Enzyme Catalysis at High Hydrostatic Pressure

Vom Promotionsausschuss der
Technischen Universität Hamburg
zur Erlangung des akademischen Grades

Doktor-Ingenieurin (Dr.-Ing.)

genehmigte Dissertation (Monografie)

von
Marlene Schmalle

aus
Göttingen

2024

Gutachter

1. Gutachter Prof. Dr. rer. nat. Andreas Liese
2. Prof. Dr.-Ing. Ralf Pörtner
3. Dr. Jürgen Kuballa

Vorsitzender: Prof. Dr.-Ing. Michael Schlüter

Tag der mündlichen Prüfung

11. November 2024

Identifier

DOI: https://doi.org/10.15480/882.13865

Handle: https://hdl.handle.net/11420/52336

Für meine Eltern

Acknowledgement

First of all, I would like to express my gratitude to Prof. Andreas Liese for the opportunity to do my PhD in his institute as well as, for his valuable supervision and unconditional support and trust.

I would like to thank Prof. Ralf Pörtner for reviewing my thesis as second examiner. Furthermore, I would like to thank Prof. Michael Schlüter for chairing the examination.

A special thanks goes to my cooperation partners Dr. Jürgen Kuballa, Dr. Miriam Aßmann and Kristin Hölting (GALAB Laboratories GmbH) for the successful project cooperation. Furthermore, I would like to thank Dr. Jürgen Kuballa for reviewing my thesis as third examiner.

I would like to express my heartfelt gratitude to the incredible team I had the privilege to work with throughout my PhD journey. Your unwavering support, insightful discussions, and collaborative spirit have been invaluable to the progress and completion of this thesis. Thank you for being a constant source of motivation and for making this journey as fulfilling as it was challenging.

I want to sincerely thank my group leader, Dr. Paul Bubenheim, for his constant support and guidance during my PhD. I am truly grateful for his mentorship and the great atmosphere he created in our group.

A big thank you to my fantastic office colleagues—Jens, Luca, Leon, and Giovanni. Working with you was always a pleasure, and your support, good humor, and insightful discussions made coming to work something to look forward to every day!

A special thanks goes to Jan Philipp, Jens, and Lukas for their valuable feedback during our long discussions about this thesis and for their support in proofreading the manuscript.

Without the help of my amazing students and interns, achieving these results would not have been possible. A heartfelt thank you to Daniel, Sophie, Nicole, Vincent, Luan, Henry, Robert, Monica, and Jana for your hard work and for making our time in the lab both productive and fun.

I would like to express my deepest gratitude to my family and friends for their unwavering support and encouragement throughout this journey. To my family, thank you for always believing in me and being a constant source of strength. To my friends, your patience, understanding, and moments of joy helped me stay balanced and motivated. I could not have done this without your love and support.

My biggest thanks go to my husband Lukas. His love, patience and endless support have been my anchor throughout this journey.

Abstract

In the past, several methods have been developed to improve the application of the biocatalysts, such as immobilizing enzymes on support materials to ensure reusability, improve stability, and maintain their activity. Furthermore, the use of non-aqueous media and genetic engineering has been applied to further enhance the enzyme performance with respect to stability, activity and selectivity. However, the evaluation of additional or synergistic process parameters is still part of research with the aim of enabling the application of enzymes in chemical synthesis. Recently, the application and effect of high hydrostatic pressure (HHP) to enzymatic catalyzed reactions is becoming increasingly important. This thesis explored the synergistic potential of combining common and innovative methods to improve enzyme performance with superior stabilization and enzyme activity, thereby contributing to the development of more efficient biocatalysts.

In order to investigate the effect of HHP on three different enzymes, a reactor concept was designed first. A continuously operated packed bed reactor (PBR) was selected to fulfill the requirement for continuous operation as part of process intensification and to enable quick and easy adjustment of process parameters. An appropriate immobilization method was developed for two selected lipases to ensure their application in a packed bed reactor (PBR) with the highest loading of the enzyme immobilizates possible. In particular, mechanical stability during continuous reactor operation under ambient and high hydrostatic pressure conditions and the leaching of enzymes from the carrier were investigated. After the establishment of the HHP reactor system, the influence of HHP on the enzyme performance including enzyme stability, activity, selectivity and kinetic parameters was investigated representing the core of the thesis. Three industrially relevant enzymes, *Candida rugosa* lipase (CRL) and *Candida antarctica* lipase B (CalB) from enzyme class 3 (EC 3), as well as *Ruegeria pomeroyi* polyphosphate kinase (PPK) of EC 2 were chosen to investigate the impact of HHP of up to 1200 bar. This investigation aims to determine the intra- and inter-enzyme-class-specific effects of HHP on the enzyme properties.

Particularly, the lipase-catalyzed transesterification reaction was used for a detailed study of the effect of HHP, as it allowed the investigation of both stability and activity changes, as well as changes in selectivity. This was of great interest as regio- as well as enantioselectivity differentiates enzymes from chemical catalysts. Additionally, the investigation included the effect of HHP on the kinetic parameters and characteristics of CRL. The resulting kinetic parameters v_{max}, $K_{M,vin,}$ $K_{M,PP}$ and $K_{i,vin}$ were adapted to the experimental data using Michaelis-Menten type kinetics at ambient and high pressure.

HHP was investigated as a synergistic and possible process intensification parameter for the cofactor regeneration process catalyzed by the industrially relevant PPK. The applicability of the enzyme immobilizates and their performance in a continuously operated reactor system were studied and compared with results obtained in a discontinuously operated stirred tank reactor (STR).

Therefore, the objective of this work was to conceptualize and investigate the operability of a continuously operated high pressure reactor system. The influence of HHP on different classes of enzymes was investigated as a complementary process parameter in the conceptualized reactor system.

Kurzzusammenfassung

Verschiedene Methoden zur Verbesserung von Biokatalysatoren, wie die Immobilisierung von Enzymen auf Trägermaterialien, wurden entwickelt, um die Wiederverwendbarkeit zu gewährleisten und die Stabilität sowie die Aktivität zu verbessern. Darüber hinaus werden nichtwässrige Medien und Gentechnik eingesetzt, um die Leistung von Enzymen in Bezug auf Stabilität, Aktivität und Selektivität zusätzlich zu verbessern. Heute gewinnt die Anwendung von hohem hydrostatischem Druck auf biologische Reaktionen als zusätzlicher Prozessparameter in verschiedenen Bereichen der Biotechnologie zunehmend an Bedeutung. In dieser Arbeit wurde das synergetische Potenzial der Kombination dieser Methoden zur Verbesserung der Enzymleistung untersucht, um eine höhere Stabilität und Enzymaktivität zu erreichen und so zur Entwicklung effizienterer Biokatalysatoren beizutragen.

Um den Einfluss des hydrostatischen Drucks auf drei ausgewählte Enzyme – zwei Lipasen und eine Kinase – untersuchen zu können, musste zunächst ein geeigneter Reaktortyp entwickelt werden. Um kontinuierlichen Betrieb zu gewährleisten wurde ein Festbettreaktor (engl. packed bed reactor; PBR) ausgewählt, der eine schnelle und einfache Anpassung der Prozessparameter ermöglicht. Anschließend wurden die ausgewählten Enzyme immobilisiert, um ihre Verwendung im PBR zu ermöglichen. Um eine möglichst hohe Beladung der Enzymimmobilisate zu erreichen, wurde eine geeignete Immobilisierungsmethode für die beiden ausgewählten Lipasen evaluiert. Um sicherzustellen, dass die Immobilisate für den Einsatz im kontinuierlichen Reaktor geeignet waren, mussten verschiedene Parameter und Effekte untersucht werden. Insbesondere galt es, die mechanische Stabilität der Immobilisate während des Reaktorbetriebs zu gewährleisten und ein Verlust der Enzyme vom Träger auszuschließen. Nach dem Aufbau des Hochdruckreaktorsystems, der Charakterisierung der Enzymimmobilisate und der Sicherstellung ihrer Verwendbarkeit wurde die zentrale Forschungsfrage dieser Arbeit umgesetzt: die Untersuchung des Einflusses des hohen hydrostatischen Drucks auf die enzymatische Leistungsfähigkeit. Dazu wurde der Einfluss des hohen hydrostatischen Drucks auf alle wichtigen Eigenschaften der Enzyme, wie Stabilität, Aktivität und Selektivität, untersucht und die kinetischen Parameter ermittelt.

Drei Enzyme von industrieller Bedeutung wurden ausgewählt, um zu untersuchen, wie die Anwendung von HHP bis zu 1200 bar diese Eigenschaften innerhalb einer Enzymklasse und für verschiedene Enzymklassen beeinflusst: die Lipasen *Candida rugosa* Lipase (CRL) und *Candida antarctica* Lipase B (CalB) aus der Enzymklasse 3 sowie die *Ruegeria pomeroyi* Polyphosphat Kinase (PPK) aus der Enzymklasse 2.

Die Lipase-katalysierte Umesterungsreaktion war für die detaillierte Untersuchung des Druckeinflusses von besonderem Interesse, da neben dem Einfluss auf Stabilität und Aktivität der Enzyme auch die Änderung der Selektivität untersucht werden konnte. Die Selektivität ist eine der herausragendsten Eigenschaften von Enzymen gegenüber chemischen Katalysatoren und muss daher besonders berücksichtigt werden. Der Einfluss des Drucks auf die kinetischen Parameter der CRL wurde zusätzlich untersucht, Die resultierenden kinetischen Parameter

v_{max}, $K_{M,vin,}$ $K_{M,PP}$ und $K_{i,vin}$ wurden mit Hilfe der Michaelis-Menten-Kinetik bei Umgebungsdruck und hohem Druck an die experimentellen Daten angepasst, um den Einfluss auf die kinetischen Eigenschaften von CRL zu bestimmen.

Der hydrostatische Druck wurde darüber hinaus auch als möglicher Prozessintensivierungsparameter für die industriell relevante PPK und deren katalysierte Cofaktorregeneration untersucht. Die Eignung des Enzymimmobilisats und die Durchführbarkeit der Reaktion im kontinuierlich betriebenen Reaktorsystem wurden untersucht und mit den Ergebnissen aus dem diskontinuierlich betriebenen Satzreaktor verglichen.

Das Ziel dieser Arbeit war es, ein kontinuierlich betriebenes Hochdruckreaktorsystem zu konzipieren und auf seine Funktionsfähigkeit hin zu untersuchen. Darüber hinaus wurde der Einfluss von HHP auf verschiedene Enzymklassen als ergänzender Prozessparameter für verschiedene Enzyme in dem konzipierten Reaktorsystem untersucht.

Contents

List of Figures

List of Tables

Abbreviations

Abbreviation	Meaning
BPR	back-pressure regulator
BSA	bovine serum albumin
CalB	*Candida antarctica* lipase B
CDP	cytidine-5'-triphosphate
CMP	cytidine-5'-diphosphate
CRL	*Candida rugosa* lipase
CTP	cytidine-5'-triphosphate
DI water	deionized water
DMSO	dimethyl sulfoxide
EC	enzyme class
GC	gas chromatography with flame ionization detector
H_2O	water
HCl	hydrochloric acid
HHP	high hydrostatic pressure
HPLC	high pressure liquid chromatography
ID	inner diameter
$MgCl_2$	magnesium chloride
Na_2HPO_4	disodium phosphate
NaCl	sodium chloride
NaH_2PO_4	sodium diphosphate
NaOH	sodium hydroxide
Na_3PO_4	sodium phosphate
NTPs	nucleoside triphosphates
OS	overhead shaker
PBR	packed bed reactor
*p*NP	*para*-Nitrophenol
*p*NPA	*para*-Nitrophenol acetate
polyP	polyphosphate
PP	*(R/S)*-1-phenyl-2-propanol
PPA	*(R/S)*-1-phenyl-2-propanyl acetate
PPK	*Ruegeria pomeroyi* polyphosphate kinase
PPKs	polyphosphate kinases
PU	pressure generation unit
RMSD	root-mean-squared deviation
rpm	revolutions per minute
R-PP	*(R)*-1-phenyl-2-propanol

R-PPA	*(R)*-1-phenyl-2-propanyl acetate
SEM	scanning electron microscopy
SP	shaking plate
S-PP	*(S)*-1-phenyl-2-propanol
S-PPA	*(S)*-1-phenyl-2-propanyl acetate
STR	stirred tank reactor
TR	tube roller
UHPLC	ultra high pressure liquid chromatography
vin	vinyl acetate

List of Symbols

Symbol	Unit	Parameter
$\dot{V}$	$L \cdot min^{-1}$	flow rate
$\bar{t}$	min^{-1}	mean residence time
a_w	-	water activity
c	$mmol \cdot mL^{-1}$	concentration
$c(t)$	$mmol \cdot mL^{-1}$	the concentration at sampling time
c/c_0	-	measured enzyme concentration of the immobilization solution in relation to the initial protein concentration of the immobilization solution
c_0	$mmol \cdot mL^{-1}$	initial concentration
c_{CDP}	$mmol \cdot L^{-1}$	CDP concentration
c_E	$mg \cdot mL^{-1}$	enzyme concentration
$c_{E,0}$	$mg \cdot mL^{-1}$	initial enzyme concentration
c_{polyP}	$mmol \cdot L^{-1}$	polyP concentration
c_{PP}	$mmol \cdot L^{-1}$	PP concentration
c_S	$mmol \cdot L^{-1}$	substrate concentration
c_{vin}	$mmol \cdot L^{-1}$	vin concentration
d	-	days
E	-	enantioselectivity
EA	$U \cdot mg_{carrier}^{-1}$	carrier-specific activity
EA_{free}	$U \cdot mg_{enzyme}^{-1}$	activity of the enzymes before
EA_{immo}	$U \cdot mg_{enzyme}^{-1}$	activity of the immobilized enzyme
ee	-	enantiomeric excess
ee_P	-	enantiomeric excess with respect to the product
EP	-	enzyme product complex
ES	-	enzyme substrate complex
Ex	-	extinction
$F\text{-}curve$	-	cumulative residence time distribution function
E	-	free enzyme
i	-	index
ID	µm	inner diameter
k_d	min^{-1}	deactivation constant
K_I	$mmol \cdot L^{-1}$	inhibition constant
$K_{I,polyP}$	$mmol \cdot L^{-1}$	inhibition constant for vin
$K_{I,vin}$	$mmol \cdot L^{-1}$	inhibition constant for PP
K_M	$mmol \cdot L^{-1}$	Michaelis-Menten constant
$K_{M,CDP}$	$mmol \cdot L^{-1}$	Michaelis-Menten constant for CDP
$K_{M,polyP}$	$mmol \cdot L^{-1}$	Michaelis-Menten constant for polyP
$K_{M,PP}$	$mmol \cdot L^{-1}$	Michaelis-Menten constant for PP
$K_{M,vin}$	$mmol \cdot L^{-1}$	Michaelis-Menten constant for vin
m	-	amount of repetitions
m_{CalB}	mg	mass of CalB

$m_{carrier}$	g	amount of carrier
m_{CRL}	mg	masse of CRL
$m_{enzyme,immo}$	mg	mass of immobilized enzyme
m_{immo}	mg	amount of immobilized enzyme
m_{PPK}	mg	mass of PPK
$m_{solution}$	mg	amount of enzyme in the solution
$n_{(R)\text{-}P}$	mol	amount of *R*-enantiomer of the product
$n_{(S)\text{-}P}$	mol	amount of *S*-enantiomer of the product
n_t	mol	initial substrate amount
$n_{t=0}$	-	number of repeated experiments
P	-	free product
p	bar	pressure
R	$J \cdot mol^{-1} \cdot K^{-1}$	ideal gas constant
r	$\mu mol \cdot min^{-1}$	reaction rate
S	-	free substrate
T	°C or K	temperature
t	min or h	time
$t_{1/2}$	min^{-1}	half-life
v	$\mu mol \cdot min^{-1}$	reaction rate
V	L	volume
v_{max}	$U \cdot mg^{-1}$	maximum reaction rate
V_R	mL	volume of the empty reactor
w	cm	width of cuvette
X	%	conversion
x	$mmol \cdot L^{-1}$	experimental value
$x_{m,i}$	$mmol \cdot L^{-1}/U \cdot mg^{-1}$	measured values
x_{si}	$mmol \cdot L^{-1}/U \cdot mg^{-1}$	predicted values
Y_{EA}	%	activity yield
Y_{immo}	%	immobilization yield
Δ	-	difference
Δc	$mmol \cdot mL^{-1}$	difference in concentration
Δc_{CTP}	$mmol \cdot mL^{-1}$	difference in CTP concentration
Δc_{PP}	$mmol \cdot mL^{-1}$	difference in PP concentration
$\Delta V^{\neq}$	$cm^{-3} \cdot mol^{-1}$	activation volume
ε	$L \cdot \mu mol^{-1} \cdot cm^{-1}$	extinction coefficient
τ	min^{-1}	hydrodynamic residence time
∂	-	partial derivative

1. Introduction

Biocatalysts are often used as an alternative to chemical catalysts in a wide range of reactions and processes. The use of biocatalysts, such as enzymes, instead of chemical catalysts, offers several advantages. They possess high activity at typically milder reaction conditions, which leads to reduced energy costs in many applications. Furthermore, enzymes are mainly reaction, substrate and regiospecific as well as enantioselective. However, a major drawback is their sensitivity to harsh reaction conditions such as high temperature, extreme pH, and aggressive chemicals.[1–3]

In the past, several methods have been developed to improve biocatalysts, including immobilization of enzymes in or on support materials to ensure biocatalyst reusability or to improve enzyme stability and activity. The same results can be obtained by using non-aqueous media or by genetic modification of the enzyme [2]. In particular, the operation of enzyme-catalyzed reactions in organic solvents provides the opportunity to perform biotransformations other than those naturally catalyzed by enzymes. This greatly expands the application range of enzymes in industry.[4–6] Generally, the operation mode, in which a reaction is carried out, should also be considered. Thus, the choice of a suitable reactor can have a significant influence on the efficiency of the process.[7–10] While most biocatalytic reactions are still performed in batch reactors, transferring them to continuous flow reactors can make the processes more productive, more sustainable, and easier to control [9]. Furthermore, replacing batch processes with continuous processes represents an additional factor contributing to the implementation of effective biotransformations and is the key to process intensification [7–9].

In recent years, a new method and its impact on biological systems has been increasingly studied in various fields of biotechnology: the application of high pressure to biological reactions [1,2]. High pressure is used in many areas of the food industry, but also has a wide range of potential applications in pharmaceutical and chemical industry [2,11,12]. In 2009, Eisenmenger *et al.* described the use of high pressure to increase the stability and/or activity of 25 different enzymes [2]. A varying degree of influence on enzyme stability and/or enzyme activity has been observed, although this is also dependent on other experimental parameters, including temperature and reaction medium. Therefore, in addition to the specific investigation of the influence of high pressure on immobilized enzymes, a more detailed consideration of the influence of the solvent, especially of organic phases, is required.[2,13] Overall, the combination of the previously described methods to stabilize and enhance the activity of enzymes will lead to further improvement of biocatalysts [14].

This work was funded by the German Federal Ministry of Education and Research (BMBF) due to its relevance for various industrial sectors and was part of the strategic alliance "prot P.S.I.". The thesis with the project number 031B0723 was carried out in close cooperation with

the industrial partner GALAB Laboratories GmbH. One of the reaction systems investigated is used by this company.

Previous investigations of the effect of HHP on enzymes have focused mainly on lipase-catalyzed reactions, which is reasonable since lipases are the most relevant enzymes in industry.[13–20] To further understand the influence of HHP on enzyme systems, it is necessary to investigate different enzymes from different enzyme classes in a comparable manner.[2,13,14] Therefore, inter and intra enzyme class specific HHP effects were investigated. Two enzyme class 3 lipases, which naturally catalyze the hydrolysis of fats while catalyzing many other reactions in unconventional reaction media, and the enzyme class 2 transferase PPK, which regenerates cofactors, were selected.[21–23]

First, the transesterification reaction of vinyl acetate with *(R)*/*(S)*-1-Phenyl-2-propanol to *(R)*/*(S)*-1-Phenyl-2-propanyl acetate and acetaldehyde catalyzed by immobilized lipases *Candida rugosa* lipase and immobilized *Candida antarctica* lipase B under ambient and HHP was studied (Figure 1). Transesterification reactions are of interest for the production of biodiesel, flavoring and fragrance substances, and many more renewable chemicals.[20,24,25]

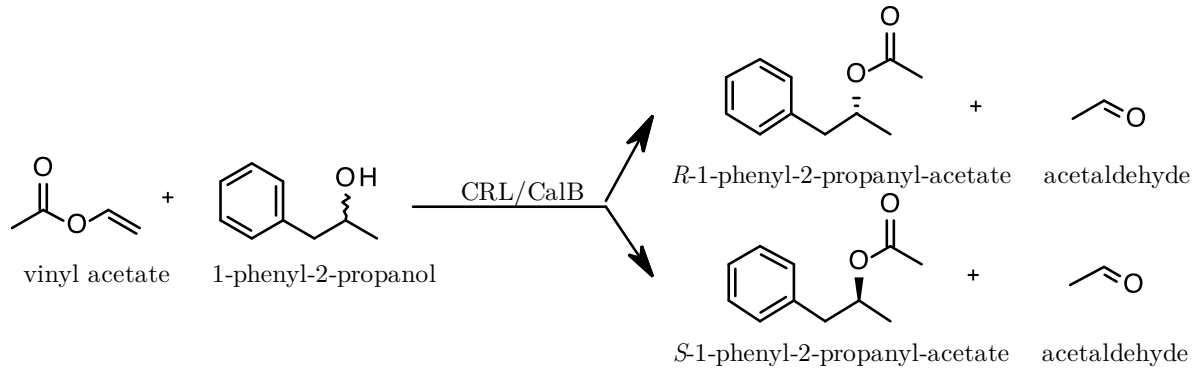

Figure 1: Transesterification by *Candida rugosa* lipase and *Candida antarctica* lipase B.

Second, the reaction kinetics and the impact of HHP on immobilized polyphosphate kinase from *Ruegeria pomeroyi* is comprehensively investigated for a cytidine-5'-diphosphate (CDP) phosphorylation to the cofactor cytidine-5'-triphosphate (CTP) (Figure 2). Due to high costs and inhibition phenomena resulting from the stoichiometric use of cofactors, cofactor-dependent biocatalysis can be challenging.[26,27] Thus, an efficient and cost-reduced cofactor regeneration process could have multiple applications in industrially relevant processes [26–29].

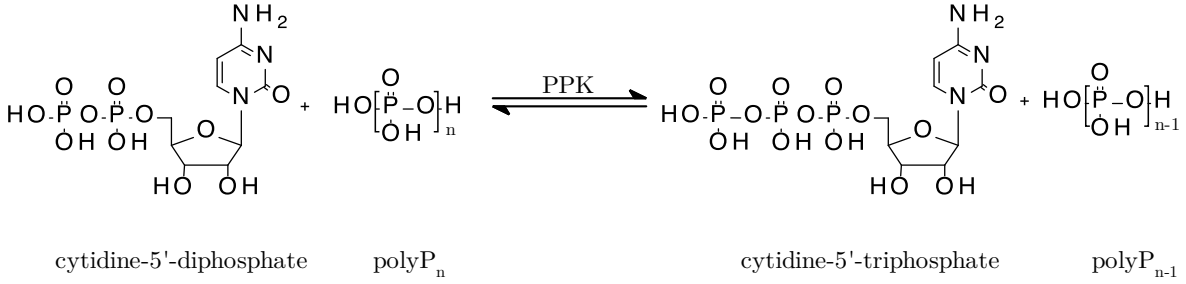

Figure 2: CDP phosphorylation by *Ruegeria pomeroyi* polyphosphate kinase.

In this thesis, the influence of HHP up to 1,200 bar on enzyme activity, stability, and selectivity is investigated. Therefore, a continuous high pressure reactor was conceptualized to provide a suitable set-up to analyze the influence of HHP on enzymes. A detailed study of the immobilizates was carried out to determine the immobilization process and their suitability for use in the continuous hydrostatic high pressure reactor. Furthermore, this continuous high pressure reactor set-up provides the possibility to analyze the kinetics of immobilized enzymes in an accelerated and simplified manner. Therefore, the influence of HHP on kinetic parameters was investigated as well. Overall, this study should contribute to a better understanding of the influence of HHP on enzyme properties and establish HHP as a complementary process parameter in various biocatalytical reactions.

1.1. Improvement of Enzymatic Catalyzed Reactions

A variety of approaches are available to further enhance the potential of enzymatic catalysis for industrial applications. These include immobilization, the use of organic solvents, or performing the reaction under high pressure. All these methods can affect the stability, activity, and selectivity of enzymes.[2] In the following section, these methods will be explained and recent developments in these areas will be discussed.

1.1.1. Immobilization of Enzymes

Immobilization of enzymes is described as "physical delineation or localization of enzymes in a confined space while maintaining catalytic activity" [30]. This method is used to increase productivity (ratio of the amount of the product to the amount of catalyst used) and conversion (the amount of substance converted in relation to the initial amount of substance at the start of the reaction) as well as reusability of biocatalysts [31]. It can significantly improve the economic efficiency of the biocatalysts used: on the one hand, the enzymes can be used more frequently, and on the other hand, costs for separating the enzymes from the product are reduced [3,32].

There are different methods to immobilize biocatalysts: attaching of enzymes on a support which can be covalent or noncovalent by, e.g., adsorption, furthermore, enclosing the enzymes in a polymer, a membrane or encapsulation of the enzymes. In addition, enzymes can be covalently cross-linked to each other. The choice of immobilization method depends on the intended application of the enzymes.[31,33] With regard to process intensification, immobilization can enable the use of continuously operated reactors since the immobilizates are retained in the reactor and therefore meet the requirements of industrial applications [34].

Immobilization can change the kinetic parameters, activity (velocity at which the substrate is converted), and stability of the enzymes. On the one hand, the immobilization matrix used and the associated change in the microenvironment have a major influence on this.[33] However, immobilization can also lead to a reduction in the activity of the enzyme, usually due to steric hindrances, such as restriction of dynamics or blockage of the active site as well as changes in surface hydrophobicity or charge. On the other hand, usually the enzyme stability at high temperatures is positively affected.[33] Generally, the reasons for stabilization are to protect the

enzyme from interaction with molecules, to prevent promotion by shear stress and to increase the rigidity of the enzyme structure to reduce conformational change [35].
Therefore, in addition to the choice of the right biocatalyst, the choice of a suitable immobilization method is of great importance for the optimal performance of a biotransformation [31,33].
Detailed immobilization techniques as well as their benefits and drawbacks are discussed in detail in Jaeger *et al.* in 2018 and Sharma in 2012 [3,36].

Description of the Immobilization Characteristics

Various parameters can be used to assess the efficiency of enzyme immobilization. These parameters indicate the effectiveness of enzyme immobilization and the performance to be expected. The definition of these parameters and their calculation is done according to Liese *et al.* in 2018.[3] Among others, the immobilization yield (Y_{immo}), the activity yield (Y_{EA}) as well as the carrier-specific activity (EA) of the enzyme for different carrier materials, immobilization durations and experimental temperatures are calculated to describe the performance of the immobilization process.

The Y_{immo} [%] provides information on the amount of the enzyme that is successfully immobilized on the carrier. The amount of immobilized enzyme (m_{immo} [mg]) is related to the mass of enzyme in the solution at the beginning of the immobilization ($m_{solution}$ [mg]) It is calculated using the following Equation 1-1.

$$Y_{immo} = \frac{m_{immo}}{m_{solution}} \cdot 100 \qquad 1\text{-}1$$

The activity yield Y_{EA} [%] describes how much activity the enzyme retains during immobilization. To calculate this parameter, the activity of the immobilized enzyme (EA_{immo} [$U \cdot mg_{enzyme}^{-1}$]) is related to the activity of the enzymes before immobilization (EA_{free} [$U \cdot mg_{enzyme}^{-1}$])

$$Y_{EA} = \frac{EA_{immo}}{EA_{free}} \cdot 100 \qquad 1\text{-}2$$

In addition, the EA [$U \cdot mg_{carrier}^{-1}$] is considered. This parameter is used to describe the catalytic performance of the immobilizate. The activity of the immobilizate multiplied by the mass of immobilized enzyme ($m_{enzyme,immo}$ [mg]) in relation to the amount of carrier ($m_{carrier}$ [g]) is referred to as carrier-specific activity.

$$EA = \frac{EA_{immo} \cdot m_{enzym,\ immo}}{m_{carrier}} \qquad 1\text{-}3$$

1.1.2. Biocatalysis in Unconventional Media

In the last decades, the use of organic solvents, mainly *n*-hexane, has been extensively studied in biotechnology. It has been found that the choice of solvent and the resulting different polarities, in addition to changing the reaction conditions, has an impact on the activity and the stability of the enzymes.[2,5,6]

The use of enzymes in their natural aqueous reaction media can limit the opportunities for industrial bioconversions, particularly for the production of specialty chemicals and polymers. Many of these compounds are insoluble in water. Moreover, water can cause undesirable side reactions or even degrade the organic reagents used.[4] Furthermore, enzymes are able to catalyze reactions other than those they catalyze in water. In particular, lipases catalyze transesterification, aminolysis and thiotransesterification in anhydrous solvents [4,37]. The products of these reactions, fine chemicals, flavors and fragrances, are of great commercial interest, which illustrates the large industrial potential of lipases [6,38]. In addition, product recovery in aqueous systems may be more difficult than in organic solvents. The use of unconventional and unnatural reaction media is a promising way to improve enzyme performance. For example, the technological utility of enzymes can be significantly increased by using organic solvents instead of aqueous reaction media, since the use of the former changes the properties of the enzymes.[4,5] Conversely, the use of organic solvents can reduce the enzyme activity in organic solvents. Enzymes lose some of their flexibility as a certain number of water molecules are essential on the enzyme surface to provide the necessary conformational mobility and catalytic activity. This effect can be avoided or even reversed by adding small amounts (<1 vol.-%) of water.[4,39] The effect of the amount of water in an organic solvent on the enzyme activity is related to the water activity (a_w), as it denotes the amount of available water for the reaction system. [40,41] This amount of water in the organic solvent has an influence on the hydration shell of the enzyme and this influencing the enzyme activity. [39,40,42] The effect of water on the enzyme activity strongly depends on the type of organic solvent and the group of enzyme [4,39,40].

However, the direct effect of the solvent on the activity is not systematic and cannot be accurately predicted [3]. Several cases of improved enzyme stability in non-aqueous media against thermal inactivation have been reported in literature, again related to the water content in the organic solvent. Nevertheless, the half-life of the enzyme decreases if the water content is too high.[4,43,44] The choice of solvent influences the selectivity of the enzyme, and since selectivity is an important objective in the application of biocatalytic processes, the use of organic solvents could be a key to optimization. When using anhydrous organic solvent, the selectivity of an enzyme can be affected in several ways. A change in substrate-, stereo-, regio-, and chemoselectivity is possible depending on the organic solvent or solvent mixture.[3,4,44]

In addition to the advantages described, there are also disadvantages related to the use of organic solvents. Mutagenicity, teratogenicity, carcinogenicity and/or reprotoxicity may be associated with many of these solvents. Furthermore, these organic solvents are manly petrol

based and therefore not environmentally sustainable [45]. As a consequence, a wise selection and efficient use of organic solvents is necessary.[46]

In order to comprehensively optimize a process, it is therefore essential to study the influence of the solvent on the enzymatic catalysis and to combine these results with other strategies to increase enzyme activity and stability in order to achieve the best possible biotransformation with the highest yield over the longest period of time.[2]

1.1.3. Biological Systems Under High Hydrostatic Pressure

The influence of high pressure on biological systems, including proteins, enzymes, prokaryotic, eukaryotic and tissue cells, has been the subject of increasing research over the past years [1,2,11,47]. To investigate this influence, different types of high pressure are used. The pressure can be generated by compressed gas, supercritical carbon dioxide, or hydrostatic pressure. In this study, the effects of hydrostatic pressure on activity, stability and enantioselectivity are examined.[2]

Over the past decades, the high hydrostatic pressure technology has gained considerable attention in the food industry. As a non-thermal food pasteurization method, HHP offers several benefits, including the ability to inactivate microorganisms while preserving the nutritional components of food.[2,47] While this part of the industry focuses on the deactivation of unwanted microorganisms or enzymes, scientists in the 1980s began to investigate the beneficial influence of hydrostatic pressure on enzymatically catalyzed reactions [2,47,48]. In general, the effect of hydrostatic pressure on enzymes can be divided into two phenomena: first, the influence on activity and second, the influence on stability.[2]

Changes in Enzyme Activity by High Pressure

Biological systems are exposed to pressures of up to 1,100 bar in nature (deep sea, Mariana Trench) and up to 6000 bar in industrial processes, especially in the food industry [2,46,47]. Studies on enzymes showed that high pressure above 10,000 bar leads to the denaturation of enzymes, as the primary structure of enzymes is stable only up to this pressure, while the secondary structure is already irreversible denatured at pressures over 4,000 bar. At pressures below 2,000 bar, in most cases only the tertiary and quaternary structure of the enzyme changes. These structural changes of the enzymes can have significant influence on the activity of the enzyme [16,51,52].

In addition to direct changes of pressure on the structure of enzymes, any changes in the surrounding medium, solvent, or substrate, will also affect the structure of the enzyme or the chemical reaction. These changes include a change in pH, density or viscosity. [2,53] The reaction mechanism can be influenced by high pressure as well. Based on Le Chatelier´s principle, the yield of some enzymatic reactions may be elevated directly by increasing the pressure, if the systems volume change due to the reaction is negative. Due to the pressure application, the thermodynamic equilibrium of a chemical reaction with negative reaction volume decreases, as the reaction is shifted to the side of the products and the yield is thus increased.[1,47,52]

For enzymatically catalyzed reactions, the pressure dependence of the equilibrium can be described by the Eyring equation. The activation volume $\Delta V^{\neq}$ [$cm^{-3} \cdot mol^{-1}$] represents the total molar volume change between the ground states and the activated states and describes the dependence of the reaction rate on the pressure.[2] Using the Eyring equation, the pressure dependence of the reaction rate can be estimated, where p [bar] is the pressure, r [$\mu mol \cdot min^{-1}$] the reaction rate, R [$J \cdot mol^{-1} \cdot K^{-1}$] is the ideal gas constant and T [K] the temperature. [2]

$$\left(\frac{\partial \ln r}{\partial p}\right)_T = - \frac{\Delta V^{\neq}}{RT} \qquad 1\text{-}4$$

Nevertheless, the Eyring equation can only be considered as an approximation for the description of the pressure dependence of biocatalytic reactions, because in contrast to chemical catalysis, the physical meaning of $\Delta V^{\neq}$ in biocatalysis is less precisely described.[2,47]
Furthermore, the substrate specificity of an enzyme can be altered if the conversion of a substrate leads to a product with a smaller volume [1,2]. However, this behavior cannot provide information about the enantioselectivity of the enzymes [54,55].

Stabilizing Effect of High Pressure

In addition to changes in enzyme activity, pressure can also alter the stability of enzymes. The processes by which HHP stabilizes enzymes are not yet fully understood. Intramolecular interactions, hydration of charged groups, disruption of bound water, and stabilization of hydrogen bonds may all play a role in the pressure effects on intra- and intermolecular interactions within enzymes.[2]
Pressure is suitable for studying changes in protein structures because the comparatively low energy input (kJ per mole) has no effect on covalent bonds — in contrast to the thermally induced unfolding of proteins, where more than 102 kJ per mole are introduced into the system.[1] Therefore, this method can be used to study changes in non-covalent bonds such as hydrogen bonding, change in hydration, or spacing of unbound atoms. Another difference in the structural change of proteins, e.g., enzymes, due to pressure compared to temperature is that the enzyme undergoes a different structural change than in the case of a temperature-induced system change.[1] At pressures below 2,000 bar, only intermolecular distances and the conformation of the enzymes (tertiary and quaternary) are changed, but not the covalent bonds [54]. However, if the change in enzyme structure is too great, the enzyme denatures; this can be caused by temperature or pressure. Figure 3 shows an example of the pressure and temperature range in which an enzyme is present in its native state (inside the circle).

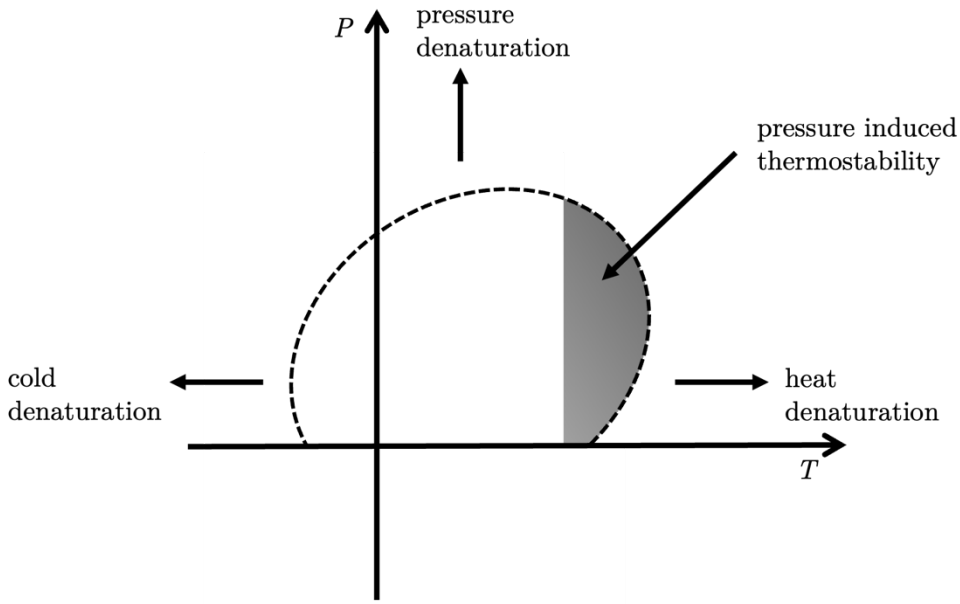

Figure 3: Schematic representation of native (inside the circle) and denatured (outside the circle) regions of an enzyme in the pressure/temperature diagram modified according to Winter *et al.* 2007 and Mishra *et al.* (2014) [54,56].

Figure 3 shows a p,T-stability diagram of an enzyme, where inside the circle the enzyme is in its native state and active. Outside of the circle the enzyme is unfolded and therefore inactive. It is shown that, as with increasing temperature, there is an upper limit for the pressure above which enzymes denature. It can be seen in the figure; the effect of heat denaturation can be compensated by increasing hydrostatic pressures as indicated in the grey colored region. The shape and position of this specific circle depend on the individual enzyme, therefore different enzymes can exhibit a different stability behavior depending on pressure and temperature. The native enzyme state at high hydrostatic pressures can be maintained by reducing the temperature. Most studies have focused on hydrolases classified as EC 3, which includes lipases.[2] The optimal pressure range in which increased stability and activity of the enzymes could be observed was 2,000 – 3,000 bar for most lipases [2,13,14,16]. Pressure-induced activity increases of up to 840 % in organic solvents have also been described in literature for other hydrolases.[2] If the reaction rate of an enzymatic reaction is limited by the thermosensitivity of the enzyme, pressure-induced thermostability may overcome this thermosensitivity. During the initial stages of thermal inactivation, an enzyme might lose essential water molecules, leading to structural misfolding. High pressure can impede this process due to its positive effect on the hydration of both charged and non-polar groups. Effectively, the application of HHP strengthens the enzyme hydration shell and promotes the hydration of the enzyme.[1,57,58] The increased substrate turnover at higher temperatures can thus realize optimized reaction conditions [1,54]. Pressure-induced temperature stability has been demonstrated in literature for several enzymes classes, including amylases, lipases, and polymerases [2,59].

Therefore, in addition to pressure, immobilization of the enzymes and the use of organic solvents can have a positive influence on stability, activity and enantioselectivity. The aim of this thesis is to investigate these influencing factors and their interaction, particularly the effect

of hydrostatic pressure on enzymes, in order to determine optimized reaction conditions for the investigated biotransformations.

1.2. Modes of Reactor Operation

In biotechnology, most experiments performed under HHP are carried out in a batch process. The substrate is first added to the free enzymes in suspension and the reactor is then pressurized. After a certain reaction time, the reactor is depressurized and the reaction mixture is analyzed.[2,60] Discontinuously operated STR offer a high flexibility in operation and a scale-up of processes is enabled comparatively easy. In contrast, the mixing efficiency in STR is limited, which can lead to mass transfer limitation.[61] Furthermore, the production rate may be low and product quality can vary from batch to batch [62].

In recent years, the replacement of batch processes with continuous processes has been an additional factor contributing to the implementation of sustainable transformations and is considered as a key to process intensification.[7–9] A continuously operated reactor is operated as follows: The substrates are continuously pumped into a reactor at a fixed flow rate where the chemical reaction takes place as the flow passes through the reactor. To maintain a constant volume level and working volume, an equal quantity of reactor content compared to the inlet flow is discarded at the reactor outlet.[63] The continuously operated reactor can be realized as a packed bed reactor, also known as fixed bed reactor, a membrane reactor, a wall-coated reactor, or a flow coil reactor. In a PBR, the biocatalyst is fixed on a carrier material by immobilization and therefore retained inside the reactor as the substrate solution flows through the reactor.[9]

PBRs can be operated under HHP, with pressurization achieved by high pressure pumps and back-pressure devices located downstream of the enzyme-containing reactor.[64] At the outlet, the product stream leaves the reactor and the packed bed or the biocatalyst itself inside the reactor remains unchanged [3,9]. Thereby, purification of the product is simplified, since no biocatalyst has to be removed from the final product [9,65]. Continuous operated flow reactors offer numerous advantages, including enhanced mass and heat transfer, better mixing performance, higher space-time yield, easier control of pressure and temperature compared to batch processes, resulting in significant process intensification [7–9,64]. As a consequence of the resulting concentration profile of substrate and product, undesirable side or subsequent reactions of the product can be suppressed [66,67]. The concentrations of the product and reactants are constant at steady-state, which can simplify the downstream processes [68].

To overcome inhibition phenomena, e.g., regeneration of cofactors, operating in a continuous reactor is advantageous, especially for large scale industrial applications. In particular, if a follow up reaction of the product occurs, the continuous flow reactor with a packed bed should be selected, as the highest product concentration is reached only at the end of the reactor.[3] The continuously operated process can be easily optimized by fine-tuning of parameters such as flow rate, pressure, and temperature. This also contributes to facilitating the scale-up of flow processes compared to batch processes.[7,9,65,69] Thus, the establishment of more flexible

continuously operated reactors and the use of immobilized enzymes can contribute to the development of advanced enzymatically catalyzed reactions on an industrial scale and the possibility of conducting experiments under HHP [7,10,27,70]. The immobilization of enzymes enables conducting experiments continuously under high pressure, as they are present in a fixed bed in the PBR [68].

1.3. Enzyme Kinetics

The investigation of enzyme kinetics describes the manner and rate at which an enzyme converts one or more substrates into one or more products [3,71]. This rate is defined as reaction rate r or reaction velocity v, which is affected by several parameters. These parameters include biocatalyst type, temperature, pressure, concentration of product and substrate.[71] However, a reaction is always limited by the chemical equilibrium dictated by the thermodynamics of the chemical reaction. By definition a catalyst increases the reaction rate without being consumed, but it cannot change the thermodynamic equilibrium of the reaction. This equilibrium will change when a change in concentration, temperature or pressure occurs. This shift to a altered equilibrium is known as the Le Chatelier's principle.[3]

The determined enzyme kinetics and the corresponding kinetic parameters represent the basis for the design of suitable reactors and processes and their estimation is of upmost importance for the determination of achievable yields and the establishment of an economic process [3,71]. A detailed description about enzyme kinetics is given by Bisswanger (2000) and Jaeger, Liese, and Syldatk (2018) [3,72].

Since kinetic constants are important parameters for characterizing and describing the performance of enzymes, the influence of HHP on them is investigated in this thesis. A detailed explanation of the kinetic model chosen to describe the enzyme kinetics in this thesis is given in 1.3.1, and a description of how to calculate the kinetic parameters using this model is given in 1.3.2.

1.3.1. Michaelis-Menten Theory

Several models have been established for the mathematical description of enzyme kinetics. The most widely used model is based on the Michaelis-Menten theory, first described by Michaelis and Menten (1913) [3,73]. The mathematic background and the detailed derivation is given by Bisswanger (2000) and Jaeger, Liese, and Syldatk (2018) [3,72].

Assuming steady-state conditions, the mechanism consists of two steps: the building of the enzymes-substrate complex (ES) out of the substrate (S) and the free enzyme (E). The steady-state condition describes that the formation and decomposition of the enzyme-substrate complex occurs at the same rate.[72] The enzyme-substrate complex is stabilized by the enzyme, which leads to a decisive reduction of the necessary activation energy. The substrate is converted to the product (P) resulting in the enzyme-product complex (EP). The second step

of the mechanism is the dissociation of the product and the free enzyme.[3,74] This is given in the following Equation 1-5.

$$E+S \rightleftharpoons ES \rightleftharpoons EP \longrightarrow E+P \qquad 1\text{-}5$$

The equation can be simplified by the assumptions that the back reaction from EP to ES is neglectable and that the formation of the enzyme-product complex from enzyme and product can be omitted because of low product concentration, resulting in Equation 1-6.[72]

$$E+S \rightleftharpoons ES \longrightarrow E+P \qquad 1\text{-}6$$

Assuming further simplifications, including that the rate-limiting step is the dissociation of the ES complex, the following equation can be derived for the reaction rate [75]. The details of the simplifications and assumptions are described in detail in Bisswanger *et al.* in 2000 [72]. In Equation 1-7 v [µmol ·min^{-1}] is the reaction rate depending on the substrate concentration c_S [mmol ·L^{-1}], maximum reaction rate v_{max} [U ·mg^{-1}] and the Michaelis-Menten constant K_M [mmol ·L^{-1}] [72].

$$v = \frac{v_{max} \cdot c_S}{K_M + c_S} \qquad 1\text{-}7$$

The Michaelis-Menten constant K_M, expresses the affinity of the enzyme to the substrate. It indicates the specific substrate concentration at which half of the maximum activity is reached, given in Equation 1-8.

$$K_M = \frac{v_{max}}{2} \qquad 1\text{-}8$$

The equation can be altered to describe the chosen model reaction. Since all selected model reactions in this thesis have two substrates, the equation must be extended by one term. This equation is called double substrate-Michaelis-Menten kinetics, assuming that both substrates binding at the same active center of the enzyme.[3]
The transesterification reaction of vinyl acetate (vin) with *(R/S)*-1-Phenyl-2-propanol (PP) to *(R/S)*-1-Phenyl-2-propanyl acetate (PPA) and acetaldehyde was investigated. In this thesis the transesterification reaction is catalyzed by two enzymes CRL and CalB. The Michaelis-Menten equation of the transesterification reaction is given in Equation 1-9.

$$v = v_{max} \cdot \frac{c_{PP}}{K_{M,PP} + c_{PP}} \cdot \frac{c_{vin}}{K_{M,vin} + c_{vin}} \qquad 1\text{-}9$$

The exact mechanism of this reaction is not known. For simplicity, Michaelis-Menten is used without mechanistic information. Nevertheless, since both substrates bind to one active site of the enzyme, there is only one reaction specific maximum reaction rate v_{max}, whereas each substrate has a Michaelis-Menten constant K_M. This results in $K_{M,PP}$ for the 1-Phenyl-2-propanol and $K_{M,vin}$ for 1-Phenyl-2-propanyl acetate.

The phosphorylation of CDP with polyphosphate (polyP) to CTP is catalyzed by polyphosphate kinase 2-3 from *Ruegeria pomeroyi*. Since there are two substrates binding to the active site of the enzyme, the double substrate-Michaelis-Menten kinetics is also applied for this reaction, and the corresponding equation is given in Equation 1-10.

$$v = v_{max} \cdot \frac{c_{CDP}}{K_{M,CDP} + c_{CDP}} \cdot \frac{c_{polyP}}{K_{M,polyP} + c_{polyP}} \qquad 1\text{-}10$$

The reaction rate v is depending on the maximum reaction rate v_{max} and the K_M values of CDP and PP and on the concentration of the substrates.

Enzyme Inhibition

The reaction rate of an enzyme-catalyzed reaction can be reduced by a substance which is called inhibitor. These are molecules that, e.g., bind to the active site of the enzyme and block it from catalyzing a reaction.[36] Two main mechanisms are distinguished: a reversible and an irreversible reaction.
For the reversible inhibition a molecule binds to the enzyme or the enzyme-substrate complex. The inhibitor can be a product or the substrate of the catalyzed reaction. In the case of an irreversible inhibition, the inhibitor is usually a reactive molecule that irreversibly binds to the enzyme and causes its inactivation.[3] The inhibitors can be organic chemicals, inorganic metals or biosynthetic compounds besides product or substrate [36]:

The reversible inhibition can be divided into three types: competitive, uncompetitive, and non-competitive inhibition. These differ in the way they interact with the enzyme or enzyme-substrate complex. The change in kinetic parameters is also different for each type of inhibition. Inhibition phenomena and how to deal with them have been described in considerable detail by Sharma in 2012.[36]
All enzymes studied in this thesis showing an inhibition by one of their substrates. The Michaelis-Menten equation must therefore be modified according to the three different inhibition types to take this inhibition phenomenon into account. The dissociation constant K_I [mmol $\cdot$L^{-1}] describes the affinity between enzyme and inhibitor, which is vinyl acetate for the transesterification reaction and polyphosphate for the CDP phosphorylation.

The Michaelis-Menten equations with uncompetitive, non-competitive and competitive inhibition by vinyl acetate are given in Equation 1-11, 1-12 and 1-13, respectively.

$$v = v_{max} \cdot \frac{c_{PP}}{K_{M,PP} + c_{PP}} \cdot \frac{c_{vin}}{K_{M,vin} + c_{vin} \cdot (1 + \frac{c_{vin}}{K_{I,vin}})} \quad 1\text{-}11$$

$$v = v_{max} \cdot \frac{c_{PP}}{K_{M,PP} + c_{PP}} \cdot \frac{c_{vin}}{(K_{M,vin} + c_{vin}) \cdot (1 + \frac{c_{vin}}{K_{I,vin}})} \quad 1\text{-}12$$

$$v = v_{max} \cdot \frac{c_{PP}}{K_{M,PP} + c_{PP}} \cdot \frac{c_{vin}}{K_{M,vin} \cdot (1 + \frac{c_{vin}}{K_{I,vin}}) + c_{vin}} \quad 1\text{-}13$$

The Michaelis-Menten equation with uncompetitive, non-competitive and competitive inhibition by polyphosphate is given in Equation 1-14, 1-15 and 1-16, respectively.

$$v = v_{max} \cdot \frac{c_{CDP}}{K_{M,CDP} + c_{CDP}} \cdot \frac{c_{polyP}}{K_{M,polyP} + c_{polyP} \cdot (1 + \frac{c_{polyP}}{K_{I,polyP}})} \quad 1\text{-}14$$

$$v = v_{max} \cdot \frac{c_{CDP}}{K_{M,CDP} + c_{CDP}} \cdot \frac{c_{polyP}}{(K_{M,polyP} + c_{polyP}) \cdot (1 + \frac{c_{polyP}}{K_{I,polyP}})} \quad 1\text{-}15$$

$$v = v_{max} \cdot \frac{c_{CDP}}{K_{M,CDP} + c_{CDP}} \cdot \frac{c_{polyP}}{K_{M,polyP} \cdot (1 + \frac{c_{polyP}}{K_{I,polyP}}) + c_{polyP}} \quad 1\text{-}16$$

There are several methods for obtaining kinetic parameters of enzyme-catalyzed reactions. Kinetic parameters cannot be measured directly but must be determined via the reaction rate equation, which is based on a specific kinetic model. Generally, changes in the concentration of at least one reactant are measured as a function of time.

One method is to measure the initial rate of the reaction. The initial rate is the rate of the reaction when the substrate concentration is relatively high and a maximum substrate conversion of 10 % is reached. This means that the back reaction becomes negligible and the reaction rate depends only on the forward reaction.[3] Another way to determine enzyme kinetics is to analyze the progression curve, where the time course of a biochemical reaction is analyzed.[74]

These measurements provide kinetic constants while using kinetic models such as Michaelis-Menten kinetic to determine the Michaelis-Menten constant K_M and maximum reaction rate v_{max} [72]:

1.3.2. Kinetic Parameter Estimation

Kinetic parameters are determined based on the Michaelis-Menten theory (see 1.3.1), which is extensively described in literature as in Jaeger *et al.* (2018) and Sharma (2012) [3,36]:

As kinetic parameters are not measurable directly, they need to be estimated using a kinetic model.[3] Initial rate experiments are performed measuring the reaction rate at low substrate

conversion, below 10 % of the equilibrium concentration.[3] This data is used to determine the kinetic parameters by model parameter adaption in MATLAB using a nonlinear regression method (nlinfit function, MATLAB 2019a) [76]. The kinetic parameters, i.e., K_M, v_{max}, K_I are fitted to process data and three different models which differ in the type of inhibition, i.e., competitive, non-competitive, and uncompetitive, are applied [75]. The kinetic model parameters are estimated using an iterative least squares estimation [3,36,75].

The root mean square deviation (RMSD [mmol $\cdot L^{-1}/U \cdot mg^{-1}$]) is determined in order to decide which kinetic model and which type of inhibition represents the experimental data best. The RMSD is calculated according to Equation 1-17 and describes the difference between the values predicted by the kinetic model $x_{s,I}$ [mmol $\cdot L^{-1}/U \cdot mg^{-1}$] and measured values $x_{m,I}$ [mmol $\cdot L^{-1}/U \cdot mg^{-1}$] divided by the number of data points n [-].

$$RMSD = \sqrt{\frac{\sum_{i=1}^{m} \left(x_{s,i} - x_{m,i}\right)^2}{n}} \qquad 1\text{-}17$$

The data of the kinetic constants and the corresponding confidence interval with respect to the inhibition types and the 95 % confidence interval indicating the variation of an estimated particular model parameter and the location of the true model parameter for a chosen confidence level are calculated. The mathematical script is given in 8.7.[77]

1.4. Cofactor Regeneration

A huge variety of cofactors such as nucleoside triphosphates (NTPs) can be found in almost every element of cellular life, the most common NTP being adenosine triphosphate [23,26,27,78–81]. Also in industry, the demand for biologically catalyzed reactions, which are often dependent on cofactors, is increasing [26,82]. However, the cost of stoichiometric amounts of cofactors and their potential to inhibit enzymes at high concentrations are challenging [26,27]. Therefore, there is an interest for stable cofactor regeneration systems to make enzymatically-catalyzed reactions industrially competitive [7,23,26–29,83,84]. Although different ways of cofactor regeneration have been studied, i.e., chemical, microbial, photochemical, and electrochemical, an enzymatic way to regenerate NTPs could be the most promising.[26,27] In addition to higher selectivity, the compatibility of the substrates, intermediates, and products of other reaction steps with the reaction system is a key factor [26,27,79].

One way to overcome the issue of enzyme inhibition by high cofactor concentration is to use polyphosphate kinases (PPKs) which use inexpensive and stable polyphosphate salts as phosphate donors to enzymatically regenerate NTPs [23,27,79,85,86].

Polyphosphate kinases can be classified into two groups, PPK1, which can synthesize polyphosphate reversibly, and PPK2 which catalyzes the phosphorylation of nucleotides using polyP as phosphate donor. PPK2-3 from *Ruegeria pomeroyi* further belongs to subfamily I, which accepts dinucleotides as substrate.[79,83,87,88] A detailed review from 2021 about the division

of PPKs into classes and subclasses is presented by Tavanti *et al.* [83]. PPKs are capable to regenerate adenosine 5'-triphosphate, uridine 5'-triphosphate or cytidine 5′-triphosphate from the corresponding diphosphorylated nucleotides [23,29,79,89,90].

The combination of polyphosphate as a cheap inorganic phosphate donor and the flexible, versatile enzymes is promising and has great potential for integration into a wide range of industrial processes [23,26,29,79,84,91]. To be successfully applied, the enzyme needs to be further characterized, including a detailed description of the kinetics of PPKs [23,79]. Optimization in terms of activity and stability is needed to develop a suitable cofactor regeneration system that could be transferred to large-scale production applications [7].

2. Aim of the Thesis

The aim of this thesis is to evaluate the application of high hydrostatic pressure on enzymatically catalyzed reactions as a new parameter in reaction optimization in order to make biocatalysis more competitive with chemically catalyzed reactions. The application of HHP will be investigated both individually and in combination with other process intensification methods such as enzyme immobilization, continuous process operation, and the use of organic solvents. [1–3] All of these methods have a significant impact on the efficiency of the catalyzed process. Therefore, their influence on the overall process must be studied in detail. [7–10,14].

The immobilization of enzymes is one major step to enable the application of a biologically catalyzed reaction in a continuously operated reactor. A detailed study of the immobilizates will be conducted to determine their suitability for the application in the continuous high pressure reactor as well as the adsorption of substrate and product on the immobilization material and the resulting activity of the enzymes after immobilization. In addition, the mechanical characterization under HHP will be carried out.

A continuous HHP reactor will be conceptualized to provide a stable biocatalytic reaction system and an effective method to analyze the influence of hydrostatic pressure on enzymes. In addition, this continuous HHP reactor enables the fast analysis of immobilized enzymes kinetics as a function of various flow rates and substrate concentrations. The HHP set-up will be characterized in terms of mass transfer limitation and mean residence time to ensure the set-up of non-limiting process conditions and the achievement of an optimal reactor operation. Three enzymes of industrial importance, two lipases (EC 3) and one polyphosphate kinase (EC 2), are selected to investigate the influence of the application of HHP up to 1,200 bar on different classes of enzymes.

In addition to the industrial application of lipases, cofactor regeneration is another important field of biocatalysis to make enzymatically catalyzed reactions more industrially competitive. The dependence of certain industrially relevant enzymes on cofactors is one of the major drawbacks for the application of enzymes in the industry. Since there is an increasing need for stable cofactor regeneration systems and the stoichiometric use of cofactors is not economically and potentially leads to inhibition phenomena, a cofactor regeneration reaction will be investigated under HHP.[23,26,83] The results obtained will then be used to systematically investigate enzyme and enzyme class-specific characteristics, such as changes in thermostability, activity, and enantioselectivity as a result of HHP application.[2] Furthermore, understanding the pressure-induced changes in kinetic parameters is crucial for further and comprehensive process intensification of biotechnological processes.

3. Materials & Methods

In the following section, all materials used, and their manufacturers are listed. In addition, all methods used to investigate the effects of HHP on enzymes together with all primary experimental methods are listed here. Some experiments are carried out at the Institute of Technical Biocatalysis (TU Hamburg) as well as at GALAB Laboratories GmbH (GALAB). The experiments to investigate the PPK are carried out at the project's cooperation partner GALAB, while the experiments to investigate the CRL and the CalB are carried out at TU Hamburg.

3.1. Chemicals

Cytidine-5'-monophosphate disodium salt (CMP), cytidine-5'-diphosphate disodium salt and cytidine-5'-triphosphate triphosphate disodium salt were bought from Biosynth Carbosynth (Compton, United Kingdom).

All other chemicals were purchased form Carl Roth (Karlsruhe, Germany), Merck KGaA (Darmstadt, Germany) or Sigma-Aldrich Chemie GmbH (Munich, Germany) and are analytical grade or higher, if not mentioned differently. 1-Phenyl-2-propanyl acetate was purchased from abcr GmbH (Karlsruhe, Germany). *Candida rugosa* lipase and *Candida antarctica* lipase B were provided by c-LEcta GmbH (Leipzig, Germany). Both were recombinant expressed in *Pichia pastoris*. CRL is lyophilized whereas CalB is in solution.

3.2. Devices

The devices used are summarized with details of their manufacturer. The devices used at the TU Hamburg are given in Table 1 and the devices used at GALAB are given in Table 2.

Table 1: List of devices used with their corresponding manufacturer used at TU Hamburg.

Device	Name/Description	Manufacturer
Pipettes	Research®, Reference® 10, 100, 1000, 5000 µL	Eppendorf Research®, Eppendorf SE, Germany
Gas chromatograph	7890B	Agilent Technologies, Santa Clara, USA
Gas chromatograph column	CP-ChiraSil-DEX CB 25 m x 0.25mm x 0.25µm	Agilent Technologies, Santa Clara, USA
Magnetic stirrer	IKA Plate RCT Digital	IKA-Werke, Staufen im Breisgau, Germany
Laboratory balance	MC1 Laboratory LC 2200 P	Sartorius AG, Göttingen, Germany
Plate reader	Infinite® M200 pro	TECAN, Männedorf, Switzerland
Microplate	96 well plate	Greiner Bio-One GmbH, Frickenhausen, Germany
Vortex mixer	Vortex-Genie 2	Scientific Industries Inc., New York, USA
Enzyme carrier	ECR 1090, ECR 1030	Purolite, King of Prussia, USA
Fused silica tubing	TNFS800010 ID: 25 µm	VICI Jour, Schenkon, Switzerland
Back-pressure regulator	JR-BPR3	VICI Jour, Schenkon, Switzerland
Stainless steel capillaries	SUS COIL PIPE; 0.1 mm x 4 m	Shimadzu Corporation, Kyōto, Japan
UHPLC column	30 x 3 mm, 50 x 3 mm, empty	ISERA GmbH, Düren, Germany
UHPLC oven	CTO-40C	Shimadzu Corporation, Kyōto, Japan
UHPLC pump	LC-40D X3	Shimadzu Corporation, Kyōto, Japan
tube roller	-	Ortho Diagnostic Systems, West-Germany
overhead shaker	-	Ismatec S. A., Zürich
shaking plate	Certomat R	B. Braun Melsungen AG, West-Germany
Desiccator	8211	Glaswerk Wertheim, Germany
Cellulose round filter	12 – 15 µm	Carl Roth GmbH, Karlsruhe, Germany
Molecular sieve	4A	
Scanning electron microscope	Leo Gemini 1530	Zeiss, Oberkochen, Germany

Table 2: List of devices used with their corresponding manufacturer used at GALAB.

Device	Name/Description	Manufacturer
Pipettes	Research®, Reference® 10, 100, 1000, 5000 µL	Eppendorf Research®, Eppendorf SE, Germany
Water bath	5B	JULABO GmbH, Seelbach, Germany
UHPLC pump	ACQUITY – Binary Solvent Manager	Waters Corporation, Milford, USA
UHPLC column	30 x 3 mm empty	ISERA GmbH, Düren, Germany
UHPLC oven	ACQUITY- column Manager	Waters Corporation, Milford, USA
HPLC	HPLC 1100 with VWD detector	Agilent, Santa Clara, USA
HPLC column	Exsil 300 C18 column	Exmere Ltd, Carnforth, UK
UHPLC column	30 x 3 mm, 50 x 3 mm, empty	ISERA GmbH, Düren, Germany
Vortex mixer	Vortex-Genie 2	Scientific Industries Inc., New York, USA
Enzyme carrier	ECR8209M	Purolite, King of Prussia, USA
Centrifuge	MiniStar silverline	VWR, Radnor, USA
Back-pressure regulator	JR-BPR3	VICI Jour, Schenkon, Switzerland
Stainless steel capillaries	SUS COIL PIPE; 0.1 mm*4 m	Shimadzu Corporation, Kyōto, Japan
Membrane pump	Membrane pump ME 2C NT	Vacuubrand GmbH & Co. KG, Wertheim, Germany
Bottle topper filter	Nalgene™	Thermo Fisher Scientific, Wirral, Germany
Membrane filters	membrane filters 3 µm	Sartorius AG, Göttingen, Germany
Ultracentrifuge units	Vivaspin™10 kDa Cut-off	Sartorius AG, Göttingen, Germany
Sample mixer	MXIC1 sample mixer	Dynal Biotech Ltd, Bromborough, UK

3.3. Buffers

In this thesis, different buffers based on deionized water (DI water) are used. Furthermore, all aqueous solutions are prepared using DI water.

Immobilization Buffer for Lipases

100.0 mmol $\cdot$ L^{-1} sodium phosphate (Na_3PO_4) buffer at pH 7 is used for immobilization of CRL and CalB. The buffer is prepared according to Table 3. The pH is adjusted using sodium hydroxide (NaOH) or hydrochloric acid (HCl) if needed.

Table 3: Immobilization buffer for Lipases.

Component	Amount
$Na_2HPO_4 \cdot 7H_2O$	4.04 g
$NaH_2PO_4 \cdot H_2O$	0.68 g
H_2O	ad 200 mL

Immobilization Buffer for Polyphosphate Kinase

For immobilization of PPK a 20.0 $mmol \cdot L^{-1}$ Na_3PO_4 buffer at pH 7.4 is used. The buffer is prepared according to Table 4. The pH is adjusted using NaOH or HCl if needed.

Table 4: Immobilization buffer for PPK.

Component	Amount
$Na_2HPO_4 \cdot 7H_2O$	0.14 g
$NaH_2PO_4 \cdot H_2O$	0.80 g
H_2O	ad 200 mL

Buffer for Free Polyphosphate Kinase

For free PPK a 50.0 $mmol \cdot L^{-1}$ Na_3PO_4 buffer at pH 7.4 is used. The buffer is prepared according to Table 5. The pH is adjusted using NaOH or HCl if needed.

Table 5: Buffer for free PPK.

Component	Amount
$Na_2HPO_4 \cdot 7H_2O$	0.14 g
$NaH_2PO_4 \cdot H_2O$	0.80 g
Imidazole	150 $mmol \cdot L^{-1}$
NaCl	300 $mmol \cdot L^{-1}$
H_2O	ad 200 mL

Reaction System Buffer for Immobilized Polyphosphate Kinase

The reaction system buffer contains 50.0 mmol · L^{-1} Na_3PO_4 and 30.0 mmol · L^{-1} $MgCl_2$. The pH is set to 7.4 using 5 M NaOH. Depending on the performed experiment, the solution contains CDP or polyP in varying concentration. The buffer is prepared according to Table 6.

Table 6: Reaction system buffer for immobilized PPK.

Component	Concentration [mmol · L^{-1}]
Na_3PO_4	50.0
$MgCl_2$	30.0
CDP	0.0-85.0
polyP	0.0-800.0

High Pressure Liquid Chromatography Buffer

The mobile phase for the High Pressure Liquid Chromatography (HPLC) contains 80 % 20.0 mmol · L^{-1} tetrabutylammonium bromide in 20.0 mmol · L^{-1} potassium phosphate buffer at pH 7 and 20 % acetonitrile. The pH is adjusted using NaOH or HCl if needed. The buffer is prepared according to Table 7.

Table 7: HPLC buffer for the phosphorylation catalyzed by PPK.

Component	Concentration [mmol · L^{-1}]
Aqueous solution (80 %)	
Tetrabutylammonium bromide	20.0
Potassium phosphate buffer	20.0
Acetonitrile (20 %)	

3.4. Analytics

The following section discusses the analytical methods which are used and their implementation.

3.4.1. Gas Chromatography

All substrates and products from the transesterification reaction are analyzed using gas chromatography (GC) with flame ionization detector. To separate the enantiomers of substrate and product, a chiral column with an inner diameter of 0.25 mm and a length of 25 m is required, specifications given in Table 1. To be able to analyze a large concentration range as precisely as possible, two different concentration ranges are calibrated, one from 0.1 to 5.0 mmol · L^{-1} and the other one from 1.0 to 200.0 mmol · L^{-1}. The inlet temperature is set to 250 °C and 1 µL respectively 0.5 µL of sample are injected. For the lower concentration range the split is set to 1:60 while it is 1:400 for the calibration range from 1 to 200.0 mmol · L^{-1}. The following conditions are the same for both calibration ranges. Hydrogen with a flowrate of 2 mL · min^{-1} is used as carrier gas. The oven temperature is set to 105 °C for 15 min. Typical resulting retention times are $t_{S\text{-PPA}} = 11.6$ min, $t_{S\text{-PP}} = 12.6$ min, $t_{R\text{-PP}} = 13.1$ min and $t_{R\text{-PPA}} = 13.7$ min. The resulting chromatograms and the calibration are shown in the Appendix 8.1.

3.4.2. High Pressure Liquid Chromatography

Samples from the phosphorylation of CDP are analyzed by HPLC using a C18 column, specifications given in Table 2. To prevent precipitation of salts in the HPLC column, samples are prepared prior to analysis. For this, 100 µL sample are mixed for 5 seconds with 50 µL isopropanol using a vortex mixer. The samples are then centrifuged for 1 minute. 25 L of the supernatant are diluted with 975 L water and then transferred to HPLC-vials. The mobile phase containing 80 vol.-% 20.0 mmol · L^{-1} tetrabutylammonium bromide in 20.0 mmol · L^{-1} potassium phosphate buffer at pH 7 and 20 vol.-% acetonitrile is heated to 40 °C. The flow rate is set to 0.8 mL · min^{-1} and the detector wavelength to 272 nm. Typical resulting retention times are $t_{CMP} = 3.4$ min, $t_{CDP} = 4.7$ min and $t_{CTP} = 5.6$ min. The resulting chromatograms and the calibration are shown in the Appendix 8.2.

3.4.3. Bradford Assay

To determine enzyme concentration of various solutions, the enzyme loading of the immobilizate, and to track the immobilization process, the free enzyme concentration is measured using the Bradford assay, which is performed according to T. Zor and Z. Selinger (1996) [92]. 200 µL of Bradford solution are mixed with 50 µL of sample and are incubated for 5 min at 25 °C in the plate reader and are shaken at 432 rpm. The standard protein bovine serum albumin (BSA) is used for calibration. The specifications are given in Table 1. A calibration is generated using eight different BSA concentrations from 0 to 200 µL · mL^{-1}. The adsorption at a wavelength of 595 nm and 405 nm is measured and the ratio of the two values

is plotted against the concentration, as is shown in Figure 4. The concentration of experimental samples is calculated using the linearized calibration values. Samples are diluted 1:10 and 1:20 with DI water prior to measurement to obtain absorbance in the calibrated range.

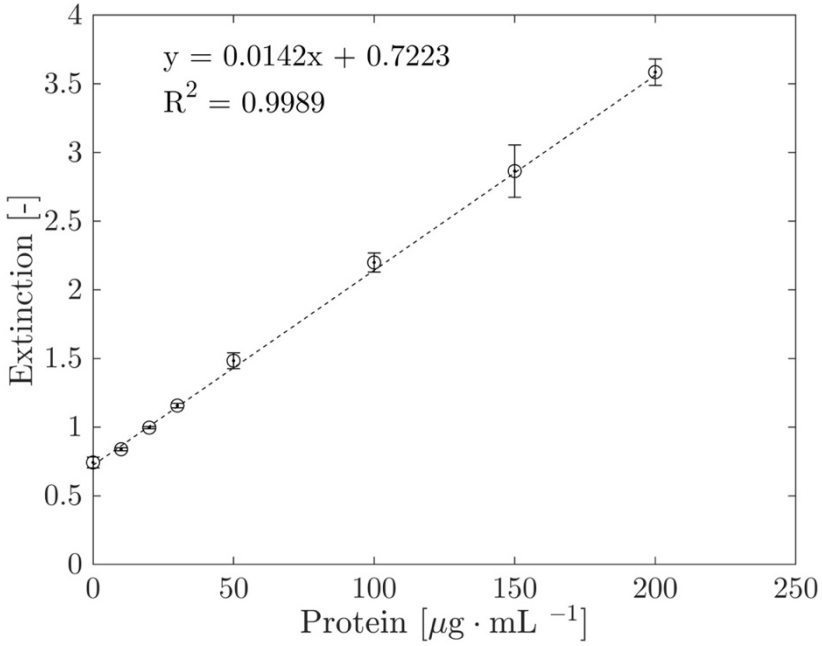

Figure 4: Calibration of the protein concentration of BSA determined according to T. Zor and Z. Selinger (1996)[92].

3.4.4. *para*-Nitrophenol Assay

The standard activity assay for hydrolases with *para*-nitrophenol acetate (*p*NPA) as substrate is applied in this thesis [93]. The hydrolytically cleaved product *para*-nitrophenol (*p*NP) exhibits optical activity at a wavelength of 405 nm. In order to use the activity test for the measurement of free lipase and immobilized lipase, the extinction coefficient (ε $[\mathrm{L \cdot \mu mol^{-1} \cdot cm^{-1}}]$) is determined first. It is calculated using the Lambert-Beer law according to Equation 3-1. This law states that the absorbance (Ex [-]) and the concentration of the optically active molecule *p*NP are proportional to each other. Therefore, the concentration of the product (c [$\mathrm{mmol \cdot mL^{-1}}$]) can be determined by measuring the absorbance using the width of the cuvette (w [cm]).[93]

$$Ex = \varepsilon \cdot w \cdot c \qquad 3\text{-}1$$

To determine ε, a dilution series is prepared first. For this purpose, a 2.0 $\mathrm{mmol \cdot L^{-1}}$ stock solution of *p*NP is diluted with deionized water in micro reaction vessel covering a concentration range from 10 to 1000 $\mathrm{\mu mol \cdot L^{-1}}$, as is shown in Figure 5.

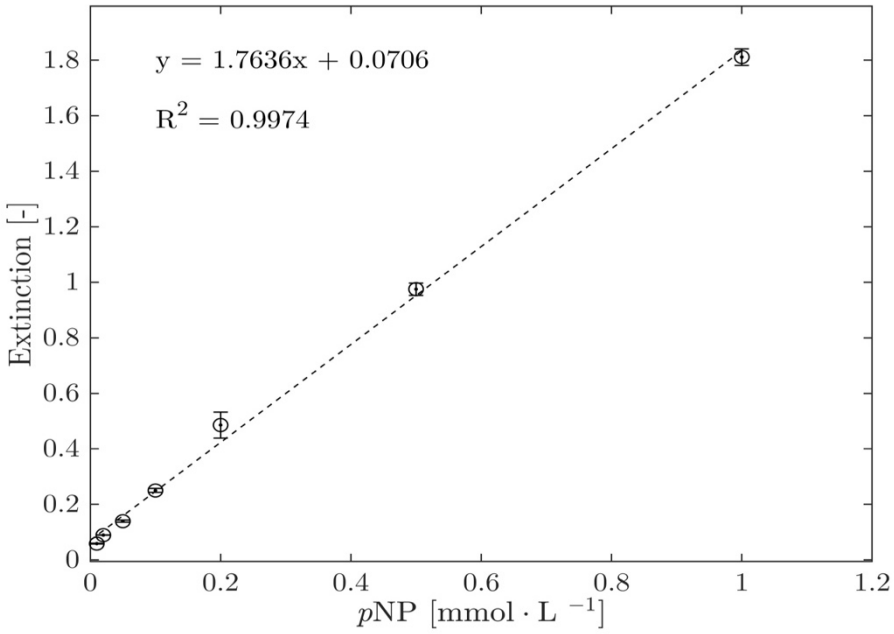

Figure 5: Determination of the extinction coefficient of *p*NP.

According to Equation. 3-1, the extinction coefficient ε is determined to be 3.04 L · µmol^{-1} · cm^{-1}. A 10.0 mmol · L^{-1} *p*NPA solution is prepared for the activity assay. For this purpose, 0.018 g *p*NPA are dissolved in 10.0 mL dimethyl sulfoxide (DMSO). The activity assay is performed differently depending on the state of the lipase (free or immobilized). Due to an error in plate reader method, all measurements are performed at a wavelength of 435 nm instead of 405 nm as planned. However, since all samples are subsequently measured at this wavelength, there is no systematical error within the measurement series.

Free Lipase Activity Assay

Using the *para*-nitrophenol assay described previously, the activity of free lipase is determined. For this purpose, Na_3PO_4 buffer at pH 6.7 is diluted 1:100 and 900 µL of the solution are added to micro reaction tubes. This is followed by the addition of 100 µL of 10 mol · L^{-1} *p*NPA in DMSO. Subsequently, 10 µL of free lipase, which was previously diluted 1:10 with DI water, are pipetted into the micro reaction vials. The tubes are sealed and shaken briefly by hand. To determine the activity, triplets of 100 µL each are taken and are transferred to a microplate. The change in absorbance is measured for one minute using the microplate reader at a wavelength of 435 nm. The activity is calculated from the absorbance data obtained using the previously determined extinction coefficient.

Immobilized Lipase Activity Assay

For the activity assay of immobilized lipase, 0.01 g of dried immobilized lipase is weighed into GC vials. 1900 µL of 1:100 diluted Na_3PO4 buffer at pH 6.7 and 100 µL of 10.0 mol · L^{-1} *p*NPA acetate are added to the immobilizate and vortexed for 10 seconds. Samples are taken at 0, 1, 2, 3, 4, and 5 min and the absorbance is measured using the plate reader at a wavelength of

435 nm. These measurements are performed in triplicates. The activity is calculated from the absorbance data obtained using the previously determined extinction coefficient.

3.5. Evaluation of Errors

Errors that occur during experiments can be divided into two groups: statistic and systematic errors. Systematic errors are based on uncertainties in the experimental values due to uncertainties in the calibration of the instrument used to measure the values. These uncertainties are quantified by performing an additional calibration in an independent experiment. For example, a chemical standard with known concentration is measured in the GC used. [94] This has not been carried out in this thesis.

The statistical error results from the limited accuracy of a measurement. It can be derived from the measurement equipment, the measured quantities, and the operator. The standard deviation of a series of independent measurements can be used to evaluate and reduce the estimated statistical error. Although a reduction of the statistical error is important, the systematic error is not affected. [94,95]

To reduce the statistical errors in this thesis, repetitive measurements of values, e.g., substrate and product concentrations, as well as the evaluation of the measurement methods were applied. Measurement errors can accumulate if several values are measured and used to calculate subsequent values with them. A common method to assess and acknowledge the single error of an individual experimental value is to calculate the propagation of uncertainty. In general, the propagation of uncertainty can be formulated as Equation 3-2, where y is the function to calculated value, u_y is the uncertainty of the calculated function, $u_{1,2,\dots}$ denotes the standard deviation of the different values to calculate the function y. [94–96]

$$u_y = \sqrt{\left(\frac{\partial y}{\partial x_1} \cdot u_1\right)^2 + \left(\frac{\partial y}{\partial x_2} \cdot u_2\right)^2 + \dots} \qquad 3\text{-}2$$

Furthermore, the analytical methods were validated by determining the uncertainty of the measurements. In addition, to calibrate the analytical instrument, a sample was measured multiple times, and the standard deviation was calculated. Figure 6 gives the values of the individual measurements for the GC analytics, as well as the mean value with standard deviation.

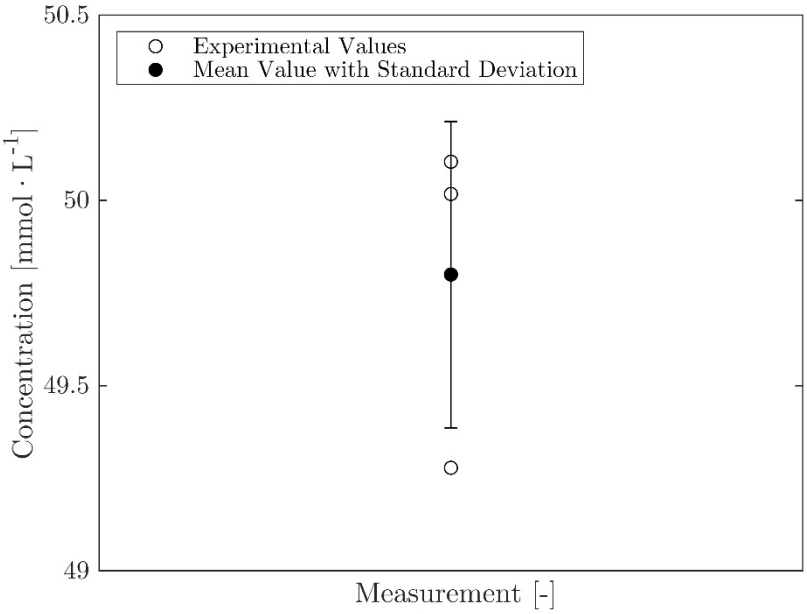

Figure 6: Determination of the uncertainty of the GC analysis.

The standard deviation of the measurement is determined to be 0.4 mmol ·L^{-1} for the GC analysis, resulting in a relative error of 0.8 %. Reasons for the deviations between the individual measurements from each other are variations in the inserted amount of sample, changes in the carrier gas, as well as possible fluctuations in the temperature profile of the analytical device.[97] The other analytical methods were also evaluated in analogously procedures, which is given in Table 8.

Table 8: Determination of the uncertainty of the analytical devices.

Device	Measurement range	Value for error calculation	Determined error absolute	Determined error relative
GC	0.01-5.0 mmol ·L^{-1}	0.03 mmol ·L^{-1}	0.002 mmol ·L^{-1}	5.0 %
GC	1.0-200.0 mmol ·L^{-1}	50.0 mmol ·L^{-1}	0.4 mmol ·L^{-1}	0.8 %
HPLC	0.01-2 mmol ·L^{-1}	1 mmol ·L^{-1}	0.01 mmol ·L^{-1}	0.5 %
Plate reader	0.0-200 µg ·mL^{-1}	10 µg ·mL^{-1}	0.3 µg ·mL^{-1}	2.7 %
Balance	0.001-220 g	-	0.1 mg	max. 2 %

Deviations between different samples of the same preparation could be explained by measurement or handling errors. To overcome this phenomenon and to reduce the statistical errors, multiple samples were analyzed, and the standard deviation was calculated analogous to the example of GC analytics.

3.6. Characterization of Enzyme Immobilizates

The enzymes are immobilized for use in the continuous HHP reactor. The lipases are immobilized adsorptively, whereas the PPK is immobilized covalently. The absorption behavior of the substrate and product on the carriers, as well as the swelling behavior in the organic solvent, are investigated. Furthermore, the mechanical stability and the surface properties of the particles are examined.

3.6.1. Adsorption Experiments

Adsorption experiments are performed to ensure that neither the substrate nor the product is adsorbed onto the immobilization supports. Two different carriers from Purolite namely ECR 1090 (macroporous styrene) and ECR 1030 (divinylbenzene/methacrylate) are tested. The particle size of both resins is specified between 300-710 µm, while the pore diameter differs from 900-1100 Å for ECR 1090 to 200-300 Å for ECR 1030. The carriers are indicated as mechanically stable and suitable for use in organic solvents by the manufacturer.

An amount of 0.05 g carrier is weighed into a 1.5 mL screw neck vial and 1 mL of a 1, 10 or 100.0 mmol $\cdot$ L^{-1} solution containing either PP or PPA is added. All different variations are conducted in duplicates for 100.0 mmol $\cdot$ L^{-1} and in quintuplicate for 1.0 mmol $\cdot$ L^{-1} and 10.0 mmol $\cdot$ L^{-1}. For negative control three additional vails are filled with the same solutions but without carrier. The vails are incubated for 7 days on a heating shaker with 1000 rpm at 35 °C. After incubation, 100 µL of sample are analyzed using GC method described in 3.4.1.

3.6.2. Immobilization Procedure

The immobilization procedure for the three different enzymes used is described in the following paragraph. While the immobilization procedure was previously optimized, the immobilization process for the CRL and CalB is investigated in the scope of this thesis.

The immobilization is performed using different devices: tube roller (TR), overhead shaker (OS), shaking plate (SP) which are displayed in Figure 7.

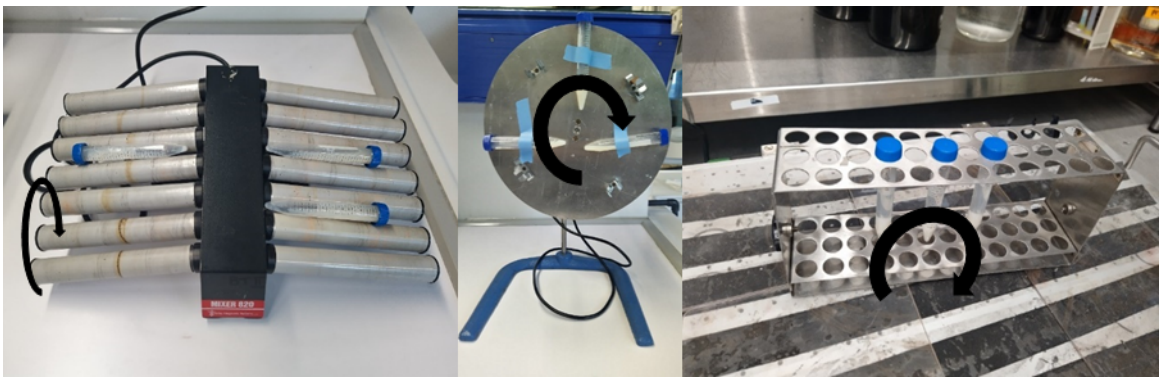

Figure 7: Immobilization set-ups: tube roller, overhead shaker, shaking plate (left to right).

The sample tubes are placed between the rollers of the tube roller, which move the contents of the tubes evenly by rotating and tilting them at the same time. This creates a radial as well as an axial movement. In the overhead shaker immobilization set-up, the sample tubes are

attached to a circularly rotating plate. The contents of the tubes undergo a radial movement. The shaker plate generates an orbital movement and therefore an axial mixing of the sample tubes. The sample tubes are fixed in a holder. The plate is set to 100 rpm.

The immobilization of the two lipases CalB and CRL are performed according to the instructions of Purolite [98]. All modifications and additional information along with the procedure are given below.

3.6.2.1. Candida antarctica Lipase B

Investigation of Immobilization Performance

All experiments for immobilization performance screening are carried out with an immobilization buffer at pH 6.7. For immobilization 1.75 g of wet carrier which is equal to 0.5 g dry carrier are added into a 15 mL falcon tube together with 4 mL immobilization buffer. The falcon tube is carefully shaken. Afterwards, the washing buffer is discarded using a 5 mL pasteur pipette without removing the carrier particles. 1 mL enzyme solution and 3 mL buffer solution are added to the washed carriers and carefully shaken. The first sample is taken immediately. Subsequently, the sample tubes are fixed in the respective experimental set-ups (tube roller, overhead shaker, shaking plate). The temperature of the investigation was 4, 20 and 40 °C. Samples are taken at 0, 0.5, 1, 2, 4, and 6 respectively 24 hours. 50 µL of the sample are taken into the micro reaction vessel and diluted with 450 µL of DI water. The enzyme concentration of the supernatant is determined using the Bradford assay as described in 3.4.3. The immobilization was terminated after 24 h and immobilizates are dried for further use. For this purpose, the immobilizates are first filtered to separate the remaining enzyme solution. Subsequent rinsing with 4 mL of buffer solution removed any residual free enzyme. The wet immobilizates collected on the filter are then dried in two steps. First, the filters are placed upside down on weighing boats and are stored in the refrigerator at 7 °C for 3 to 4 days. After the filter paper had dried completely and the immobilized particles had been detached from it, the immobilizates are placed in a desiccator containing silica at 50 mbar to adsorb the remaining moisture at 4 °C. After 2-3 days, the immobilizates are removed and the dried immobilizates are stored in micro reaction vessels at 7 °C.

Immobilization for High Hydrostatic Pressure Experiments

All immobilizates used to investigate the influence of HHP on enzyme performance are prepared using immobilization buffer at pH 7. Therefore 8.77 g of wet carrier are added into a 50 mL falcon tube with 10 mL immobilization buffer. The falcon tube is carefully shaken. Afterwards the supernatant washing buffer is removed using a 5 mL pasteur pipette. 5 mL of buffer and 5 mL of CalB solution are added to the enzyme carriers placed on the TR at 25 °C for 3 h. Samples are taken at 0, 0.5, 1, 2, and 3 h. 25 µL of the sample are transferred into the micro reaction vessel and diluted with 975 µL of DI water. The enzyme concentration of the

supernatant is determined using the Bradford assay as described in 3.4.3. The immobilization was terminated after 3 h and immobilizates are dried for further use. The detailed method for washing and subsequent drying of the immobilizates of CalB is described in the previously paragraph. Table 32 in the Appendix 8.4 gives the number of the immobilization procedure in accelerating number and the method used for immobilization with the resulting enzyme loading and the immobilization yield.

3.6.2.2. Candida rugosa Lipase

Investigation of Immobilization Performance

All experiments for immobilization performance screening are carried out with an immobilization buffer at pH 6.7. Therefore 0.5 g of wet carrier are added into a 15 mL falcon tube and 2 mL of 200.0 mmol $\cdot$ L^{-1} Na_3PO_4 immobilization buffer is added. The falcon tube is carefully shaken. Afterwards the washing buffer is removed using a 5 mL Pasteur pipette, without removing any carrier particles. 0.01 g CRL and 2 mL of 200.0 mmol $\cdot$ L^{-1} Na_3PO_4 immobilization buffer are added to the enzyme carriers placed on the tube roller, overhead shaker or shaking plate at 4 and 20 °C for 24 h. A sample of the enzyme solution is taken immediately to determine the initial CRL concentration. Samples are taken at 1 h, 2 h, 4 h, 6 h, and 24 h. 50 µL of the sample are taken into the micro reaction vessel and diluted with 950 µL of DI water. The enzyme concentration of the supernatant is determined using the Bradford assay according to 3.4.3 Bradford Assay. The immobilization was terminated after 24 h and immobilizates are dried for further use as previously described for CalB.

Immobilization for High Hydrostatic Pressure Experiments

All immobilizates used to investigate the influence of HHP on enzyme performance are prepared using immobilization buffer at pH 7. Therefore 8.77 g of wet carrier are added into a 50 mL falcon tube and 10 mL immobilization buffer are added. The falcon tube is carefully shaken. Afterwards the washing buffer is removed using a 5 mL Pasteur pipette, without removing any carrier particles. 0.1 g CRL and 10 mL of immobilization buffer are added to the enzyme carriers and placed on the tube roller at room temperature 25 °C for 3 h. Samples are taken at 0, 0.5, 1, 2, and 3 h. 25 µL of the sample are taken into the micro reaction vessel and diluted with 975 µL of DI water. The enzyme concentration of the supernatant is determined using the Bradford assay according to 3.4.3 Bradford Assay. The immobilization was terminated after 3 h and immobilizates are dried for further use as previously described for CalB. Table 31 in the Appendix 8.3 gives the number of the immobilization procedure in accelerating number and the method used for immobilization with the resulting enzyme loading and the immobilization yield.

3.6.2.3. Polyphosphate Kinase from *Ruegeria pomeroyi*

The production and the immobilization of PPK is done within the framework of the cooperation with GALAB Laboratories GmbH (Hamburg) in the project „UfIB: Bioprozesse unter Druck in neuen Anwendungsfeldern – BioproDruck“.

Polyphosphate kinase from *Ruegeria pomeroyi* is recombinantly expressed in *Escherichia coli* BL21(DE3)_pET22b_rpppk2-3, which has already been described by Gottschalk *et al.* (2021) [29].

PPK is provided immobilized on Purolite carriers ECR8209M. A maximum enzyme load of 86.4 $mg_{PPK} \cdot g_{carrier}^{-1}$ is achieved. All specific activity data is given in relation to the mass of enzyme ($U \cdot mg_{PPK}^{-1}$). The immobilization method for this enzyme has already been described by Reich *et al.* (2022) [99].

3.6.3. Influence of Water Content of the Solvent on the Enzyme Activity

Specific activity of CalB and CRL depending on the water content of the solvent is measured. Therefore 0.1 g of immobilized CRL (immobilization batch TR 6) and CalB (immobilization batch TR 7) is weighed into 1.5 mL HPLC vails. A 10.0 $mmol \cdot L^{-1}$ PP and 2712.5 $mmol \cdot L^{-1}$ vinyl acetate in heptane solution is dehydrated using a molecular sieve. 1 mL substrate solution containing 0,1,2,4,8, 9, and 10 µL DI water is added to the lipase and is incubated for 1 h at 35 °C on the thermo shaker at 500 rpm. The experiments are performed in triplicates.

The specific activity of the CRL and CalB in the STR in batch mode is calculated according to Equation 3-3 where Δc [$mmol \cdot mL^{-1}$] is the converted substrate PP; t [min] is the time, and m_{CRL} [mg] the mass of immobilized enzyme.

$$\text{specific activity} = \frac{\frac{\Delta c}{t}}{m_{CRL}} \qquad 3\text{-}3$$

3.6.4. Investigation of the Storage Stability of Lipase Immobilizates

The storage stability of CRL and CalB is investigated to ensure the usage of the immobilizate over a longer time. After drying, the immobilizates are stored at 7 °C in the refrigerator. 0.1 g of immobilized CRL and CalB is weighed into 1.5 mL HPLC vails. 1 mL substrate solution containing 10.0 $mmol \cdot L^{-1}$ PP and 2712.5 $mmol \cdot L^{-1}$ vinyl acetate in heptane solution is added. The lipases are incubated for 1 h at 35 °C on the thermo shaker at 500 rpm. The experiments are performed after 1, 6, 19, 36, 78, and 100 days of storage for TR 21 (CRL) and TR 22 (CalB) as well as day 19, 36, 78, 100 for TR 19 (CalB). The experiments are performed in triplicates and activity is calculated according to Equation 3-3.

The storage stability values at day 78 and 100 are measured with the other GC and the corresponding calibration.

3.6.5. Investigation of Mechanical Stability of Carriers

Mechanical stability is another important characteristic of the enzyme carrier. Scanning electron microscopy (SEM) images are taken from the particles to investigate change of the particles and the particle surface after different treatments, e.g., immobilization, usage in the continuously operated high pressure reactor, etc. The differently treated particles are given in Table 9.

Table 9: Differently treated particles for carrier stability experiments.

Particles number	Treatment	Enzyme
1	Untreated ECR 1090	-
2	Immobilized	CRL
3	Immobilized	CalB
4	1 h thermo shaker experiment, 1000 rmp	CRL
5	Usage in the continuously operated high pressure reactor, 3 h, ambient pressure	CRL
6	Usage in the continuously operated high pressure reactor, 3 h, 800 bar	CRL
7	Usage in the continuously operated high pressure reactor, 3 h, ambient pressure	CalB
8	Usage in the continuously operated high pressure reactor, 3 h, 800 bar	CalB

SEM images are taken with the Leo Gemini 1530 with an acceleration voltage of 2 kV and a magnification of 52-times, the specifications are given in Table 1. The particles are first coated with 50 nm gold in argon atmosphere.

3.6.6. Investigation of Enzyme Leaching from the Carriers

To determine enzyme leaching from the carrier, 200 mL of 10.0 mmol $\cdot$ L^{-1} PP and 434.0 mmol $\cdot$ L^{-1} vinyl acetate solution is pumped through a 3 x 30 mm column filled with 0.1 g immobilizate (TR 21) at 35 °C with a flow rate of 1 mL $\cdot$ min^{-1}. The solution is collected in a 250 mL bottle. Samples are taken at 0, 3, 5, 16, and 73 days. The conversion of the substrate is determined via GC.

3.7. Investigations in Stirred Tank Reactor in Batch Operation Mode

Prior to the investigation of the CRL and the PPK in the continuous high hydrostatic pressure system, experiments will be conducted in a batch STR to provide a better classification of the reactor performance. The thermodynamically maximum possible turnover, i.e., state of equilibrium, is determined to set the limits for the kinetic studies.

The kinetic parameters of CRL are investigated in the STR for comparison with the kinetic parameters that are determined in the PBR.

3.7.1. Stirred Tank Reactor Experiments with *Candida rugosa* Lipase

Experiments in STR in batch mode for kinetic investigations and long-time experiments are carried out in a 25 mL tempered glass reactor with three ports, which is schematically shown in Figure 8.

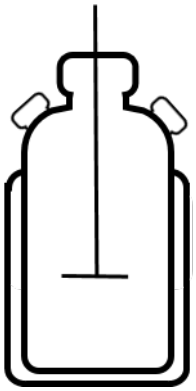

Figure 8: Scheme of the discontinuously operated stirred tank reactor.

The external heating is set to 35 °C. Two ports are sealed with rubber septa. An overhead magnetic stirrer with a magnetic stirring bar is installed. The 10 mL reaction solution is preheated to 35 °C as well. An amount of 0.1 g of the immobilized CRL is added to the vessel through a port using a funnel. Subsequently, the preheated reaction solution is added, and the port is sealed with a rubber septum afterwards. A sample of 250 µL is taken using a syringe through the septum. The reaction is started when the stirrer is set to 250 rpm. This procedure is used for all STR experiments carried out in the STR in batch operation mode.
The conversion X of PP is calculated according to Equation 3-4, where $n_{t=0}$ [mol] denotes the initial amount of substrate and n_t [mol] denotes the substrate amount at the sampling time t [min].

$$X = \frac{n_{t=0} - n_t}{n_{t=0}} \qquad 3\text{-}4$$

3.7.1.1. Thermodynamic Equilibrium of the Transesterification Reaction

To investigate the thermodynamic equilibrium, immobilized CRL of the batch TR 21 is used. The reaction solution contains 10.0 mmol · L^{-1} PP and 864.0 mmol · L^{-1} vinyl acetate in heptane. Samples are taken at 0, 2, 5, 10, 30, 60, and 180 min. The specific activity of CRL is calculated using Equation 3-3.

3.7.1.2. Investigation of Enzyme Kinetics

To investigate the kinetics of the CRL in the STR, substrate solutions with different PP and vinyl acetate concentrations are prepared. To investigate the influence of PP on specific activity

of CRL, the substrate solution contains 1356.3 mmol · L^{-1} vinyl acetate and 5.0 mmol · L^{-1} to 100.0 mmol · L^{-1} PP in heptane. In the second part of the investigation the influence of vinyl acetate on specific activity of CRL the substrate solution contains 60.0 mmol · L^{-1} PP and 108.0 mmol · L^{-1} to 5424.0 mmol · L^{-1} vinyl acetate in heptane. Samples are taken at 0, 5, 10, 15, 20, 25, and 30 min. Immobilized CRL of the batch TR 11 is used. The activity is calculated according to Equation 3-3.

3.7.1.3. Investigation of the Kinetic Parameters

Kinetic parameters are determined based on the Michaelis-Menten theory, as explained in 1.3.2 and additionally extensively described in literature by Jaeger *et al.* (2018) and Sharma (2012) [3,100].

The parameters of the kinetic model are determined by model parameter adaption with MATLAB using a nonlinear regression method and iterative least-squares estimation (*nlinfit* function, MATLAB 2019a) [76]. The parameters are fitted to the process data, in particular the estimated activity, and three different models which differ in the type of inhibition by the inhibiting substrate, i.e., competitive, uncompetitive, non-competitive [75]. The MATLAB script used is given in 8.7.

In order to make a decision about the validity of the description of the measured values by the model, the RMSD is used, as described in Equation 1-17

By immobilizing the enzyme, changes in activity, specificity or selectivity are possible. These changes result from direct changes in the enzyme structure as well as from changes induced by the immobilization (changes in diffusion in the carrier pores, etc.). Therefore, our studies do not determine the real kinetic parameters of the native enzyme, but the apparent ones modified by the effects of immobilization such as surface polarity or diffusion limitation. [35,101]

3.7.2. Investigations in Stirred Tank Reactor in Batch Operation Mode with *Ruegeria pomeroyi* Polyphosphate Kinase

Prior to the investigation of the PPK in the continuous high hydrostatic pressure system, experiments are carried out in the STR in batch mode.

To compare the application of PPK cofactor regeneration of CTP in different operation modes, the process is performed in a stirred tank reactor and in a continuously operated PBR. The thermodynamically maximum possible turnover, i.e., state of equilibrium, is determined to set the limits for the kinetic studies.

The substrate solution for STR contains 44.0 mmol · L^{-1} CDP, 30.0 mmol · L^{-1} $MgCl_2$, 44.0 mmol · L^{-1} polyP in a 50.0 mmol · L^{-1} Na_3PO_4 buffer at pH 7.4. These reaction conditions were previously determined to be optimal within the predetermined range in 4.6.3 Investigation of *Ruegeria pomeroyi* Polyphosphate Kinase Kinetic Parameters in the Packed Bed Reactor.

The STR experiments are performed in a 25 mL thermo vessel at 40 °C, which is schematically shown in Figure 8. The reaction volume of 10 mL is preheated to 40 °C and mixed with 0.16 g

of immobilizate using an overhead magnetic stirrer at 250 rpm. 200 µL samples are taken at 0, 1, 3, 5, 10, and 60 min as well as at 24 h and 72 h.

The specific activity of the PPK in the STR is calculated according to Equation 3-5 where Δc_{CTP} [µmol · L^{-1}] is the formed product CTP, t [min] is the time, and m_{PPK} [mg] the mass of immobilized enzyme. Since degradation of CDP to CMP was observed, the activity was calculated by product formation. Moreover, no side product formation was observed, thus the selectivity of the biotransformation is one, and the product concentration can be used to calculate the activity.

$$\text{specific activity} = \frac{\Delta c_{CTP}}{m_{PPK} \cdot t} \qquad 3\text{-}5$$

3.8. Continuous High Hydrostatic Pressure System

The investigation of the effect of HHP on enzyme behavior for different reaction systems is the core objective of this thesis. Therefore, a continuous high hydrostatic pressure system is conceptualized. The continuous high hydrostatic pressure system is first built at the TU Hamburg. As part of the thesis is carried out in close collaboration with GALAB Laboratories GmbH, a second system is built to investigate the effect of hydrostatic pressure on PPK. Both set-ups consist of different components from different suppliers, namely Shimadzu and Waters, and will be described in the following.

The need for a highly flexible system is met by designing the reactor with three main components: An Ultra High Pressure Liquid Chromatography (UHPLC) pump, a high pressure vessel, and a pressure generation unit. The UHPLC pump can provide a precise flow rate with a wide pressure range up to 1,200 bar. For the high pressure vessel, a stainless steel UHPLC column is used into which the immobilized enzymes are loaded. The pressure generation unit (PU) is composed of a back-pressure regulator and restriction capillaries.

3.8.1. Continuous High Hydrostatic Pressure System at TU Hamburg

The concept of the high hydrostatic pressure reactor is shown in Figure 9, all specifications are given in Table 1. The solutions are mixed in the low-pressure mixing chamber inside the binary piston UHPLC pump. The high pressure vessel (dimensions are application-dependent) is placed into an oven and heated to 35-65 °C. The PU, which is installed after the reactor, consists of a BPR, stainless steel capillaries (ID: 100 µm). and fused silica tubing (ID: 25 µm). The BPR provides a pressure from 1-300 bar relative to atmospheric pressure. To achieve higher pressures up to 1,200 bar, stainless steel capillaries with varying length from 1 to 8 m or fused silica tubing with varying length from 0.1 to 0.3 m have been installed beforehand. The resulting back pressure is regulated by the length of the capillaries. The longer a capillary is and the smaller its inner diameter, the greater the pressure generated. Samples are taken at the outlet of the BPR in a non-pressurized environment at ambient pressure. An additional

cooling coil is installed at the outlet if the experiment is performed at higher temperatures above 45 °C. It consists of a stainless steel coil that is placed in an ice bath.

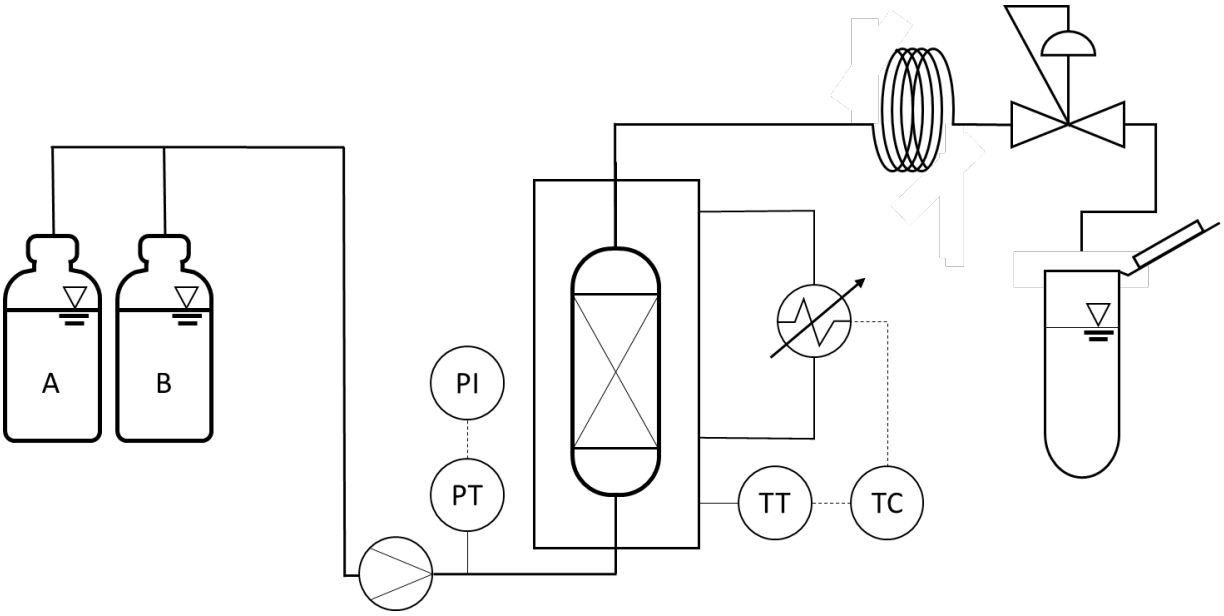

Figure 9: Scheme of the continuously operated high hydrostatic pressure set-up at TU Hamburg with temperature control (TC), temperature transmitter (TT), pressure transmitter (PT) and pressure indicator (PI) along with the pressure unit consisting of BPR, stainless steel capillaries and fused silica tubing.

The specific activity of the CRL and CalB in the PBR is calculated according to Equation 3-6 where Δc_{PP} [µmol L^{-1}] is the converted substrate PP, $\dot{V}$ [L min^{-1}] is the flow rate and $m_{CRL/CalB}$ [mg] the mass of immobilized enzyme (CRL or CalB).

$$specific\ activity = \frac{\Delta c_{PP} \cdot \dot{V}}{m_{CRL/CalB}} \qquad 3\text{-}6$$

3.8.2. Continuous High Hydrostatic Pressure System at GALAB

The highly flexible high hydrostatic pressure system at GALAB is designed out of three main components: a UHPLC pump, a high pressure vessel, and a pressure generation unit; all specifications are given in Table 2.

The concept of the high hydrostatic pressure reactor is shown in Figure 10. The bottles containing, e.g., the substrate solution, are preheated in a water bath to 40 °C. The solutions are mixed in the high pressure mixing chamber inside the binary piston of the UHPLC-pump, which provides a precise flow rate with a wide pressure range up to 800 bar. The high pressure reactor, a 30 x 3 mm empty UHPLC-column, into which the immobilized enzymes are filled, is placed into an oven and heated to 40 °C. The pressure building unit, which is installed behind the reactor, consists of a back-pressure regulator and stainless-steel capillaries. The back-pressure regulator provides a pressure from 1-300 bar relative to atmospheric pressure. To achieve higher pressures up to 800 bar, stainless steel capillaries (0.005 ’’) with varying

length from 1 to 8 m are installed according to the necessary pressure. The length of the capillaries is used to regulate the resulting back pressure. The longer a capillary is, the greater the pressure generated. Samples are taken at the outlet of the BPR in a non-pressurized environment at ambient pressure.

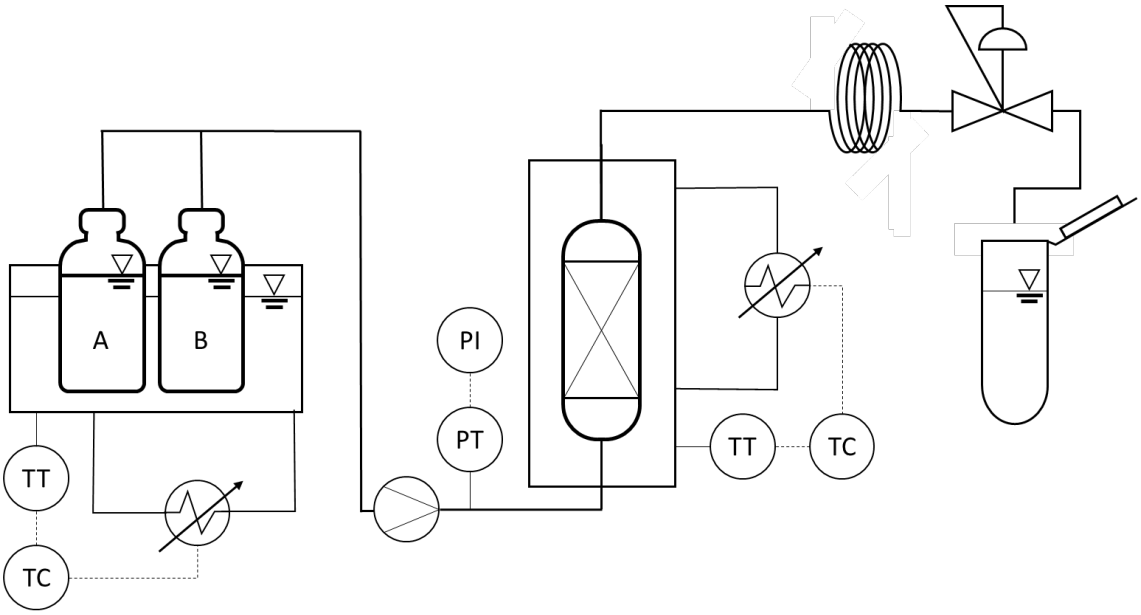

Figure 10: Scheme of the continuously operated high hydrostatic pressure set-up at GALAB with temperature control (TC), temperature transmitter (TT), pressure transmitter (PT) and pressure indicator (PI) along with the pressure unit consisting of BPR, stainless steel capillaries and fused silica tubing.

The specific activity of the PPK in the PBR is calculated according to Equation 3-7 where Δc_{CTP} [µmol · L^{-1}] is the formed product CTP; $\dot{V}$ [L min^{-1}] is the flow rate and m_{PPK} [mg] the mass of immobilized enzyme.

$$\text{specific activity} = \frac{\Delta c_{CTP} \cdot \dot{V}}{m_{PPK}} \qquad 3\text{-}7$$

3.8.3. Residence Time Experiments

Residence time experiments are performed to ensure that the reaction is in the steady-state conditions. The steady-state condition indicates that no change in concentration occurs over time. Different experiments are performed for the different continuous high hydrostatic pressure systems.

Continuous High Hydrostatic Pressure System at TU Hamburg

An empty 30 x 3 mm UHPLC column is used as high hydrostatic pressure reactor, where 0.063 g immobilizate are filled in. The reactor is flushed with 1 ml · min^{-1} solvent (2712.5 mmol · L^{-1} vinyl acetate in heptane solution) for 5 min. Subsequently the reactor is removed, and the pump is flushed with substrate solution containing 10.0 mmol · L^{-1} PP for 3 min. As tracer a substrate solution containing 10.0 mmol · L^{-1} PP is used. The reactor is reinstalled and a step signal (step change from pure solvent to a 10.0 mmol · L^{-1} substrate

solution) is applied to the reactor to determine the mean residence time ($\bar{t}$) depending on the flow rate. The time interval and duration of sampling depended on the flow rate and are shown in Table 10. For all flow rates 8 samples are collected with a volume of 250 µL each. The experiment is performed in duplicates.

Table 10: Residence time experiments continuously operated high hydrostatic pressure set-up at TU Hamburg.

Flow rate [ml · min^{-1}]	Sampling duration [s]	Sample interval [s]
0.25	480	60
0.5	240	30
1	120	15
1.5	80	10

The concentration of the substrate in the sample is determined by GC analysis. The *F*-curve of the initial concentration is calculated using Equation 3-8. The *F*-curve [-] describes the cumulative residence time distribution function, where c_0 [mmol · mL^{-1}] denotes the tracer concentration in the feed and *c(t)* [mmol · mL^{-1}] the concentration at sampling time *t* [min].

$$F = \frac{c(t)}{c_0} \qquad 3\text{-}8$$

The mean residence time $\bar{t}$ [min] can be obtained from the following Equation 3-9, where *t* [min] is the sampling time [102].

$$\bar{t} = \sum_i (1\text{-}F_i) \cdot \Delta t_i \qquad 3\text{-}9$$

Continuous High Hydrostatic Pressure System at GALAB

An empty 30 x 3 mm UHPLC column is used as high hydrostatic pressure reactor, where 0.174 g wet immobilizate are filled in. The reactor is flushed with 1 ml · min^{-1} reaction system buffer of PPK containing neither CDP nor polyP for 5 min. Subsequently the reactor is removed, and the pump is flushed with substrate solution containing 44.0 mmol · L^{-1} CDP for 2 min. As tracer a substrate solution containing 44.0 mmol · L^{-1} CDP is used. The reactor is reinstalled and a step signal (step change from pure solvent to a 10.0 mmol · L^{-1}substrate solution) is applied to the reactor to determine the mean residence time depending on the flow rate. The time interval and duration of sampling depended on the flow rate and are given in Table 10. For all flow rates 6 to 8 samples are collected with a volume of 250 µL each. The experiment is performed six times for each flow rate.

Table 11: Residence time experiments continuously operated high hydrostatic pressure set-up at GALAB.

Flow rate [ml · min^{-1}]	Sampling duration [s]	Sample interval [s]
0.5	180	30
0.75	150	20
1	120	15
1.25	90	12
1.5	60	10

The concentration of substrate in the sample is determined by HPLC analysis. The *F*-curve of the initial concentration and the mean residence time is calculated using Equation 3-8 and Equation 3-9, respectively. [102]

3.8.4. Investigation of Mass Transfer Limitation

To investigate a potential mass transfer limitation the continuous high hydrostatic pressure system at TU Hamburg and GALAB are used. Different investigations for the two stet-ups were performed to determine mass transfer limitation.

Continuous High Hydrostatic Pressure System at TU Hamburg

A mass transfer limitation in the system is investigated for flow rates from 0.25 to 1.5 ml · min^{-1}. The same reactor bed is used for all experiments, and the volume of the empty reactor is 212 µL. The same number of 9 hydrodynamic residence times up to the sampling point is realized for all experiments with different flow rates by different experiment durations. The hydrodynamic residence time τ [min^{-1}] was calculated according to Equation 3-10, where V_R [mL] is the volume of the empty reactor and $\dot{V}$ [L min^{-1}] the flow rate.

$$\tau = \frac{V_R}{\dot{V}} \qquad 3\text{-}10$$

The sample is taken according to Table 12. The activity of CRL is calculated according to Equation 3-6.

Table 12: Mass transfer limitation experiments CRL.

Flow rate [ml · min^{-1}]	Time point of sampling [s]
0.25	480
0.5	240
1	120
1.5	80

Continuous High Hydrostatic Pressure System at GALAB

A mass transfer limitation in the system is investigated for flow rates from 0.5 to 1.5 ml · min^{-1}. The same reactor bed is used for all experiments, and the volume of the empty reactor is

212 µL. To ensure, that the reactor is in steady-state conditions 7-9 hydrodynamic residence times are waited before the sampling point. The hydrodynamic residence time τ was calculated according to Equation 3-10, The sample is taken according to Table 13. The activity of PPK is calculated according to Equation 3-7.

Table 13: Mass transfer limitation experiments PPK.

Flow rate [ml · min^{-1}]	Time point of sampling [s]
0.5	180
0.75	150
1	120
1.25	90
1.5	60

3.9. Continuous Flow Biocatalysis

The continuous flow biocatalysis paragraph describes the experiments which are performed in the conceptualized Continuous High Hydrostatic Pressure System which is described in 3.8 "Continuous High Hydrostatic Pressure System". The experiments to investigate the kinetic parameters of PPK and the influence of high hydrostatic pressure on the PPK are performed using the High Hydrostatic Pressure System at GALAB which is described in 3.8.2. The experiments to investigate the kinetic parameters of CRL and CalB and the influence of high hydrostatic pressure on CRL and CalB are performed using the High Hydrostatic Pressure System at TU Hamburg which is described in 3.8.1.

3.9.1. *Candida rugosa* Lipase in Continuously Operated Packed Bed Reactor

The following paragraph describes the experiments using CRL in the High Hydrostatic Pressure System at TU Hamburg. First, the stability of the CRL under ambient and high pressure is investigated, followed by the investigation of the influence of hydrostatic pressure on the activity, selectivity, and kinetic parameters of CRL. All experiments are carried out at 35 °C.

3.9.1.1. Investigation of Process Stability of *Candida rugosa* Lipase

The stability experiments are performed to assess the process stability of CRL and to validate that the performance of the CRL for HHP or kinetic measurements is consistent over the experiment time. A 30 x 3 mm UHPLC column is used as high hydrostatic pressure reactor and filled with 0.055 g immobilizate (TR 21). The reactor is flushed with 1 ml · min^{-1} heptane containing 864.0 mmol · L^{-1} vinyl acetate for 5 min. Subsequently, a flow rate of 0.5 mL · min^{-1} with a PP concentration of 60.0 mmol · L^{-1} PP in heptane containing 864.0 mmol · L^{-1} vinyl acetate is adjusted. Samples of 250 µL each are taken for 2 h.

The stability of CRL is determined at 1 bar and 800 bar. The deactivation constant k_d [min^{-1}] is calculated from the experimental results between 40 min and 120 min experimental time using Equation 3-11, where t [min] is time of sampling, c_E [$mg \cdot mL^{-1}$] is the enzyme concentration and $c_{E,0}$ [$mg \cdot mL^{-1}$] is the initial enzyme concentration.

$$c_E = c_{E,0} \cdot e^{-k_d \cdot t} \qquad 3\text{-}11$$

The half-life $t_{1/2}$ [min^{-1}] is calculated using Equation 3-12. The experiment is performed in triplicates with a new reactor being filled each time.

$$t_{1/2} = \frac{ln(2)}{k_d} \qquad 3\text{-}12$$

3.9.1.2. High Hydrostatic Pressure Experiment

The influence of HHP on CLR activity and selectivity is investigated. Therefore, a 50 x 3 mm UHPLC column is used as high hydrostatic pressure reactor and filled with 0.1 g immobilizate (TR 13). The reactor is flushed with 0.35 $mL \cdot min^{-1}$ of substrate solution containing 10.0 $mmol \cdot L^{-1}$ PP and 864.0 $mmol \cdot L^{-1}$ vinyl acetate in heptane for 60 min. Subsequently, a flow rate of 0.35 $mL \cdot min^{-1}$ with a PP concentration of 10.0 $mmol \cdot L^{-1}$ in heptane containing 864.0 $mmol \cdot L^{-1}$ vinyl acetate is adjusted at the desired pressure and held for 15 min.
The specific activity of CRL is first determined at ambient pressure and then the hydrostatic pressure is increased to 100 bar. Samples are collected and the pressure is subsequently reduced to ambient pressure followed by an increase to the next higher pressure. Subsequently, the same procedure is used for all pressure levels. Three samples of each 250 µL are taken at each pressure level, which are 100, 200, 400, 600, 800, 1000, and 1,200 bar.

To investigate the effect of hydrostatic pressure on the selectivity of CRL on the transesterification reaction, the enantiomeric excess (ee [-]) is determined since both the product and the substrate are enantiomers. ee is the excess of one enantiomer present relative to the total amount of both enantiomers. The enantiomeric excess of the product ee_P and is calculated according to Equation 3-13, where $n_{(R)\text{-}P}$ [mol] denotes the R enantiomer of the product and $n_{(R)\text{-}S}$ [mol] denotes the R enantiomer of the substrate.[3]

$$ee_P = \frac{n_{(R)\text{-}P} - n_{(S)\text{-}P}}{n_{(R)\text{-}P} + n_{(S)\text{-}P}} \qquad 3\text{-}13$$

To describe the selectivity of the enzyme, the enantioselectivity (E [-]) is calculated. This describes the ratio of the reaction rate constants of the two enantiomers to each other. A detailed description of the dependency of the enantiomeric excess and the conversion is

described by Liese *et al.* (2013) and Jaeger *et al.* (2024) [40,103].The E of the product, which is independent of the conversion X [%], is calculated according to Equation 3-14.[3]

$$E = \frac{ln[1 - X \cdot (1 + ee_P)]}{ln[1 - X \cdot (1 - ee_P)]} \qquad 3\text{-}14$$

3.9.1.3. Kinetic Experiment in the Continuous High Hydrostatic Pressure Reactor

The kinetic of CRL and the kinetic parameters are investigated at ambient pressure (1 bar) and 800 bar.

A 30 x 3 mm UHPLC column is used as high hydrostatic pressure reactor and is filled with 0.06 g immobilizate (TR 21). The reactor is flushed with 1 ml · min^{-1} solvent of substrate solution containing 10.0 mmol · L^{-1} PP and 864.0 mmol · L^{-1} vinyl acetate in heptane for 5 min. Subsequently, the flow rate is increased to 1.5 ml · min^{-1} for 20 min. The pressure is set to 800 bar if the experiment is performed under high pressure and held for 15 min. If the experiment is carried out at ambient pressure, the ambient pressure is kept for 15 min as well. The different substrate concentrations for the investigation of the kinetic parameters of CRL are provided using the mixing chamber of the pump. Two solutions A and B are prepared in heptane according to Table 14 and Table 15.

Table 14: Investigation of the influence of PP on the activity of CRL.

	solution A [mmol · L^{-1}]	solution B [mmol · L^{-1}]
PP	100.0	0.0
vinyl acetate	864.0	864.0

Table 15: Investigation of the influence of vinyl acetate on the activity of CRL.

	solution A [mmol · L^{-1}]	solution B [mmol · L^{-1}]
PP	60.0	60.0
vinyl acetate	3255.0	0.0

Both solutions are connected to the UHPLC input A and B. By varying the composition of the pumped liquid, the concentration of PP or vinyl acetate is changed from 100 % to 0.5 % and from 100 % to 1 %, respectively. Three samples are taken after 2 min of equilibration. Afterwards, the composition of the two substrates is changed from 0.5 % to 100 % (PP) and from 1 % to 100 % (vinyl acetate), respectively in accelerating order. In total 6 samples are taken for each substrate composition. The experiment is performed three times for each substrate with a new reactor filled for each experiment. The specific activity of the CRL in the PBR is calculated according to Equation 3-6. The kinetic parameters are investigated according to 3.7.1.3.

3.9.2. *Candida antarctica* Lipase B in Continuously Operated Packed Bed Reactor

The following paragraph describes the experiments using CalB in the High Hydrostatic Pressure System at TU Hamburg.

3.9.2.1. Investigation of Process Stability of *Candida antarctica* Lipase B

The stability experiment is performed to assess the process stability of the enzyme and to characterize the reactor operation. These experiments validate that the performance of the CalB is constantly consistent over the experiment time. A 50 x 3 mm UHPLC column is used as high hydrostatic pressure reactor and filled with 0.1 g immobilizate (TR 12). The reactor is flushed with 1 ml $\cdot$ min^{-1} heptane containing 864.0 mmol $\cdot$ L^{-1} vinyl acetate for 5 min. A flow rate of 0.5 mL $\cdot$ min^{-1} with a PP concentration of 10.0 mmol $\cdot$ L^{-1} PP in heptane containing 864.0 mmol $\cdot$ L^{-1} vinyl acetate is adjusted. Samples of 250 µL each are taken for 5 h. The temperature of the experiment is set to 35 °C.

3.9.2.2. High Hydrostatic Pressure Experiment

To determine the influence of HHP on the specific activity of CalB, a 50 x 3 mm UHPLC column is used as high hydrostatic pressure reactor and is filled with 0.1 g immobilizate of the immobilization batch TR 15, TR 17, and TR 18.The overview of used immobilization batches to investigate the activity in dependency on pressure and temperature is given in 8.5. The reactor is flushed with 0.5 mL $\cdot$ min^{-1} of substrate solution containing 10.0 mmol $\cdot$ L^{-1} PP and 864.0 mmol $\cdot$ L^{-1} vinyl acetate in heptane for 90 min. In each experiment, the influence of two pressures on the activity and the selectivity of CalB are investigated. The pressure to be investigated is applied and held for 45 min. The pressure is reduced to 1 bar and held for 45 min before it is increased to the second pressure to be investigated. The pressure levels to be investigated are 400 and 600 bar as well as 800 and 1,200 bar. Each experiment is performed at 35 °C, 45 °C, 55 °C, and 65 °C. The experiments are performed in duplicates.

To investigate the effect of pressure on the selectivity of CRL on the transesterification reaction, the enantiomeric excess is calculated since both the product and the substrate are enantiomers. The *ee* of the product is calculated according to Equation 3-13.

For a description of the selectivity of the enzyme, the enantioselectivity *E* is calculated. The *E* of the product is calculated according to Equation 3-13.

3.9.3. *Ruegeria pomeroyi* Polyphosphate Kinase in Continuously Operated Packed Bed Reactor

For the determination of the kinetic parameter of the PPK a substrate conversion below 10 % of the thermodynamic equilibrium is required [3]. In order to achieve this low level of conversion in the PBR, the amount of enzymes has to be kept at a low value. In order to use the same reactor and to obtain a similar reactor bed, the carrier with immobilized enzyme was mixed with unloaded carriers, i.e. 25 % carrier with immobilized enzyme mixed with 75 % unloaded carriers. In the following, the mixture is denoted as carrier load of "25/75". A carrier load of "50/50" is selected for pressure experiments and stability investigation. In both cases, the reactor is filled with wet immobilizate using a funnel. Subsequently, the reactor is purged with air to remove excess liquid and to determine the mass of the carriers inside the reactor. For short-term storage (< 1 week), the reactor is filled with 50.0 mmol $\cdot$ L^{-1} Na_3PO_4 buffer at pH 7.4.

3.9.3.1. Investigation of Process Stability of *Ruegeria pomeroyi* Polyphosphate Kinase

For the stability investigation, the 30 x 3 mm stainless steel column is filled with 0.17 immobilized PPK (carrier load of "50/50", described in 3.9.3) and installed in the oven at 40 °C. The substrate solution contains 25.0 mmol $\cdot$ L^{-1} CDP, 30.0 mmol $\cdot$ L^{-1} $MgCl_2$, 44.0 mmol $\cdot$ L^{-1} polyP in a 50.0 mmol $\cdot$ L^{-1} Na_3PO_4 buffer at pH 7.4. The flow rate is adjusted to 0.5 mL $\cdot$ min^{-1}. Samples are taken over a period of 5 h. The deactivation constant k_d is calculated from the experimental results using Equation 3-11. The half-life is calculated using Equation 3-12. The experiment is performed in triplicates with a new packed bed reactor prepared each time.

3.9.3.2. High Hydrostatic Pressure Experiment

Pressure experiments are carried out at 100, 200, 400, 600, and 800 bar in ascending order. To avoid a pressure-induced systematic error reference, experiments are carried out at 1 bar at the beginning, after 400 bar and at the end of the experiment. To apply the desired pressure to the system, a BPR and stainless steel capillaries are used as described in 3.8.2 "Continuous High Hydrostatic Pressure System at GALAB". The reactor filled with 0.16 g immobilizate (carrier load of "50/50", as described in 3.9.3) is installed in the 40 °C tempered oven. The substrate solution contains 30.0 mmol $\cdot$ L^{-1} CDP, 44.0 mmol $\cdot$ L^{-1} polyP, and 30.0 mmol $\cdot$ L^{-1}

$MgCl_2$ and is prepared in 50.0 mmol · L^{-1} Na_3PO_4 buffer. The pH is set to 7.4 using 5 mol · L^{-1} NaOH. The flow rate is set to 1 mL · min^{-1}. A 250 µL sample is taken after 4, 6, 8, and 10 min on each pressure level. The activity is calculated according to Equation 3-7. The experiments are performed in triplicates.

3.9.3.3. Investigation of PPK Kinetics

Kinetic measurements are performed in the continuously operated reactor filled with 0.16 g of carrier (carrier load of "25/75", as described in 3.9.3). Different substrate concentrations are provided using the described reactor set-up in 3.8.2.
Two solutions A and B are prepared in 50.0 mmol · L^{-1} Na_3PO_4 buffer according to Table 16 and Table 17 with 30.0 mmol · L^{-1} $MgCl_2$ in both solutions. The pH is set to 7.4 using 5 mol · L^{-1} NaOH.

Table 16: Investigation of the influence of CDP on the activity of polyphosphate kinase.

	solution A [mmol · L^{-1}]	solution B [mmol · L^{-1}]
CDP	85.0	0.0
polyP	44.0	44.0

Table 17: Investigation of the influence of polyP on the activity of polyphosphate kinase.

	solution A [mmol · L^{-1}]	solution B [mmol · L^{-1}]
CDP	85.0	85.0
polyP	800.0	0.0

Both solutions are connected to the input A and B of the UHPLC pump and placed in a 40 °C preheated water bath. By varying the composition of the pumped liquid, the concentration of CDP, respectively of polyP, is changed from 100 % to 0.1 %. The flow rate is set to 1.5 mL · min^{-1}. Two samples are taken after equilibration time of 2 min. The specific activity of the PPK in the PBR is calculated according to Equation 3-7. The kinetic parameters are determined according to 3.7.1.3.

3.9.3.4. Comparison Between Different Reactor Operation Modes

To compare the application of the phosphorylation catalyzed by PPK in different reactor configurations, the process is operated in a stirred tank reactor and in a continuously operated PBR. The substrate solutions for experiment contains 44.0 mmol · L^{-1} CDP, 30.0 mmol · L^{-1} $MgCl_2$, 44.0 mmol · L^{-1} polyP in a 50.0 mmol · L^{-1} Na_3PO_4 buffer at pH 7.4. These reaction conditions were previously determined to be optimal in the predetermined range.
The PBR experiments are performed using 0.12 g immobilizate (carrier load of "50/50", as described in 3.9.3) in a 30 x 3 mm reactor at 40 °C. The flow rate is varied from 0.15 to

3 mL $\cdot$ min^{-1}. After 10 min of equilibration 3 samples (200 µL each) are taken. The activity is calculated using Equation 3-7. The batch mode STR experiments are described in 3.7.2.

4. Results

The following paragraph describes all results of this thesis, starting with the characterization of the immobilizates, including adsorption experiments, investigation of leaching from the carrier and the characterization of the immobilization procedures. The results of the transesterification and phosphorylation in the stirred tank reactor are then discussed. In the main part, the results of the enzymatic catalyzed reactions in the continuously operated PBR are shown. In addition to the process stability, data on the influence of HHP on the activity, stability and selectivity of the enzymes are presented.

4.1. Characterization of Enzyme Immobilizates

The results of the immobilization experiments and the preliminary tests on the suitability of the enzyme supports are presented in the following section. To ensure that the lipase immobilizates are suitable for the application in a high pressure reactor, preliminary tests are performed. The absorption behavior of the substrate and product on the carriers as well as the swelling behavior in the organic solvent are investigated. A detailed study of the immobilizates was conducted to determine their applicability for use in the continuous high pressure reactor as well as their mechanical behavior under HHP and their resulting activity after immobilization.

4.1.1. Adsorption Experiments

Two carrier materials, Purolite ECR 1090 and ECR 1030, were tested for immobilization of CRL and CalB. Adsorption experiments were performed to test the suitability of the carrier materials for 7 d to ensure that the adsorption equilibrium had been reached. Three substrate (*R*-PP and *S*-PP) and product (*R*-PPA and *S*-PPA) concentrations, ranging from 1 to 100.0 mmol $\cdot$ L^{-1}, were selected as these concentrations were used in subsequent experiments. The results are presented in the following Table 18.

Table 18: Adsorption experiments with a concentration of 1.0-100.0 mmol · L^{-1} of PPA and PP. Reaction conditions: T = 20°C; $V_{PP/PPA}$ = 1 mL; $c_{PP/PPA}$ = 1.0-100.0 mmol · L^{-1}; $m_{carrier}$ = 0.05 g; ECR 1030; ECR 1090; t = 7d.

Carrier	Adsorption in %			
Substance	*S*-PPA	*R*-PPA	*S*-PP	*R*-PP
	Concentration: 1.0 mmol · $L^{-1}$of PPA and PP			
ECR 1090	1.8 ± 2.1	0.3 ± 2.2	7.5 ± 4.2	7.0 ± 4.2
ECR 1030	6.8 ± 6.7	2.0 ± 1.4	9.8 ± 3.9	9.5 ± 4.0
	Concentration: 10.0 mmol · $L^{-1}$of PPA and PP			
ECR 1090	1.0 ± 0.5	0.9 ± 0.6	2.6 ± 1.0	2.4 ± 1.1
ECR 1030	2.7 ± 0.7	2.4 ± 0.8	5.1 ± 0.5	5.6 ± 0.5
	Concentration: 100.0 mmol · $L^{-1}$of PPA and PP			
ECR 1090	2.2 ± 1.0	1.8 ± 1.1	1.4 ± 1.3	1.1 ± 1.4
ECR 1030	0.5 ± 1.3	0.6 ± 1.3	4.7 ± 0.5	4.5 ± 0.5

The investigation revealed that at a starting concentration of 1.0 mmol · L^{-1}, 7.5 ± 4.2 % for *S*-PP and 7.0 ± 4.2 % for *R*-PP were adsorbed on the ECR 1090 carrier after 7 d of incubation. The products PPA adsorption on the ECR 1090 carrier was 1.8 ± 2.1 % and 0.3 ± 2.2 %, respectively.

At a substrate and product concentration of 10 mmol · L^{-1}, the adsorption for the products was less than 1 % and for the substrates 2.6 ± 1.0 % and 2.4 ± 1.1 %, respectively.

At a substrate and product concentration of 100.0 mmol · L^{-1}, the adsorption for the products was 2.6 ± 1.0 % and 1.8 ± 1.1 %, respectively, and for the substrates 1.4 ± 1.3 % and 1.1 ± 1.4 %, respectively.

The adsorption of the substrates on the ECR 1030 support after 7 days was 9.8 ± 3.9 % and 9.5 ± 4.0 %, respectively, at a concentration of 1.0 mmol · L^{-1}. The products adsorption on the carrier was 6.8 ± 6.7 % and 2.0 ± 1.4 %, respectively.

At a concentration of the substrate and product of 10.0 mmol · L^{-1}, the percent adsorption for the products was 2.7 ± 0.7 % and 2.4 ± 0.8 %, respectively, and for the substrates it was 5.1 ± 0.5 % and 5.6 ± 0.5 %, respectively. At a concentration of the substrate and the product of 100.0 mmol · L^{-1}, the percent adsorption for the products was less than 1 % and for the substrates was 4.7 ± 0.5 % and 4.5 ± 0.5 %, respectively.

The experiment showed that the substrate adsorption was higher than product adsorption regardless of concentration. The percent adsorption of product and substrate was greater on the ECR 1030 support material than on the ECR 1090 support material at concentrations of 1 mmol · L^{-1} and 10 mmol · L^{-1}, respectively. At a product and substrate concentration of 100 mmol · L^{-1}, the adsorption of the product on the carrier ECR 1090 was 2.2 ± 1.0 % and 1.8 ± 1.1 % and therefore greater than on the carrier ECR 1030.

The different carriers are distinguished by the material they are made of. ECR 1090 is made from macroporous styrene and ECR 1030 consist of a mixture of divinylbenzene and methacrylate. Methacrylate is one of the most used immobilization material, but is reported that substrate and product adsorption can occur especially for aromatic compounds. [104,105] Therefore, the carrier material ECR 1090 was selected for further experiments. Since the adsorption of both the substrate and the product in a process was not desired, this is an important property of the enzyme carrier. [105] In addition, the handling of ECR 1090 was easier since the particles are less electrostatic than ECR 1030.

4.1.2. Characterization of Immobilization Procedure

The following section discusses the characterization of immobilization method for CRL and CalB.

4.1.2.1. Candida antarctica Lipase B

The influence of different external parameters on the immobilization process were investigated. First, the influence of temperature on immobilization was examined, followed by the influence of the immobilization method.

To investigate the influence of temperature on the immobilization process of CalB on ECR 1090, experiments were carried out at 4 °C, 22 °C, and 40 °C using the same immobilization method. Since the tube roller immobilization method is commonly used, this method was used first. For better comparability, the measured enzyme concentration of the immobilization solution was related to the initial protein concentration of the immobilization solution c/c_0. Figure 11 shows the influence of temperature on the immobilization method TR.

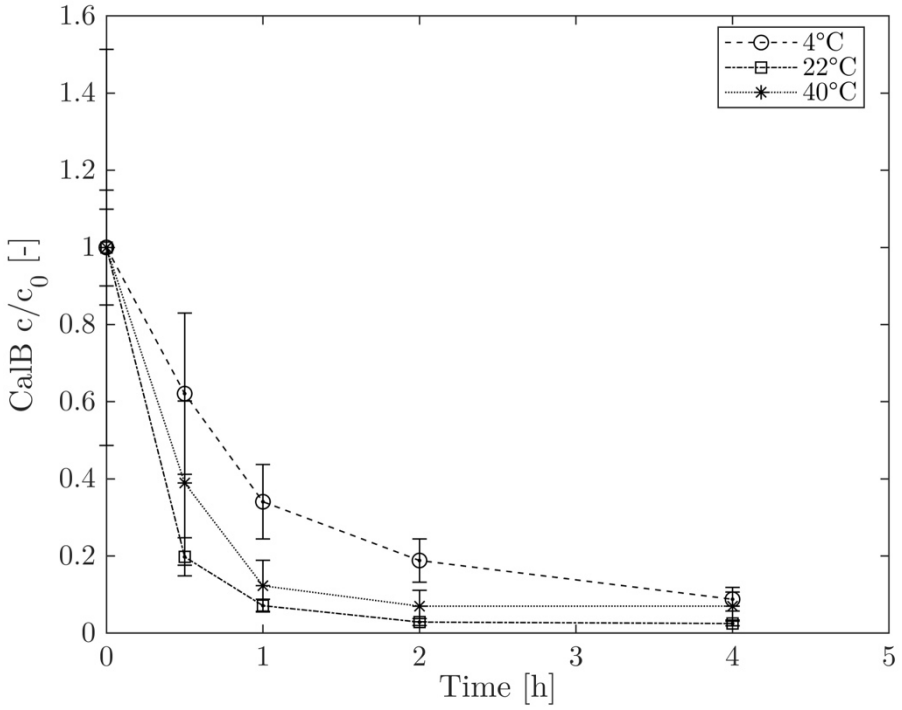

Figure 11: Influence of the temperature on the immobilization rate.
Reaction conditions: T = 4 - 40 °C; immobilization method: TR; V_{CalB} = 1 mL; V_{buffer} = 3 mL; c_{buffer} = 400.0 mmol · L^{-1}; pH = 6,7; $m_{carrier\ ECR\ 1090}$ = 1.75 g.

At the beginning of the immobilization (t= 0 h) and a temperature of 4 °C an enzyme concentration in the immobilization solution of 1679.7 ± 250.0 µg · mL^{-1} was measured. After 30 min, the enzyme concentration in the immobilization solution decreased to 1043.1 ± 314.7 µg · mL^{-1} and the ratio of the initial concentration to the current concentration was 0.6 ± 0.2. At the end of the experiment, after 4 h, c/c_0 was 0.08 ± 0.02.

The same progression of the enzyme concentration was observed for the immobilization experiments at 22 °C and 40 °C. The initial protein concentration at 22 °C was 2540.8 ± 252.6 µg · mL^{-1}. After two hours, the ratio of the initial concentration to the current concentration was 0.03 ± 0.01. At the end of the experiment, the concentration in the immobilization solution was 49.1 ± 18.4 µg · $mL^{-1}$and a c/c_0 of 0.01 ± 0.001 was determined.
At the beginning, the protein concentration at was 1236.7 ± 634.9 µg · mL^{-1} at 40 °C. After one hour, the concentration decreased to 151.9 ± 25.4 µg · $mL^{-1}$and c/c_0 was 0.12 ± 0.01. At the end of the experiment, after 6 h, the concentration was 47.0 ± 32.1 µg · $mL^{-1}$and a c/c_0 of 0.04 ± 0.03 was determined.

The enzyme concentrations in the immobilization solution decreased regardless of the experimental temperature of the TR immobilization method. This decrease in enzyme concentration is indicated as adsorptive immobilization on the enzyme carrier [3]. At all temperatures, the greatest decrease in c/c_0 ratio was observed during the first hour of immobilization.

At the beginning of the experiment, the entire surface is available for adsorption and no enzymes are bound to the support material. Since adsorption is an equilibrium process, a concentration equilibrium for the adsorbent is reached over time.[106] If the immobilizing solution has a high enzyme concentration, as in this case, more enzyme will be immobilized on the support compared to a lower enzyme concentration [107]. After 2 h, the protein concentrations in the immobilization solutions at 22 °C and 40 °C were constant, whereas at 4 °C, the enzyme concentration in the immobilization solution reached equilibrium after 4 h.

Since the terminal enzyme concentration of the immobilization solutions was approximately the same at all temperatures, it can be assumed that temperature influence on immobilization yield can be neglected in the selected temperature range for experiments that are carried out over 4. This phenomenon was already described by Siódmiak *et al.* in 2023 for CalB. The immobilization of CalB was performed at 4 °C to 37 °C. The relative activity value was above 90 %, independent of the experimental temperature.[108] This was confirmed by Dobreva in 1987 for an enzyme preparation with milk clotting activity at 25 °C and 4 °C [109]. Nevertheless, it is necessary to investigate the influence of the immobilization process, since external factors such as temperature, pH or the polarity of the solvent can have a significant influence on the success of immobilization [110].

In addition, the influence of the immobilization method on the success of the immobilization has also been studied. The variation of the immobilization set-ups for a temperature 22 °C and TR, SP and OS is shown in Figure 12.

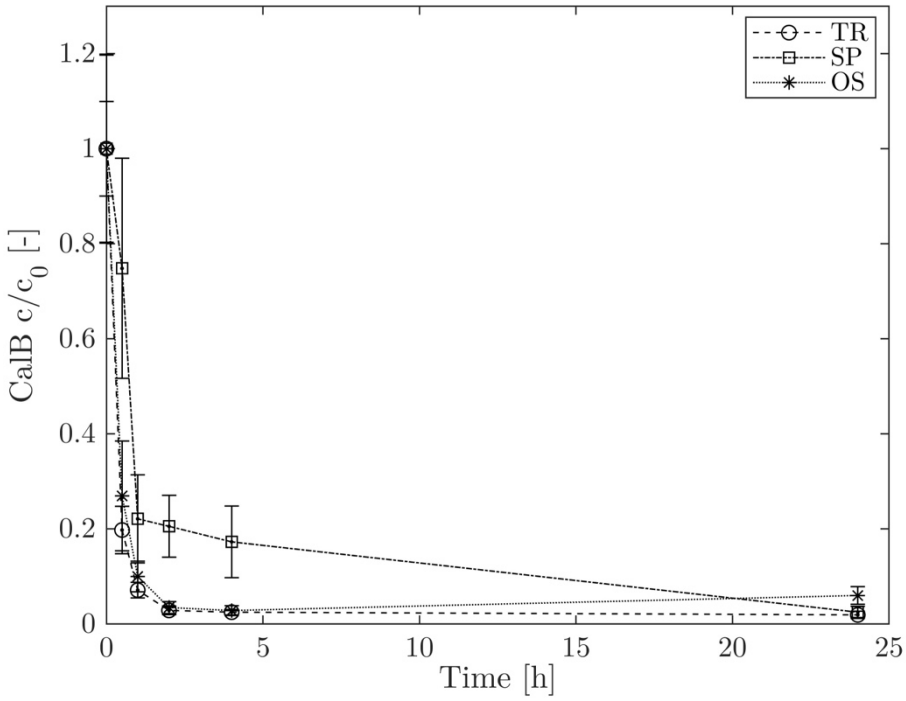

Figure 12: Influence of the immobilization method on the immobilization rate.
Reaction conditions: $T = 22$ °C; immobilization method: TR, SP, OS; $V_{CalB} = 1$ mL; $V_{buffer} = 3$ mL; $c_{buffer} = 400.0$ mmol · L^{-1}; pH = 6,7; $m_{carrier\ ECR\ 1090} = 1.75$ g.

The initial enzyme concentration in the immobilization solution of the TR experiment was 2540.8 ± 252.6 µg · mL^{-1}. After one hour, the ratio of the initial concentration to the actual concentration c/c_0 was 0.07 ± 0.02. After 4 hours, c/c_0 was 0.03 ± 0.01 and the enzyme concentration was 63.4 µg · mL^{-1}. After 24 hours, the concentration in the immobilization solution was 49.1 µg · mL^{-1} and the c/c_0 ratio was 0.02 ± 0.01.

The initial enzyme concentration of the OS experiment was 1701.6 ± 335.5 µg · mL^{-1}. After half an hour, c/c_0 was 0.27 ± 0.12 and the concentration was 459.1 ± 174.5 µg · mL^{-1}. After two hours, the ratio of the initial concentration to the actual concentration was 0.03 ± 0.01. At the end of the experiment, the concentration in the immobilization solution was 102.7 ± 24.0 µg · mL^{-1} and the ratio of c/c_0 was 0.06 ± 0.02.

The initial protein concentration of the SP experiment at 0 hours was 1615.8 ± 321.1 µg · mL^{-1}. After 4 h of the experiment, the ratio of the initial concentration to the actual concentration was 0.17 ± 0.08. After 24 hours, the concentration in the immobilization solution was 40.3 µg · mL^{-1} and the ratio c/c_0 was 0.03 ± 0.01.

Figure 12 shows that the enzyme concentrations of the immobilization solutions of the TR and SP experiment decreased over time. Between 0 and 30 min, the protein concentration of the SP method decreased less than the protein concentration of the immobilization solutions of the TR and OS experiments. After 2 hours, the protein concentration in the immobilization solution of the TR experiment was constant. The enzyme concentration of the experiment using the SP decreased until the end of the experiment. In addition, Figure 12 shows that the protein concentration of the immobilization solution of the experiment using the OS decreased between 0 and 4 hours (0.028 [-]), then slightly increased again until the end of the experiment (0.060 [-]). At the end of the experiment, after 24 hours, 2 % to 3 % of the initial amount of enzymes was still in solution.

It can be concluded that the progression of the measured to initial enzyme concentration ratio differ for the selected immobilization methods. This could be related to the different types of movement depending on the immobilization method. The overhead shaker moves the immobilization solution radially, the shaking plate moves the immobilization solution axially, while the tube roller moves the solution both, radially and axially. Due to the limited mobility of the support materials and the exclusively axial or radial movement, the solution is mixed less effectively and thus less enzyme can be adsorbed on the support material [107]. The combined direction of movement of the tube roller mixes the immobilizing solution more uniformly and ensures constant mixing. This results in more frequent contact between the enzyme and the carrier material compared to a purely axial movement. Thus the protein concentration in the immobilization solution decreases more quickly.[111,112] Furthermore, the tube roller in contrast to the other set-ups provides a more uniform distribution. This circumstance explains in addition why the protein concentration of the shaking plate experiment decreases less rapidly than the concentrations of the immobilization solutions of the TR and OS experiments. These differences in immobilization conditions have a significant impact on the immobilization

efficiency and should be taken into account when aiming for a low a ratio between measured and initial enzyme concentration [113].

All other combinations of temperature and immobilization set-up variations are summarized in Table 19. The performance of each immobilization method was investigated for the selected temperatures.
TR at 22 °C was selected as the most effective method for the immobilization of CalB in terms of the highest immobilization yield of 98.1 ± 0.8 %. The activity test was exemplarily described for this combination of parameters.

Investigation of Immobilizate Activity

The specific activity of CalB immobilized on ECR 1090 at 22 °C on the TR was 1339.8 ± 16.8 $U \cdot g_{carrier}^{-1}$ with an activity yield of 419.6 ± 5.3 %.
Table 19 presents all immobilization yields and activity data from the experiments with different combinations of parameters.

Table 19: Immobilization experiment of CalB at different temperatures and set-ups.
Reaction conditions: T = 4 - 40 °C; immobilization method: TR, SP, TR; V_{CalB} = 1 mL; V_{buffer} = 3 mL; c_{buffer} = 400.0 mmol · L^{-1}; pH = 6,7; $m_{carrier\ ECR\ 1090}$ = 1.75 g.

Immobilization set-up	Temperature [°C]	Immobilization yield [%]	Activity yield [%]	Carrier-specific activity [U · $g_{carrier}^{-1}$]
tube roller	4	92.4 ± 1.5	540.4 ± 20.3	1075.0 ± 40.5
	22	98.1 ± 0.8	419.6 ± 5.3	1339.8 ± 16.8
	40	93.8 ± 3.3	1133.2 ± 8.8	1326.3 ± 10.3
overhead shaker	4	88.8 ± 4.3	751.5 ± 18.1	1193.7 ± 28.8
	22	94.0 ± 1.9	578.6 ± 22.9	1184.2 ± 46.9
	40	95.8 ± 2.1	712.1 ± 8.3	1520.5 ± 17.8
shaking plate	4	78.5 ± 3.9	273.9 ± 14.1	485.8 ± 25.0
	22	97.5 ± 1.2	423.1 ± 11.0	1305.3 ± 33.8
	40	98.2 ± 1.1	873.5 ± 5.7	1917.4 ± 12.5

A comparison of the reaction parameters of the TR immobilization method shows that the maximum immobilization yield and carrier-specific activity, but also the lowest activity yield, was achieved at 22 °C. The activity yield provides information on how much activity the enzyme retains upon immobilization. Despite the comparatively low value of 419.6 ± 5.3 %, this value was above 100 %. An activity yield of 100 % means that the enzyme does not lose any activity over the immobilization process. Furthermore, an activity yield of above 100 % means that the specific activity of CalB was increased by immobilization compared to the unimmobilized form in all experiments. Lipases are activated at interphases, which takes place through immobilization. [114,115] This was previously described by Mateo *et al.* in 2007 as so called "hyperactivation" [35]. Mateo *et al.* stated that the active center of lipases that are adsorptively immobilized on hydrophobic supports is more often the opened form, which causes the increased activity [35]. The relatively low specific activity compared to the high immobilization yield can be explained by the process of adsorption. During adsorption, a monomolecular enzyme layer is initially formed, i.e., the surface of the carrier material is initially completely covered by enzyme. This is followed by the formation of further, multi-molecular layers, resulting in a

higher overall loading of the carrier material. These multiple layered enzyme cause steric hindering themselves as well as conformation changes of the enzyme, leading to loss of the enzyme activity.[107,108,112]

The highest immobilization performance is achieved at 22 °C for the TR method, this combination of immobilization method and process temperature is used for all subsequent immobilizations of CalB.

Immobilization of CalB for High Hydrostatic Pressure Experiments

Since the highest immobilization performance is achieved at 22 °C for the TR, this method is used for all subsequent immobilizations at the 5 g carrier scale for PBR applications. As an example, the 22 st immobilization of CalB with the tube roller is plotted in Figure 13. The resulting immobilized enzymes are further named TR22.

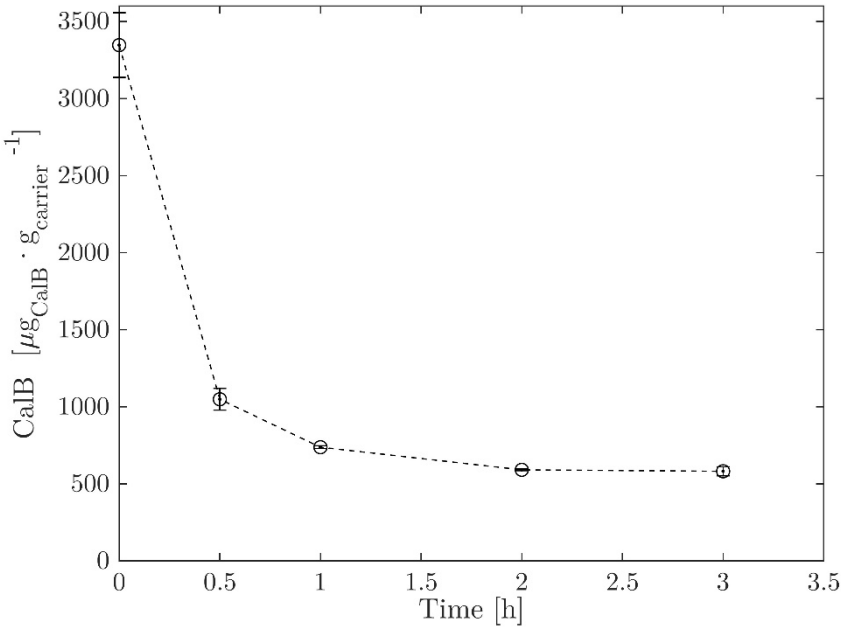

Figure 13: Immobilization of CalB. Enzyme concentration over time of the immobilization batch TR 22. Reaction conditions: $T = 20$ °C; immobilization method: TR; $V_{CalB} = 5$ mL; $V_{buffer} = 5$ mL; $c_{buffer} = 100.0$ mmol $\cdot$ L^{-1}; pH = 7; $m_{carrier;\ ECR\ 1090} = 8.77$ g.

The enzyme concentration in the supernatant of the immobilization process TR 22 was initially 3346.8 ± 209.5 µg $\cdot$ mL^{-1} and decreased to 1049.3 ± 71.1 µg $\cdot$ mL^{-1} after 0.5 h and 3 h of immobilization the enzyme concentration of the supernatant further declined to 591.6 ± 5.0 µg $\cdot$ mL^{-1} and 582.4 ± 29.6 µg $\cdot$ mL^{-1}, respectively. This data was used to calculate the immobilization yield of 82.6 % and an enzyme loading of the carrier of 11.1 $mg_{CalB} \cdot g_{carrier}$.

The immobilization yield and enzyme loading of the carriers of all other immobilizations performed in this thesis are given in the supplementary information in Table 32.

4.1.2.2. Candida rugosa Lipase

The optimal immobilization method for CRL was also investigated using the TR, OS, and SP set-ups. In addition, the temperature of the immobilization process was varied from 4 °C and 20 °C. The experimental results are shown in Figure 14. The actual concentration of the supernatant is plotted related to the initial concentration of the enzyme solution at the beginning of the immobilization.

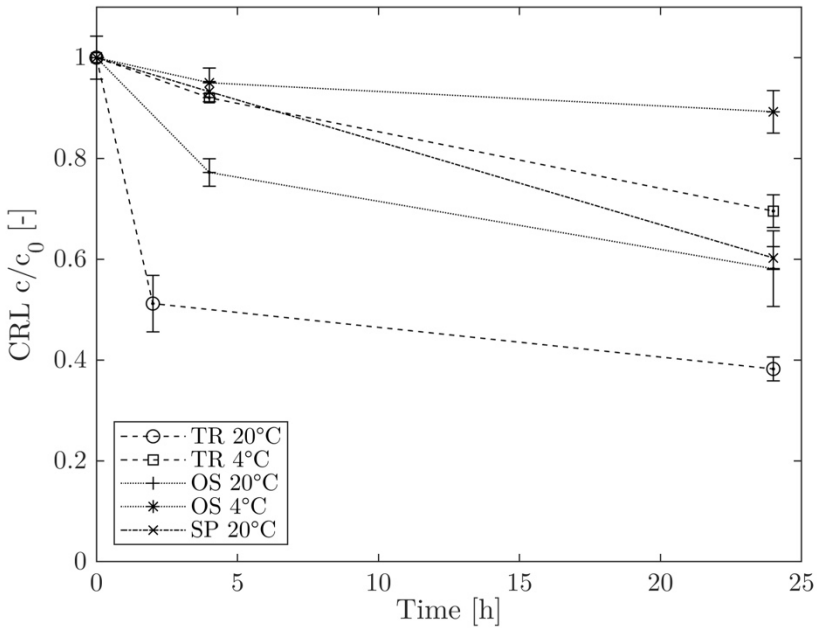

Figure 14: Immobilization experiments of CRL at 20 and 4 °C. Progression of c/c_0 of the different immobilization methods over time.
Reaction conditions: $T = 4 – 20$ °C; immobilization method: TR; $m_{CRL} = 0.01$ g; $V_{buffer} = 2$ mL; $c_{buffer} = 100.0$ mmol · L^{-1}; pH = 7; $m_{carrier;\ ECR\ 1090} = 0.5$ g.

The initial CRL concentration in the immobilization solution of the TR experiments at 20 °C and 4 °C was 315.8 µg · mL^{-1} ($n = 1$) and 342.7 µg · mL^{-1} ($n = 1$). After 2 h and 4 h the CRL concentration was 161.7 ± 17.7 µg · mL^{-1} at 20 °C and 315.4 ± 2.8 µg · mL^{-1} at 4 °C, respectively. The CRL concentration after 24 h of immobilization was 120.7 ± 7.6 µg · mL^{-1} at 20 °C and 238.4 ± 11.1 µg · mL^{-1} at 4 °C.

The initial CRL concentration in the immobilization solution of the OS experiments at 20 °C and 4 °C was 299.5 ± 12.7 µg · mL^{-1} and 342.7 µg · mL^{-1} ($n = 1$). After 4 h the CRL concentration was 231.3 ± 8.1 µg · mL^{-1} and 325.6 ± 10.0 µg · mL^{-1}. The CRL Concentration after 24 h of immobilization was 174.1 ± 22.5 µg · mL^{-1} at 20 °C and 305.9 ± 14.5 µg · mL^{-1} at 4 °C.

The initial CRL concentration in the immobilization solution of the PS experiment at 20 °C was 299.5 ± 12.7 µg · mL^{-1}. After 4 h of immobilization the CRL concentration declined to

279.3 ± 5.6 µg · mL^{-1}. The CRL concentration after 24 h of immobilization was 180.5 ± 6.8 µg · mL^{-1}.

The CRL concentration in the supernatant of the immobilization solution decreased over 24 h in all experiments. The decrease in enzyme concentration in the supernatant suggests that the CRL was adsorptively immobilized [3]. For a better comparison, the immobilization yields as well as the enzyme loading of the supports are summarized in Table 20.

Table 20: Immobilization experiment for CRL at different temperatures and set-ups.

	Immobilization yield [%]	Enzyme load [$\mu g_{enzyme} \cdot g_{carrier}^{-1}$]
tube roller 20 °C	61.0 ± 2.4	770.3 ± 30.2
tube roller 4 °C	29.2 ± 3.2	400.8 ± 44.5
overhead shaker 20 °C	44.3 ± 7.0	522.7 ± 87.5
overhead shaker 4 °C	8.3 ± 4.2	113.8 ± 57.9
Plate Shaker 20 °C	39.8 ± 1.7	468.8 ± 35.1

The immobilization yield for immobilizations performed with the tube roller was 61.0 ± 2.4 % (experiment temperature 20 °C) and 29.2 ± 3.2 % (experiment temperature 4 °C) with an enzyme load on the carrier of 770.3 ± 30.2 $\mu g_{enzyme} \cdot g_{carrier}^{-1}$ and 400.8 ± 44.5 $\mu g_{enzyme} \cdot g_{carrier}^{-1}$. The immobilization yield for immobilizations performed with the overhead shaker was 44.3 ± 7.0 % (experiment temperature 20 °C) and 8.3 ± 4.2 % (experiment temperature 4 °C) with an enzyme load on the carrier of 522.7 ± 87.5 $\mu g_{enzyme} \cdot g_{carrier}^{-1}$ and 113.8 ± 57.9 $\mu g_{enzyme} \cdot g_{carrier}^{-1}$. The immobilization of CRL with the Plate Shaker yielded an immobilization yield 39.8 ± 1.7 % while an enzyme load on the carrier of 468.8 ± 35.1 $\mu g_{enzyme} \cdot g_{carrier}^{-1}$ was achieved.

The influence of temperature on the immobilization process was investigated for the TR and the OS. For both immobilization set-ups the immobilization yield is higher when the temperature during the process is set to 20 °C compared to 4 °C. The temperature dependence of the immobilization process was confirmed by the results of Guisan (2006), who described that the success of immobilization can be significantly affected by external factors such as temperature [110]. The highest achieved immobilization yield was 61.0 ± 2.4 % using the TR and performing the immobilization at 20 °C. Therefore, this combination of immobilization method and process temperature is used for all subsequent immobilizations of CRL.

Immobilization of CRL for High Hydrostatic Pressure Experiments

Since the highest immobilization performance is achieved at 20 °C for the TR, this method is used for all subsequent immobilizations at the 5 g carrier scale for PBR applications. Exemplarily, immobilization 21 with the tube roller (TR 21) is shown in Figure 15.

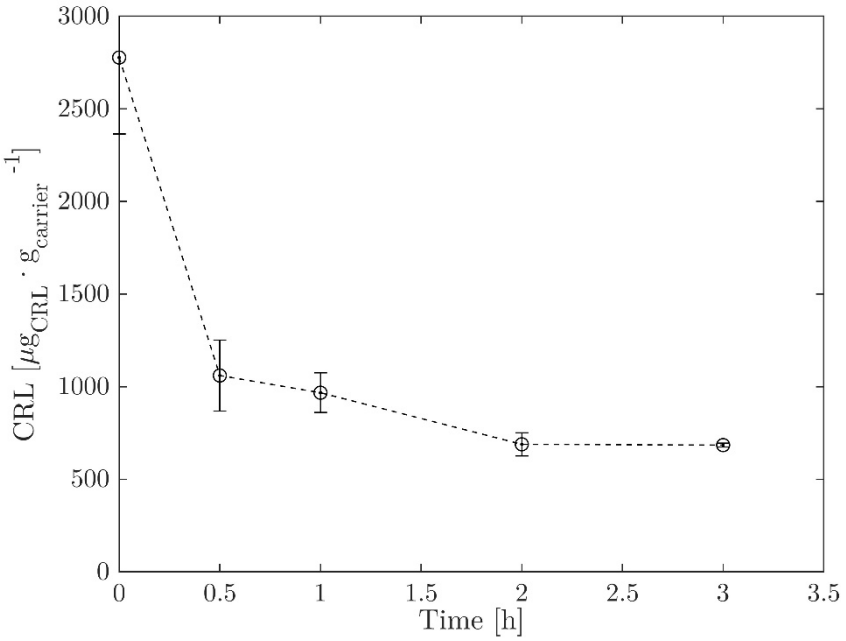

Figure 15: Immobilization of CRL. Enzyme concentration over time of the immobilization batch TR 21. Reaction conditions: $T = 20$ °C; immobilization method: TR; $V_{buffer} = 10$ mL; $c_{buffer} = 100.0$ mmol · L^{-1}; pH = 7; $m_{CRL} = 0.1$ g; $m_{carrier;\ ECR\ 1090} = 8.77$ g.

The enzyme concentration in the supernatant of the immobilization solution TR 21 was initially 2776.9 ± 413.1 µg · mL^{-1} and decreased to 1060.2 ± 191.9 µg · mL^{-1} at 0.5 h and 3 h of immobilization, the enzyme concentration of the supernatant was 689.0 ± 62.7 µg · mL^{-1} and 684.6 ± 10.9 µg · mL^{-1}, respectively. This data was used to calculate the immobilization yield of 75.4 % and an enzyme loading of the carrier of 8.4 $mg_{CRL} \cdot g_{carrier}$.

The immobilization yield and enzyme loading of the carriers of all other immobilizations that were performed in this thesis are given in the supplementary information in Table 31.
The investigation focused on the specificities of the immobilization process for two different enzymes, CalB and CRL. Various variables, including temperature and immobilization techniques, were examined. Notably, the tube roller method at room temperature proved to be the most effective approach, in terms of enzyme loading on the carrier, allowing for uniform immobilization.

4.1.3. Influence of Water Content of the Solvent on the Enzyme Activity

The amount of water in organic solvents can influence the activity of an enzyme. On the one hand, enzymes are losing parts of their flexibility since essential water molecules are needed on the enzyme surface to ensure the necessary conformational mobility and catalytic activity.[39,116] This effect can be avoided or even reversed by adding small amounts of water.[4] Nevertheless,

on the other hand, these rigidity of enzymes in almost water free solvents can be beneficial. As a result of the absence of water, various crystalline enzymes retain their native structure and thus their catalytic activity even in anhydrous organic solvents.[4,39] Therefore, the dependency of the specific activity of immobilized CRL and CalB on the water content of the organic solvent was determined. The solubility of water in heptane is extremely low with 3 µL ·mL^{-1} at 20°C and slightly increasing at higher temperatures [117,118]. The solubility of water in vinyl acetate is 1 µL ·mL^{-1} at 20°C.[119] However, the solubility of water in mixtures of organic solutions may differ from that of pure substances and is additionally influenced by the temperature of the mixture.[46,120] The organic solvents were previously desaturated using a molecular sieve and a certain amount of waste was added. The water/heptane-vinyl acetate mixture was monophasic for all combinations.

The specific activity of immobilized CalB was measured in relation to the water content of the solvent heptane and the results are given in Figure 16.

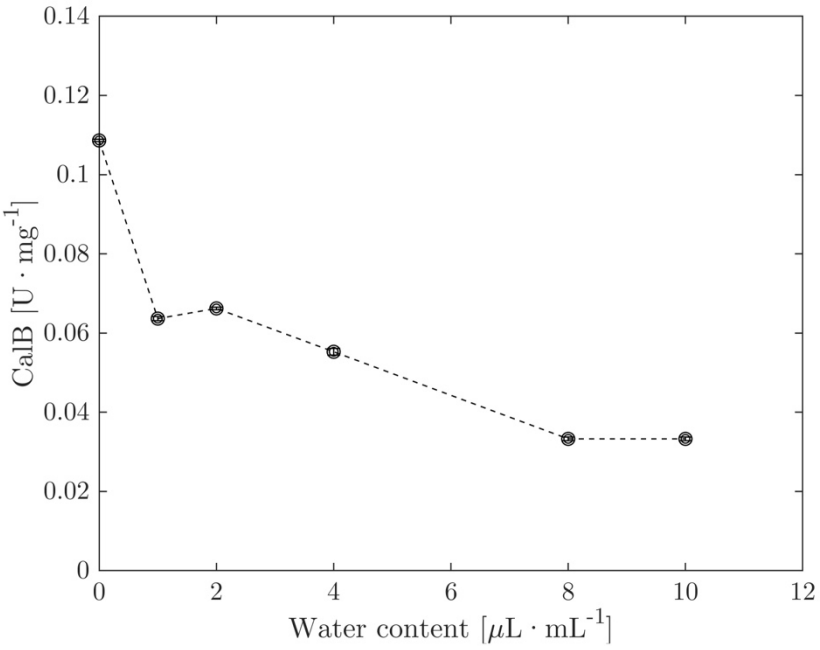

Figure 16: Specific activity of immobilized CalB as a function of water content of the reaction system.
Reaction conditions: T = 35 °C; $V_{reaction}$ = 1 mL; solvent: heptane; c_{PP} = 10.0 mmol ·L^{-1}; c_{vin} = 2712.5 mmol ·L^{-1}; V_{water} = 0-8 µL; m_{TR17} = 0.01 g; ECR 1090; m_{CalB} = 0.3017 mg; t = 1 h; 500 rpm; n = 3.

The activity of CalB in a water free solvent was determined to be 0.1 U · mg^{-1}. At a water content of 1 µL · mL^{-1} and 2 µL · mL^{-1} a catalytic activity of 0.06 and 0.07 U · mg^{-1} was determined. At the highest water content of 10 µL the lowest specific activity of CalB 0.03 U · mg^{-1} was measured. Therefore, the activity of CalB decreased with increasing water content.

Since the influence of water content is also reported for CRL, the specific activity of immobilized CRL was measured in relation to the water content of the solvent heptane. The results are shown in Figure 17.

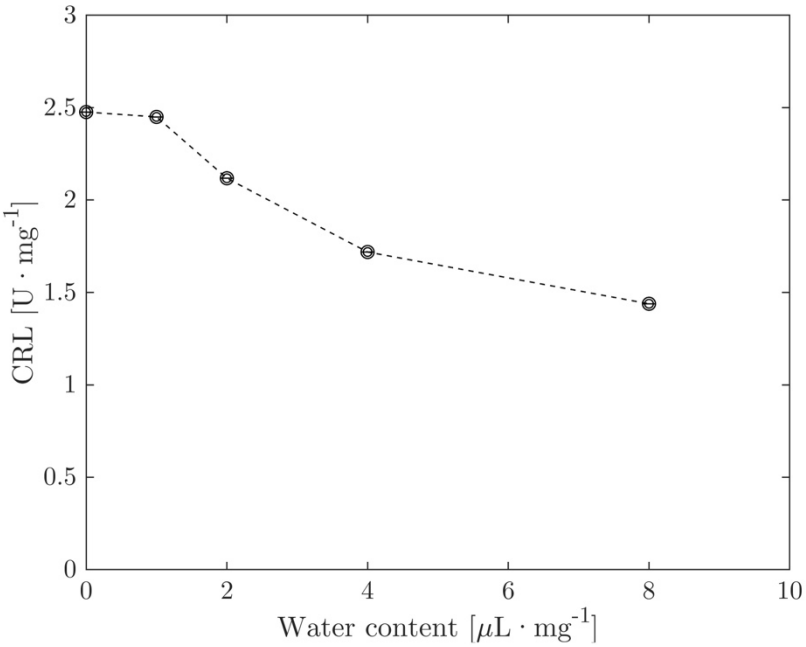

Figure 17: Specific activity of immobilized CRL as a function of water content of the reaction system.
Reaction conditions: T = 35 °C; $V_{reaction}$ = 1 mL; solvent: heptane; c_{PP} = 10.0 mmol ·L^{-1}; c_{vin} = 2712.5 mmol ·L^{-1}; V_{water} = 0-8 µL; m_{TR16} = 0.01 g; ECR 1090; m_{CRL} = 0.0196 mg; t = 1 h; 500 rpm; n = 3.

The activity of CRL in a water free solvent was determined to be 2.5 U · mg^{-1}. The activity of CRL at a water content of 1 µL · mL^{-1} and 2 µL · mL^{-1} was 2.5 and 2.1 U · mg^{-1}. At the highest water content of 8 µL · mL^{-1} the lowest activity of CRL was determined to be 1.4 U · mg^{-1}. As shown for CalB, the catalytic activity of CRL decreased with increasing water content.

The activity of CalB decreased by one third with increasing water content from 0 to 10 µL · mL^{-1}. Furthermore, the activity of CRL decreased as well when the water content of the solvent was increased. A 58 % decrease in activity was observed for a water content increase from 0 to 8 µL · mL^{-1}. However, there is a necessary amount of water molecules on the surface of enzymes to ensure catalytic activity, which depends on the enzyme and the used solvent [4,75]. Herbst *et al.* (2014) investigated the effect of water content in hexane for the same CRL reaction system. It was shown that the activity of CRL increased with increasing water content of up to 6 µL · mL^{-1} of the solvent. Nevertheless, at a water content higher than 6 µL · mL^{-1} the CRL activity slightly decreased.[43] Whereas Bornscheuer *et al.* found that the activity of lipases from other origin in organic solvents decreases with increasing water content [121].
Although the data indicates that a lower water content leads to higher activity of both lipases, a solvent completely saturated with water was used for further experiments. When using the solvents in the continuously operated PBR, it is not possible to use an anhydrous solvent because the solution bottles are open for pressure equalization. However, the use of the solvent saturated with water ensures that the water content of the solvent can be kept constant for all experiments.

4.1.4. Investigation of the Storage Stability of Lipase Immobilizates

The CRL and CalB immobilizates are stored at 7 °C in the refrigerator after drying. To ensure that all experiments can be carried out with the same batch of immobilized enzymes and that the specific activity is comparable in all experiments, the activity of immobilized CRL and CalB was measured over 100 days after finishing the drying process, as described in 3.6.4. The specific activity of CRL as a function of storage time was measured and the results are given in Figure 18.

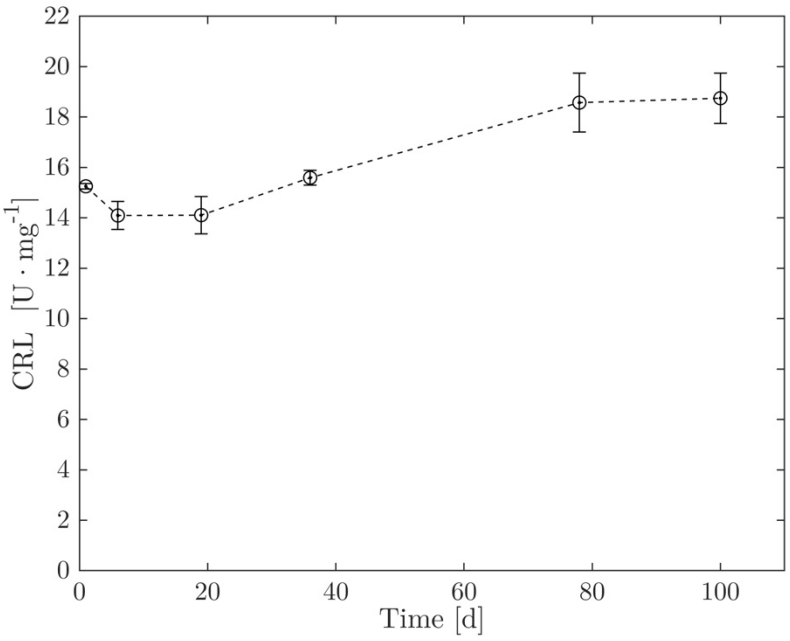

Figure 18: Storage Stability of CRL. Change in specific activity of CRL over storage time.
Reaction conditions: $T_{storage} = 4$ °C; $T = 35$ °C; $V_{reaction} = 1$ mL; solvent: heptane; $c_{PP} = 10.0$ mmol ·L^{-1}; $c_{vin} = 2712.5$ mmol ·L^{-1}; $m_{TR21} = 0.01$ g; ECR 1090; $m_{CRL} = 0.0837$mg; $t = 1$ h; 500 rpm; $n = 3$.

After 24 h the activity of CRL was determined to be 15.3 ± 0.7 U · mg^{-1}. The activity of CRL at day 19 and 36 was 14.1 ± 0.7 U · mg^{-1}and 15.6 ± 0.7 U · mg^{-1}, respectively. At day 78 and 100 the specific activity of CRL increased to 18.6 ± 0.6 U · mg^{-1} and 18.8 ± 0.7 U · mg^{-1}, respectively.

The specific activity of CalB as a function of time was measured and the results are given in Figure 19.

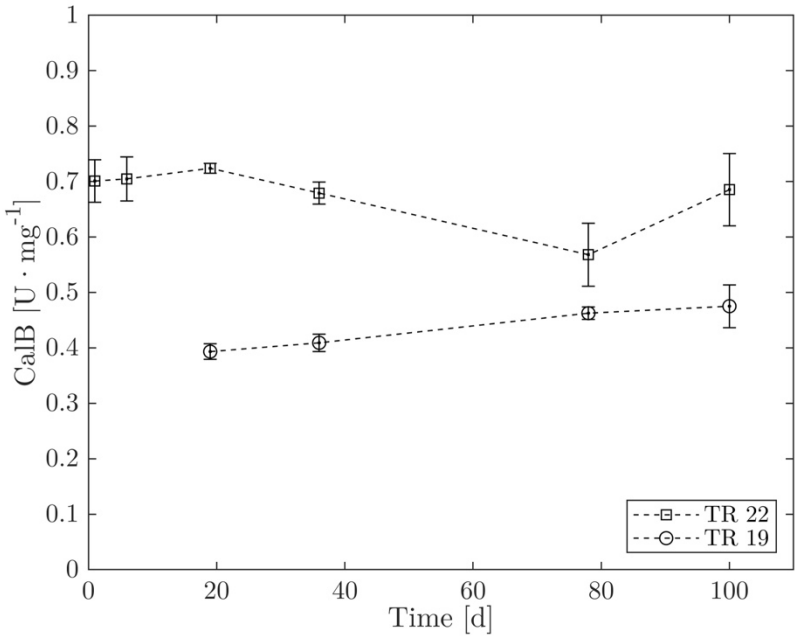

Figure 19: Storage Stability of CalB. Change in specific activity of CalB over storage time.
Reaction conditions: $T_{storage}$ = 4 °C; T = 35 °C; $V_{reaction}$ = 1 mL; solvent: heptane; c_{PP} = 10.0 mmol ·L^{-1}; c_{vin} = 2712.5 mmol ·L^{-1}; $m_{TR19/TR22}$ = 0.01 g; ECR 1090; m_{CalB} = 0.211 / 0.158 mg; t = 1 h; 500 rpm; n = 3.

At the first day of the investigation the activity of CalB (TR 22) was determined to be 0.7 ± 0.04 U · mg^{-1}. The activity of CalB at day 19 and 100 was 0.7 ± 0.01 U · mg^{-1}and 0.7 ± 0.07 U · mg^{-1}, respectively.
The change of specific activity over time was investigated for a different immobilization batch as well. The activity of the immobilization batch TR 19 of day 19 and 100 was 0.4 ± 0.01 U · mg^{-1} and 0.5 ± 0.04 U · mg^{-1}, respectively.

A decrease in stability could not be detected within 100 storage days. The slight fluctuations in activity could be related to measurement or handling errors. Furthermore, the activity experiment on day 78 and 100 was performed with another GC and therefore with a new calibration for substrate and product, which explains the different activity values. Aghaei *et al.* (2021) investigated the storage stability of immobilized CRL on epoxy-activated cloisite 30B at 4 °C. After 30 days, the relative activity of the immobilized biocatalyst had fallen to 87.3 % with respect to the initial activity.[122] Siódmiak *et al.* determined a residual activity of 89.9 % after 7 days of storage at 4 °C, while no decrease in activity was detected for CalB [108]. The results presented suggest that all CRL and CalB immobilizates can be used over a long period of time without deactivation.

4.1.5. Investigation of Mechanical Stability of Carriers

The mechanical stability of the enzyme carrier was investigated to ensure their suitability for application in the different reactors as well as in organic solvents and under high hydrostatic pressure. To investigate the change of the immobilizate and their surface, SEM images were taken from the particles after different treatments, e.g., untreated carrier, carriers after

immobilization or after the usage in the continuously operated high pressure reactor. The exact treatment for each particle batch is shown in Table 9. SEM images of the differently treated enzymes carriers are shown in Figure 20.

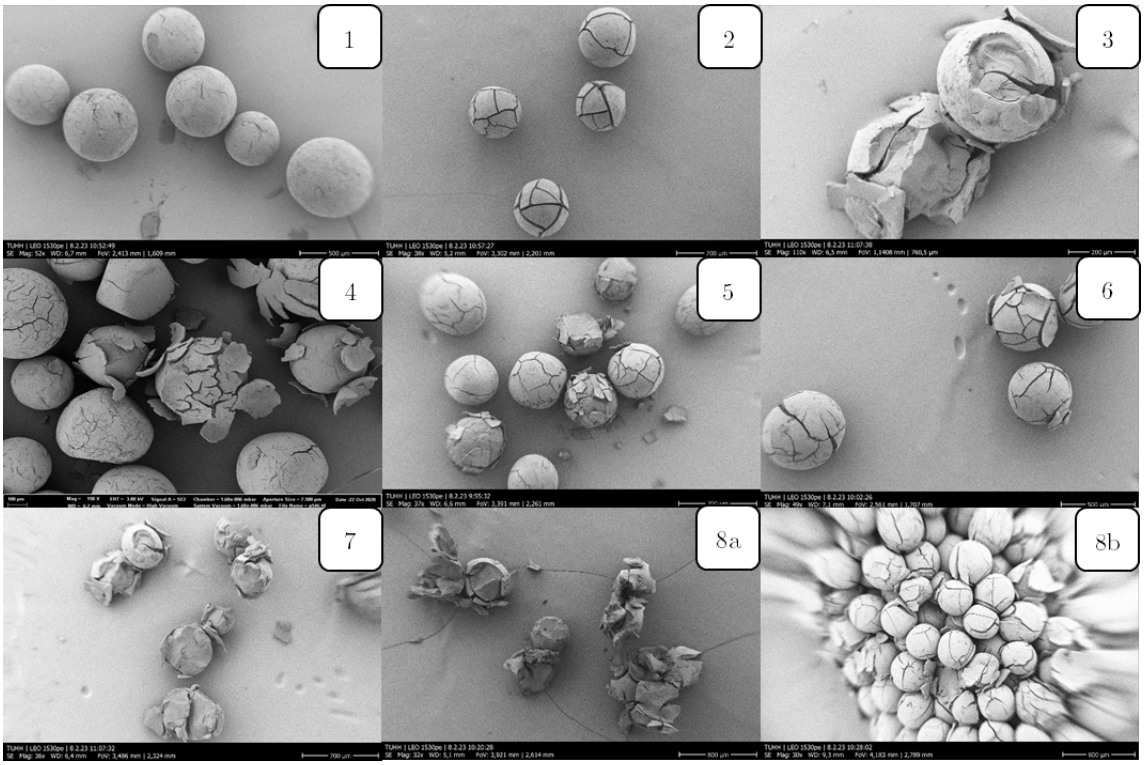

Figure 20: SEM images of immobilizate particle Purolite ECR 1090 with different treatments. 1. Untreated ECR 1090; 2. CRL immobilizate; 3. CalB immobilizate; 4. CRL immobilizate 1 h thermo shaker experiment, 1000 rmp; 5. CRL Immobilizate 3 h in HHP reactor at ambient pressure; 6. CRL Immobilizate 3 h in HHP reactor at 800 bar; 7. CalB Immobilizate 3 h in HHP reactor at ambient pressure; 8. CalB Immobilizate 3 h in HHP reactor at 800 bar.

Figure 20-*1* shows an untreated and dried particle. It can be seen that the untreated particles already have small cracks or an uneven surface. Figure 20-*2* and Figure 20-*3* show the particles after immobilization with CRL and CalB, respectively. Compared to Figure 20-*1*, larger cracks are visible in the surface of the particle with immobilized CRL in Figure 20-*2* but are intact and have an intact round shape. In Figure 20-*3*, the immobilization with CalB has caused cracks in the carrier and partially destroyed the particles. Figure 20-*4* shows the CRL immobilizates after being used for 1 h on the thermo shaker at 1000 rpm. The particles have larger cracks and are partially broken. Figure 20-*5* and Figure 20-*6* show the immobilized particles (CRL) after being used in organic solvent in the continuously operated high hydrostatic pressure reactor, as described in 3.9.1.2. The particles in Figure 20-*5* were used for an experiment at ambient pressure, whereas the particles in Figure 20-*6* were used for an experiment at 800 bar. The particles have more cracks than in Figure 20-*2*, and some surface destruction has occurred. These damages are smaller compared to the particles in Figure 20-*4* after use in the thermos shaker for 1 . Furthermore, no difference can be found between Figure 20-*5* and Figure 20-*6*. Figure 20-*7* and Figure 20-*8a* show the immobilized particles (CalB) after being used in the continuously operated high hydrostatic pressure reactor. The particles

in Figure 20-*7* were used for an experiment at ambient pressure, whereas the particles in Figure 20-*8a* were used for an experiment at 800 bar. It can be seen that most of the particles have a more damaged surface than the particles in in Figure 20-*3*. Furthermore, no difference can be found between Figure 20-*7* and Figure 20-*8a*. Figure 20-*8b* shows the particles from the reactor bed of the test performed at 800 bar. The particles stuck together. In order to obtain a single particle for the recording, they had to be carefully removed from the solid bed. The particles in the fixed bed have cracks in the surface and that they are partially destroyed, but the majority of the particles are present as intact spherical particles. SEM imaging showed that the immobilization already caused cracks (CRL) or destruction of the particles (CalB) when the enzymes were immobilized. Partial destruction of the particles can be observed, especially during immobilization of CalB. This can possibly be explained by the deposition of salts or glycerol from the enzyme solution on the particles [105]. Particles (CRL) were destroyed by thermo shaker application, even though an overhead magentic stirrer was used [123]. This means that the mechanical stress caused by the stirrer is greater than that caused by the use of a continuous reactor. Furthermore, no difference can be found between Figure 20-*5* and Figure 20-*6*, and respectively Figure 20-*7* and Figure 20-*8* which concludes that the influence of HHP on the particles is less severe than by other treatments.

The particles are therefore suitable for utilization in a continuously operated high pressure reactor from the point of view of mechanical stability. This is essential for the use of biocatalysts in stable processes and their reusability.[124] Since the mechanical stability of the carrier was confirmed, further investigations were carried out to test their suitability for the catalytic performance and stability of the enzymes.

4.1.6. Investigation of Enzyme Leaching from the Carriers

The effluent of a continuously operated high hydrostatic pressure reactor with a packed bed with immobilized CRL was collected in a bottle. As it was not possible to determine the enzyme concentration in the effluent, the leaching of the enzyme from the packed bed was determined by measuring the conversion of the PP over time in the collected solution. The results are given in Figure 21.

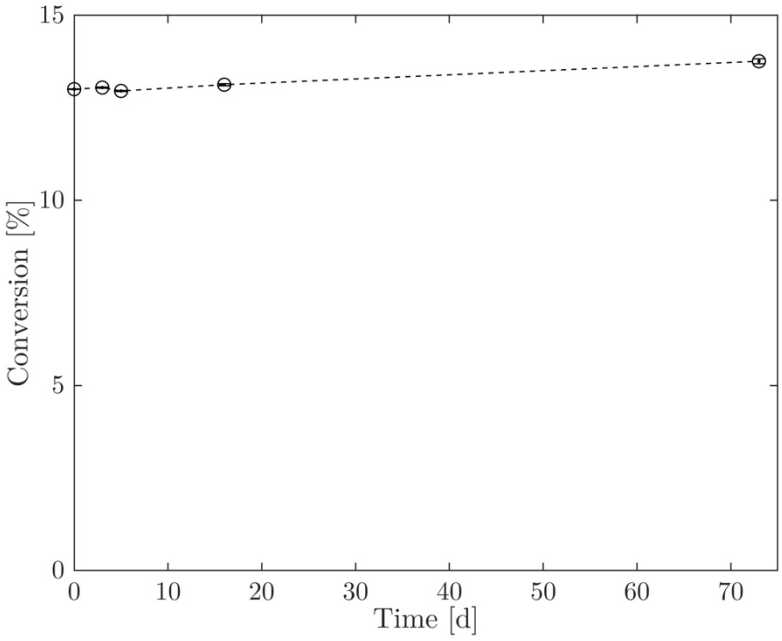

Figure 21: Leaching of CRL from enzyme carrier. Conversion of PP over time.
Reaction conditions: $T_{storage}$ = 20 °C; $V_{reaction}$ = 250 mL; solvent: heptane; c_{PP} = 50.0 mmol ·L^{-1}; c_{vin} = 434.0 mmol ·L^{-1}; m_{TR21} = 0.01 g; ECR 1090; m_{CRL} = 0.0837mg; n = 3.

The conversion of PP was 13.0 % at the beginning of the investigation. With increasing time, the conversion decreased to 12.9 % at day 5 and further increased at day 16 and at day 73 to 13.1 % and 13.8 %, respectively. Overall, the conversion increased by 0.8 % within 73 days. Since the conversion increased only slightly, it can be assumed that no enzyme leached from the carrier. The increase in conversion could be explained by measurement or handling errors.

4.1.7. Summary Characterization of Enzyme Immobilizates

In this section, the immobilization of the enzymes and tests on the suitability of the enzyme carriers were investigated. The carrier material ECR 1090 was found to be suitable for immobilization and mechanically stable under high hydrostatic pressure conditions. For CRL and CalB, a suitable immobilization method was identified that could be also transferred to a larger scale. In addition, the storage stability of the immobilizates was confirmed and no leaching of enzymes from the carrier material was observed. Therefore, the enzyme immobilizates are suitable for the use in a continuously operated high hydrostatic pressure reactor.

4.2. Enzyme Characterization in the Stirred Tank Reactor in Batch Operation Mode

Prior to investigations of the CRL and the PPK in the continuous high hydrostatic pressure reactor system, experiments were carried out in batch mode. The efficiency of the synthesis essentially depends on the choice of a suitable reactor type for enzymatic reactions.[3] Although the replacement of batch processes with continuous processes has begun in the field of biocatalysis, the simplest way to perform an enzymatic catalyzed reaction is still the discontinuously operated stirred tank reactor.[7–9]

The thermodynamic maximum possible turnover, i.e., state of equilibrium, was determined to set the limits for the kinetic studies. The specific activity of CRL and PPK was investigated in STR as well as in PBR for later comparison. The kinetic parameters of CRL in the STR were compared with those from the PBR experiments.

4.2.1. *Candida rugosa* Lipase Application in the Stirred Tank Reactor

Experiments to determine the specific activity and the kinetic parameters in a discontinuously operated stirred tank reactor were carried out in a thermo vessel at 30 °C, given in 3.7.1. The state of equilibrium was investigated, giving the limits for investigating the kinetic parameters in the STR.

4.2.1.1. Investigation of the Thermodynamic Equilibrium of the Transesterification Reaction

The reaction was carried out starting with the substrate PP and vinyl acetate. Immobilized CRL was used, and the reaction process was monitored by means of continuous sampling according to 3.7.1.1. The conversion of PP over time is shown in Figure 22.

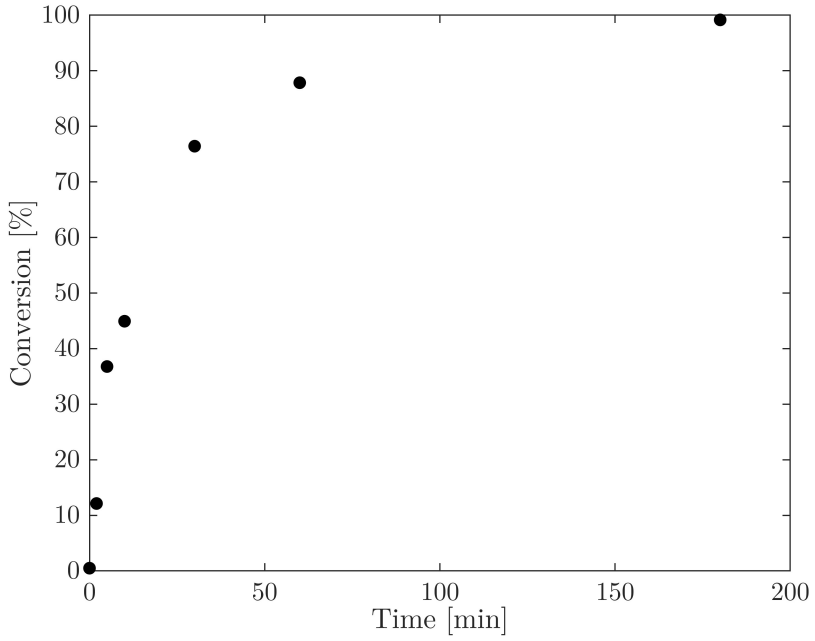

Figure 22: Thermodynamic equilibrium of the transesterification in the STR. Conversion of PP over time. Reaction conditions: T = 35 °C; $V_{reaction}$ = 10 mL; solvent: heptane; c_{PP} = 10.0 mmol ·L^{-1}; c_{vin} = 864.0 mmol ·L^{-1}; m_{TR21} = 0.1 g; m_{CRL} = 0.0837 mg; ECR 1090; 250 rpm; n = 1.

The conversion of PP at 2 min was 12.1 % and increased from 87.9 % after 60 min to 100.0 % after 180 min. Products of the reaction were PPA and vinyl alcohol. Unless stabilized, vinyl alcohol is immediately isomerized to its tautomer acetaldehyde.[125] A back reaction is thus completely avoided and therefore the reaction is irreversible.[116,126]

Since the thermodynamic equilibrium of the transesterification reaction starting from PP and vinyl acetate showed 100.0 % conversion of PP, the kinetic experiments can be performed with a maximal conversion of the substrate of 10.0 %. These 10.0 % of conversion are equal to 10.0 % of the maximal conversion. In the range of substrate conversion from 0.0 % to 10.0 %, the activity of the enzyme is assumed to be approximately linear according to the Michaelis–Menten theory.[3]

4.2.1.2. Investigation of the Kinetic Parameters of *Candida rugosa* Lipase in the Discontinuously Operated Stirred Tank Reactor

For investigation of the kinetics, the dependence of the activity of CRL on the PP and vinyl acetate concentration in relation to the mass of enzyme (U · mg$_{PPK}^{-1}$) was determind. The specific activity of the CRL was calculated using Equation 3-3. The specific activity of CRL as a function of PP and vinyl acetate is given in Figure 23.

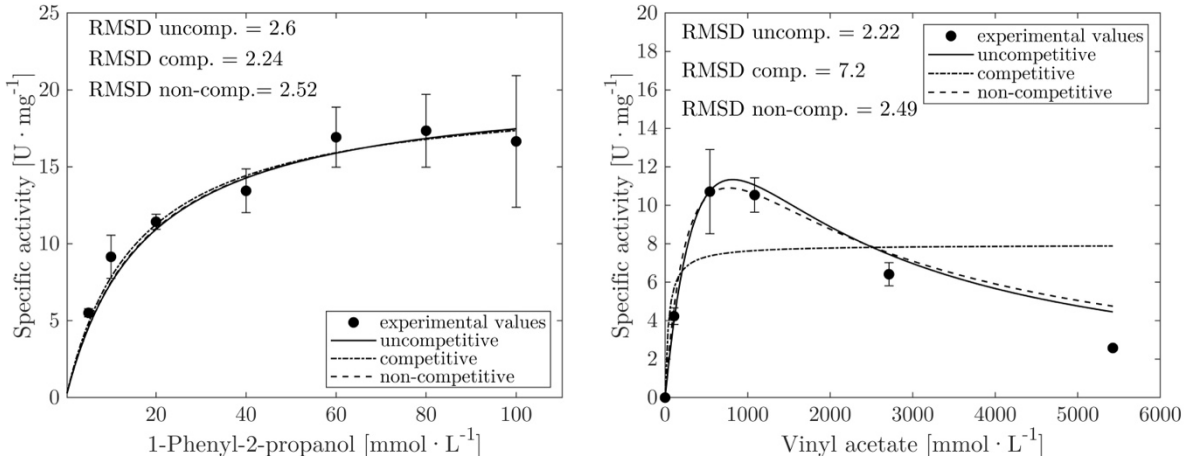

Figure 23: Investigation of kinetic parameters of CRL in STR. Reaction rates were measured during the first 20 minutes of the investigation.

Reaction conditions: $T = 35$ °C; $V_{reaction} = 10$ mL; solvent: heptane; $c_{PP} = 0.0 – 100.0$ mmol ·L^{-1}; $c_{vin} = 0.0 – 5425.0$ mmol ·L^{-1}; $m_{TR11} = 0.1$ g; ECR 1090; $m_{CRL} = 0.0098$ g; $m_{CRL} = 0.0098$ mg; $t = 1$ h; 250 rpm; $n = 3$.

The specific activity of CRL at a constant concentration of vinyl acetate of 1356.3 mmol · L^{-1} and a PP concentration of 5.0 mmol · L^{-1} and 40.0 mmol · L^{-1} was 5.5 U · mg^{-1} and 13.4 U · mg^{-1}, respectively. At a concentration of 60.0 mmol · L^{-1} and 100.0 mmol · L^{-1} the specific activity was 16.9 U · mg^{-1} and 16.7 U · mg^{-1}, respectively.

At a constant concentration of PP of 100.0 mmol · L^{-1} and a vinyl acetate concentration of 108.0 mmol · L^{-1} the specific activity of CRL was 4.2 U · mg^{-1}, respectively. At a concentration of vinyl acetate of 542.5 mmol · L^{-1} the highest specific activity of 10.7 U · mg^{-1} was measured. At concentrations higher than that, the specific activity of CRL decreased to 10.5 U · mg^{-1} at 1085.0 mmol · L^{-1} and further to 2.6 U · mg^{-1} at 5425.0 mmol · L^{-1}.

Optimal substrate concentrations in this set-up and under the given reaction conditions were determined to be PP concentration of 100.0 mmol · L^{-1} and a vinyl acetate concentration of 864.0 mmol · L^{-1} resulting in a CRL activity of 26.6 U · mg^{-1}. The influence of high pressure on the CRL activity and the stability of CRLs were further investigated under these optimal substrate concentrations. The decrease in activity at higher substrate concentrations of vinyl acetate indicated a substrate inhibition [100]. The substrate inhibition of CRL by vinyl acetate was previously described by Palocci *et al.* (2008) [127].

To characterize the CRL, the kinetic parameters were determined. Based on the evaluated activity data as a function of PP and vinyl acetate, substrate inhibition by vinyl acetate was determined. Kinetic parameters were determined by using three equations based on the Michaelis-Menten theory to describe the enzyme activity in dependency of the substrate concentration and type of inhibition. These equations describe competitive, uncompetitive and non-competitive inhibition by vinyl acetate and, in addition, the affinity of the enzyme to the substrate (K_M-value, Michaelis-Menten constant) and the maximum reaction rate (v_{max}) were taken into concideration.[3,75,100] The measured activity values were used to determine the kinetic

parameters $K_{M,PP}$, $K_{M,vin}$, v_{max} and $K_{I,\ vin}$ by using the *nlinfit* algorithm in MATLAB, see 3.7.1.3. The data is given in Table 21.

Table 21: Kinetic parameters of the transesterification reaction by CRL in a stirred tank reactor.

	Uncompetitive inhibition		competitive inhibition		noncompetitive inhibition	
	calculated	95 % confidence interval	calculated	95 % confidence interval	calculated	95 % confidence interval
v_{max} [U · mg^{-1}]	88.1	± 122.3	114.4	± 9.7 · 10^{9}	118.6	± 1.3 · 10^{6}
$K_{M,PP}$ [mmol · L^{-1}]	17.6	± 6.8	15.7	± 12.5	17.2	± 6.8
$K_{M,vin}$ [mmol · L^{-1}]	742.4	± 1512.4	239.1	± 2.0 · 10^{10}	771.6	± 8.5 · 10^{6}
$K_{I,vin}$ [mmol · L^{-1}]	900.3	±1 582.5	51.9	± 9.6 · 10^{8}	771.6	± 8.5 · 10^{6}
RMSD PP [U · mg^{-1}]	2.6		2.3		2.5	
RMSD vin [U · mg^{-1}]	2.2		7.2		2.5	

The data of the kinetic constants and the corresponding confidence interval with regard to the inhibition types are given in Table 21. The 95 % confidence interval indicates the variation of an estimated particular model parameter and the location of the true model parameter for a chosen uncertainty level. The 95 % confidence interval for v_{max} was determined to be 88.1 ± 122.3 U · mg^{-1} for uncompetitive, 114.4 ± 9.7 · 10^{9}U · mg^{-1} for non-competitive and 118.6 ± 1.3 · 10^{6} U · mg^{-1} for competitive inhibition. The kinetic parameters describe the dependence of the activity of CRL on vinyl acetate $K_{M,vin}$ and $K_{I,vin}$ are 742.4 mmol · L^{-1} and 900.3 mmol · L^{-1} for uncompetitive, 239.1 mmol · L^{-1} and 51.9 mmol · L^{-1} for non-competitive and 771.6 mmol · L^{-1} and 771.6 mmol · L^{-1} for competitive inhibition, respectively. As the experiments were carried out in a STR, the number of concentration variations was limited, resulting in relatively wide confidence intervals as for example with v_{max} (88.1 ± 122.3 U · mg^{-1}). In addition, the deviation of the individual experiments was partly large for an accurate prediction of kinetic parameters.

Zhao *et al.* (2015) investigated a specific activity of immobilized CRL of 2.37 U · g^{-1} for the same transesterification reaction in hexane, which is one decade lower than the determined activity in this study [14]. Nevertheless, it was mentioned that due to covalent immobilization, the enzyme loses the majority of its activity while the activity stays the same or is even enhanced when lipases are adoptively immobilized [14,35,128]. Pencreac'h et. Al (2001) investigated

a specific activity of CRL in heptane of 53 $U \cdot g^{-1}$ for a hydrolysis [129]. However, since the activity of lipase is strongly dependent on the properties if the reaction solution, the water content of the solvent, the temperature and the reaction to be catalyzed, and the specific activity values are within a comparable range [116].
In order to obtain a prediction about the accuracy of the model's description of the measured data, the RMSD was used. The RMSD describes the difference between the measured data and predicted values of the model. RMSD data is given in Table 29. The deviation of the predicted from the measured values for the PP-dependent activity of CRL was 2.6 $U \cdot mg^{-1}$ for uncompetitive inhibition, 2.3 $U \cdot mg^{-1}$ for uncompetitive inhibition, and 2.5 $U \cdot mg^{-1}$ for non-competitive inhibition. The RMSD was 2.2 $U \cdot mg^{-1}$ for uncompetitive, 7.2 $U \cdot mg^{-1}$ for competitive inhibition, and 2.5 $U \cdot mg^{-1}$ for non-competitive inhibition for the vinyl acetate-dependent activity.
The confidence interval for the predicted kinetic parameters for uncompetitive inhibition gave the lowest values compared to the other types of inhibition (see Table 29). Since the lowest RMSD was determined for uncompetitive inhibition additionally, this inhibition type was selected for the following investigations The model parameters for uncompetitive inhibition were determined by using Equation 1-11. Nevertheless, this is only an assumption and the real mechanism of the type of inhibition cannot be conclusively determined with these calculations.

Optimal substrate concentrations based on the kinetic parameter investigation which resulted in the highest specific activity of CRL were 742.4 $mmol \cdot L^{-1}$ vinyl acetate and a PP concentration of 100.0 $mmol \cdot L^{-1}$. In particular, if inhibition by one of the substrates occurs, also known as substrate surplus inhibition, the choice of the right reactor type is important. To keep the substrate concentration in a suitable range, the reaction should be carried out in a CSTR (continuously stirred tank reactor) or a fed batch reactor. In these reactor types the concentration of the inhibitor can be kept low.[3]

Since the focus of this research was to study the influence of HHP on the performance of enzymes, the reactor not only had to fulfill the best possible configuration for substrate inhibition, but also the requirements for high pressure.

Although a large number of studies on enzymes have been performed under high pressure in batch processes and the technical implementation is comparatively simple, not all effects on the enzymes could be studied sufficiently well. The enzymes are often added to the substrate under ambient pressure and then pressurized, after which the pressure is released for a certain time and the sample is removed.[2,60] Therefore, depending on the type of the enzyme, it is not possible to measure the initial reaction rate to determine the kinetic data; the enzyme catalyzes the reaction too quickly. A more viable option is to use a continuously operated reactor packed bed reactor.[9] By using a pressure build-up unit and a suitable pump, every point in the reaction process can be targeted and the desired pressure can be set-up fast. Sampling takes place in the range of ambient pressure (see 3.8). The immobilized enzymes are firmly enclosed in the

PBR and retained by frits. Therefore, no reaction takes place in the range of the ambient pressure. The replacement of batch processes with continuous processes has been an additional factor that contributed to the implementation of sustainable transformations and is the key to process intensification [7–9]. Therefore, it is more appropriate to study the effects of HHP in a continuously operated process. Subsequently, another enzyme, PPK, was also investigated in the STR to determine whether its application in the continuous PBR would also be reasonable.

4.2.2. *Ruegeria pomeroyi* Polyphosphate Kinase Application in Stirred Tank Reactor

The application of immobilized enzymes can be carried out in several different reactors. Particular attention was paid to the comparison between a discontinuously operated STR and a continuously operated PBR, as explained in the introduction. The cofactor regeneration of CTP catalyzed by PPK was performed in a 10 mL thermo vessel to investigate the thermodynamic equilibrium and the specific activity of PPK in batch mode. The reaction process was monitored by means of continuous sampling according to 3.7.2. The conversion of CDP in the STR over time is shown in Figure 24.

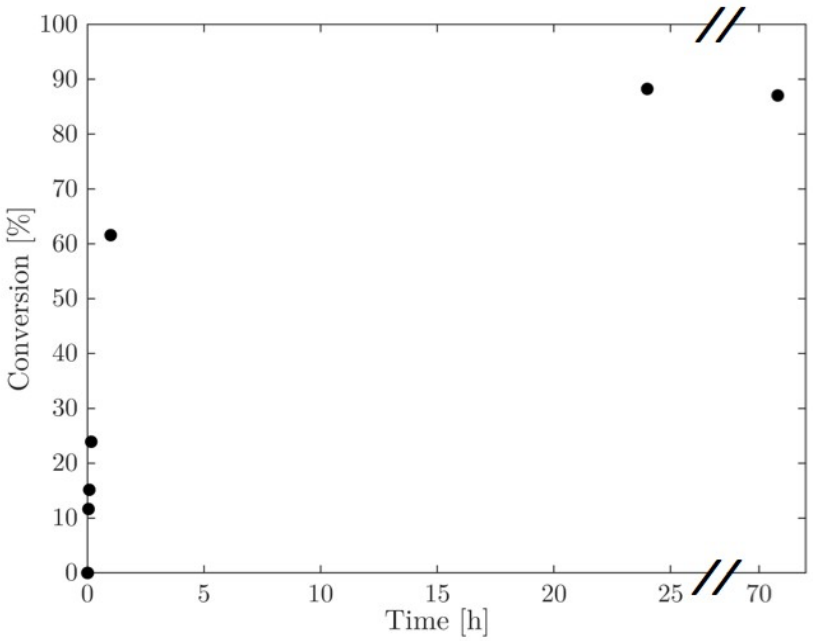

Figure 24: Thermodynamic equilibrium of the phosphorylation reaction in STR.
Reaction conditions: T= 40 °C; $V_{reaction}$= 10 mL; solvent: Na_3PO_4 buffer; c_{buffer} = 50.0 mmol · L^{-1}; pH = 7.4; c_{polyP} = 44.0 mmol ·L^{-1}; c_{CDP} = 30.0 mmol ·L^{-1}; c_{MgCl2} = 30.0 mmol ·L^{-1}; $m_{immobilizate}$ = 0.1 g; m_{PPK} = 0.0415 mg; 250 rpm; n = 1.

The conversion of CDP at 3 min was 11.7 % and increased to 61.6 % after 60 min and further to 88.3 % after 24 h.

As the thermodynamic equilibrium of the phosphorylation reaction starting form CDP and polyP was 88.0 % CDP conversion, the kinetic experiments can be performed with a maximal conversion of 8.8 %, which represents 10.0% of the total conversion. In the range of 0.0 % to

8.8 % substrate conversion the activity of the enzyme is assumed to be almost linear according to the Michaelis–Menten theory.[3]

The specific activity of PPK was determined using Equation 3-5. The initial reaction rate, which is equivalent with the specific activity of PPK, was calculated after 3 min of reaction time with 0.87 $U \cdot mg^{-1}$.

4.2.3. Summary Enzyme Characterization in the Stirred Tank Reactor in Batch Operation Mode

Prior to the continuous high hydrostatic pressure reactor experiments, the reactions catalyzed by CRL and PPK were investigated in a STR in batch operation mode to determine the synthesis efficiency and influence of the substrate concentrations on the specific enzyme activity.

Both reaction systems, the transesterification catalyzed by CRL and the phosphorylation by PPK, were successfully conducted in the discontinuously operated STR. The transesterification reaction reached a 100 % conversion equilibrium, making it possible to perform kinetic experiments with up to 10 % substrate conversion as the enzyme activity is still linear. For CRL, optimal reaction conditions in the STR were determined to be 100.0 $mmol \cdot L^{-1}$ PP and 864.0 $mmol \cdot L^{-1}$ vinyl acetate. A specific activity of 26.6 $U \cdot mg^{-1}$ was measured. Uncompetitive inhibition by vinyl acetate provided the best fit to the kinetic data.

The phosphorylation reaction catalyzed by PPK reached 88 % conversion equilibrium with an initial reaction rate of 0.87 $U \cdot mg^{-1}$ at 8.8 % substrate conversion.

These results guide the design of the continuous high hydrostatic pressure reactor experiments, highlighting the importance of optimal substrate concentrations and determination of inhibition effects for enzymatic efficiency.

4.3. Characterization of the High Hydrostatic Pressure Set-up

The following section discusses the characterization of the high hydrostatic pressure set-up. This characterization is of utmost importance as it discusses possible phenomena that can occur in a continuously operated packed bed reactor.

4.3.1. Establishment of Steady-State Conditions in the Packed Bed Reactor

In order to ensure steady-state conditions when the reaction in the continuously operated packed bed reactor is investigated, the activity of CRL was determined in the first 120 min of the experiment. The hydrodynamic residence time was determined to 0.87 ± 0.01 min at a flow rate of 0.5 mL · min^{-1}. The CRL activity of six individual experiments, each with a newly loaded reactor bed, is plotted against time in Figure 25.

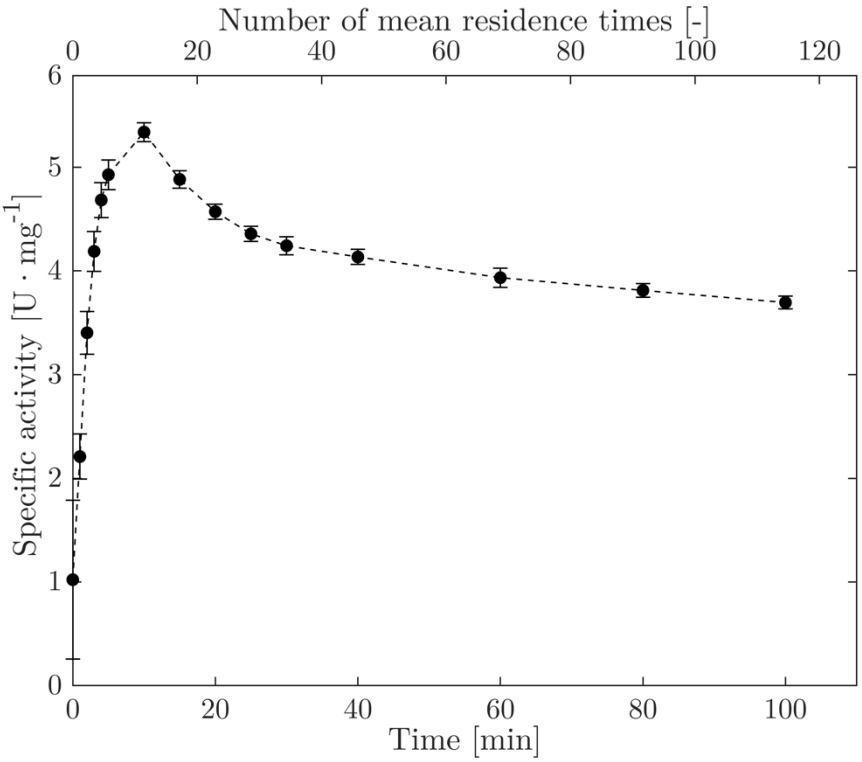

Figure 25: Establishment of steady-state conditions of PBR filled with CRL immobilizate at ambient pressure. Reaction conditions: $T = 35$ °C; $\dot{V}$ =0.5 ml·min^{-1}; solvent: heptane; $c_{PP} = 10$ mmol · L^{-1}; $c_{vin} = 864.0$ mmol·L^{-1}; reactor dimensions: 30 x 3 mm; $\bar{t} = 0.87 \pm 0.01$ min; $m_{TR21} = 0.1$ g; ECR 1090; $m_{CRL} = 0.0837$ mg; $t = 100$ min; $n = 3$.

The specific the activity of CRL was 3.4 ± 0.2 U · mg^{-1} at 2 min and increased to 5.3 ± 0.1 U · mg^{-1} after 10 min of reactor operation. At 20 min and 80 min the activity was 4.6 ± 0.1 U · mg^{-1} and 3.8 ± 0.1 U · mg^{-1}, respectively.

In each experiment, CRL activity increased during the first 10 min of reactor operation. Subsequently, the activity decreased. This phenomenon is not due to insufficient mixing of the reactor, as the mean residence time is 0.87 min which is equal to 11 residence times. The increase in activity up to 10 min of the experiment could be explained by a flow induced compression of the packed bed. The decrease of the CRL activity could be explained by the

subsequent formation of channeling in the reactor bed, swelling of the particles or denaturation of the enzyme.[3,130,131] In particular, the declining course of activity over time can be explained by the deactivation of the CRL [3].

4.3.2. Residence Time Experiments in Packed Bed Reactor

Residence time experiments were performed to ensure that the reaction was in steady-state conditions. A step signal was applied and the concentration of the tracer, which was in both cases the substrate of the reaction was measured at the reactor outlet. Different experiments were performed for the different continuous high hydrostatic pressure systems.

Continuous High Hydrostatic Pressure System at TU Hamburg

The F-curve of the experiments, which represents the sum curve of the residence time distribution, is plotted in Figure 26.

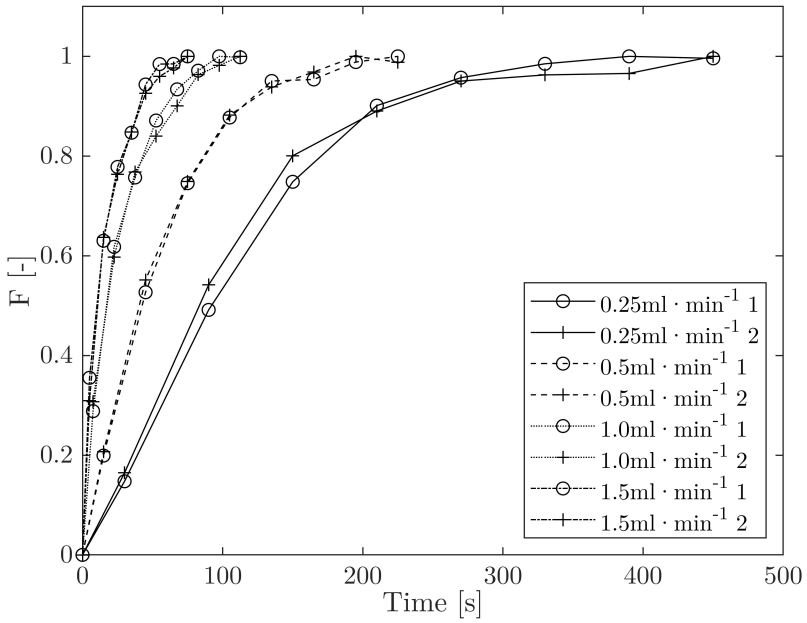

Figure 26: Determination of the mean residence time. Sum curve of the residence time distributions from two experiments *F*-curve.
Reaction conditions: T = 35 °C; $\dot{V}$ = 0.25-1.5 ml ·min^{-1}; solvent: heptane; c_{PP} = 10.0 mmol ·L^{-1}; c_{vin} = 864.0 mmol ·L^{-1}; reactor dimensions: 30 x 3 mm; m_{TR21} = 0.0627 g; ECR 1090; t = 80 – 480 s; n = 2.

The mean residence time was calculated according to Equation 3-9 and is given in Table 22.

Table 22: Mean residence time as a function of the flow rate of the continuous high hydrostatic pressure system at TU Hamburg.

Flow rate [ml · min^{-1}]	mean residence time [min]
0.25	1.75 ± 0.02
0.5	0.87 ± 0.01
1.0	0.40 ± 0.01
1.5	0.38 ± 0.01

The mean residence time at a flow rate of 1.0 mL · min^{-1} was 0.40 min while $\bar{t}$ was 0.38 min at a flow rate of 1.5 mL · min^{-1}. The flow rate of the substrate at the experiments to determine the kinetic parameters was 1.5 mL · min^{-1}; the waiting time was chosen to be 2 min which is 5 – fold the mean residence time. To determine the effects of HHP on the enzyme activity, a flow rate of 1 mL · min^{-1} was selected. To provide more time to reach the steady-state condition, while the time for the experiment was kept as short as possible to avoid enzyme denaturation during the experiment, the first sample was taken after 5 min which, is equal to 12 mean residence times.

Continuous High Hydrostatic Pressure System at GALAB

The calculated residence time is plotted against the flow rates in Figure 27, the mean residence time is given in Table 23.

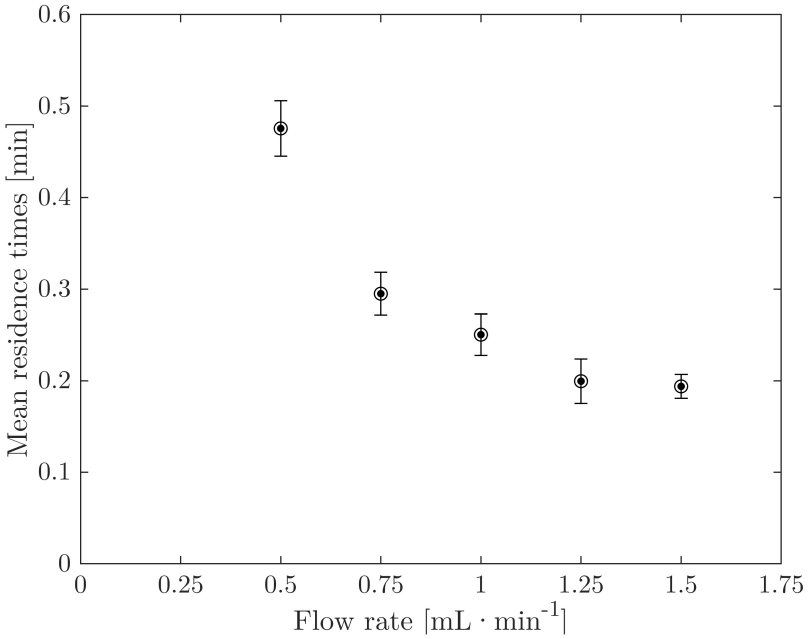

Figure 27: Determination of the mean residence time in dependency of the flow rate.
Reaction conditions: T = 40 °C; $\dot{V}$ = 0.25-1.5 ml ·min^{-1}; solvent: Na_3PO_4 buffer; c_{buffer} = 50.0 mmol · L^{-1}; pH = 7.4; c_{polyP} = 44.0 mmol ·L^{-1}; c_{CDP} = 30.0 mmol ·L^{-1}; c_{MgCl2} = 30.0 mmol ·L^{-1}; $m_{immobilizate}$ = 0.1742 g; reactor dimensions: 30 x 3 mm; t = 60 – 180 s; n = 6.

The mean residence time at a flow rate of 0.5 mL · min^{-1} was 0.48 min while $\bar{t}$ was 0.19 min at a flow rate of 1.5 mL · min^{-1}. The flow rate of the substrate feed in the experiments to determine

the kinetic parameters was 1.5 mL · min^{-1}; the waiting time was chosen to be 2 min which is 10-fold the mean residence time. For determining the effects of HHP on the enzyme activity, a flow rate of 1 mL · min^{-1} was selected. The first sample was taken after 4 min which is equal to 15 mean residence times. Since the mean residence time was determine using the F-curve, interactions between the immobilization carrier and the tracer could not be quantified which might have affected these results.

Table 23: Mean residence time in dependency of the flow rate of the continuous high hydrostatic pressure system at GALAB.

Flow rate [ml · min^{-1}]	mean residence time [min]
0.5	0.48 ± 0.03
0.75	0.30 ± 0.02
1	0.25 ± 0.02
1.25	0.20 ± 0.02
1.5	0.19 ± 0.01

4.3.3. Investigation of Mass Transfer Limitation in Packed Bed Reactor

A potential mass transfer limitation is one of the most important parameters to be studied in the process of setting up a continuously operated RBR. Therefore, different flow rates and the resulting enzyme activity were calculated to identify this potential limitation. The investigation of the mass transfer limitation was performed for both high hydrostatic pressure systems.

Continuous High Hydrostatic Pressure System at TU Hamburg

The activity of CRL in dependency of the flow rate, as well as the mean residence time, at the continuous high hydrostatic pressure system at TU Hamburg is given in Figure 28.

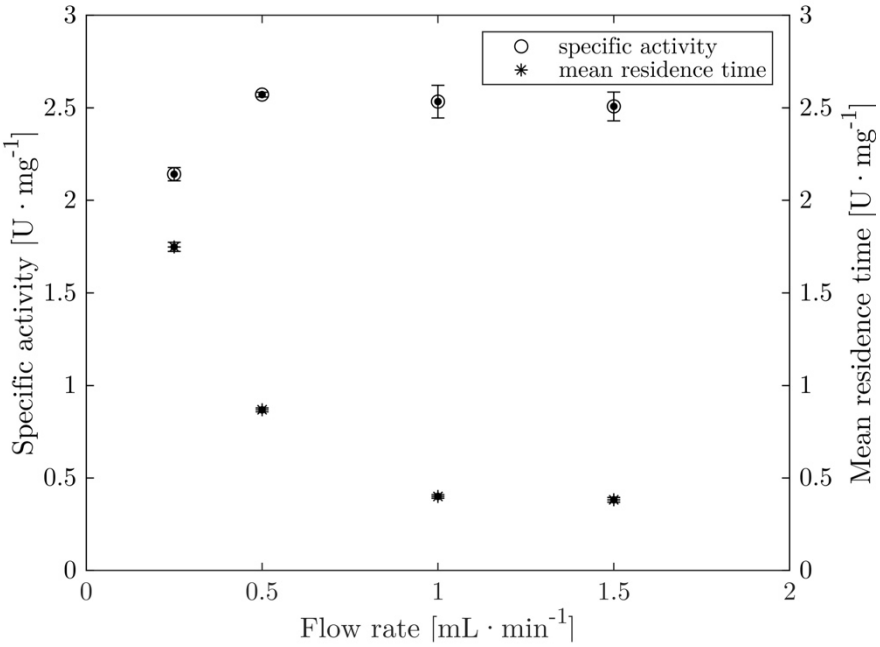

Figure 28: Determination of Mass transfer limitation in PBR with immobilized CRL. Activity and mean residence time as a function of the flow rate.
Reaction conditions: T = 35 °C; $\dot{V}$ = 0.25-1.5 ml ·min^{-1}; solvent: heptane; c_{PP} = 10.0 mmol ·L^{-1}; c_{vin} = 864.0 mmol ·L^{-1}; reactor dimensions: 30 x 3 mm; m_{TR21} = 0.0627 g; ECR 1090; t = 80 - 480 s; n = 2.

The activity of the CRL was determined to be 2.5 ± 0.03 U · mg^{-1} for increasing flow rates from 0.5 to 1.5 mL · min^{-1}. The activity of CRL at a flow rate of 0.25 mL · min^{-1} is 2.1 ± 0.04 U · mg^{-1}. Since the activity of CRL at a flow rate above 0.25 mL · min^{-1} was higher, a mass transfer limitation was assumed at flow rates lower than 0.5 mL · min^{-1}.[131] As the experiments to determine the kinetic parameters, as described in 3.9.1.3, and the pressure experiment, as described in 3.9.1.2, were carried out at a flow rate of 1.5 mL · min^{-1} and 1.0 mL · min^{-1} respectively, it was assumed that lower mass transfer limitation occurred at these flow rates.

Continuous High Hydrostatic Pressure System at GALAB

The activity of PPK as a function of the flow rate is given in Figure 29. The activity of the PPK was determined to be 0.8 ± 0.1 U · mg^{-1} for increasing flow rates from 0.5 to 3.0 mL · min^{-1}. The activity of PPK at a flow rate of 0.15 mL · min^{-1} was 0.6°U · mg^{-1}.

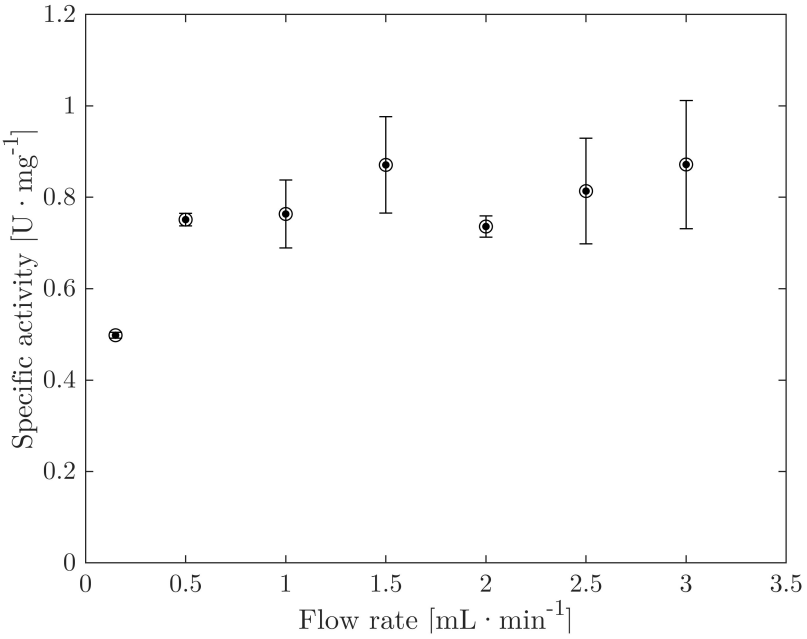

Figure 29: Determination of mass transfer limitation in PBR with immobilized PPK. Activity as a function of the flow rate.
Reaction conditions: $T = 40$ °C; $\dot{V} = 0.15$-1.5 ml ·min^{-1}; solvent: Na_3PO_4 buffer; $c_{buffer} = 50.0$ mmol · L^{-1}; pH = 7.4; $c_{polyP} = 44.0$ mmol ·L^{-1}; $c_{CDP} = 30.0$ mmol ·L^{-1}; $c_{MgCl2} = 30.0$ mmol ·L^{-1}; $m_{immobilizate} = 0.166$ g; $m_{PPK} = 0.0415$ g reactor dimensions: 30 x 3 mm; $t = 60$ - 180 s; $n = 3$.

As the activity of PPK at a flow rate above 0.5 mL · min^{-1} was higher than the activity at lower flow rates, a higher mass transfer limitation, which is potentially external, was assumed at flow rates lower than 0.15 mL · min^{-1}.[131] Since the experiments to determine the kinetic parameters and the pressure experiment, as described in 3.9.1.3 and 3.9.1.2, are performed at a flow rate of 1.5 mL · min^{-1} and 1.0 mL · min^{-1} respectively, it was assumed that lower mass transfer limitation occurs at these flow rates. To further compare the activity of the PPK in different reaction modes, the activity was calculated for the batch mode. The activity of the PPK was determined to be 0.8 ± 0.1 U · mg^{-1} for flow rates from 0.5 to 3.0 mL · min^{-1}.

4.3.4. Summary Characterization of the High Hydrostatic Pressure Set-up

The high hydrostatic pressure set-ups at TU Hamburg by Shimadzu and at GALAB by Waters were characterized to ensure the suitability of the set-ups to investigate the influence of high hydrostatic pressure on the enzyme performance. When immobilized CRL was applied in the HHP reactor, a time dependent establishment of the steady-state conditions was observed. To ensure steady-state conditions in the continuously operated packed bed reactor, the system was flushed for at least 10 min before investigating effects in the HHP system. Nevertheless, a similar phenomenon was not investigated for the immobilized PPK in the HHP set-up at GALAB. As these enzymes, carriers and solvents are different, the effect observed for immobilized CRL was only specific for this combination of reaction set-up and conditions.
The mean residence time in the reactor set-ups was carried out analogously for both set-ups. At a flow rate of 1 mL · min^{-1}, the mean residence time was 0.40 min for the TU Hamburg set-

up, while it was 0.25 min for the GALAB set-up. These differences were due to different types of pumps installed and different void volumes of solvent in the capillaries to and from the reactors.

Based on the results, the high hydrostatic pressure set-ups at TU Hamburg by Shimadzu and at GALAB by Waters were both found to be suitable for the investigation of the influence of high hydrostatic pressure on the enzyme performance.

4.4. Characterization of *Candida rugosa* Lipase in Continuously Operated Packed Bed Reactor

The following section describes the experiments using CRL in the High Hydrostatic Pressure System at TU Hamburg. First, the stability of the CRL was investigated under ambient and HHP followed by the investigation of the influence of HHP on the activity, and selectivity of CRL. In addition, the enzyme kinetics of CRL were studied at ambient and elevated pressure of 800 bar.

4.4.1. Stability Experiments Under High Hydrostatic Pressure

Experiments were performed to assess the process stability of the enzyme and to characterize the reactor operation for different hydrostatic pressure conditions. These experiments validate that the performance of the CRL for pressure or kinetic measurements is consistent over the time of the experiment. The immobilized CRL was kept in the continuously operated PBR for 2 h. The results of the activity change over time are shown in Figure 30.

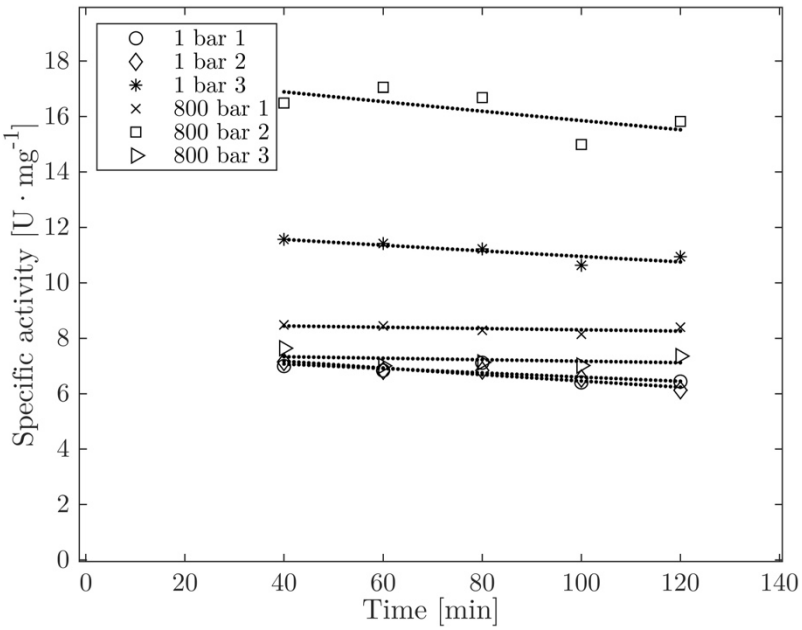

Figure 30: Investigation of CRL Stability at 1 bar and 800 bar. Specific activity of CRL over time.
Reaction conditions: $T = 35$ °C; $\dot{V} = 0.5$ ml ·min^{-1}; solvent: heptane; $c_{PP} = 60.0$ mmol ·L^{-1}; $c_{vin} = 864.0$ mmol ·L^{-1}; reactor dimensions: 30 x 3 mm; $\bar{t} = 0.87 \pm 0.01$ min; $m_{TR21} = 0.0533$ g; ECR 1090; $m_{CRL} = 0.446$ mg; $n = 3$.

In all experiments, the activity decreased slightly over time. The deactivation constant k_d was calculated from the experimental results. The data is given in Table 24.

Table 24: Deactivation constant and mean half-life of immobilized CRL at 1 and 800 bar.

	1 bar			800 bar		
experiment number	1	2	3	1	2	3
k_d [min^{-1}]	$1.2 \cdot 10^{-03}$	$1.8 \cdot 10^{-03}$	$9.0 \cdot 10^{-04}$	$2.8 \cdot 10^{-04}$	$1.1 \cdot 10^{-03}$	$3.7 \cdot 10^{-04}$
$t_{1/2}$ [min]	600.8	395.7	764.1	2496.2	657.6	1857.5

The decrease of enzyme activity over time can be explained by different phenomena. Thermal deactivation may be one explanation for a decrease in enzyme activity over time. A decrease of enzyme activity as a result of enzyme leaching from the carrier is in this application unlikely, as it was determined that no enzyme leaching was occurring as described in 4.1.6 [131]. The experiment was performed with six different packed columns, therefore the specific activity of the CRL varied. This could be due to the error-prone loading of the packed bed in terms of the amount of immobilizate and the structure of the bed [131]. Despite the relatively large error of the experiment, the mean half-life at 800 bar is increased compared to the mean half-life at 1 bar.
Nevertheless, the mean half-life at 1 bar and 35 °C was approximately 5 times longer than the longest experiment performed of 120 min described in 3.9.1.3. With consideration of the loss of activity during the experiment, the duration of the experiment was acceptable even though the stability of the enzyme cannot be verified as high ($t_{1/2} \geq$ 50 - 100 days).[132]

Literature references support these results. Hei and Clark (1994) showed an increase in half-life for hydrogenases from different origins by increasing the pressure from 1 to 507 bar [49]. At 80 bar and 60 °C, Lozano *et al.* investigated an enhanced half-life for CalB [133]. Marie-Olive *et al.* (2000) showed that the half-life of *Saccharomyces cerevisiae* invertase increased when pressures up to 2,000 bar were applied at 60 °C. Depending on the enzyme type and source, the hydrostatic pressure range that protects the enzyme from thermal inactivation varied.[134] Further examples were described by Eisenmenger *et al.* (2009)[2].

4.4.2. Dependence of Activity and Selectivity on Pressure

Among other aspects, the investigation of the influence of HHP on the performance of CRL was the main focus of this thesis. Enzyme performance is characterized by both activity and selectivity, so the influence of HHP on both parameters was investigated.

The specific activity of CRL in the PBR was determined using Equation 3-6. Since the experiment was performed with up to three different packed columns, the specific activity of

the CRL varied. This could be due to the error-prone loading of the packed bed in terms of the amount of immobilizate and the structure of the bed [131]. Figure 31 shows the relative activity of CRL with increasing hydrostatic pressure.

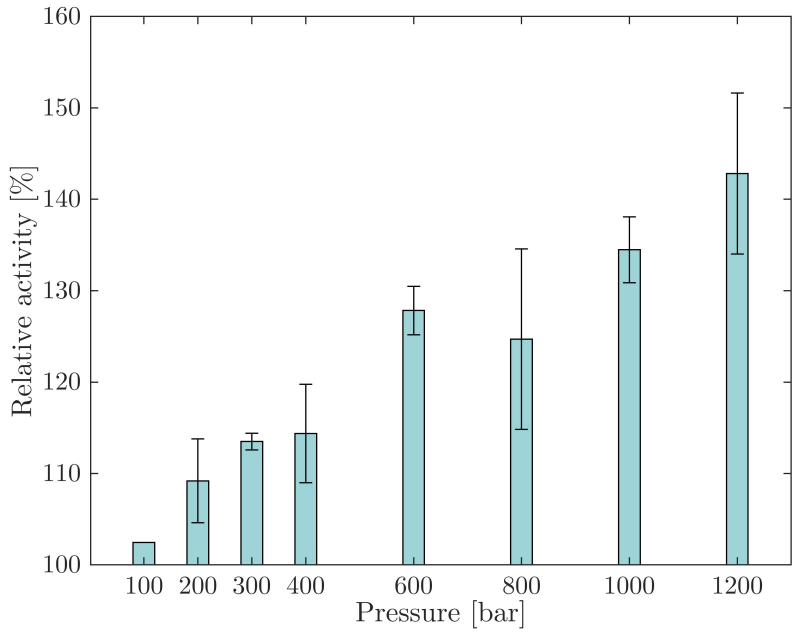

Figure 31: Investigation of the pressure induced increase of CRL activity. Relative activity as a function of pressure. Reaction conditions: $T = 35$ °C; $\dot{V} = 0.35$ ml ·min^{-1}; solvent: heptane; $c_{PP} = 10.0$ mmol ·L^{-1}; $c_{vin} = 2712.5$ mmol ·L^{-1}; p = 1-1,200 bar; reactor dimensions: 50 x 3 mm; $m_{TR13} = 0.1$ g; ECR 1090; $m_{CRL} = 0.120$ mg; n = 1-3.

All presented values are related to the activity of CRL at ambient pressure for each series of measurements. In relation to the activity of CRL at 1 bar, the activity was increased by 9.2 ± 4.6 % at 200 bar, 14.4 ± 5.4 % at 400 bar and 24.7 ± 9.9 % at 800 bar. A hydrostatic pressure of 1,200 bar resulted in the highest activity increase of 42.8 ± 8.8 %.

HHP can improve enzyme activities by altering the enzyme structure and changing the physical properties of both the substrate and the solvent [2,135–138]. Different enzymes show a maximum of activity enhancement at different pressure levels and it is reported that that the activity remains constant or decreases at a certain pressure [2,13,137–139]. Eisenmenger *et al.* (2009) described the effect of pressure on lipases from various organisms. Eight different lipases showed a pressure induced activity enhancement at pressures between 80 and 3500 bar.[2] Herbst *et al.* (2014) found that the increase of pressure from 500 to 2,000 bar led to an increase in the activity of CRL, dependent on the reaction temperature. At 35 °C the increase of activity between 1 and 500 bar was 170 % when water (1 µL ·mL^{-1}) was added to the organic solvent.[43] Furthermore, Chen *et al.* (2016) investigated the effect of HHP on a transesterification reaction catalyzed by CRL. An activating effect was found below 3,000 bar resulting in an activity increase of 90 %. At pressures higher than 4,000 bar, the activity of CRL was reduced compared to the activity at ambient pressure. In addition, Chen *et al.* (2016) pointed out that the activity

and the effect of HHP on the activity of CRL strictly depends on the solvent in which the reaction was performed.[15]

Enantioselectivity is an essential advantage of enzymes over chemical catalysts and therefore an elementary parameter in the characterization of an enzyme. Therefore, the enantiomeric selectivity of the CRL was another important parameter to investigate.
As the conversion of the measurement at different pressures is not the same, the enantiomeric excess *ee* is not directly comparable. The enantioselectivity *E* or *E*-value is used as a decision criterion on the selectivity of the CRL as it is independent of the conversion, it is calculated according to Equation 3-14. This criterion can be used since the reaction is irreversible, as described in 4.2.1.1. The *E*-value of the transesterification catalyzed by CRL is plotted in Figure 32.

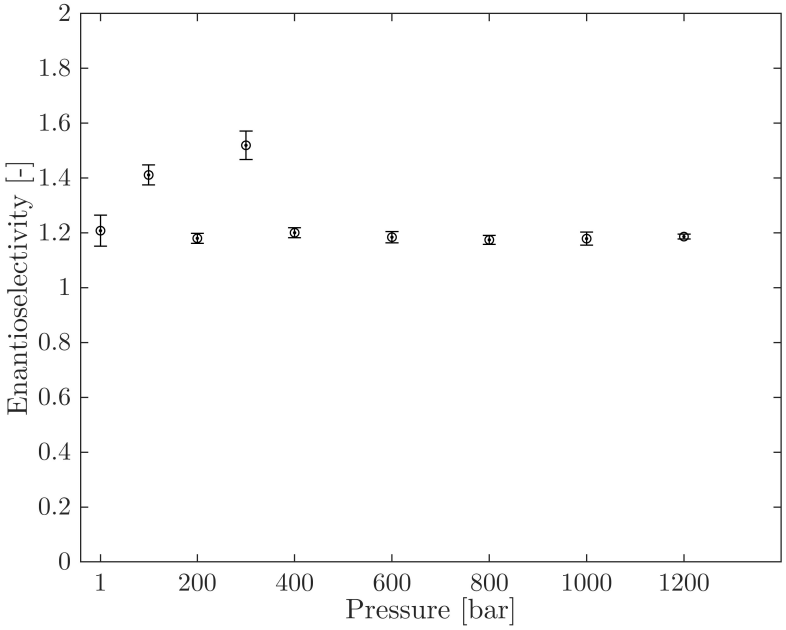

Figure 32: Investigation of pressure induced change of CRL enantioselectivity. *E*-value of product over pressure. Reaction conditions: $T = 35$ °C; $\dot{V} = 0.35$ ml ·min^{-1}; solvent: heptane; $c_{PP} = 10.0$ mmol ·L^{-1}; $c_{vin} = 2712.5$ mmol ·L^{-1}; p = 1-1,200 bar; reactor dimensions: 50 x 3 mm; $m_{TR13} = 0.1$ g; ECR 1090; $m_{CRL} = 0.120$ mg; n = 1-3.

The *E*-value of the reaction was 1.2 ± 0.1 at ambient pressure. At 400 bar and 1,000 bar the value was 1.2 ± 0.02 and 1.2 ± 0.02, respectively. An *E*-value of maximum 1.5 is not industrially relevant since only reactions with an enantioselectivity of over 35 are interesting for industrial production processes.[3] Furthermore, the HHP does not change the enantioselectivity of the enzyme of the transesterification. Herbst *et al.* (2014) found that the increase of pressure from 500 to 2,000 bar led to an increase in the enantioselectivity of CRL dependent on the reaction solvent. Below 500 bar a decrease in enantioselectivity was observed. Although an increase in enantioselectivity was detected for all tested solvents, hexane,

tetrahydrofuran, and a mixture of both, it was different for each solvent, which leads to the assumption that the solvent has an influence on the enantioselectivity as well [43,140]. Kahlow *et al.* (2001) described a pressure-dependent enantioselectivity of CRL on the transesterification of menthol. CRLs enantioselectivity decreased from an *E*-value of 55 at 1 bar to an *E*-value of 9 at 100 bar [141]. Furthermore, Zhao *et al.* (2015) investigated that the enantiomeric selectivity depends on the water content of the solvent and the level of pressure [14]. Even at ambient pressure, the choice of solvent has an influence on the enantioselectivity of the corresponding enzyme reaction [3].

Overall CRL is known to be not enantioselective, which was first described by Kazlauskas *et al.* (1991) especially for acyclic substrates like the PP used [126,142,143]. The crystal structure of the CRL shows a relatively large active center, which leads to low enantioselective for aliphatic substrates [144].

4.4.3. Investigation of the Kinetic Parameters of *Candida rugosa* Lipase in Packed Bed Reactor

For the investigation of the kinetic parameters, the dependence of the specific activity of CRL on the PP and vinyl acetate concentration in relation to the mass of enzyme ($U \cdot mg_{PPK}^{-1}$) was measured at ambient and high pressure (800 bar) and given in Figure 33. The activity of the CRL was calculated using Equation 3-6.

A. ambient pressure

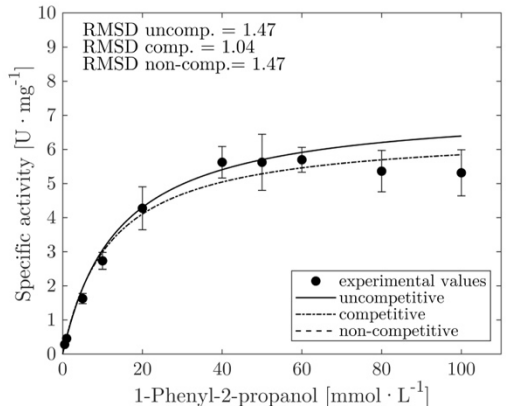

B. ambient pressure

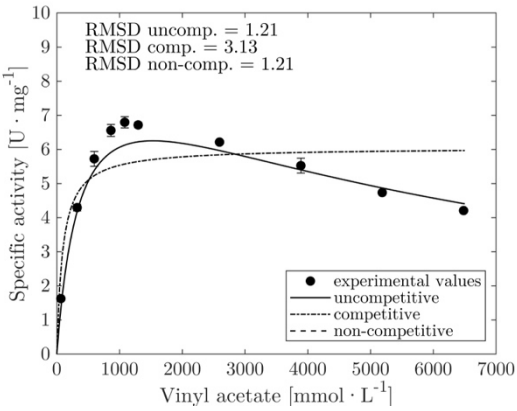

C. 800 bar

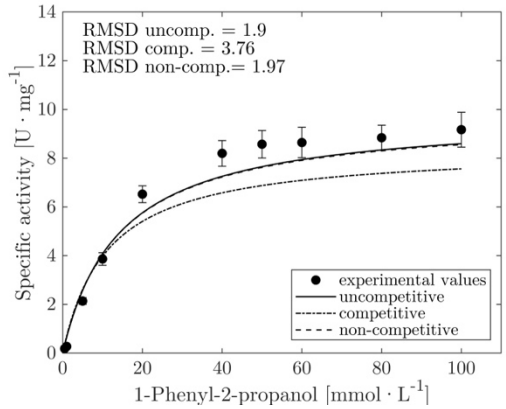

D. 800 bar

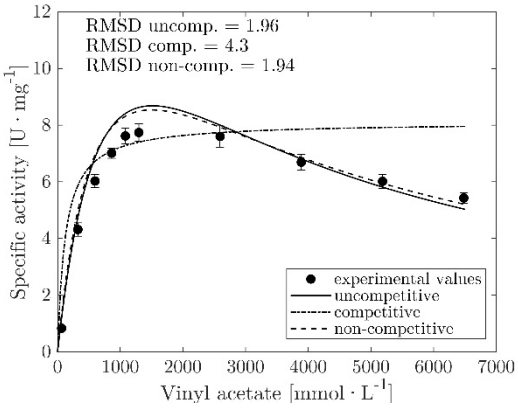

Figure 33: Investigation of kinetic parameters of CRL in PBR at ambient (A,B) and high hydrostatic pressure of 800 bar (C, D). Specific activity over substrate concentration.
Reaction conditions: $T = 35$ °C; $\dot{V} = 1.5$ ml ·min^{-1}; solvent: heptane; A/C: $c_{PP} = 0.0 - 100.0$ mmol ·L^{-1}; $c_{vin} = 864.0$ mmol ·L^{-1}; B/D: $c_{PP} = 60.0$ mmol ·L^{-1}; $c_{vin} = 0.0 - 5425.0$ mmol ·L^{-1}; $m_{TR21} = 0.0533$ g; ECR 1090; $m_{CRL} = 0.446$ mg; $t_{sampling} = 2$ min; 250 rpm; p = 1-800 bar; reactor dimensions: 30 x 3 mm; $\bar{t} = 0.38 \pm 0.01$ min; $n = 3$.

Figure 33 A and B show the results of the investigation of the kinetics CRL at ambient pressure. Figure 33 C and D show the results of the investigation at 800 bar. In Figure 33 A the activity in relation to the PP concentration is shown. The activity of CRL increased with increasing substrate concentration up to 4.3 U · mg^{-1} at a PP concentration of 20.0 mmol · L^{-1}. At higher PP concentrations the specific activity remained constant for 50.0, 60.0 and 80.0 mmol · L^{-1} with 5.6 U · mg^{-1} 5.7 U · mg^{-1} 5.4 U · mg^{-1}. In Figure 33 B the activity in relation of the vinyl acetate concentration is depicted. The activity of the CRL increased with increasing substrate concentration up to 6.8 U · mg^{-1} at a vinyl acetate concentration of 1082.4 mmol · L^{-1}. At higher vinyl acetate concentration, the activity decreased to 6.2 U · mg^{-1} and 4.7 U · mg^{-1} at 2592.6 mmol · L^{-1} and 5185.3 mmol · L^{-1}, respectively.
Figure 33 C shows the activity in relation to the PP concentration at 800 bar. The activity of CRL increased with increasing substrate concentration up to 6.5 U · mg^{-1} at a PP concentration of 20.0 mmol · L^{-1}. At higher PP concentrations the specific activity remained nearly constant for 50.0 and 80.0 mmol · L^{-1} with 8.6 U · mg^{-1} and 8.8 U · mg^{-1}, respectively. Figure 33 D shows

the activity in relation of the vinyl acetate concentration at 800 bar. The activity of the CRL increased with increasing substrate concentration up to 7.7 $U \cdot mg^{-1}$ at a vinyl acetate concentration of 1296.3 $mmol \cdot L^{-1}$. At higher vinyl acetate concentrations, the activity decreased to 7.6 $U \cdot mg^{-1}$ and 6.0 $U \cdot mg^{-1}$ at 2592.6 $mmol \cdot L^{-1}$ and 5185.3 $mmol \cdot L^{-1}$, respectively. These results lead to the assumption that the CRL is inhibited by the substrate vinyl acetate at concentrations higher than 391.0 $mmol \cdot L^{-1}$ and 1020.7 $mmol \cdot L^{-1}$, at 1 bar and 800 bar, respectively, if uncompetitive inhibition is assumed. This confirms the results from 4.2.1.2 where the kinetics of CRL in the STR were determined. A substrate inhibition of CRL by vinyl acetate was described by Palocci *et al.* (2008) and Zhong *et al.* (2013) [127,145].

To further characterize the CRL, the kinetic parameters were determined. The parameters were fitted to the three inhibition types to take into account the substrate inhibition by vinyl acetate. Based on the evaluated activity data as a function of PP and vinyl acetate, a substrate inhibition by vinyl acetate was determined. The kinetic parameters were determined as previously described for the transesterification reaction operated in the STR, as described in 3.7.1.3. The data of the kinetic constants and the corresponding confidence interval regarding the inhibition types are given in Table 25 at ambient pressure and in Table 26 at 800 bar.

Table 25: Estimated model parameters according to the type of inhibition with RMSD for CRL at ambient pressure.

	uncompetitive inhibition		competitive inhibition		noncompetitive inhibition	
	calculated	95 % confidence interval	calculated	95 % confidence interval	calculated	95 % confidence interval
v_{max} [$U \cdot mg^{-1}$]	11.6	± 3.9	10.2	± $2.6 \cdot 10^{7}$	12.5	± 5.7
$K_{M,PP}$ [$mmol \cdot L^{-1}$]	13.8	± 7.1	11.9	± 11.3	13.8	± 7.1
$K_{M,vin}$ [$mmol \cdot L^{-1}$]	391.0	± 320.2	131.8	± $3.4 \cdot 10^{8}$	420.5	± 395.5
$K_{I,vin}$ [$mmol \cdot L^{-1}$]	5999.7	± 4556.1	323.0	± $2.0 \cdot 10^{9}$	5579.2	± 4913.2
RMSD [$U \cdot mg^{-1}$] PP	1.5		1.0		1.5	
RMSD [$U \cdot mg^{-1}$] vin	1.2		3.1		1.2	

Table 26: Estimated model parameters according to the type of inhibition with RMSD for CRL at 800 bar.

	uncompetitive inhibition		competitive inhibition		noncompetitive inhibition	
	calculated	95 % confidence interval	calculated	95 % confidence interval	calculated	95 % confidence interval
v_{max} [U · mg^{-1}]	25.2	± 18.2	30.5	± 2.2 · 10^{8}	42.1	± 2.1 · 10^{5}
$K_{M,PP}$ [mmol · L^{-1}]	14.1	± 7.7	11.1	± 14.0	13.9	± 7.8
$K_{M,vin}$ [mmol · L^{-1}]	1020.7	± 1203.5	391.5	± 2.8 · 10^{9}	1500.7	± 7.4 · 10^{6}
$K_{I,vin}$ [mmol · L^{-1}]	2242.1	± 2439.0	179.8	± 6.2 · 10^{8}	1501.0	± 7.4 · 10^{6}
RMSD [U · mg^{-1}] PP	1.9		3.8		2.0	
RMSD [U · mg^{-1}] vin	2.0		4.3		1.9	

Due to the large confidence interval at ambient pressure and 800 bar, competitive inhibition can be excluded. Furthermore, the large confidence interval of the noncompetitive imbibition type at 800 bar led to the exclusion of this type of inhibition for the transesterification reaction. Reasonable values for the 95 % confidence interval were predicted for the uncompetitive inhibition type. Together with the predictions of the kinetic parameters in the discontinuously operated STR, it was assumed that the uncompetitive inhibition type is the most reasonable description of the reaction system.

The calculated value and the 95 % confidence interval for v_{max} for uncompetitive inhibition at ambient pressure was determined to be 11.6 ± 3.9 U · mg^{-1} and 25.2 ± 18.2 U · mg^{-1} at 800 bar. For $K_{M,PP}$ a value of 13.8 ± 7.1 mmol · L^{-1} was predicted at ambient pressure and 14.1 ± 7.8 mmol · L^{-1} at 800 bar. The kinetic parameters $K_{M,vin}$ and $K_{I,vin}$ describe the dependence of the activity and inhibition of CRL from vinyl acetate. $K_{M,vin}$ and $K_{I,vin}$ were determined to 391.0 mmol · L^{-1} and 5999.7 mmol · L^{-1} at ambient pressure as well as 1020.7 mmol · L^{-1} and 2242.1 mmol · L^{-1} at 800 bar, respectively.

In order to obtain a prediction about the accuracy of the model's description of the measured data, the RMSD was used, as described in 4.2.1.2. A RMSD value of 1.5 U · mg^{-1} (PP) and 1.2 U · mg^{-1} (vinyl acetate) was calculated for ambient pressure and 1.9 U · mg^{-1} (PP) and 2.0 U · mg^{-1} (vinyl acetate) at 800 bar for uncompetitive inhibition. The complete data is listed in Table 25 and in Table 26.

The RMSD is lowest for the uncompetitive inhibition type and the 95 % confidence interval is also lowest for the uncompetitive inhibition. Overall, the uncompetitive inhibition type provides the most conclusive data, and therefore this type of inhibition is assumed for CRL by

vinyl acetate. Additionally, this inhibition type was as well determined when the kinetic parameters were studied in batch operation mode in the STR, as described in 4.2.1.2. Furthermore, the substrate surplus inhibition which is determined for this reaction system by vinyl acetate is described by Jaeger *et al.* (2024) as a special case of the uncompetitive inhibition type.[40]

The changes in the dependence of the specific activation of CRL on PP and vinyl acetate are shown in Figure 34 A and B.

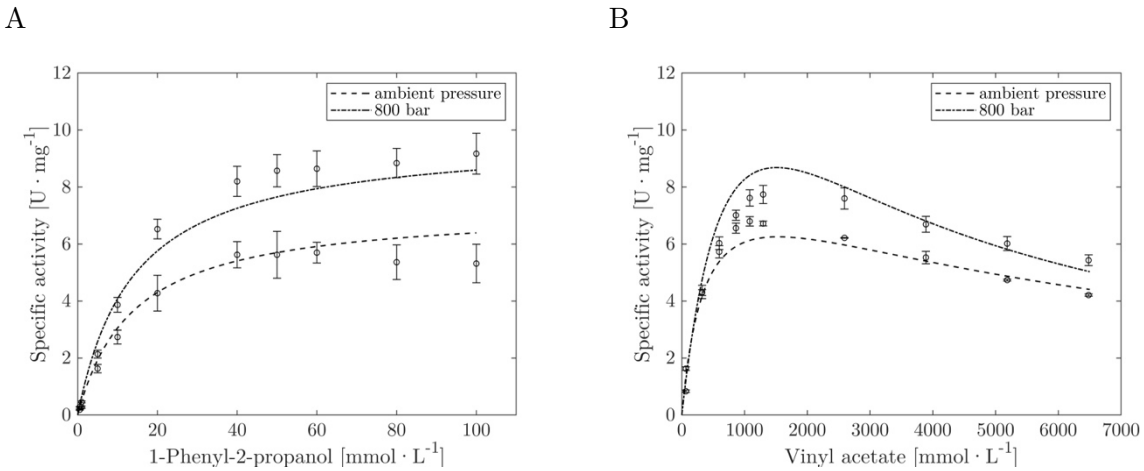

Figure 34: Investigation of the kinetic parameters of CRL in the PBR at ambient and high pressure. Specific activity over substrate concentration.
Reaction conditions: $T = 35$ °C; $\dot{V} = 1.5$ ml ·min^{-1}; solvent: heptane; $c_{PP} = 0.0$ - 100 mmol ·L^{-1}; $c_{vin} = 0.0$ – 5425.0 mmol ·L^{-1}; $m_{TR21} = 0.0533$ g; $m_{CRL} = 0.446$ mg; ECR 1090; $t_{sampling} = 2$ min; 250 rpm; $p = 1$-800 bar; reactor dimensions: 30 x 3 mm; $\bar{t} = 0.38 \pm 0.01$ min; $n = 3$.

The v_{max} increased by the factor 2.2 with increasing pressure from ambient to 800 bar which indicates enhanced specific activity of CRL, while the $K_{M,PP}$ value was unchanged. The K_M indicates the affinity of enzyme to the substrate, therefore no change in the interaction between the enzyme and the substrate PP is expected [3].
The K_M-value of the second substrate vinyl acetate changed from 391.0 mmol · L^{-1} at ambient pressure to 1020.7 mmol · L^{-1} at 800 bar, which indicates that the affinity towards the substrate vinyl acetate decreased. To achieve the maximum reaction rate, a higher substrate concentration of vinyl acetate is required [75]. The $K_{I,vin}$-value decreased from 5999.7 mmol · L^{-1} at ambient pressure to 2242.1 mmol · L^{-1} at HHP. The K_I-value describes the equilibrium constant for the dissociation of the enzyme inhibitor complexes [100]. This indicates that the inhibitor concentration is reduced by a factor of 2.6 therefore the increase of the pressure from 1 bar to 800 bar leads to more severe substrate inhibition by vinyl acetate.

Eisenmenger *et al.* (2010) investigated the CalB catalyzed synthesis of isoamyl acetate in hexane at pressures up to 2500 bar. A 10-fold increase of v_{max} when pressure was increased from 1 bar to 2,000 bar was found. The K_M-value at 40 °C increased by the factor 15 resulting in a

lower affinity to the substrate which is unfavorable for an enzymatic catalyzed reaction. At 80 °C no effect on the K_M-value was found.[146] Knop *et al.* (2023) investigated the effect of high pressure up to 200 bar on a formate dehydrogenase. The K_M-value of formate decreased with increasing pressure while the initial reaction rate of the reaction increased. [136] Chen *et al.* (2017*)* investigated the effect of high pressure on a *Rhizopus chinensis* lipase (RCL) catalyzing the hydrolysis of 4-nitrophenolpalmitate in an aqueous system. The K_M-value decreased by 25.5 % and v_{max} increased by 24.4 % when pressure was increased from 1 bar to 2,000 bar. If pressure was increased further up to 4,000 bar, the K_M-value increased while v_{max} decreased.[147] The shift of the catalytic parameters of the RCL were related to the volume changes during the formation of the reaction transition state [148]. It is known that enzyme performance can be modified by pressure-induced conformational changes [147].

In the case of the substrate surplus inhibition described here, carrying out the enzymatic reaction in a continuously operated flow reactor is not advantageous, because the concentration of the inhibitor must be kept as low as possible and this is not practical to achieve maximum yield in this type of reactor.[3] In the case of the investigated reaction carrying out the reaction in the PBR since vinyl acetate has a K_I-value of 5999.7 mmol · L^{-1} at ambient pressure to 2242.1 mmol · L^{-1} at 800 bar may be applicable. At ambient pressure a maximum specific activity of 6.4 U · mg^{-1} was achieved at a PP concentration of 100.0 mmol · L^{-1} and 862.0 mmol · L^{-1} of vinyl acetate. At a pressure of 800 bar the maximum specific activity of CRL was 8.7 U · mg^{-1} at a PP concentration of 60.0 mmol · L^{-1} and 1526.9 mmol · L^{-1} of vinyl acetate. The transesterification reaction studied here is an equimolar reaction, i.e., one molecule of each substrate is used. In this case, the reaction is limited by the non-inhibiting substrate PP, as the maximum reaction rate is reached at lower concentrations than the concentration at which substrate inhibition occurs from the vinyl acetate. It is possible to work with a substrate excess of the inhibiting vinyl acetate of 8-fold at ambient pressure and 25-fold at 800 bar. Nevertheless, even at this excess of vinyl acetate of 8 to 25-fold the inhibiting concentration of vinyl acetate of 5999.7 mmol · L^{-1} at ambient pressure to 2242.1 mmol · L^{-1} at high pressure is not reached.
It can therefore be concluded that, for this particular case, the reaction can be taken out in the PBR, as this reactor concept allows the determination of the influence of HHP on the enzyme activity and selectivity of the CRL.

4.4.4. Summary Characterization of *Candida rugosa* Lipase in Continuously Operated Packed Bed Reactor

The application of the CRL in the continuously operated HHP reactor was investigated in terms of stability, activity, and enantioselectivity at ambient and elevated pressure of up to 1,200 bar. Furthermore, the enzyme kinetics of CRL were studied at ambient and elevated hydrostatic pressure.

Despite the relatively large experimental error, the mean half-life at 800 bar was increased compared to the mean half-life at 1 bar. An increase of enzyme activity at 1,200 bar resulted in the highest activity increase of 42.8 ± 8.8 %. In contrast, no influence of HHP on the enantioselectivity of CRL could be determined.

To further characterize the CRL, the kinetic parameters and the probable inhibition type were determined. CRL exhibit substrate inhibition by vinyl acetate at ambient and elevated pressures. The calculated value and the corresponding 95 % confidence interval for v_{max} were determined to be 11.6 ± 3.9 U · mg^{-1} at ambient pressure and 25.2 ± 18.2 U · mg^{-1} at 800 bar for the assumption of uncompetitive inhibition. For $K_{M,PP}$ a value of 13.8 ± 7.1 mmol · L^{-1} was calculated at ambient pressure and a value of 14.1 ± 7.8 mmol · L^{-1} at 800 bar. The kinetic parameters $K_{M,vin}$ and $K_{I,vin}$, describing the dependence of the activity and inhibition of CRL from vinyl acetate, were determined to 391.0 mmol · L^{-1} and 5999.7 mmol · L^{-1} at ambient pressure as well as 1020.7 mmol · L^{-1} and 2242.1 mmol · L^{-1} at 800 bar, respectively.

The v_{max} increased by the factor 2.2 with increasing pressure from ambient to 800 bar, which indicates an enhanced specific activity of CRL, while the $K_{M,PP}$-value was unchanged. The K_M indicates the affinity of enzyme to the substrate, therefore no change in the interaction between the enzyme and the substrate PP is to be expected [3]. The K_M-value of the second substrate vinyl acetate increased, indicating that the affinity towards the substrate vinyl acetate decreased. To achieve the maximum reaction rate, a higher substrate concentration of vinyl acetate is required [75]. The $K_{I,vin}$-value decreased from 5999.7 mmol · L^{-1} at ambient pressure to 2242.1 mmol · L^{-1} at 800 bar. The K_I-value describes the equilibrium constant for the dissociation of the enzyme inhibitor complexes [100]. This indicates that the inhibitor concentration is reduced by a factor of 2.6, and therefore, the increase in the pressure from 1 bar to 800 bar results in more severe substrate inhibition by vinyl acetate.

Overall, these results indicate that performing an enzymatic reaction at different hydrostatic pressures can influence the kinetic parameters and might therefore be an interesting parameter to adjust the enzyme performance for a more successful application of enzymes in various industrial processes.

4.5. Characterization of *Candida antarctica* Lipase B in the Continuously Operated Packed Bed Reactor

The following section describes the experiments using CalB in the High Hydrostatic Pressure System at TU Hamburg. First, the stability of the CalB was investigated under ambient pressure followed by the investigation of the influence of hydrostatic pressure on the activity, and selectivity of CalB.

4.5.1. Investigation of the Stability of *Candida antarctica* Lipase B

The change in the specific activity of CalB over time was investigated to ensure that the biocatalyst was stable throughout the duration of the experiment and to determine the

influence of pressure on enzyme stability and activity. The activity of CalB is given as a function of time in Figure 35.

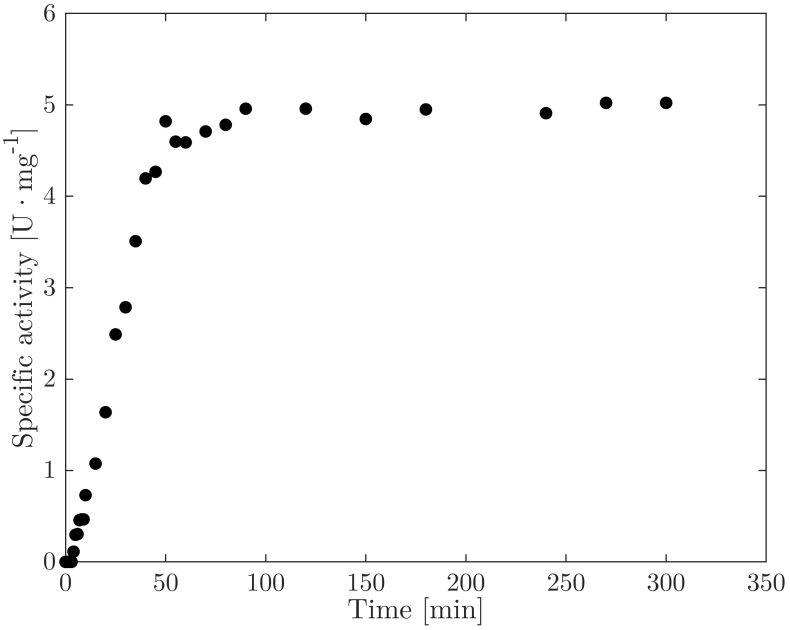

Figure 35: Investigation of process stability of CalB. Specific activity over time.
Reaction conditions: $T = 35$ °C; $\dot{V} = 0.5$ ml ·min^{-1}; solvent: heptane; $c_{PP} = 10.0$ mmol ·L^{-1}; $c_{vin} = 864.0$ mmol ·L^{-1}; reactor dimensions: 50 x 3 mm; $m_{TR12} = 0.1701$ g; ECR 1090; $m_{CalB} = 0.195$ mg; $t = 300$ min; $p = 1$ bar; $n = 1$.

As shown in Figure 35, the activity of CalB increased from 0.3 U · mg^{-1} at 5 min to 2.8 U · mg^{-1} at 30 min. and to 5.0 U · mg^{-1} after 90 min. Subsequently, the specific activity stayed nearly constant until the end of the experiment, up to 300 min. The mean residence time was determined to ensure that this phenomenon was not a result of, e.g., backmixing of the reactor content. A mean residence time of 1.04 min was calculated at a flow rate of 0.5 ml · min^{-1}, as described in 3.8.3. The increase in activity until 90 min can activity could be explained by the subsequent formation of channeling in the reactor bed or swelling of the particles.[3,130,131] A similar effect was investigated for immobilized CRL in the PBR, as described in 4.3.1.
Thus, in the following experiments, a waiting period of 90 min was observed before the experiment was started.
The results presented are consistent with former investigations. Immobilized CalB has been described as a temperature stable enzyme, e.g., it shows activity in the synthesis of acetic acid isopentyl ester in n-hexane at 100 °C [149]. Whitaker *et al.* (1989) investigated the stability in the continuous acidolysis of soybean oil and lauric acid using immobilized CalB; a half-life of 500 hours at 80 °C and over 2500 hours at 60 °C was measured [150].

4.5.2. Investigation of the Activity in Dependence of Pressure and Temperature

To investigate the influence of high pressure up to 1,200 bar on the activity of CalB, the influence of two HHP steps was studied per experiment. The first HHP stage was preceded by

90 min at 1 bar to achieve steady-state conditions as described in 4.5.1. After each HHP step, the pressure was reduced to 1 bar in order to get a comparative specific activity value for CalB. In addition to applying the HHP steps to 400, 600, 800 and 1,200 bar, the transesterification reaction was carried out at 35 °C, 45 °C, 55 °C, and 65 °C. An overview of the performed experiments is given in the appendix in Table 34.
The activity was calculated using Equation 3-6. Figure 36 shows the activity of CalB at different HHP and temperatures.

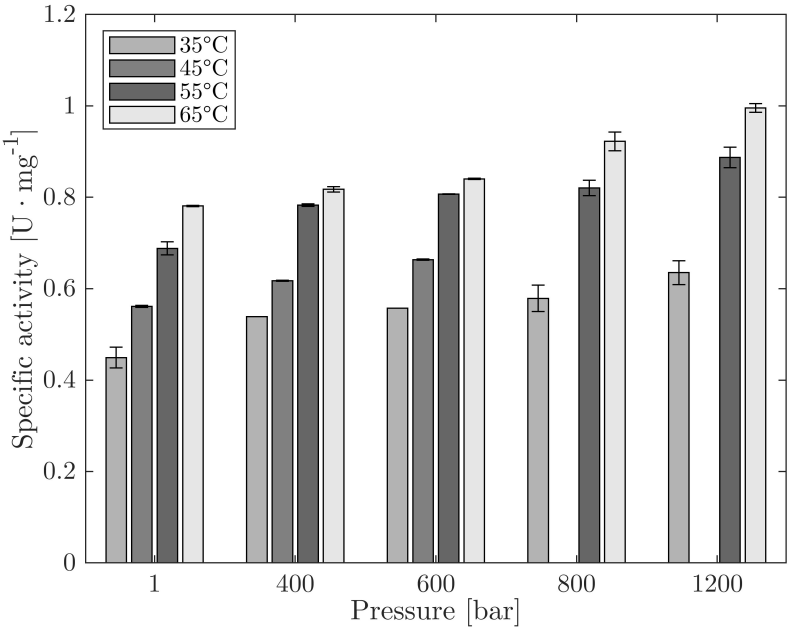

Figure 36: Investigation of the activity in dependence of pressure and temperature. Specific activity of CalB as a function of pressure in dependence of temperature.
Reaction conditions: T = 35-65 °C; $\dot{V}$ = 0.5 ml ·min^{-1}; solvent: heptane; c_{PP} = 10.0 mmol ·L^{-1}; c_{vin} = 864.0 mmol ·L^{-1}; reactor dimensions: 50 x 3 mm; $m_{TR15/TR18}$ = 0.15 g; ECR 1090; m_{CalB} = 0.195/0.741 mg; p = 1 bar; n = 1-2.

At 1 bar and 1,200 bar, the specific activity of CalB at 35 °C was 0.5 ± 0.02 U · mg^{-1} and 0.7 ± 0.03 U · mg^{-1}, respectively. With increasing temperature, the activity of CalB increased to 0.7 ± 0.01 U · mg^{-1} and 0.9 ± 0.02 U · mg^{-1} at 1 bar, respectively 1,200 bar at 55 °C. All data is given in Table 34 in the appendix. The results presented show that the specific activity of CalB increases with increasing temperature regardless of the pressure. This is in accordance to findings of Romero *et al.* (2005) who observed a linear increase in CalB activity in the temperature range from 30 °C to 65 °C for the production of isoamyl acetate in hexane [149].

The activity data of the 45 °C experiment at 800 bar and 1,200 bar are excluded from Figure 36 because these experiments were performed with a different batch of immobilizate. The immobilization batch used in the experiment at 45 °C and 800/1,200 bar was TR 18. The TR 18 immobilization batch had an immobilization loading of 6.0 $mg_{CalB} \cdot g_{carrier}^{-1}$, while TR 15 batch had an immobilization loading of 17.4 $mg_{CalB} \cdot g_{carrier}^{-1}$. Thus, the immobilization batch TR 18 had an enzyme loading approximately 65.3 % lower than the batch TR 15. Nevertheless,

comparable activities could be measured with the immobilization batch TR 18. Thus, at 35 °C and 1 bar, an activity of 0.7 U · mg^{-1} (35 °C and 400/600 bar) was measured with TR 18 and an activity of 1.2 U · mg^{-1} (35 °C and 400/600 bar) with TR 15. Here, accumulation of the enzyme on the carrier surface in multiple layers could be a possible reason for the reduced specific activity, even though batch TR 15 provided a high loading of enzyme. Thus, a high density of enzyme occupancy on the carrier surface can lead to mutual restriction of the neighboring enzyme molecules. The associated steric hindrance with regard to substrate accessibility in the active site is reflected in a low specific activity.[151]
To overcome this, the increase in activity in relation to the activity at 1 bar was calculated to compare the results with each other. The results are given in Table 27.

Table 27: Increase in activity in relation to the activity at 1 bar in percent. Investigating of activity in dependency on pressure and temperature.

Temperature	Increase in activity in relation to the activity at 1 bar [%]			
[°C]	400 bar	600 bar	800 bar	1,200 bar
35	18.8 ± 0.8	26.2 ± 4.2	28.9 ± 0.1	41.4 ± 1.3
45	10.0 ± 0.3	18.2 ± 0.2	27.3 ± 0.8	42.3 ± 2.3
55	11.7 ± 3.3	15.0 ± 3.0	19.2 ± 2.5	28.9 ± 0.6
65	7.7 ± 0.1	10.7 ± 1.1	18.1 ± 2.9	27.5± 1.5

The increase in activity was 41.4 ± 1.3 % from 1 to 1,200 bar at 35 °C, 42.3 ± 2.3 at 45 °C and 27.5 ± 1.5 % at 65 °C. Therefore, the activity of CalB increases with temperature as the HHP is elevated. The effect of pressure induced activation is higher at lower temperatures.

Similar effects were investigated by Vilareal *et al.* (2007) for the temperature-induced pressure activation in an aqueous environment in the hydrolysis of naringin by naringinase. The initial reaction rates at 25 °C, 30 °C, 35 °C, and 40 °C were studied at 1600 bar and compared to the initial reaction rate at 1 bar and the corresponding temperature. The highest pressure activation was observed at 30 °C with an activity increase of 94 %. In contrast, an increase of 25 %, 10 %, and 15 % was measured at 25 °C, 35 °C and 40 °C, respectively.[152] Eisenmenger *et al.* (2009) investigated the combined effect of pressure and temperature on CalB activity in organic solvent as well. The activity of CalB was higher at higher temperatures for all pressures from 1 to 600 bar. The CalB activity increased by 110 % at ambient pressure when the temperature was increased from 40 to 80 °C, while the activity increased by 239 % at 3500 bar at the same temperature increase. [13] This higher increase in enzyme activity at higher temperatures and pressures was explained by a shift in the tertiary structure surrounding the active site allowing greater substrate interaction [153]. Further examples of lipase activation by high pressure are given by Eisenmenger *et al.* (2009). The increase of CalB activity was described for different catalyzed reactions in variant solvents and by different methods of pressurization, namely HHP or the use of supercritical carbon dioxide.[2] Romero *et al.* (2005)

investigated CalB activity in dependence on pressure in supercritical carbon dioxide. No effect of pressure between 80 and 300 bar on the activity of CalB was found. [149] The level of increase in the specific activity of CalB depends on all these parameters and therefore no general statement can be made about the specific influence of high pressure on the activity of CalB.

4.5.3. Influence of Pressure on Selectivity

In the following section, the enantioselectivity with respect to the formation of the *R*-enantiomer of the product *R*-PPA of immobilized CalB under HHP is evaluated, as the enantioselectivity of the enzyme is the most valuable property, especially in industrial processes [154,155]. The enantioselectivity *E* with respect to the *R*-enantiomer product at steady-state is plotted in Figure 37 against the corresponding HHP levels.

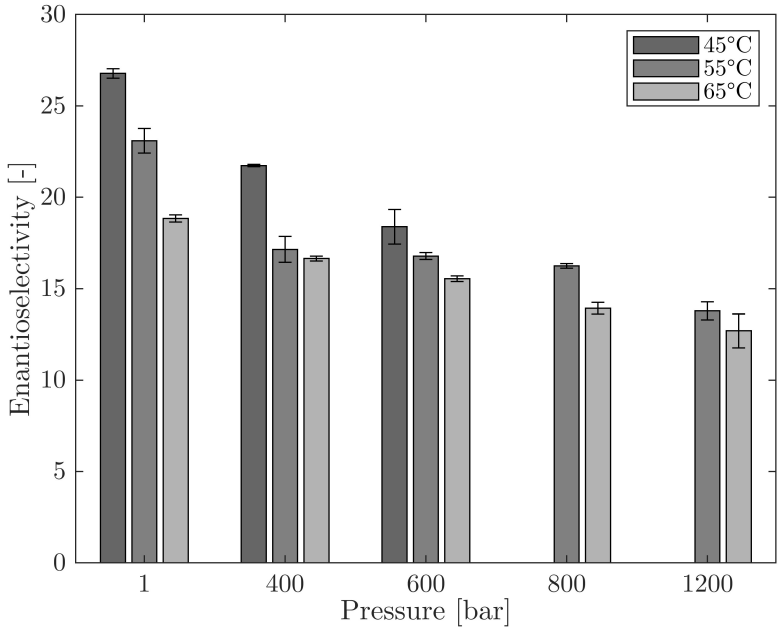

Figure 37: Investigation of the enantioselectivity of CalB in dependence of pressure and temperature. Reaction conditions: T = 45-65 °C; $\dot{V}$ = 0.5 ml ·min^{-1}; solvent: heptane; c_{PP} = 10.0 mmol ·L^{-1}; c_{vin} = 864.0 mmol ·L^{-1}; reactor dimensions: 50 x 3 mm; $m_{TR15/TR18}$ = 0.15 g; ECR 1090; m_{CalB} = 0.195/0.741 mg; p = 1 bar; n = 1-2.

Due to the high deviation caused by handling errors with the samples before analysis, the data of the experiments carried out at 35 °C are excluded from this investigation. Furthermore, the data set measured at 45 °C and 800 bar and 1,200 bar are not included, because another batch of immobilizates was used for these experiments described in 4.5.2.

The *E*-value of CalB at 45 °C and at ambient pressure was 26.8 ± 0.3, 21.7 ± 0.1 at 400 bar, and 18.4 ± 1.0 at 600 bar, respectively. At 65 °C the enantioselectivity was 20.8 ± 0.4 at ambient pressure, 16.7 ± 0.1 at 400 bar and 12.7 ± 0.9 at 1,200 bar, respectively. A pressure-dependent decrease of the enantioselectivity with respect to the *R* - enantiomer of the product was observed. At 65 °C the enantioselectivity decreased by 39.0 % when the pressure was increased from ambient to 1,200 bar. For all three investigated temperatures the enantioselectivity decreased with increasing pressure.

CalB is known to be highly enantioselective, making this property one of the most important parameters of this biocatalyst [155,156]. Nevertheless, CalB showed different *E*-values from 220 to 278 for a transesterification using different substrates [156]. This was described by Schönstein *et al.* (2013): The enantioselectivity was depending on the substrate and varied between an *E*-value of 1 to over 200. In addition, the enantioselectivity varied between 45 and over 200 depending on the solvent used. [157] In addition to the choice of the solvent, the water content also has an influence on the enantioselectivity of the corresponding enzyme reaction [3,155,157,158]. Léonard-Nevers *et al.* (2009) investigated the effect of the water content of the reaction media on the enantioselectivity and the resulting hydration of the biocatalyst for an acylation catalyzed by CalB. The enantioselectivity decreased with increasing water content because of changes at the enzyme surface.[155] Csajági *et. al* (2008) found no significant effect of pressures up to 120 bar on the selectivity on an acylation of racemic alcohols by CalB. Moreover, the enantioselectivity of CalB changed with temperature. While the *E*-value was 25 at 20 °C, it was reduced to 7 at 50 °C. [159] Ottosson *et al.* found no effect of pressure on the enantioselectivity of CalB in hexane at 214 bar compared to ambient pressure [158]. Therefore, the selectivity of CalB depends on multiple factors and pressure is indicated as one of them.
Since reactions with an enantioselectivity of over 35 are interesting for process development, the presented reaction with a maximal *E*-value of 26.8 at 45 °C can be considered as not industrially relevant [3]. Nevertheless, the application showed that the process parameter *pressure* changed the enantioselectivity of the enzyme of the transesterification. Even though the enantioselectivity was further decreased, this might be an interesting application for a biocatalytic reaction in which the undesired product is formed in excess under ambient conditions.

4.5.4. Summary Characterization of *Candida antarctica* Lipase B in the Continuously Operated Packed Bed Reactor

The stability and activity of CalB were studied in a continuously operated packed bed reactor at ambient and elevated hydrostatic pressures up to 1,200 bar and temperatures ranging from 35 °C to 65 °C.
These results are consistent with previous studies showing that immobilized CalB remains stable at high temperatures up to 65 °C.
The specific activity of CalB increased with temperature, independent of pressure. The activity of CalB at 35 °C increased from 0.5 ± 0.02 U · mg^{-1} at 1 bar to 0.7 ± 0.03 U · mg^{-1} at 1,200 bar. At 35 °C and 1,200 bar, the highest activity increase of 41.4 %, compared to the activity at 1 bar, was observed. Higher temperatures showed similar results, with the highest increases observed at lower temperatures.
These observations support previous studies showing that enzyme activity is dependent on both temperature and pressure, probably due to structural changes that enhance substrate interaction.

The enantioselectivity of CalB in the formation of the *R*-enantiomer of the product *R*-PPA under HHP was also evaluated, focusing on the practical value of this property in industrial processes. At 45 °C, the E-value decreased from 26.8 ± 0.3 at ambient pressure to 18.4 ± 1.0 at 600 bar. At 65 °C it decreased from 20.8 ± 0.4 at ambient pressure to 12.7 ± 0.9 at 1,200 bar. Thus, the enantioselectivity decreased consistently with increasing pressure.
While the highest enantioselectivity observed (E-value of 26.8 at 45 °C) may not be industrially relevant, the study demonstrates that hydrostatic pressure and temperature can modulate enzyme selectivity as well as enzyme activity, which may be useful for processes where a change in the product ratio is advantageous under certain conditions.

4.6. Characterization of *Ruegeria pomeroyi* Polyphosphate Kinase in the Continuously Operated Packed Bed Reactor

In order to use PPK for cofactor regeneration in reaction cascades, a detailed study of the stability, the kinetics of the enzyme and the determination of kinetic parameters based on the Michaelis-Menten theory were investigated. These parameters were fitted to experimental data considering three different types of inhibition (competitive, uncompetitive and non-competitive inhibition) to describe substrate inhibition by polyP. Furthermore, the change in specific activity under HHP up to 800 bar was investigated and a comparison of different operation modes was carried out.

4.6.1. Investigation of the Stability of Polyphosphate Kinase

Experiments were performed to assess the process stability and performance consistency of the enzyme and to characterize the reactor operation itself. The PBR containing the immobilized PPK was continuously operated for 5 h. The results of the activity change over time are shown in Figure 3.

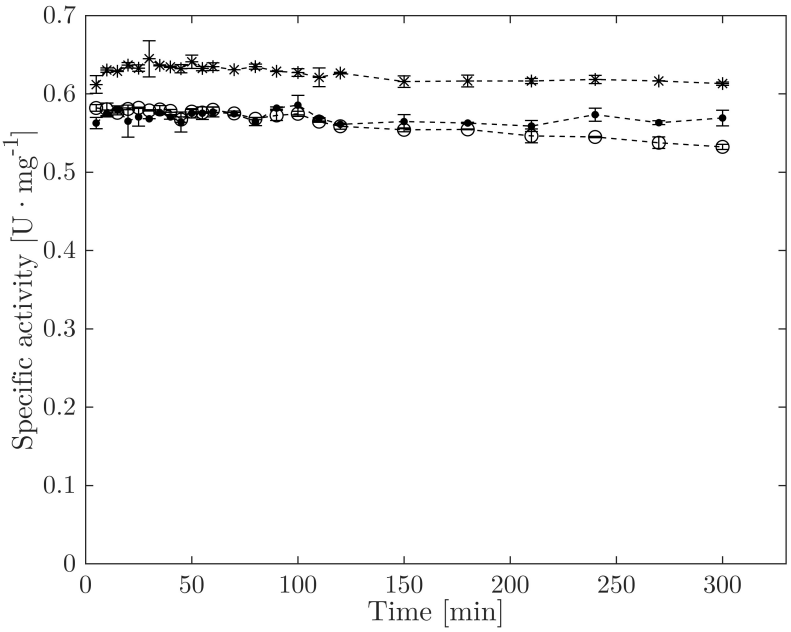

Figure 38: Investigation of polyphosphate kinase stability. Activity of PPK as a function of time.

Reaction conditions: $T = 40$ °C; $\dot{V} = 0.5$ ml $\cdot$min^{-1}; solvent: Na_3PO_4 buffer; $c_{buffer} = 50.0$ mmol $\cdot$ L^{-1}; pH = 7.4; $c_{polyP} = 44.0$ mmol $\cdot$L^{-1}; $c_{CDP} = 25.0$ mmol $\cdot$L^{-1}; $c_{MgCl2} = 30.0$ mmol $\cdot$L^{-1}; $m_{PPK} = 6.80$ mg(o), 6.58 mg(*), 7.11 mg($\cdot$); reactor dimensions: 30 x 3 mm; $\bar{t} = 0.48 \pm 0.03$ min; $n = 3$.

The PPK activity of the three individual experiments, each with new immobilizate, decreased over time in all experiments. The deactivation constant k_d was calculated from the experimental results. The corresponding data is summarized in Table 28.

Table 28: Determination of the deactivation constant and half-life of immobilized PPK.

	experiment 1	experiment 2	experiment 3
k_d [h^{-1}]	$3.14 \cdot 10^{-04}$	$1.38 \cdot 10^{-04}$	$5.39 \cdot 10^{-05}$
$t_{1/2}$ [h]	36.8	83.6	214.3

The half-life of PPK was calculated according to the Equation 3.8.3. The experiments yielded an average half-life of 111.6 h. The decrease of enzymatic activity could be due to thermal deactivation, as the temperature of the experiment was 40 °C [3]. However, it could also be a consequence of the leaching of enzymes from the carrier [3,100,131,160]. The effect of activity loss of immobilized enzymes is comprehensively described in Liese and Hilterhaus (2012) [131]. Nevertheless, the lowest measured half-life was 20-times longer than the longest experiment performed with 110 min described in 3.9.3.3. Taking into account the loss in activity during the experiment for the investigation of the PPK kinetics, the duration of the experiment was acceptable even though the stability of the enzyme could not be verified as high ($t_{1/2} \geq$ 50 - 100 days) [132].

4.6.2. Activity Enhancement by High Pressure

The exposure of PPK to HHP and the investigation of activity changes were the main aspects of this thesis. The specific activity of PPK was determined using Equation 3-7. The results of three experiments are given in Figure 6 A, each experiment labeled is with a different symbol. For each experiment, a new reactor bed was packed with approximate 0.17 g of carrier (carrier load of “50/50”, as described in 3.9.3), resulting in a different amount of enzyme for each run. The specific activity at a pressure of 1 bar was 0.5 U $\cdot$ mg^{-1} (o), 0.7 U $\cdot$ mg^{-1} ($\bullet$) and 0.5 U $\cdot$ mg^{-1} (+), at 200 bar 0.6 U $\cdot$ mg^{-1} (o), 0.7 U $\cdot$ mg^{-1} ($\bullet$) and 0.5 U $\cdot$ mg^{-1} (+) and at 600 bar 0.6 U $\cdot$ mg^{-1} (o), 0.8 U $\cdot$ mg^{-1} ($\bullet$) and 0.6 U $\cdot$ mg^{-1} (+). For all these experiments the activity at ambient pressure was the lowest, while the activity of PPK at 600 bar, respectively 800 bar for the third measurement (+), was the highest. The variations between the specific activity of the three packed reactor beds (o, $\bullet$, +) could be due to the error-prone loading of the packed bed with regard to the amount of immobilizate and the structure of the bed.[131]

A B

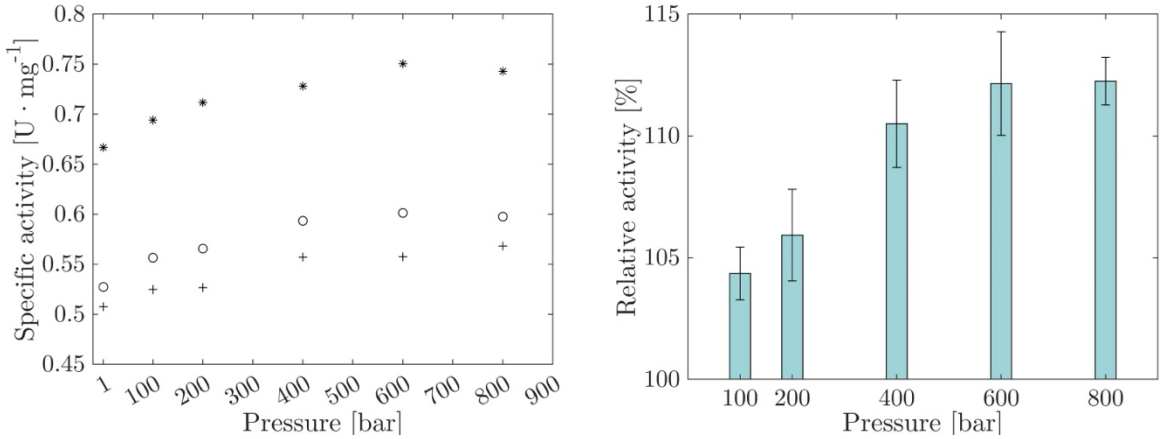

Figure 39: Investigation of polyphosphate kinase activity under pressure. A: Specific activity of PPK as a function of pressure. B: relative activity of PPK as a function of pressure.
Reaction conditions: $T = 40$ °C; $\dot{V} = 1.0$ ml $\cdot$min^{-1}; solvent: Na_3PO_4 buffer; $c_{buffer} = 50.0$ mmol $\cdot$ L^{-1}; pH = 7.4; $c_{polyP} = 44.0$ mmol $\cdot$L^{-1}; $c_{CDP} = 30.0$ mmol $\cdot$L^{-1}; $c_{MgCl2} = 30.0$ mmol $\cdot$L^{-1}; $m_{PPK} = 8.07$ mg (o), 7.18 mg (*), 7.48 mg (+); reactor dimensions: 30 x 3 mm; $\bar{t} = 0.25 \pm 0.01$ min; $n = 3$.

Figure 39 B shows the relative activity of PPK related to the activity of PPK at ambient pressure. In relation to the activity of PPK at ambient pressure, the activity at ,200 bar was 5.9 ± 1.8 % and at 400 bar 10.5 ± 1.2 %. A hydrostatic pressure increased to 600 bar and 800 bar resulted in the highest increase in activity of 12.2 ± 2.1 % and 12.3 ± 0.9 %, which are about the same value. As conclusion it is possible to state that HHP can improve enzyme activities either by altering the enzyme structure, enzyme dynamics, or changing the physical properties of both the substrate and solvent. Pressure may affect all of these phenomena to varying degrees. However, with the methods used in this thesis, it is not possible to distinguish which of these phenomena, alone or in combination, is responsible for the increase in enzyme activity. [2,135–138,161,162]. Different enzymes show a maximum of activity enhancement at different pressure levels. It is reported that the activity remains constant or decreases [2,13,137–139]. The effect of pressure on the activity of a few transferases was studied; among others, γ-glutamyl transferase showed a 35 % increase of activity at 3,000 bar and a reduction of the activity over 4,000 bar [135,163].

4.6.3. Investigation of *Ruegeria pomeroyi* Polyphosphate Kinase Kinetic Parameters in the Packed Bed Reactor

For the investigation of the kinetics, the dependence of the specific activity of PPK on the CDP and polyP concentration in relation to the mass of enzyme ($U \cdot mg_{PPK}^{-1}$) was measured. The specific activity was calculated using Equation 3-7. In Figure 40 the measured specific activity of PPK in relation to the CDP concentration is shown. Additionally, the predicted specific activities in dependency of the different inhibition types are given in Figure 40. For the uncompetitive and the non-competitive inhibition, the same specific activity values were predicted. Therefore, the data is not visible in the Figure 40 and Figure 41.

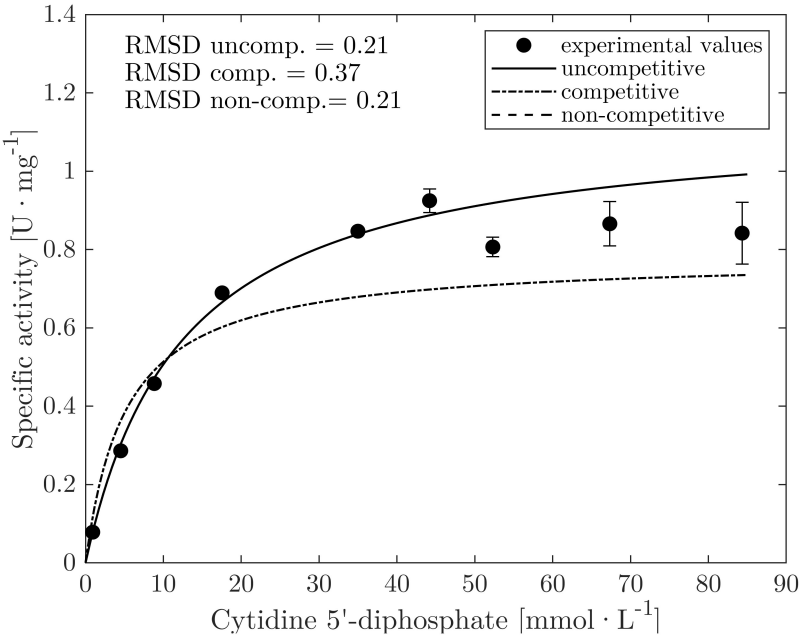

Figure 40: Investigation of kinetic parameters of PPK in PBR at ambient pressure. Specific activity over CDP concentration.

Reaction conditions: $T = 40$ °C; $\dot{V} = 1.5$ ml ·min^{-1}; solvent: Na_3PO_4 buffer; $c_{buffer} = 50.0$ mmol · L^{-1}; pH = 7.4; $c_{polyP} = 44.0$ mmol ·L^{-1}; $c_{CDP} = 1.0$-85.0 mmol ·L^{-1}; $c_{MgCl2} = 30.0$ mmol ·L^{-1}; $m_{PPK} = 3.59$ mg; reactor dimensions: 30 x 3 mm; $\bar{t} = 0.19 \pm 0.01$ min; $n = 6$.

The activity of PPK increased with increasing substrate concentration up to 0.9 ± 0.03 U · mg^{-1} for a CDP concentration of 44.0 mmol · L^{-1}. At higher CDP concentrations the specific activity remained nearly constant for 52.0, 67.0 and 84.0 mmol · L^{-1} with 0.8 ± 0.02 U · mg^{-1} 0.9 ± 0.1 U · mg^{-1} 0.8 ± 0.1 U · mg^{-1}.

From the results presented, it can be concluded that a high CDP concentration up to 84.0 mmol · L^{-1} had no inhibitory effect. However, Gottschalk *et al.* (2021) described substrate inhibition by other dinucleotides, adenosine diphosphate (ADP) and uridine diphosphate (UDP) for the same PPK, at concentrations higher than 15 mmol · L^{-1} and free enzyme [29]. Furthermore, different specific activities of PPK were reported for different nucleotides [23,29,90,164,165]. The structural difference between ADP, which is a purine nucleotide, and CDP and UDP, which are pyrimidine nucleotides, may be the reason for this. These effects are also described by Nahálka (2009) for *Silicibacter pomeroyi* PPKs [90]. In addition, immobilized enzymes may show a different behavior compared to free enzymes with regard to inhibition of substrate, product, and other inhibitors [101,166,167].

In Figure 41 the activity in relation to the polyP concentration is depicted.

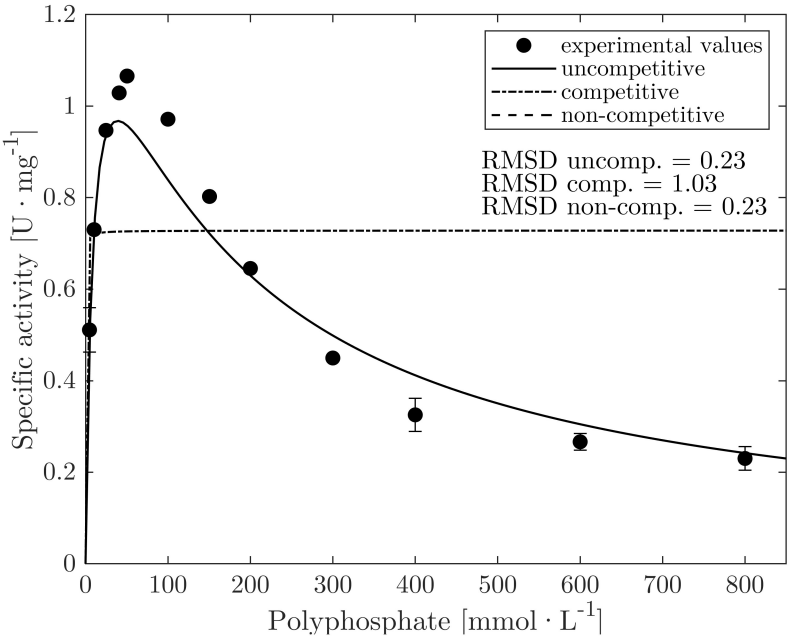

Figure 41: Investigation of kinetic parameters of PPK in PBR at ambient pressure. Specific activity over polyP concentration.

Reaction conditions: T= 40 °C; $\dot{V}$ = 1.5 ml ·min^{-1}; solvent: Na_3PO_4 buffer; c_{buffer} = 50.0 mmol · L^{-1}; pH= 7.4; c_{polyP} = 5-800 mmol ·L^{-1}; c_{CDP} = 70 mmol ·L^{-1}; c_{MgCl2} = 30 mmol ·L^{-1}; m_{PPK} = 3.59 mg; reactor dimensions: 30 x 3 mm; $\bar{t}$ = 0.19 ± 0.01 min; n = 6.

The activity of the PPK increased with increasing substrate concentration up to 1.1 ± 0.01 U · mg^{-1} at a polyP concentration of 50.0 mmol · L^{-1}. At higher polyP concentrations the activity decreased to 0.5 ± 0.01 U · mg^{-1} and 0.2 ± 0.03 U · mg^{-1} at 300.0 mmol · L^{-1} and 800.0 mmol · L^{-1}, respectively. These results lead to the assumption that the PPK is inhibited by the substrate polyP at concentrations higher than 50.0 mmol · L^{-1}, which was previously described by Tavanti *et al.* (2021) as well [23,83]. Moreover, Tavanti *et al.* (2021) found substrate inhibition from polyP for several PPKs from different organisms for concentrations higher than 100 mmol · L^{-1} [83]. Suzuki *et al.* (2018) stated that polyP inhibition at concentrations higher than 25 mmol · L^{-1} for a PPK from *Deinococcus proteolyticus* is present [84]. An inhibitory effect by polyP was also discovered for other polyphosphate kinases [80]. Gottschalk *et al.* (2021) found no inhibition of the same PPK by polyP up to a concentration of 40 mmol · L^{-1} [29]. Compared to the results from previous studies by Gottschalk *et al.* (2021), the activity of PPK was comparatively low. The activity of PPK was reported to be 3.7 U · mg^{-1} for an ADP/polyP system and 14.8 U · mg^{-1} for an UDP/polyP system. Gottschalk *et al.* (2021) found the lowest activity for a CDP/polyP system, which is confirmed by the results of Achbergerová *et al.* in 2014.[29,87] The reaction conditions in these experiments differ from those in this thesis in terms of reaction buffer, salt concentration and substrate concentration.

Nevertheless, to date, no specific activity data for immobilized PPK has been reported in the literature. Therefore, in this section, the activities of free PPK are compared with immobilized PPK, even though it is known that the immobilization of enzymes can lead to a change in both

activity and specificity.[35,101] In addition, the experiments to investigate the kinetic parameters of the PPKs were carried out under different reaction conditions, such as temperature, pH or salt concentrations, which may have an influence on the kinetic parameters.[168]

The activity of polyphosphate kinases is significantly influenced not only by the concentration of the polyP donor, but also by its chain length [23,81,84,86]. It was reported that PPKs prefer longer chain polyPs and are inhibited by short chains of polyP, whereby the mechanism of polyP consumption has not yet been sufficiently described [23]. Lelièvre *et al.* (2020) found that the activity of *Deinococcus geothermalis* PPK2-3 was higher at lower concentrations of long polyP chains with 25 or 45 phosphate residues [86]. Similarly, *Thermus thermophilus* PPK has a preference for using long-chain polyP consisting of more than 25 phosphate residues [81]. Most PPKs prefer polyphosphates with chain lengths from 10 to 100 residues [23,81,86,165]. Since the mean length of polyP used in this experiment was 78 residues (see Appendix 0), an inhibition resulting from the length of the polyP is improbable. Therefore, this data is used to determine the kinetic parameters of the cofactor regeneration by PPK.

Determination of the Kinetic Parameters of the PPK

The kinetic parameters of PPK for the phosphorylation of CDP were fitted to experimental data using different equations based on the Michaelis-Menten theory to describe the substrate or product inhibition in a mechanistic suitable manner.

Based on the evaluated specific activity data as a function of the CDP and polyP, substrate inhibition by polyP was determined. According to the Michaelis-Menten theory three equations describing the enzyme activity as a function of substrate concentrations and inhibitions were set-up. These equations describe competitive, uncompetitive and non-competitive inhibition by polyP.[3,75,100] The measured activity values were used to determine the kinetic parameters $K_{M,CDP}$, $K_{M,polyP}$, v_{max} and $K_{I,polyP}$ by using *nlinfit* (MATLAB).

The data of the kinetic constants and the corresponding confidence interval with regard to the inhibition types are given in Table 29. The value of v_{max} and its 95 % confidence interval was determined to 1.7 ± 0.4 U · mg^{-1} for uncompetitive, 1.8 ± 0.5 U · mg^{-1} for non-competitive and 4.6 ± 21.3*10^{9} U · mg^{-1} for competitive inhibition. The same value of 12.4 mmol · L^{-1} was predicted for $K_{M,CDP}$ for uncompetitive and non-competitive inhibition, while 5.2 mmol · L^{-1} was predicted for competitive inhibition. The kinetic parameters describing the dependence of the activity of PPK from polyP $K_{M,polyP}$ and $K_{I,polyP}$ were 9.4 mmol · L^{-1} and 163.0 mmol · L^{-1} for uncompetitive, 10.0 mmol · L^{-1} and 153.0 mmol · L^{-1} for non-competitive and 0.7 mmol · L^{-1} and 0.1 mmol · L^{-1} for competitive inhibition, respectively. Compared to Gottschalk *et al.* (2021), v_{max} is comparatively low. The activity of PPK was 3.7 U · mg^{-1} for an ADP/polyP System and 14.8 U · mg^{-1} for an UDP/polyP System. Nevertheless, it was mentioned that the lowest activity was found for a CDP/polyP system. The K_M for ADP was determined to be 0.9 mmol · L^{-1} at Gottschalk *et al.* (2021) in contrast to 12.4 mmol · L^{-1} for CDP in this thesis.[29] A low K_M-value

indicates that a comparatively low substrate concentration is needed to reach the maximum reaction rate and therefore corresponds to a high affinity to the substrate [3]. This implies that compared to Gottschalk *et al.* (2021) the PPK has a lower affinity to CDP than ADP [29]. Similar results were found by Kuroda *et al.* (1997), who determined the lowest affinity (high K_M value) of *Escherichia coli* PPK to CDP, while the affinity was the highest towards ADP [78]. It should be noted that the polyphosphate kinase was not only of different origin, but also in a different physical form. While Gottschalk *et al.* (2021) and Kuroda *et al.* (1997) used free enzymes, the PPK used in this thesis was present in immobilized form [29,78]. By immobilization, changes in activity, specificity, or selectivity are possible. These changes result from direct changes in the enzyme structure as well as from changes induced by the immobilization, e.g., changes in diffusion of substrate in the carrier pores.[35,101]

Table 29: Estimated model parameters according to the type of inhibition with RMSD for PPK.

	uncompetitive inhibition		competitive inhibition		noncompetitive inhibition	
	calculated	95 % confidence interval	calculated	95 % confidence interval	calculated	95 % confidence interval
v_{max} [U mg^{-1}]	1.7	± 0.4	4.576	± 21.3·10^{9}	1.8	± 0.5
$K_{M,CDP}$ [mmol · L^{-1}]	12.4	± 6.3	5.184	± 11.7	12.4	± 6.3
$K_{M,polyP}$ [mmol · L^{-1}]	9.4	± 5.7	0.697	± 3.24·10^{9}	10.0	± 6.8
$K_{I,polyP}$ [mmol · L^{-1}]	163.0	± 74.5	0.144	± 137.9·10^{6}	153.0	± 79.7
RMSD [U · mg^{-1}] CDP	0.2		0.4		0.2	
RMSD [U · mg^{-1}] polyP	0.2		1.0		0.2	

In order to obtain a prediction of the accuracy of the kinetic model's description of the measured data, the RMSD was used. The data is given in Table 29. The deviation of the predicted from the measured values for the CDP-dependent activity of PPK was 0.4 for competitive inhibition and 0.2 for uncompetitive and non-competitive inhibition. The RMSD for uncompetitive and non-competitive inhibition for the polyP-dependent activity was 0.2. The estimated model parameters, which had an RMSD of 1.0, do not adequately describe the competitive inhibition.

The confidence interval for the predicted kinetic parameters for uncompetitive inhibition gave the lowest values compared to the other types of inhibition as well as the lowest RMSD (see Table 29). In addition, the investigated substrate surplus inhibition by polyP is described by Jaeger *et al.* (2024) as a special case of the uncompetitive inhibition type.[40] Thus, it is assumed that the inhibition by polyP is following an uncompetitive inhibition model. The model parameters for uncompetitive inhibition were determined by using Equation 1-14. Nevertheless, this is only an assumption and the real mechanism of the type of inhibition cannot be conclusively determined with these calculations. It has been shown that the conceptualized high hydrostatic pressure reactor set-up can be used for different types and classes of immobilized enzymes and a wide range of hydrostatic pressures, flow rates, and substrate concentrations.

Furthermore, the simplified and user-friendly determination of kinetic parameters and activity as well as stability of the data were demonstrated. These findings could be used to further improve biocatalytical processes and support the design of new production processes.

4.6.4. Summary Characterization of *Ruegeria pomeroyi* Polyphosphate Kinase in the Continuously Operated Packed Bed Reactor

The investigation aimed to evaluate the stability and kinetic parameters of PPK for the potential regenerating of cofactors within reaction cascades. In addition, the effect of HHP on the enzyme activity was investigated.

The process with immobilized PPK was operated in a continuously PBR for 5 hours. The enzyme activity decreased over time with an average half-life of 111.6 hours. HHP up to 800 bar improved the PPK activity, possibly by altering the enzyme structure, dynamics or substrate/solvent properties. Furthermore, the kinetic parameters of PPK as a function of CDP and polyP were determined to be 44 mmol $\cdot$ L^{-1} CDP and 50 mmol $\cdot$ L^{-1} polyP, with a maximal specific activity of 1.7 U $\cdot$ mg^{-1}. Uncompetitive inhibition by polyP provided the best fit to the kinetic data and was assumed for further investigations.

The enhancement of enzyme activity under HHP offers the potential for improved biocatalytic processes. The results support the development of more efficient biocatalytic systems and the design of new production processes that take advantage of the potential stability and enhanced activity of immobilized enzymes under HHP.

5. Comprehensive Discussion and Outlook

The following section discusses the results of the work presented and gives an outlook on the potential of applying high pressure to biocatalytic reactions. The reactor design and the enzymes were studied intensively. First, the suitability of the enzyme immobilizates for the application in a continuous high hydrostatic pressure packed bed reactor and the reactor set-up itself are highlighted. In particular, the obtained results for the different enzymes CRL, CalB and PPK are compared to illustrate the influence of hydrostatic pressure on the enzyme performance. Furthermore, the comparison of two reactor operation modes for the CRL and the PPK are presented and discussed. Conclusively, an outlook is given for further research on the influence of high pressure on enzymatically catalyzed reactions.

5.1. Characterization of Enzyme Immobilizates and Reactor

The choice of an enzyme carrier for immobilization depends on different properties. Although immobilization on solid supports is an established technique and a key technique in biocatalysis, offering enhanced stability and reusability, there are no defined guidelines for choosing the most suitable solid support for a specific application.[105,123]

The selection of an appropriate solid support depends on several critical factors, including enzyme activity, stability, mechanical robustness, and susceptibility to substrate and product adsorption [3,105,123]. The choice depends on the carrier-specific effects on enzyme activity and stability as well as other application-specific factors. This is particularly relevant when immobilized enzymes are used in a flow process under harsh reaction conditions, including high acidity or basicity, elevated temperatures and high concentrations of organic solvents, as well as the use of HHP.[2,40,1693] However, the mechanical stability of the enzyme support, the physicochemical parameters such as the hydrophobicity of the carrier as well as the potential adsorption of product and substrate on the surface are decisive [33,105]. Furthermore, an uniform shape of the carrier particles is important for application in continuously operated processes since the pressure drop in fixed-bed reactors increases with the width of the particle size distribution [123].

In this thesis, various support materials were characterized in detail to determine their suitability for enzyme immobilization. The adsorption behavior of these materials was thoroughly evaluated, with the percentage of substrate and product adsorption playing a critical role in the selection of the support material. To ensure that there is no impact on the process, lower adsorption was considered more favorable.[105] The carrier material ECR 1090 was selected, which showed an adsorption of the product PPA of 2.6 ± 1.0 % after 7 days of incubation, based on a 100.0 mmol $\cdot$ L^{-1} PPA solution.

The investigation focused on the specificities of the immobilization process for two different enzymes, CalB and CRL. Various variables, including temperature and immobilization techniques, were examined. Notably, the tube roller method at room temperature proved to be the most effective approach, in terms of enzyme loading on the carrier, allowing for uniform immobilization.

Addressing the critical concern of enzyme leaching, which can undermine activity and lead to product contamination, no detectable leaching for CRL was determind.[3,75,123] This finding further support the usability of the enzyme immobilizates.

By investigating the effect of water content, this thesis showed that enzyme activity is closely related to the water content of the solvent. Both CalB and CRL showed decreasing activity with increasing water content in the solvent, emphasizing the importance of optimal water content for catalytic efficiency.[4,75,121] Storage stability emerged as a positive outcome, with both CRL and CalB maintaining their activity over a 100-day storage.

Mechanical stability, a key consideration for practical applications, was addressed by SEM imaging, which revealed particle damage during the immobilization procedure. However, the particles exhibited adequate mechanical stability for continuous operation and high pressure environments, which is a fundamental property for ensuring process robustness in biocatalytic applications.

In conclusion, this thesis provides a comprehensive overview of various factors that influence enzyme immobilization on solid supports. It gives valuable insights into process optimization for specific applications and highlights the importance of parameters such as support material, immobilization methodology, and mechanical stability. Together, these findings contribute to the advancement of biocatalytic processes with improved stability and efficiency. However, the results indicate that the selection of immobilizates and their application is highly specific and further guidelines to improve process development and optimization could be useful.

The selection of the right reactor set-up and its characterization is also crucial for a successful determination of the influence of high pressure on enzyme performance.

In recent years, replacing batch processes with continuous processes has been an additional factor that contributes to the implementation of sustainable transformations and is the key to process intensification.[7–9] Nevertheless, there are phenomena that need to be studied before a process can be carried out in continuously operated reactors.

The immobilized CRL and CalB showed an equilibration phenomenon in the continuously operated PBR which is shown in Figure 42.

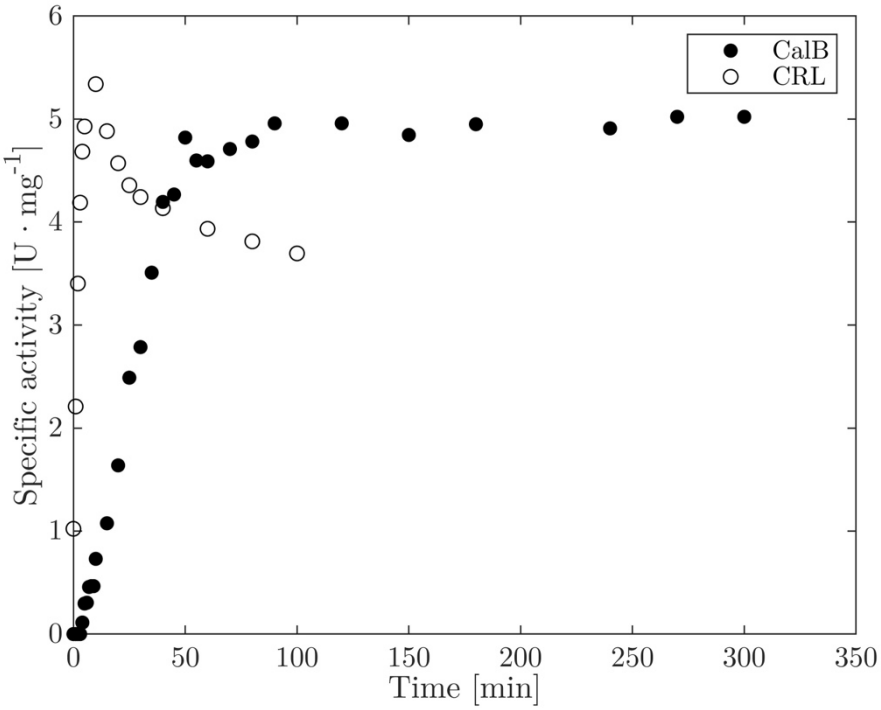

Figure 42: Establishment of steady-state conditions of PBR filled with CRL and CalB immobilizate at ambient pressure.

Reaction conditions CalB: $T = 35$ °C; $\dot{V} = 0.5$ ml ·min^{-1}; solvent: heptane; $c_{PP} = 10.0$ mmol ·L^{-1}; $c_{vin} = 864.0$ mmol ·L^{-1}; reactor dimensions: 50 x 3 mm; $m_{TR12} = 0.1701$ g; ECR 1090; $m_{CalB} = 0.195$ mg; $t = 300$ min; $p = 1$ bar; $n = 1$.

Reaction conditions CRL: $T = 35$ °C; $\dot{V}$ =0.5 ml·min^{-1}; solvent: heptane; $c_{PP} = 10$ mmol · L^{-1}; $c_{vin} = 864.0$ mmol·L^{-1}; reactor dimensions: 30 x 3 mm; $\bar{t} = 0.87 \pm 0.01$ min; $m_{TR21} = 0.1$ g; ECR 1090; $m_{CRL} = 0.0837$ mg; $t = 100$ min; $n = 3$.

In each experimental approach, the CRL activity increased in the first 10 min of the experiment and then slightly decreased. The CalB showed an increase in the first 80 min, while no decrease of enzyme activity over the reaction progress was observed. This phenomenon is not due to insufficient mixing of the reactor, as the mean residence time is 0.87 min at a flow rate of 0.5 mL · min^{-1} and thus corresponds to 11 mean residence times for experiments carried out with immobilized CRL. The increase of activity until 10 min for CRL immobilizates, respectively 80 min for CalB immobilizates of experiment, can be explained by the re-orientation of the packed bed.[3,130,131]

The mean residence time $\bar{t}$ at a flow rate of 1.0 mL · min^{-1} in high pressure experiments was 0.40 min while $\bar{t}$ is 0.38 min at a flow rate of 1.5 mL · min^{-1} in kinetic experiments. Appropriate steady-state residence times were determined so that the kinetic parameters of CRL were studied with 5 residence times before sampling. When investigating the influence of HHP, 12 residence times were waited before sampling, while other authors have stated that three to four residence times are sufficient to reach steady-state.[170,171]

Potential mass transfer limitation is one of the most important parameters to be investigated.[3,131] Therefore, different flow rates and the resulting enzyme activity were calculated to identify this potential limitation. The activity of CRL at a flow rate higher than

0.25 mL · min^{-1} was higher than the activity at lower flow rates. Therefore, a mass transfer limitation was assumed at flow rates lower than 0.5 mL · min^{-1}.[131] Since the experiments to determine the kinetic parameters and pressure experiments are carried out at a flow rate of 1.5 mL · min^{-1} and 1.0 mL · min^{-1} respectively, it was assumed that lower mass transfer limitation occurred at theses flow rates.

The mean residence time of the CDP phosphorylation reactor system was characterized as well. A mean residence time $\bar{t}$ of 0.25 ± 0.02 min at flow rate of 1.0 mL · min^{-1} in high pressure experiments and 0.19 ± 0.01 min at a flow rate of 1.5 mL · min^{-1} in kinetic experiments was determined, respectively. Similar to the investigation with CRL and CalB, appropriate steady-state conditions were determined for experiments with PPK. For the kinetic experiments, no sampling was performed for 10 residence times. In addition, no sampling was performed for 15 residence times to investigate the influence of HHP.

The results of the characterization of the high hydrostatic continuously operated packed bed reactor and the results of the characterization of the enzyme immobilizates showed that the immobilizates of PPK, CalB and CRL were suitable for use in the conceptualized HHP reactor.

5.2. Comparison of Discontinuously Operated Stirred Tank Reactor and Continuously Operated Packed Bed Reactor

Immobilized enzymes can be applied in different types of reactors. In this thesis, particular attention was paid to the comparison of a discontinuously operated STR and the conceptualized continuously operated PBR, as explained in the introduction.

The transesterification reaction catalyzed by CRL was initially performed in a 10 mL thermovessel in batch operation mode to determine possible substrate inhibition and optimal substrate concentrations for this set-up. A maximum conversion of PP of 100.0 % was achieved when carrying out the reaction in the STR. Therefore, kinetic experiments were performed with a maximal conversion of the substrate of 10.0 %. In the range of substrate conversion from 0.0 % to 10.0 %, the activity of the enzyme is assumed to be linear according to the Michaelis-Menten theory.[3] Furthermore, an uncompetitive substrate inhibition by vinyl acetate resulting in an optimal PP concentration of 100.0 mmol · L^{-1} and 868.0 mmol · L^{-1} vinyl acetate with a maximum CRL activity of 11.3 U · mg^{-1} was determined. Even though many biotransformations are carried out in batch mode, not all effects on the enzymatic performance can be studied sufficiently due to the simplified technical realization [2,60]. A viable option for studying further enzyme characteristics is the use of a continuously operated reactor, such as a packed bed reactor operated as plug flow reactor [9]. Especially the investigation of the influence of HHP on the enzyme performance was subsequently investigated in this reactor configuration.

For both reactor operation modes the kinetic parameters were estimated according to the Michaelis-Menten theory using a nonlinear regression method (nlinfit function, MATLAB 2019a) [76]. The uncompetitive inhibition by vinyl acetate was confirmed when the reaction was carried out in the PBR. The maximum reaction rate predicted by the model was

11.6 ± 3.9 U · mg^{-1} in comparison to 88.1 ± 122.3 U · mg^{-1} in STR, although the measured maximum reaction rates of 6.4 U · mg^{-1} in the PBR and 11.3 U · mg^{-1} in the STR were similar. The $K_{M,PP}$ value at ambient pressure in the PBR was 17.6 mmol · L^{-1} while it was 13.8 mmol · L^{-1} in the STR. One reason for the deviation in the predicted kinetic parameters is that different immobilization batches were used to investigate the enzyme kinetics for the different operation modes. Under ambient pressure, the maximum achievable specific activity was 6.4 U · mg^{-1} at a PP concentration of 100.0 mmol · L^{-1} and 862.1 mmol · L^{-1} of vinyl acetate. The optimal conditions investigated in the PBR were similar to the results from the STR, even if the kinetic parameters differed in some cases. The data is given in Table 30.

Table 30: Estimated model parameters for uncompetitive inhibition with RMSD for CRL at ambient pressure investigated in stirred tank reactor and in PBR.

	Stirred Tank Reactor		Packed Bed Reactor	
	calculated	95 % confidence interval	calculated	95 % confidence interval
v_{max} [U · mg^{-1}]	88.1	± 122.3	11.6	± 3.9
$K_{M,PP}$ [mmol · L^{-1}]	17.6	± 6.8	13.8	± 7.1
$K_{M,vin}$ [mmol · L^{-1}]	742.4	± 1512.4	391.0	± 320.2
$K_{I,vin}$ [mmol · L^{-1}]	900.3	± 1582.5	5999.7	± 4556.1
RMSD PP	2.6		1.5	
RMSD vin	2.2		1.2	

A comparison of the enzyme performance is beneficial to determine the best reactor operation mode. Csajági *et al.* (2008) compared the enantioselectivities and productivities of different lipases in different reactor operating modes. While the enantioselectivities were not affected by the choice of operation mode, the productivities were improved when the process was applied in a continuous flow reactor instead of a discontinuously operated stirred tank reactor.[159] In contrast, Liese *et al.* (2013) report that the optical purity of a product at the reactor outlet depends not only on the enantioselectivity of the catalyst, i.e. the kinetics, but also on the reactor configuration. The selectivity of the enzyme remains the same, but the reactor selectivity is different due to the varying backmixing in different reactor conmfigurations.[103]

Due to different hydrodynamic conditions, the determined kinetic parameters for the immobilized enzyme may vary in different reactor set-ups, especially when the reaction is carried out in discontinuously operated stirred tank reactors and continuously operated packed-bed reactors [172]. Furthermore, the determination of these kinetic parameters of immobilized enzymes in continuously operated packed-bed reactors can be affected by mass transfer limitation as well as by channeling in the reactor bed or swelling of the particles.[3,130,131,172] The selection of the reactor type for the evaluation of the kinetic parameters is important for the development of an industrial process, because an insufficient determination of the kinetic parameters will cause challenges in scale-up. For the optimization of the reaction system, it is therefore advantageous to carry out the kinetic data in a reactor as similar as possible to the reactor system in which the biotalalytic reaction will be conducted. In addition to the possibility of high sampling number and a good control of the reaction conditions, the set-up should be similar to the reaction set-up in which the process will be carried out on a larger scale.[173]

In the case of substrate surplus inhibition, it is not advantageous to perform the reaction in a continuously operated PBR without recycle stream as the concentration of inhibitor must be kept as low as possible, which is not practical to achieve maximum conversion of the substrates from this type of reactor [3]. However, if the PBR is operated as a CSTR with a recycle stream, this can also be of advantage in the case of substrate surplus inhibition due to outflow conditions resulting in a low inhibitor concentration.[131] In the case of the reaction investigated here, however, it makes sense to carry out the reaction in the PBR, since vinyl acetate has a K_I-value of 5999.7 mmol $\cdot$ L^{-1} at ambient pressure to 2242.1 mmol $\cdot$ L^{-1} at HHP. At ambient pressure, the maximum specific activity of CRL can be achieved at a PP concentration of 100.0 mmol $\cdot$ L^{-1} and 862.1 mmol $\cdot$ L^{-1} of vinyl acetate. At a pressure of 800 bar the maximum specific activity of CRL was achieved at a PP concentration of 60.0 mmol $\cdot$ L^{-1} and 1526.9 mmol $\cdot$ L^{-1} of vinyl acetate. The transesterification reaction studied here is an equimolar reaction in which both substrates are converted in identical molar amounts. In this case, the reaction is limited by the non-inhibiting substrate PP, as the maximum reaction rate is reached at lower concentrations than the concentration at which substrate inhibition by vinyl acetate occurs. It is possible to work with a substrate excess of the inhibiting vinyl acetate, which in this case is 8-fold at ambient pressure and 25-fold at 800 bar. It can therefore be concluded that, for this particular case, the reaction can be taken out in the PBR, as this reactor concept allows the determination of the influence of HHP on the enzyme activity and selectivity of the CRL.

Furthermore, the application of PPK was investigated in both a discontinuous stirred tank reactor and a continuously operated packed bed reactor. To compare the activity of the enzymes in the two different reactor types, the specific activity of PPK in the STR was calculated after 3 min reaction time, whereas the specific activity of PPK in the PBR was determined at a flow rate of 1.5 mL $\cdot$ min^{-1}. Since the conversion at this point was 7.1 % for

the STR and 4.2 % for the PBR, both were in the range for initial reaction rate determination [3]. The activity of the enzymes in the STR and the specific activity of the enzymes in the packed bed reactor, both 0.87 $U \cdot mg^{-1}$, are comparable. The process in continuous operation mode should be preferred due to the retention of immobilized PPK leading to a reduced catalyst consumption as well as the operational advantages of this operation mode. Therefore, this thesis enables the application of PPK in a continuously operated PBR.[7,65,69,174,175]

Several other examples are given in literature where a change from batch to continuous flow operation mode was advantageous for the overall process. These improvements are: increased yield in a shorter time[176] and, additionally, a higher enantioselectivity[65], in addition to the advantages which result from the reactor itself[7,65,69,174,175], such as continuous manufacturing of chemicals, optimized heat transfer[8,174,175], and increasing the economics of large-scale production [9].

For both reaction systems, it could be shown that the application in the continuously operated bed reactor is useful. When the reactions were carried out in the STR, the limits for the investigation of the kinetic parameters were determined, which could also be determined for the CRL in the STR. However, the PPK showed the same activity in both reactor types, which supports the thesis that the application in the continuous reactor is reasonable. This study could not be carried out for the CRL because different immobilized batches were used which had different specific activities due to different loadings of the carriers. The present results suggest that enzyme activity in a STR and a packed bed reactor are comparable, with no determinable mass transfer limitation in both reactors. Thus, the application of PPK and CRL in a continuously operated PBR is established and offers a promising integration into further processes.[7,65,69,174,175]

5.3. Enzyme Performance at High Hydrostatic Pressure

The investigation of the influence of HHP on the performance of enzymes from different enzyme classes was the main focus of this thesis. An important characteristic of an enzyme is its specific activity in the selected reaction system and under the given reaction conditions. The influence of HHP on the activity of CRL, CalB, and PPK was investigated. In addition, the influence of hydrostatic pressure on the selectivity and on the kinetic parameters of the enzymes was studied as well.

The influence of HHP was investigated for the two lipases CRL and CalB. Additionally, the combined effect of pressure and temperature was studied for CalB.

In relation to the activity of CRL at 1 bar, the activity of CRL was increased by 9.2 ± 4.6 % at 200 bar and 24.7 ± 9.9 % at 800 bar at a temperature of 35 °C. A hydrostatic pressure of 1,200 bar resulted in the highest activity increase of 42.8 ± 8.8 %. The increase in specific activity of CalB was 41.4 ± 1.3 % from 1 to 1,200 bar at 35 °C and 27.5 ± 1.5 % at 65 °C. Therefore, it can be concluded that the effect of pressure induced activation on CalB is higher at lower temperatures. In conclusion, the effect of pressure induced activation on the enzyme is the highest for the lowest investigated temperature of 35 °C. Both lipases showed a pressure-

induced increase in activity, the activity increased by over 40.0 % when the pressure was raised from ambient pressure to 1,200 bar.

Furthermore, the stability of CRL was investigated at ambient and high pressure. Despite the relatively large error of the experiment, the mean half-life at 800 bar is increased compared to the mean half-life at 1 bar. The activity of CalB was constant over 300 min, indicating that the enzyme was stable over the course of the experiment.

Literature references support these results [149,150]. While immobilized CalB has been described as a temperature stable enzyme even above 100 °C, the effect of pressure on the stability of this enzyme was not feasible.[149,150] The effect of pressure on the CRL was previously investigated: Hei and Clark (1994) showed an increase in half-life for hydrogenases of different origins by increasing the pressure from 1 to 507 bar [49]. At 80 bar and 60 °C Lozano *et al.* (2004) investigated an enhanced half-life of CalB [133]. Marie-Olive *et al.* (2000) showed that the half-life of *Saccharomyces cerevisiae* invertase increased when pressures up to 2,000 bar were applied.

Overall, depending on the enzyme type and source, the HHP range that protects the enzyme from thermal inactivation varied [134]. Further examples were described by Eisenmenger *et al.* (2009) [2].

In addition to the specific activity and stability, the selectivity of CRL and CalB was investigated. The enantioselectivity E of the transesterification was determined and used as decision criteria. For the CRL, a maximum E-value of 1.5 was determined, which did not change with pressure. It can be concluded that HHP-induced changes in enantioselectivity are not industrially relevant [3].

An E-value of 20.8 ± 0.4 at ambient pressure and 12.7 ± 0.9 at 1,200 bar at 65 °C was determined for the CalB catalyzed transesterification reaction. A pressure-dependent decrease of the enantioselectivity with respect to the R-enantiomer of the product was observed. As for the CRL, the enantioselectivity of CalB with a maximum value of 26.8 at ambient pressure at 45 °C is not industrially relevant [3]. For all three investigated temperatures the enantioselectivity was decreasing with increasing pressure, thus making the enzyme less enantioselective. Csajági *et al.* 2008 investigated the enantioselectivity of different lipases. While CRL showed a low E-value of 4.0, the CalB showed a E-value of over 200. Overall, the enantioselectivity of lipases was found to differ depending on the origin of the enzyme.[159] There are some major structural differences between the two investigated lipases. While CRL has a lid covering the active site[140], CalB does not [177]. This structural difference has been reported to be a potential cause for the different enantioselectivities of these two lipases [140]. This could be an explanation for the differences in the behavior of enantioselectivity under HHP. Since the performance of enzymatically catalyzed reactions under high pressure can also influence the selectivity, the application in various areas of industry is of interest. This is related to the increased interest in enantiomerically pure products and the different properties of the

enantiomers and is particularly important in the pharmaceutical industry and the production of fine chemicals.[3,75]

The influence of HHP on the kinetic parameters of CRL was investigated at ambient pressure and 800 bar. The v_{max} increased by the factor 2.2 indicating high specific activity of CRL, while the $K_{M,PP}$ value did not change. The K_M value indicates the affinity of the enzyme to the substrate, i.e., the interaction between the enzyme and the substrate, which does not change [3]. The K_M-value of the second substrate vinyl acetate changed from 391.0 mmol · L^{-1} at ambient pressure to 1020.7 mmol · L^{-1} at high pressure. Therefore, the affinity towards the substrate vinyl acetate decreased. To achieve the maximum reaction rate, a higher substrate concentration of vinyl acetate is required.[75] The $K_{I,vin}$-value decreased from 5999.7 mmol · L^{-1} at ambient pressure to 2242.1 mmol · L^{-1} at high pressure. The K_I-value describes the equilibrium constant for the dissociation of enzyme inhibitor complexes [100]. This indicates that the inhibitor concentration is reduced by a factor of 2.6. Increasing the pressure from 1 bar to 800 bar therefore leads to greater substrate inhibition. However, it has been shown that HHP can be used as an appropriate method for directly influencing kinetic parameters of the catalyzed transesterification reaction by CRL.

Besides studying the effect of HHP on the enzymatic performance of two lipases, another enzyme from a different class was investigated as well. PPK is a transferase from enzyme class 2 regenerating cofactors, while the lipases from enzyme class 3 are hydrolases catalyzing hydrolysis of fats and many other reactions in non-conventional reaction media [21–23]. PPK showed an optimum of pressure induced activation at 600 to 800 bar of 12.0 %, while both lipases showed a constant increase over the course of pressure up to 1,200 bar. These behaviors was already reported by Eisenmenger *et al.* (2009) [2].

The impact on the biocatalyst performance for three enzymes from two enzyme classes was investigated in this thesis. For all three reaction systems, the main focus was to investigate the influence of HHP on the activity of the enzymes. Overall, the application of HHP increased the activity of all three investigated enzymes up to 40.0 % which is shown in Figure 43.

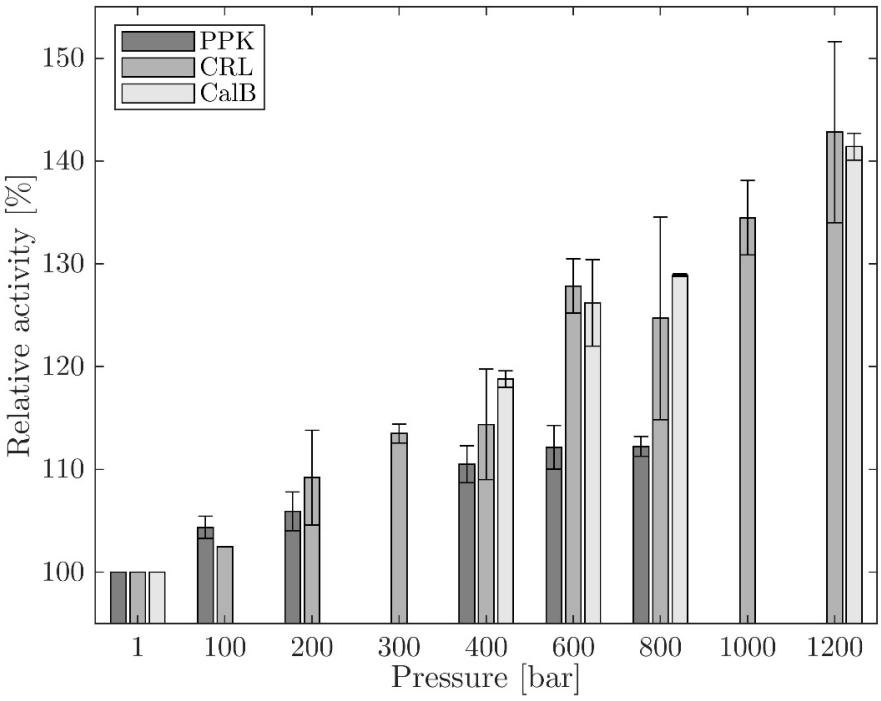

Figure 43: Investigation of the pressure induced increase of CRL, PPK and CalB activity. Relative activity as a function of pressure.

Reaction conditions PPK: $T = 40$ °C; $\dot{V} = 1.0$ ml $\cdot$min^{-1}; solvent: Na_3PO_4 buffer; $c_{buffer} = 50.0$ mmol $\cdot$ L^{-1}; pH = 7.4; $c_{polyP} = 44.0$ mmol $\cdot$L^{-1}; $c_{CDP} = 30.0$ mmol $\cdot$L^{-1}; $c_{MgCl2} = 30.0$ mmol $\cdot$L^{-1}; $m_{PPK} = 8.07$ mg; reactor dimensions: 30 x 3 mm; p = 1-800 bar; $n = 3$. Reaction conditions CalB: $T = 35$ °C; $\dot{V} = 0.5$ ml $\cdot$min^{-1}; solvent: heptane; $c_{PP} = 10.0$ mmol $\cdot$L^{-1}; $c_{vin} = 864.0$ mmol $\cdot$L^{-1}; reactor dimensions: 50 x 3 mm; $m_{TR15/TR18} = 0.15$ g; ECR 1090; m_{CalB}(TR15) = 0.195 mg; m_{CalB}(TR18) = 0.741 mg; p = 1-1,000 bar; n = 1-2. Reaction conditions CRL: $T = 35$ °C; $\dot{V} = 0.35$ ml $\cdot$min^{-1}; solvent: heptane; $c_{PP} = 10.0$ mmol $\cdot$L^{-1}; $c_{vin} = 2712.5$ mmol $\cdot$L^{-1}; p = 1-1,200 bar; reactor dimensions: 50 x 3 mm; $m_{TR13} = 0.1$ g; ECR 1090; $m_{CRL} = 0.120$ mg; n = 1-3.

Furthermore, the stability was increased by a factor of 2.8 and the kinetic parameters of CRL were changed by HHP. While the selectivity of CRL was not changed by HHP, the selectivity of CalB slightly decreased.

The complex effects of high pressure have to be researched further to fully exploit its potential as a complementary process parameter [2].

Jaworek *et al.* (2021) showed that the combination of temperature, a co-solvent and high pressure influenced the kinetic parameters of a formate dehydrogenase. Similar results were obtained in this thesis. Overall, it was shown that the application of various strategies to improve enzyme performance, including the application of HHP, can be beneficial.[178]

The investment and operating costs for high pressure equipment must be taken into account when designing a new biotechnological process [2]. However, as this technology is widely used in the food industry and is therefore under constant development, the cost of high pressure equipment, especially on a small scale, is decreasing [2,179,180].

5.4. Enhancing Enzyme Performance Under High Pressure: Optimized Analysis and Future Directions

In order to further advance and intensify research on the influence of HHP on enzymatically catalyzed reactions, new approaches can be pursued and, in particular, the analysis of the processes can be optimized. These improvements will contribute significantly to the understanding of the influence of pressure on enzymatic reaction systems.

The suitable and durable immobilization of enzyme for the application in HHP reactors is crucial for the subsequent investigation of the influence of HHP on enzymatically catalyzed reactions. Further development and optimization of the immobilization of the enzymes would be valuable to refine process development.

Optimized analytics, in the sense of in- or on-line measurement of substrates and products, represents an essential deepening of the understanding of the influence of HHP on enzyme systems. In addition to faster data evaluation, a larger amount of data can be recorded and analyzed. This can be accomplished, for example, by an on-line nuclear magnetic resonance spectrometer located at the reactor outlet.

Various strategies can be used to further improve the understanding of the influence of HHP on enzyme systems. Intensified analytics can contribute to a better understanding of the behavior of enzymes inside the reactor. The concentration profile of substrates and products in the column can be measured with point-by-point analysis, not just the concentration at the end of the reactor. An alternative to classical immobilizates is the use of 3D printed packings to improve enzyme performance with respect to mass transfer limitations. However, these structures can have a poor surface-to-volume ratio, which must be considered when choosing this type of enzyme carrier. The use of micro-CT in addition to SEM allows the study of immobilizates and reactor packings. Furthermore, differences in the reactor bed and immobilizates before and after the application of HHP can be detected in detail. In particular, the pressure range to be investigated should be extended by more powerful pumps in order to fully exploit the effect of HHP on enzyme performance. In order to investigate the influence of HHP on enzyme performance more comprehensively, it is necessary to extend this pressure range up to 2000 bar, since above this pressure the tertiary structure of the enzyme is irreversibly denatured and thus its ability to catalyze is affected.

Particular attention should be paid to the study of changes in the kinetic parameters of enzymes under pressure, as enzyme kinetics are the basis for the use and the understanding of enzymes in a biotechnological process. The application of high pressure to optimize enzymes is a new and interesting process parameter because the technology is already available from the food industry and the cost of this technology is falling due to constant innovation. Today, due to the comparatively high cost of high pressure applications, the use of HHP could be beneficial for the manufacturer of high-margin or high-value products that are produced on a small scale were the cost of the products exceed 100 € per kg.[181] Since the selectivity of enzymatically

catalyzed reactions under high pressure is also influenced, the application in various areas of industry is of interesting. This is related to the increased interest in enantiomerically pure products and the different characteristics of the enantiomers. Furthermore, the application of HHP is not limited to individual reaction systems or to certain enzyme classes; the performance of biocatalytic reactions under HHP can be applied to all enzymes. However, it is not (yet) possible to make a complete statement about the specific application, because, as shown in this thesis, the influence of HHP on the enzyme performance and interactions with additional process parameters must be further examined to improve biocatalytical reactions in a more targeted way.

6. Summary

In this thesis, the application of HHP as a complementary process intensification method was successfully demonstrated. In addition, different enzyme immobilization materials and methods as well as reactor design were evaluated with a particular focus on the impact of HHP on enzyme performance and kinetic parameters.

The choice of the carrier and carrier material for enzyme immobilization is complex, considering factors such as enzyme activity, stability, mechanical robustness, and proneness to substrate and product adsorption. This thesis investigated the immobilization of two enzymes, CalB and CRL, and three immobilization methods. The tube roller method at room temperature was the most effective approach, with no detectable leaching for CRL observed, emphasizing its applicability. Storage stability was confirmed for both CRL and CalB for over 110 days. The mechanical stability was assessed by SEM, revealing adequate robustness for continuous operation and the application in high pressure environments.

The immobilized CRL and CalB showed an equilibrium phenomenon in the PBR until 10 and 80 min of reactor operation, respectively. As the activity of immobilized CRL increased with flow rates higher than 0.25 $mL \cdot min^{-1}$, a mass transfer limitation was assumed at flow rates lower than 0.5 $mL \cdot min^{-1}$. A comparable effect was also determined for the third immobilized enzyme, PPK, assuming a higher, potentially external, mass transfer limitation at flow rates below 0.15 $mL \cdot min^{-1}$. In the subsequent investigations, the flow rates and sampling times for the CRL, CalB, and PPK experiments were chosen to minimize mass transfer limitations, overcome the equilibrium phenomenon, and ensure steady-state conditions, providing a basis for further investigations.

The feasibility of the reactions catalyzed by CRL and PPK in different reactor types was conducted, as this is an important issue in the development of biotechnological processes. Since most high pressure experiments are performed in the “easy to operate” STR in batch mode, this reactor type was compared to the continuously operated PBR. It was shown that the enzyme activity in a STR and PBR is comparable, with no determinable mass transfer limitation in either reactor, establishing the application of CRL and PPK in a continuously operated PBR.

Furthermore, the kinetic parameters of CRL in the two reactor types were investigated, revealing an inhibition by the substrate vinyl acetate. In the discontinuously operated STR, CRL exhibited a maximum reaction rate v_{max} of 88.1 $U \cdot mg^{-1}$ and a $K_{M,PP}$ of 17.6 $mmol \cdot L^{-1}$. In the PBR, the v_{max} was notably lower with 11.6 $U \cdot mg^{-1}$, but the $K_{M,PP}$ was comparable with 13.8 $mmol \cdot L^{-1}$. This difference can be attributed to variations in the immobilizate batches used in the two reactor types. In both reactors, the K_I for vinyl acetate was different, with a higher value in the PBR. The RMSD values for the estimated kinetic parameters were relatively low for the uncompetitive inhibition, indicating reasonable consistency of both kinetic models and adequate description of the kinetic data.

The PPK showed similar activity in both reactor types with a specific activity of 0.87 $U \cdot mg^{-1}$. This suggests that mass transfer limitations did not affect the PBR's performance. The kinetic characterization of the catalyzed cofactor regeneration revealed a substrate inhibition by polyphosphate, which is described best by the uncompetitive inhibition type according to the Michaelis-Menten theory.
The main focus of this thesis was the investigation of the influence of HHP on the performance of CRL, CalB, and PPK. For CRL and CalB, an increase in the specific activity was observed with increasing HHP. Both enzymes exhibited more than 40.0 % activity increase when exposed to 1,200 bar pressure. The stability of CRL increased at higher pressure compared to ambient pressure. The activity of CalB increased with temperature and pressure, whereas the enantioselectivity of CalB decreased under pressure, making the enzyme less specific. PPK showed an optimal pressure-induced activation range at 600-800 bar, with a specific activity increase of 12.0 %.
In addition to the determination of kinetic parameters at ambient pressure, the influence of HHP on the kinetic parameters of CRL at 800 bar was investigated. v_{max} increased by factor 2.2, indicating a high specific activity of CRL, while the $K_{M,PP}$ stayed unchanged. The K_M of the second substrate vinyl acetate changed from 391.0 $mmol \cdot L^{-1}$ at ambient pressure to 1020.7 $mmol \cdot L^{-1}$ at HHP, this means that the affinity of the enzyme towards the substrate vinyl acetate decreased. To achieve the maximum reaction rate v_{max}, a higher substrate concentration of vinyl acetate is required. The $K_{I,vin}$ decreased from 5999.7 $mmol \cdot L^{-1}$ at ambient pressure to 2242.1 $mmol \cdot L^{-1}$ at HHP. Consequently, the inhibitor concentration is reduced by a factor of 2.6. and a pressure increase from 1 bar to 800 bar leads to severe substrate inhibition.

Overall, it was shown that the enzyme immobilizates and the developed continuously operated high pressure reactor setup are suitable for conducting experiments to study the behavior of enzymes under HHP and the effects on the kinetic parameters to gain a better understanding of the process and pressure-induced changes.
The application of HHP enhanced the specific activity of all three different enzymes by up to 40.0 % and increased their stability. Furthermore, the kinetic parameters of CRL were affected by pressure. CalB's enantioselectivity slightly decreased under pressure. However, further research is needed to fully understand HHP effects on the enzyme performance.

With regard to an industrial application, HHP has been shown to be a complementary process parameter in the process intensification of enzymatically catalyzed reactions. It can complement other strategies for improving biotechnological processes, such as immobilization, genetic engineering, and the use of unconventional solvents. This opens up numerous possible applications in various areas of biocatalysis.

7. Bibliography

(1) Aertsen, A.; Meersman, F.; Hendrickx, M. E. G.; Vogel, R. F.; Michiels, C. W. Biotechnology under High Pressure: Applications and Implications. *Trends Biotechnol.* **2009**, *27* (7), 434–441. https://doi.org/10.1016/j.tibtech.2009.04.001.

(2) Eisenmenger, M. J.; Reyes-De-Corcuera, J. I. High Pressure Enhancement of Enzymes: A Review. *Enzyme Microb. Technol.* **2009**, *45* (5), 331–347. https://doi.org/10.1016/j.enzmictec.2009.08.001.

(3) Jaeger, K.-E.; Liese, A.; Syldatk, C. *Einführung in Die Enzymtechnologie*; Springer Berlin Heidelberg: Berlin, Heidelberg, 2018. https://doi.org/10.1007/978-3-662-57619-9.

(4) Klibanov, A. M. Improving Enzymes by Using Them in Organic Solvents. *Nature* **2001**, *409* (6817), 241–246. https://doi.org/10.1038/35051719.

(5) Stepankova, V.; Bidmanova, S.; Koudelakova, T.; Prokop, Z.; Chaloupkova, R.; Damborsky, J. Strategies for Stabilization of Enzymes in Organic Solvents. *ACS Catal.* **2013**, *3* (12), 2823–2836. https://doi.org/10.1021/cs400684x.

(6) Hanefeld, U.; Hollmann, F.; Paul, C. E. Biocatalysis Making Waves in Organic Chemistry. *Chem. Soc. Rev.* **2022**, *51* (2), 594–627. https://doi.org/10.1039/D1CS00100K.

(7) Britton, J.; Majumdar, S.; Weiss, G. A. Continuous Flow Biocatalysis. *Chem. Soc. Rev.* **2018**, *47* (15), 5891–5918. https://doi.org/10.1039/c7cs00906b.

(8) Santis, P.; Meyer, L.-E.; Kara, S. The Rise of Continuous Flow Biocatalysis – Fundamentals, Very Recent Developments and Future Perspectives. *React. Chem. Eng.* **2020**, *5* (12), 2155–2184. https://doi.org/10.1039/d0re00335b.

(9) Tamborini, L.; Fernandes, P.; Paradisi, F.; Molinari, F. Flow Bioreactors as Complementary Tools for Biocatalytic Process Intensification. *Trends Biotechnol.* **2018**, *36* (1), 73–88. https://doi.org/10.1016/j.tibtech.2017.09.005.

(10) Rocha, R. A.; Speight, R. E.; Scott, C. Engineering Enzyme Properties for Improved Biocatalytic Processes in Batch and Continuous Flow. *Org. Process Res. Dev.* **2022**, *26* (7), 1914–1924. https://doi.org/10.1021/acs.oprd.1c00424.

(11) Huang, Q.; Rodgers, J. M.; Hemley, R. J.; Ichiye, T. Extreme Biophysics: Enzymes under Pressure. *J. Comput. Chem.* **2017**, *38* (15), 1174–1182. https://doi.org/10.1002/jcc.24737.

(12) Patel, A. K.; Singhania, R. R.; Pandey, A. Novel Enzymatic Processes Applied to the Food Industry. *Curr. Opin. Food Sci.* **2016**, *7*, 64–72. https://doi.org/10.1016/j.cofs.2015.12.002.

(13) Eisenmenger, M. J.; Reyes-De-Corcuera, J. I. High Hydrostatic Pressure Increased Stability and Activity of Immobilized Lipase in Hexane. *Enzyme Microb. Technol.* **2009**, *45* (2), 118–125. https://doi.org/10.1016/j.enzmictec.2009.03.004.

(14) Zhao, Z.; Herbst, D.; Niemeyer, B.; He, L. High Pressure Enhances Activity and Selectivity of Candida Rugosa Lipase Immobilized onto Silica Nanoparticles in Organic Solvent. *Food Bioprod. Process.* **2015**, *96*, 240–244. https://doi.org/10.1016/j.fbp.2015.08.006.

(15) Chen, G.; Du, H.; Jiang, B.; Miao, M.; Feng, B. Activity of Candida Rugosa Lipase for Synthesis of Hexyl Octoate under High Hydrostatic Pressure and the Mechanism of This Reaction. *J. Mol. Catal. B Enzym.* **2016**, *133*, S439–S444. https://doi.org/10.1016/j.molcatb.2017.03.007.

(16) Chen, G.; Miao, M.; Jiang, B.; Jin, J.; Campanella, O. H.; Feng, B. Effects of High Hydrostatic Pressure on Lipase from Rhizopus Chinensis: I. Conformational Changes. *Innov. Food Sci. Emerg. Technol.* **2017**, *41*, 267–276. https://doi.org/10.1016/j.ifset.2017.03.016.

(17) Knez, Ž.; Habulin, M. Lipase Catalysed Esterification at High Pressure. *Biocatalysis* **1994**, *9* (1–4), 115–121. https://doi.org/10.3109/10242429408992113.

(18) Noel, M.; Combes, D. Effects of Temperature and Pressure on Rhizomucor Miehei Lipase Stability. *J. Biotechnol.* **2003**, *102* (1), 23–32. https://doi.org/10.1016/S0168-1656(02)00359-0.

(19) Sarmah, N.; Revathi, D.; Sheelu, G.; Yamuna Rani, K.; Sridhar, S.; Mehtab, V.; Sumana, C. Recent Advances on Sources and Industrial Applications of Lipases: *Biotechnol. Prog* ., 2017, Vol. 00, No. 00. *Biotechnol. Prog.* **2018**, *34* (1), 5–28. https://doi.org/10.1002/btpr.2581.

(20) Mehta, A.; Guleria, S.; Sharma, R.; Gupta, R. The Lipases and Their Applications with Emphasis on Food Industry. In *Microbial Biotechnology in Food and Health*; Elsevier, 2021; pp 143–164. https://doi.org/10.1016/B978-0-12-819813-1.00006-2.

(21) Kundys, A.; Białecka-Florjańczyk, E.; Fabiszewska, A.; Małajowicz, J. Candida Antarctica Lipase B as Catalyst for Cyclic Esters Synthesis, Their Polymerization and Degradation of Aliphatic Polyesters. *J. Polym. Environ.* **2018**, *26* (1), 396–407. https://doi.org/10.1007/s10924-017-0945-1.

(22) Gotor-Fernández, V.; Busto, E.; Gotor, V. *Candida Antarctica* Lipase B: An Ideal Biocatalyst for the Preparation of Nitrogenated Organic Compounds. *Adv. Synth. Catal.* **2006**, *348* (7–8), 797–812. https://doi.org/10.1002/adsc.200606057.

(23) Michele Tavanti; Joseph Hosford; Richard C. Lloyd; Murray J. B. Brown. Recent Developments and Challenges for the Industrial Implementation of Polyphosphate Kinases. *ChemCatChem* **2021**, *13* (16), 3565–3580. https://doi.org/10.1002/cctc.202100688.

(24) Pérez, B.; Anankanbil, S.; Guo, Z. Synthesis of Sugar Fatty Acid Esters and Their Industrial Utilizations. In *Fatty Acids*; Elsevier, 2017; pp 329–354. https://doi.org/10.1016/B978-0-12-809521-8.00010-6.

(25) Hoydonckx, H. E.; De Vos, D. E.; Chavan, S. A.; Jacobs, P. A. Esterification and Transesterification of Renewable Chemicals. *Top. Catal.* **2004**, *27* (1–4), 83–96. https://doi.org/10.1023/B:TOCA.0000013543.96438.1a.

(26) Zhao, H.; van der Donk, W. A. Regeneration of Cofactors for Use in Biocatalysis. *Curr. Opin. Biotechnol.* **2003**, *14* (6), 583–589. https://doi.org/10.1016/j.copbio.2003.09.007.

(27) Liu, W.; Wang, P. Cofactor Regeneration for Sustainable Enzymatic Biosynthesis. *Biotechnol. Adv.* **2007**, *25* (4), 369–384. https://doi.org/10.1016/j.biotechadv.2007.03.002.

(28) *Biocatalysis*; Bommarius, A. S., Riebel, B., Eds.; Wiley-VCH: Weinheim, 2010. https://doi.org/10.1002/3527602364.

(29) Johannes Gottschalk; Lea Blaschke; Miriam Aßmann; Jürgen Kuballa; Lothar Elling. Integration of a Nucleoside Triphosphate Regeneration System in the One-Pot Synthesis of UDP-Sugars and Hyaluronic Acid. *ChemCatChem* **2021**, *13* (13), 3074–3083. https://doi.org/10.1002/cctc.202100462.

(30) Katchalski-Katzir, E. Immobilized Enzymes — Learning from Past Successes and Failures. *Trends Biotechnol.* **1993**, *11* (11), 471–478. https://doi.org/10.1016/0167-7799(93)90080-S.

(31) Datta, S.; Christena, L. R.; Rajaram, Y. R. S. Enzyme Immobilization: An Overview on Techniques and Support Materials. *3 Biotech* **2013**, *3* (1), 1–9. https://doi.org/10.1007/s13205-012-0071-7.

(32) Bornscheuer, U. T. Immobilizing Enzymes: How to Create More Suitable Biocatalysts. *Angew. Chem. Int. Ed.* **2003**, *42* (29), 3336–3337. https://doi.org/10.1002/anie.200301664.

(33) Brena, B.; González-Pombo, P.; Batista-Viera, F. Immobilization of Enzymes: A Literature Survey. In *Immobilization of Enzymes and Cells*; Guisan, J. M., Ed.; Methods in Molecular Biology; Humana Press: Totowa, NJ, 2013; Vol. 1051, pp 15–31. https://doi.org/10.1007/978-1-62703-550-7_2.

(34) DiCosimo, R.; McAuliffe, J.; Poulose, A. J.; Bohlmann, G. Industrial Use of Immobilized Enzymes. *Chem. Soc. Rev.* **2013**, *42* (15), 6437–6474. https://doi.org/10.1039/C3CS35506C.

(35) Mateo, C.; Palomo, J. M.; Fernandez-Lorente, G.; Guisan, J. M.; Fernandez-Lafuente, R. Improvement of Enzyme Activity, Stability and Selectivity via Immobilization Techniques. *Enzyme Microb. Technol.* **2007**, *40* (6), 1451–1463. https://doi.org/10.1016/j.enzmictec.2007.01.018.

(36) *Enzyme Inhibition and Bioapplications*; Sharma, R. R., Ed.; InTech: New York, 2012.

(37) Guncheva, M.; Dimitrov, M.; Zhiryakova, D. Novel Nanostructured Tin Dioxide as Promising Carrier for Candida Rugosa Lipase. *Process Biochem.* **2011**, *46* (11), 2170–2177. https://doi.org/10.1016/j.procbio.2011.08.020.

(38) *Flavours and Fragrances: Chemistry, Bioprocessing and Sustainability*; Berger, R. G., Ed.; Springer: Berlin ; New York, 2007.

(39) Zaks, A.; Klibanov, A. M. The Effect of Water on Enzyme Action in Organic Media. *J. Biol. Chem.* **1988**, *263* (17), 8017–8021. https://doi.org/10.1016/S0021-9258(18)68435-2.

(40) *Introduction to Enzyme Technology*; Jaeger, K.-E., Liese, A., Syldatk, C., Eds.; Learning Materials in Biosciences; Springer International Publishing: Cham, 2024. https://doi.org/10.1007/978-3-031-42999-6.

(41) Wedberg, R.; Abildskov, J.; Peters, G. H. Protein Dynamics in Organic Media at Varying Water Activity Studied by Molecular Dynamics Simulation. *J. Phys. Chem. B* **2012**, *116* (8), 2575–2585. https://doi.org/10.1021/jp211054u.

(42) Fogarty, A. C.; Laage, D. Water Dynamics in Protein Hydration Shells: The Molecular Origins of the Dynamical Perturbation. *J. Phys. Chem. B* **2014**, *118* (28), 7715–7729. https://doi.org/10.1021/jp409805p.

(43) Herbst, D.; Peper, S.; Fernández, J. F.; Ruck, W.; Niemeyer, B. Pressure Effects on Activity and Selectivity of Candida Rugosa Lipase in Organic Solvents. *J. Mol. Catal. B Enzym.* **2014**, *100*, 104–110. https://doi.org/10.1016/j.molcatb.2013.12.002.

(44) Doukyu, N.; Ogino, H. Organic Solvent-Tolerant Enzymes. *Biochem. Eng. J.* **2010**, *48* (3), 270–282. https://doi.org/10.1016/j.bej.2009.09.009.

(45) Vovers, J.; Smith, K. H.; Stevens, G. W. Bio-Based Molecular Solvents. In *The Application of Green Solvents in Separation Processes*; Elsevier, 2017; pp 91–110. https://doi.org/10.1016/B978-0-12-805297-6.00004-8.

(46) Cortes-Clerget, M.; Yu, J.; Kincaid, J. R. A.; Walde, P.; Gallou, F.; Lipshutz, B. H. Water as the Reaction Medium in Organic Chemistry: From Our Worst Enemy to Our Best Friend. *Chem. Sci.* **2021**, *12* (12), 4237–4266. https://doi.org/10.1039/D0SC06000C.

(47) Scepankova, H.; Galante, D.; Espinoza-Suaréz, E.; Pinto, C. A.; Estevinho, L. M.; Saraiva, J. High Hydrostatic Pressure in the Modulation of Enzymatic and Organocatalysis and Life under Pressure: A Review. *Molecules* **2023**, *28* (10), 4172. https://doi.org/10.3390/molecules28104172.

(48) Morild, E. The Theory of Pressure Effects on Enzymes. In *Advances in Protein Chemistry*; Elsevier, 1981; Vol. 34, pp 93–166. https://doi.org/10.1016/S0065-3233(08)60519-7.

(49) Hei, D. J.; Clark, D. S. Pressure Stabilization of Proteins from Extreme Thermophiles. *Appl. Environ. Microbiol.* **1994**, *60* (3), 932–939. https://doi.org/10.1128/aem.60.3.932-939.1994.

(50) Tsevdou, M.; Gogou, E.; Taoukis, P. High Hydrostatic Pressure Processing of Foods. In *Green Food Processing Techniques*; Elsevier, 2019; pp 87–137. https://doi.org/10.1016/B978-0-12-815353-6.00004-5.

(51) Charlier, C.; Alderson, T. R.; Courtney, J. M.; Ying, J.; Anfinrud, P.; Bax, A. Study of Protein Folding under Native Conditions by Rapidly Switching the Hydrostatic Pressure inside an NMR Sample Cell. *Proc. Natl. Acad. Sci.* **2018**, *115* (18). https://doi.org/10.1073/pnas.1803642115.

(52) Balny, C. Pressure Effects on Weak Interactions in Biological Systems. *J. Phys. Condens. Matter* **2004**, *16* (14), S1245–S1253. https://doi.org/10.1088/0953-8984/16/14/036.

(53) De Souza Melchiors, M.; Veneral, J. G.; Furigo Junior, A.; De Oliveira, J. V.; Di Luccio, M.; Prando, L. T.; Terenzi, H.; De Oliveira, D. Effect of Compressed Fluids on the Enzymatic Activity and Structure of Lysozyme. *J. Supercrit. Fluids* **2017**, *130*, 125–132. https://doi.org/10.1016/j.supflu.2017.07.020.

(54) Roland Winter; Dahabada Lopes; Stefan Grudzielanek; Karsten Vogtt. Towards an Understanding of the Temperature/ Pressure Configurational and Free-Energy Landscape of

Biomolecules. **2007**, *32* (1), 41–97. https://doi.org/10.1515/JNETDY.2007.003.

(55) Mishra, R.; Winter, R. Cold- and Pressure-Induced Dissociation of Protein Aggregates and Amyloid Fibrils. *Angew. Chem. Int. Ed.* **2008**, *47* (35), 6518–6521. https://doi.org/10.1002/anie.200802027.

(56) Mishra, S.; Sachan, A.; Vidyarthi, A. S.; Sachan, S. G. Transformation of Ferulic Acid to 4-Vinyl Guaiacol as a Major Metabolite: A Microbial Approach. *Rev. Environ. Sci. Biotechnol.* **2014**, *13* (4), 377–385. https://doi.org/10.1007/s11157-014-9348-0.

(57) Mozhaev, V. V.; Lange, R.; Kudryashova, E. V.; Balny, C. Application of High Hydrostatic Pressure for Increasing Activity and Stability of Enzymes. *Biotechnol. Bioeng.* **2000**, *52* (2), 320–331. https://doi.org/10.1002/(SICI)1097-0290(19961020)52:2<320::AID-BIT12>3.0.CO;2-N.

(58) Knorr, D.; Heinz, V.; Buckow, R. High Pressure Application for Food Biopolymers. *Biochim. Biophys. Acta BBA - Proteins Proteomics* **2006**, *1764* (3), 619–631. https://doi.org/10.1016/j.bbapap.2006.01.017.

(59) Heinz, V.; Buckow, R.; Knorr, D. Catalytic Activity of β-Amylase from Barley in Different Pressure/Temperature Domains. *Biotechnol. Prog.* **2005**, *21* (6), 1632–1638. https://doi.org/10.1021/bp0400137.

(60) Follonier, S.; Panke, S.; Zinn, M. Pressure to Kill or Pressure to Boost: A Review on the Various Effects and Applications of Hydrostatic Pressure in Bacterial Biotechnology. *Appl. Microbiol. Biotechnol.* **2012**, *93* (5), 1805–1815. https://doi.org/10.1007/s00253-011-3854-6.

(61) Santi, M.; Sancineto, L.; Nascimento, V.; Braun Azeredo, J.; Orozco, E. V. M.; Andrade, L. H.; Gröger, H.; Santi, C. Flow Biocatalysis: A Challenging Alternative for the Synthesis of APIs and Natural Compounds. *Int. J. Mol. Sci.* **2021**, *22* (3), 990. https://doi.org/10.3390/ijms22030990.

(62) Tabatabaei, M.; Aghbashlo, M.; Dehhaghi, M.; Panahi, H. K. S.; Mollahosseini, A.; Hosseini, M.; Soufiyan, M. M. Reactor Technologies for Biodiesel Production and Processing: A Review. *Prog. Energy Combust. Sci.* **2019**, *74*, 239–303. https://doi.org/10.1016/j.pecs.2019.06.001.

(63) Lindeque, R.; Woodley, J. Reactor Selection for Effective Continuous Biocatalytic Production of Pharmaceuticals. *Catalysts* **2019**, *9* (3), 262. https://doi.org/10.3390/catal9030262.

(64) Rehbein, M. C.; Wolters, J.; Kunick, C.; Scholl, S. Continuous High-Pressure Operation of a Pharmaceutically Relevant Krapcho Dealkoxycarbonylation Reaction. *J. Flow Chem.* **2019**, *9* (2), 123–131. https://doi.org/10.1007/s41981-019-00031-2.

(65) Hugentobler, K. G.; Rasparini, M.; Thompson, L. A.; Jolley, K. E.; Blacker, A. J.; Turner, N. J. Comparison of a Batch and Flow Approach for the Lipase-Catalyzed Resolution of a Cyclopropanecarboxylate Ester, A Key Building Block for the Synthesis of Ticagrelor. *Org. Process Res. Dev.* **2017**, *21* (2), 195–199. https://doi.org/10.1021/acs.oprd.6b00346.

(66) Kragl, U.; Vasic-Racki, D.; Wandrey, C. Kontinuierliche Reaktionsführung Mit

Löslichen Enzymen: Kontinuierliche Reaktionsführung Mit Löslichen Enzymen. *Chem. Ing. Tech.* **1992**, *64* (6), 499–509. https://doi.org/10.1002/cite.330640605.

(67) Brethauer, S.; Wyman, C. E. Review: Continuous Hydrolysis and Fermentation for Cellulosic Ethanol Production. *Bioresour. Technol.* **2010**, *101* (13), 4862–4874. https://doi.org/10.1016/j.biortech.2009.11.009.

(68) Kragl, U.; Dreisbach, C. Kontinuierliche asymmetrische Synthese in einem Membranreaktor. *Angew. Chem.* **1996**, *108* (6), 684–685. https://doi.org/10.1002/ange.19961080612.

(69) Lozano, P.; Garcia-Verdugo, E.; V. Luis, S.; Pucheault, M.; Vaultier, M. (Bio)Catalytic Continuous Flow Processes in scCO2 and/or ILs: Towards Sustainable (Bio)Catalytic Synthetic Platforms. *Curr. Org. Synth.* **2011**, *8* (6), 810–823. https://doi.org/10.2174/157017911804586593.

(70) Bolivar, J. M.; López-Gallego, F. Characterization and Evaluation of Immobilized Enzymes for Applications in Flow Reactors. *Curr. Opin. Green Sustain. Chem.* **2020**, *25*, 100349. https://doi.org/10.1016/j.cogsc.2020.04.010.

(71) Ancheyta, J. *Chemical Reaction Kinetics: Concepts, Methods, and Case Studies*; John Wiley & Sons, Inc: Hoboken, NJ, 2017.

(72) Bisswanger, H.; Degtiarev, D. *Enzymkinetik: Theorie und Methoden ; [mit CD-ROM]*, 3., völlig neu bearb. Aufl.; Wiley-VCH: Weinheim, 2000.

(73) Johnson, K. A.; Goody, R. S. The Original Michaelis Constant: Translation of the 1913 Michaelis–Menten Paper. *Biochemistry* **2011**, *50* (39), 8264–8269. https://doi.org/10.1021/bi201284u.

(74) Choi, B.; Rempala, G. A.; Kim, J. K. Beyond the Michaelis-Menten Equation: Accurate and Efficient Estimation of Enzyme Kinetic Parameters. *Sci. Rep.* **2017**, *7* (1), 17018. https://doi.org/10.1038/s41598-017-17072-z.

(75) *Industrial Biotransformations*, 2., completely rev. and extended ed.; Liese, A., Ed.; Wiley-VCH: Weinheim, 2006.

(76) MATLAB. 9.7.0.1190202 (R2019b). *The MathWorks Inc.* Natick, Massachusetts.

(77) Hazra, A. Using the Confidence Interval Confidently. *J. Thorac. Dis.* **2017**, *9* (10), 4124–4129. https://doi.org/10.21037/jtd.2017.09.14.

(78) Kuroda, A.; Kornberg, A. Polyphosphate Kinase as a Nucleoside Diphosphate Kinase in Escherichia Coli and Pseudomonas Aeruginosa. *Proc. Natl. Acad. Sci.* **1997**, *94* (2), 439–442. https://doi.org/10.1073/pnas.94.2.439.

(79) Jennifer N. Andexer; Michael Richter. Emerging Enzymes for ATP Regeneration in Biocatalytic Processes. *ChemBioChem* **2015**, *16* (3), 380–386. https://doi.org/10.1002/cbic.201402550.

(80) Restiawaty, E.; Iwasa, Y.; Maya, S.; Honda, K.; Omasa, T.; Hirota, R.; Kuroda, A.; Ohtake, H. Feasibility of Thermophilic Adenosine Triphosphate-Regeneration System Using Thermus Thermophilus Polyphosphate Kinase. *Process Biochem.* **2011**, *46* (9), 1747–1752.

https://doi.org/10.1016/j.procbio.2011.05.021.

(81) Iwamoto, S.; Motomura, K.; Shinoda, Y.; Urata, M.; Kato, J.; Takiguchi, N.; Ohtake, H.; Hirota, R.; Kuroda, A. Use of an Escherichia Coli Recombinant Producing Thermostable Polyphosphate Kinase as an ATP Regenerator to Produce Fructose 1,6-Diphosphate. *Appl. Environ. Microbiol.* **2007**, *73* (17), 5676–5678. https://doi.org/10.1128/AEM.00278-07.

(82) Salvi, H. M.; Yadav, G. D. Process Intensification Using Immobilized Enzymes for the Development of White Biotechnology. *Catal. Sci. Technol.* **2021**, *11* (6), 1994–2020. https://doi.org/10.1039/D1CY00020A.

(83) Tavanti, M.; Hosford, J.; Lloyd, R. C.; Brown, M. J. B. ATP Regeneration by a Single Polyphosphate Kinase Powers Multigram-Scale Aldehyde Synthesis in Vitro. *Green Chem.* **2021**, *23* (2), 828–837. https://doi.org/10.1039/D0GC03830J.

(84) Suzuki, S.; Hara, R.; Kino, K. Production of Aminoacyl Prolines Using the Adenylation Domain of Nonribosomal Peptide Synthetase with Class III Polyphosphate Kinase 2-Mediated ATP Regeneration. *J. Biosci. Bioeng.* **2018**, *125* (6), 644–648. https://doi.org/10.1016/j.jbiosc.2017.12.023.

(85) Jendrossek, D.; Hildenbrand, J. C. Polyphosphat — Ein Unterschätztes Molekül. *BIOspektrum* **2022**, *28* (7), 691–693. https://doi.org/10.1007/s12268-022-1856-9.

(86) Lelièvre, C. M.; Balandras, M.; Petit, J.; Vergne-Vaxelaire, C.; Zaparucha, A. ATP Regeneration System in Chemoenzymatic Amide Bond Formation with Thermophilic CoA Ligase. *ChemCatChem* **2020**, *12* (4), 1184–1189. https://doi.org/10.1002/cctc.201901870.

(87) Achbergerová, L.; Nahálka, J. Degradation of Polyphosphates by Polyphosphate Kinases from Ruegeria Pomeroyi. *Biotechnol. Lett.* **2014**, *36* (10), 2029–2035. https://doi.org/10.1007/s10529-014-1566-6.

(88) Motomura, K.; Hirota, R.; Okada, M.; Ikeda, T.; Ishida, T.; Kuroda, A. A New Subfamily of Polyphosphate Kinase 2 (Class III PPK2) Catalyzes Both Nucleoside Monophosphate Phosphorylation and Nucleoside Diphosphate Phosphorylation. *Appl. Environ. Microbiol.* **2014**, *80* (8), 2602–2608. https://doi.org/10.1128/AEM.03971-13.

(89) Tzeng, C. M.; Kornberg, A. The Multiple Activities of Polyphosphate Kinase of Escherichia Coli and Their Subunit Structure Determined by Radiation Target Analysis. *J. Biol. Chem.* **2000**, *275* (6), 3977–3983. https://doi.org/10.1074/jbc.275.6.3977.

(90) Nahálka, J.; Pätoprstý, V. Enzymatic Synthesis of Sialylation Substrates Powered by a Novel Polyphosphate Kinase (PPK3). *Org. Biomol. Chem.* **2009**, *7* (9), 1778–1780. https://doi.org/10.1039/b822549b.

(91) Neville, N.; Roberge, N.; Jia, Z. Polyphosphate Kinase 2 (PPK2) Enzymes: Structure, Function, and Roles in Bacterial Physiology and Virulence. *Int. J. Mol. Sci.* **2022**, *23* (2). https://doi.org/10.3390/ijms23020670.

(92) Zor, T.; Selinger, Z. Linearization of the Bradford Protein Assay Increases Its Sensitivity: Theoretical and Experimental Studies. *Anal. Biochem.* **1996**, *236* (2), 302–308. https://doi.org/10.1006/abio.1996.0171.

(93) Anderson, J.; Byrne, T.; Woelfel, K. J.; Meany, J. E.; Spyridis, G. T.; Pocker, Y. The Hydrolysis of P-Nitrophenyl Acetate: A Versatile Reaction To Study Enzyme Kinetics. *J. Chem. Educ.* **1994**, *71* (8), 715. https://doi.org/10.1021/ed071p715.

(94) Heinrich, J.; Lyons, L. Systematic Errors. *Annu. Rev. Nucl. Part. Sci.* **2007**, *57* (1), 145–169. https://doi.org/10.1146/annurev.nucl.57.090506.123052.

(95) Bevington, P. R.; Robinson, D. K. *Data Reduction and Error Analysis for the Physical Sciences*, 3rd ed.; McGraw-Hill: Boston, 2003.

(96) Fornasini, P. *The Uncertainty in Physical Measurements: An Introduction to Data Analysis in the Physics Laboratory*; Springer: New York, 2008.

(97) Agilent 7890A Gaschromatograph Fehlerbehebung.

(98) *Purolite: Lifetech™ ECR Enzyme Immobilization Procedures Application Guide (brochure).* https://www.cphi-online.com/lifetech-ecr-resins-are-robust-enzyme-carriers-file094352.html (accessed 2023-07-14).

(99) Reich, J. A.; Aßmann, M.; Hölting, K.; Bubenheim, P.; Kuballa, J.; Liese, A. *Shift of Reaction Equilibrium at High Pressure in the Continuous Synthesis of Neuraminic Acid*; preprint; organic chemistry, 2022. https://doi.org/10.3762/bxiv.2022.11.v1.

(100) Sharma, R. *Enzyme Inhibition and Bioapplications*; Sharma, R. R., Ed.; IntechOpen: Erscheinungsort nicht ermittelbar, 2012. https://doi.org/66067.

(101) Rodrigues, R. C.; Ortiz, C.; Berenguer-Murcia, Á.; Torres, R.; Fernández-Lafuente, R. Modifying Enzyme Activity and Selectivity by Immobilization. *Chem Soc Rev* **2013**, *42* (15), 6290–6307. https://doi.org/10.1039/C2CS35231A.

(102) Baerns, M.; Hofmann, H.; Renken, A. *Chemische Reaktionstechnik*; Thieme: Stuttgart, 1987.

(103) Liese, A.; Kragl, U. Influence of the Reactor Configuration on the Enantioselectivity of a Kinetic Resolution. *Chem. Ing. Tech.* **2013**, *85* (6), 826–832. https://doi.org/10.1002/cite.201300011.

(104) Contente, M. L.; Dall'Oglio, F.; Tamborini, L.; Molinari, F.; Paradisi, F. Highly Efficient Oxidation of Amines to Aldehydes with Flow-based Biocatalysis. *ChemCatChem* **2017**, *9* (20), 3843–3848. https://doi.org/10.1002/cctc.201701147.

(105) Benítez-Mateos, A. I.; Contente, M. L. Agarose vs. Methacrylate as Material Supports for Enzyme Immobilization and Continuous Processing. *Catalysts* **2021**, *11* (7), 814. https://doi.org/10.3390/catal11070814.

(106) Datta, R.; Anand, S.; Moulick, A.; Baraniya, D.; Pathan, S. I.; Rejsek, K.; Vranova, V.; Sharma, M.; Sharma, D.; Kelkar, A.; Formanek, P. How Enzymes Are Adsorbed on Soil Solid Phase and Factors Limiting Its Activity: A Review. *Int. Agrophysics* **2017**, *31* (2), 287–302. https://doi.org/10.1515/intag-2016-0049.

(107) Cao, L. *Carrier-Bound Immobilized Enzymes: Principles, Applications and Design*; Wiley-VCH: Weinheim, 2005.

(108) Siódmiak, T.; Dulęba, J.; Haraldsson, G. G.; Siódmiak, J.; Marszałł, M. P. The Studies

of Sepharose-Immobilized Lipases: Combining Techniques for the Enhancement of Activity and Thermal Stability. *Catalysts* **2023**, *13* (5), 887. https://doi.org/10.3390/catal13050887.

(109) Dobreva, E. Einfluß Einiger Faktoren in Abhängigkeit von Den Methoden Bei Der Immobilisierung Eines Bakteriellen Enzympräparats Mit Milchkoagulationswirkung: Immobilisierung Eines Enzympräparates. *Acta Biotechnol.* **1987**, *7* (1), 49–53. https://doi.org/10.1002/abio.370070111.

(110) *Immobilization of Enzymes and Cells*, 2nd ed.; Guisan, J. M., Ed.; Methods in biotechnology; Humana Press: Totowa, N.J, 2006.

(111) Wasti, A.; Ali Awan, M. Adsorption of Textile Dye onto Modified Immobilized Activated Alumina. *J. Assoc. Arab Univ. Basic Appl. Sci.* **2016**, *20* (1), 26–31. https://doi.org/10.1016/j.jaubas.2014.10.001.

(112) Gómez, J. M.; Romero, Ma. D.; Hodaifa, G.; De La Parra, E. Adsorption of Trypsin on Commercial Silica Gel. *Eng. Life Sci.* **2009**, *9* (4), 336–341. https://doi.org/10.1002/elsc.200900018.

(113) Zhao, X.; Qi, F.; Yuan, C.; Du, W.; Liu, D. Lipase-Catalyzed Process for Biodiesel Production: Enzyme Immobilization, Process Simulation and Optimization. *Renew. Sustain. Energy Rev.* **2015**, *44*, 182–197. https://doi.org/10.1016/j.rser.2014.12.021.

(114) Palomo, J. M.; Guisan, J. M. Different Strategies for Hyperactivation of Lipase Biocatalysts. In *Lipases and Phospholipases*; Sandoval, G., Ed.; Methods in Molecular Biology; Humana Press: Totowa, NJ, 2012; Vol. 861, pp 329–341. https://doi.org/10.1007/978-1-61779-600-5_20.

(115) Verger, R. 'Interfacial Activation' of Lipases: Facts and Artifacts. *Trends Biotechnol.* **1997**, *15* (1), 32–38. https://doi.org/10.1016/S0167-7799(96)10064-0.

(116) Herbst, D.; Peper, S.; Niemeyer, B. Enzyme Catalysis in Organic Solvents: Influence of Water Content, Solvent Composition and Temperature on Candida Rugosa Lipase Catalyzed Transesterification. *J. Biotechnol.* **2012**, *162* (4), 398–403. https://doi.org/10.1016/j.jbiotec.2012.03.011.

(117) Winkelman, J. G. M.; Kraai, G. N.; Heeres, H. J. Binary, Ternary and Quaternary Liquid–Liquid Equilibria in 1-Butanol, Oleic Acid, Water and n-Heptane Mixtures. *Fluid Phase Equilibria* **2009**, *284* (2), 71–79. https://doi.org/10.1016/j.fluid.2009.06.013.

(118) Atanassova, M.; Kurteva, V. Mutual Solubilities between Ethylene Glycol and Organic Diluents: Gas Chromatography and NMR. *Molecules* **2023**, *28* (13), 5121. https://doi.org/10.3390/molecules28135121.

(119) *Makromolekulare Stoffe: Teilband 1-3*, 4th ed.; Bartl, H., Falbe, J., Eds.; Georg Thieme Verlag: Stuttgart, 1987; p b-003-113755. https://doi.org/10.1055/b-003-113755.

(120) Gao, J.; Guan, D.; Xu, D.; Zhang, L.; Zhang, Z. Measurement and Modeling of Liquid–Liquid Equilibrium for the Systems Vinyl Acetate + Acetic Acid/Ethanol + Water at 298.15 and 308.15 K. *J. Chem. Eng. Data* **2017**, *62* (4), 1240–1246. https://doi.org/10.1021/acs.jced.6b00794.

(121) Bornscheuer, U.; Herar, A.; Kreye, L.; Wendel, V.; Capewell, A.; Meyer, H. H.; Scheper, T.; Kolisis, F. N. Factors Affecting the Lipase Catalyzed Transesterification Reactions of 3-Hydroxy Esters in Organic Solvents. *Tetrahedron Asymmetry* **1993**, *4* (5), 1007–1016. https://doi.org/10.1016/S0957-4166(00)80145-7.

(122) Aghaei, H.; Yasinian, A.; Taghizadeh, A. Covalent Immobilization of Lipase from Candida Rugosa on Epoxy-Activated Cloisite 30B as a New Heterofunctional Carrier and Its Application in the Synthesis of Banana Flavor and Production of Biodiesel. *Int. J. Biol. Macromol.* **2021**, *178*, 569–579. https://doi.org/10.1016/j.ijbiomac.2021.02.146.

(123) Castiglione, K.; Weuster-Botz, D. Enzymatische Prozesse. In *Bioprozesstechnik*; Chmiel, H., Takors, R., Weuster-Botz, D., Eds.; Springer Berlin Heidelberg: Berlin, Heidelberg, 2018; pp 403–447. https://doi.org/10.1007/978-3-662-54042-8_10.

(124) Hanefeld, U.; Gardossi, L.; Magner, E. Understanding Enzyme Immobilisation. *Chem Soc Rev* **2009**, *38* (2), 453–468. https://doi.org/10.1039/B711564B.

(125) Cotton, F. A.; Francis, J. N.; Frenz, B. A.; Tsutsui, M. Structure of a Dihapto(Vinyl Alcohol) Complex of Platinum(II). *J. Am. Chem. Soc.* **1973**, *95* (8), 2483–2486. https://doi.org/10.1021/ja00789a011.

(126) Trapp, C. Untersuchungen Zu Stereoselektiven Reduktionen Ausgewählter α-Substituierter β-Ketocarbonsäureester Durch Bio-Und Chemokatalytische Transformationen. **2021**.

(127) Palocci, C.; Falconi, M.; Chronopoulou, L.; Cernia, E. Lipase-Catalyzed Regioselective Acylation of Tritylglycosides in Supercritical Carbon Dioxide. *J. Supercrit. Fluids* **2008**, *45* (1), 88–93. https://doi.org/10.1016/j.supflu.2007.11.009.

(128) Zhao, Z.; Tian, J.; Wu, Z.; Liu, J.; Zhao, D.; Shen, W.; He, L. Enhancing Enzymatic Stability of Bioactive Papers by Implanting Enzyme-Immobilized Mesoporous Silica Nanorods into Paper. *J. Mater. Chem. B* **2013**, *1* (37), 4719. https://doi.org/10.1039/c3tb20953a.

(129) Pencreac'h, G.; Baratti, J. C. Comparison of Hydrolytic Activity in Water and Heptane for Thirty-Two Commercial Lipase Preparations. *Enzyme Microb. Technol.* **2001**, *28* (4–5), 473–479. https://doi.org/10.1016/S0141-0229(00)00355-0.

(130) Spinchem. https://www.spinchem.com/media/lu2mr3ky/spinchem-applicationnote-1029.pdf (accessed 2023-08-22).

(131) Liese, A.; Hilterhaus, L. Evaluation of Immobilized Enzymes for Industrial Applications. *Chem. Soc. Rev.* **2013**, *42* (15), 6236. https://doi.org/10.1039/c3cs35511j.

(132) Buchholz, K.; Kasche, V.; Bornscheuer, U. T. *Biocatalysts and Enzyme Technology*, 2., completely rev., and enl. ed.; Wiley-Blackwell: Weinheim, 2012.

(133) Lozano, P.; Víllora, G.; Gómez, D.; Gayo, A. B.; Sánchez-Conesa, J. A.; Rubio, M.; Iborra, J. L. Membrane Reactor with Immobilized Candida Antarctica Lipase B for Ester Synthesis in Supercritical Carbon Dioxide. *J. Supercrit. Fluids* **2004**, *29* (1–2), 121–128. https://doi.org/10.1016/S0896-8446(03)00050-0.

(134) Noel Marie-Olive, M.; Athes, V.; Combes, D. Combined Effects of Pressure and

Temperature on Enzyme Stability. *High Press. Res.* **2000**, *19* (1–6), 317–322. https://doi.org/10.1080/08957950008202571.

(135) *Effect of High-Pressure Technologies on Enzymes: Science and Applications*; Leite Júnior, B. R. de C., Ed.; Foundations and frontiers in enzymology; Elsevier Science & Technology: San Diego, 2023.

(136) Knop, J.-M.; Mukherjee, S.; Jaworek, M. W.; Kriegler, S.; Manisegaran, M.; Fetahaj, Z.; Ostermeier, L.; Oliva, R.; Gault, S.; Cockell, C. S.; Winter, R. Life in Multi-Extreme Environments: Brines, Osmotic and Hydrostatic Pressure─A Physicochemical View. *Chem. Rev.* **2023**, *123* (1), 73–104. https://doi.org/10.1021/acs.chemrev.2c00491.

(137) Ostermeier, L.; Oliva, R.; Winter, R. The Multifaceted Effects of DMSO and High Hydrostatic Pressure on the Kinetic Constants of Hydrolysis Reactions Catalyzed by α-Chymotrypsin. *Phys. Chem. Chem. Phys. PCCP* **2020**, *22* (28), 16325–16333. https://doi.org/10.1039/d0cp03062g.

(138) Leite Júnior, B. R. de C.; Tribst, A. A. L.; Cristianini, M. Effect of High-Pressure Technologies on Enzymes Applied in Food Processing. In *Enzyme Inhibitors and Activators*; Senturk, M., Ed.; InTech, 2017. https://doi.org/10.5772/66629.

(139) Munir, M.; Nadeem, M.; Qureshi, T. M.; Leong, T. S. H.; Gamlath, C. J.; Martin, G. J. O.; Ashokkumar, M. Effects of High Pressure, Microwave and Ultrasound Processing on Proteins and Enzyme Activity in Dairy Systems — A Review. *Innov. Food Sci. Emerg. Technol.* **2019**, *57*, 102192. https://doi.org/10.1016/j.ifset.2019.102192.

(140) Domínguez De María, P.; Sánchez-Montero, J. M.; Sinisterra, J. V.; Alcántara, A. R. Understanding Candida Rugosa Lipases: An Overview. *Biotechnol. Adv.* **2006**, *24* (2), 180–196. https://doi.org/10.1016/j.biotechadv.2005.09.003.

(141) Kahlow, U. H. M.; Schmid, R. D.; Pleiss, J. A Model of the Pressure Dependence of the Enantioselectivity of *Candida Rugosa* Lipase towards (±)-Menthol. *Protein Sci.* **2001**, *10* (10), 1942–1952. https://doi.org/10.1110/ps.12301.

(142) Kazlauskas, R. J.; Weissfloch, A. N. E.; Rappaport, A. T.; Cuccia, L. A. A Rule to Predict Which Enantiomer of a Secondary Alcohol Reacts Faster in Reactions Catalyzed by Cholesterol Esterase, Lipase from Pseudomonas Cepacia, and Lipase from Candida Rugosa. *J. Org. Chem.* **1991**, *56* (8), 2656–2665. https://doi.org/10.1021/jo00008a016.

(143) Persichetti, R. A.; Lalonde, J. J.; Govardhan, C. P.; Khalaf, N. K.; Margolin, A. L. Candida Rugosa Lipase: Enantioselectivity Enhancements in Organic Solvents. *Tetrahedron Lett.* **1996**, *37* (36), 6507–6510. https://doi.org/10.1016/0040-4039(96)01430-X.

(144) Cygler, M.; Grochulski, P.; Kazlauskas, R. J.; Schrag, J. D.; Bouthillier, F.; Rubin, B.; Serreqi, A. N.; Gupta, A. K. A Structural Basis for the Chiral Preferences of Lipases. *J. Am. Chem. Soc.* **1994**, *116* (8), 3180–3186. https://doi.org/10.1021/ja00087a002.

(145) Zhong, X.; Qian, J.; Liu, M.; Ma, L. *Candida Rugosa* Lipase-catalyzed Synthesis of Sucrose-6-acetate in a 2-butanol/Buffer Two-phase System. *Eng. Life Sci.* **2013**, *13* (6), 563–571. https://doi.org/10.1002/elsc.201200170.

(146) Eisenmenger, M. J.; Reyes-De-Corcuera, J. I. Kinetics of Lipase Catalyzed Isoamyl Acetate Synthesis at High Hydrostatic Pressure in Hexane. *Biotechnol. Lett.* **2010**, *32* (9), 1287–1291. https://doi.org/10.1007/s10529-010-0288-7.

(147) Chen, G.; Tang, J.; Miao, M.; Jiang, B.; Jin, J.; Feng, B. Elucidation of Pressure-Induced Lid Movement and Catalysis Behavior of Rhizopus Chinensis Lipase. *Int. J. Biol. Macromol.* **2017**, *103*, 360–365. https://doi.org/10.1016/j.ijbiomac.2017.04.122.

(148) Masson, P.; Balny, C. Linear and Non-Linear Pressure Dependence of Enzyme Catalytic Parameters. *Biochim. Biophys. Acta BBA - Gen. Subj.* **2005**, *1724* (3), 440–450. https://doi.org/10.1016/j.bbagen.2005.05.003.

(149) Romero, M. D.; Calvo, L.; Alba, C.; Daneshfar, A.; Ghaziaskar, H. S. Enzymatic Synthesis of Isoamyl Acetate with Immobilized Candida Antarctica Lipase in N-Hexane. *Enzyme Microb. Technol.* **2005**, *37* (1), 42–48. https://doi.org/10.1016/j.enzmictec.2004.12.033.

(150) *Biocatalysis in Agricultural Biotechnology*; Whitaker, J. R., Sonnet, P. E., Eds.; ACS Symposium Series; American Chemical Society: Washington, DC, 1989; Vol. 389. https://doi.org/10.1021/bk-1989-0389.

(151) Rackel, H. Enzymimmobilisierung an oberflächenmodifizierten superparamagnetischen Silica-Partikeln. **2006**. https://doi.org/10.15488/6781.

(152) Vilareal, H.; Alfaia, A.; Calado, A.; Ribeiro, M. High Pressure-Temperature Effects on Enzymatic Activity: Naringin Bioconversion. *Food Chem.* **2007**, *102* (3), 565–570. https://doi.org/10.1016/j.foodchem.2006.05.033.

(153) Uppenberg, J.; Oehrner, N.; Norin, M.; Hult, K.; Kleywegt, G. J.; Patkar, S.; Waagen, V.; Anthonsen, T.; Jones, T. A. Crystallographic and Molecular-Modeling Studies of Lipase B from Candida Antarctica Reveal a Stereospecificity Pocket for Secondary Alcohols. *Biochemistry* **1995**, *34* (51), 16838–16851. https://doi.org/10.1021/bi00051a035.

(154) Otten, L. G.; Hollmann, F.; Arends, I. W. C. E. Enzyme Engineering for Enantioselectivity: From Trial-and-Error to Rational Design? *Trends Biotechnol.* **2010**, *28* (1), 46–54. https://doi.org/10.1016/j.tibtech.2009.10.001.

(155) Léonard-Nevers, V.; Marton, Z.; Lamare, S.; Hult, K.; Graber, M. Understanding Water Effect on Candida Antarctica Lipase B Activity and Enantioselectivity towards Secondary Alcohols. *J. Mol. Catal. B Enzym.* **2009**, *59* (1–3), 90–95. https://doi.org/10.1016/j.molcatb.2009.01.008.

(156) Lund, I. T.; Bøckmann, P. L.; Jacobsen, E. E. Highly Enantioselective CALB-Catalyzed Kinetic Resolution of Building Blocks for β-Blocker Atenolol. *Tetrahedron* **2016**, *72* (46), 7288–7292. https://doi.org/10.1016/j.tet.2016.02.018.

(157) Schönstein, L.; Forró, E.; Fülöp, F. Continuous-Flow Enzymatic Resolution Strategy for the Acylation of Amino Alcohols with a Remote Stereogenic Centre: Synthesis of Calycotomine Enantiomers. *Tetrahedron Asymmetry* **2013**, *24* (4), 202–206. https://doi.org/10.1016/j.tetasy.2013.01.006.

(158) Ottosson, J.; Fransson, L.; King, J. W.; Hult, K. Size as a Parameter for Solvent Effects on Candida Antarctica Lipase B Enantioselectivity. *Biochim. Biophys. Acta BBA - Protein Struct. Mol. Enzymol.* **2002**, *1594* (2), 325–334. https://doi.org/10.1016/S0167-4838(01)00324-7.

(159) Csajági, C.; Szatzker, G.; Rita Tőke, E.; Ürge, L.; Darvas, F.; Poppe, L. Enantiomer Selective Acylation of Racemic Alcohols by Lipases in Continuous-Flow Bioreactors. *Tetrahedron Asymmetry* **2008**, *19* (2), 237–246. https://doi.org/10.1016/j.tetasy.2008.01.002.

(160) Iyer, P. V.; Ananthanarayan, L. Enzyme Stability and Stabilization—Aqueous and Non-Aqueous Environment. *Process Biochem.* **2008**, *43* (10), 1019–1032. https://doi.org/10.1016/j.procbio.2008.06.004.

(161) Stiller, J. B.; Jordan Kerns, S.; Hoemberger, M.; Cho, Y.-J.; Otten, R.; Hagan, M. F.; Kern, D. Probing the Transition State in Enzyme Catalysis by High-Pressure NMR Dynamics. *Nat. Catal.* **2019**, *2* (8), 726–734. https://doi.org/10.1038/s41929-019-0307-6.

(162) Gross, M.; Jaenicke, R. Proteins under Pressure: The Influence of High Hydrostatic Pressure on Structure, Function and Assembly of Proteins and Protein Complexes. *Eur. J. Biochem.* **1994**, *221* (2), 617–630. https://doi.org/10.1111/j.1432-1033.1994.tb18774.x.

(163) Pandey, P. K.; Ramaswamy, H. S. Effect of High - Pressure Treatment of Milk on Lipase and Glutamyl Transferase Activity. *J. Food Biochem.* **2004**, *28* (6), 449–462. https://doi.org/10.1111/j.1745-4514.2004.02603.x.

(164) Hildenbrand, J. C.; Teleki, A.; Jendrossek, D. A Universal Polyphosphate Kinase: PPK2c of Ralstonia Eutropha Accepts Purine and Pyrimidine Nucleotides Including Uridine Diphosphate. *Appl. Microbiol. Biotechnol.* **2020**, *104* (15), 6659–6667. https://doi.org/10.1007/s00253-020-10706-9.

(165) Ishige, K.; Zhang, H.; Kornberg, A. Polyphosphate Kinase (PPK2), a Potent, Polyphosphate-Driven Generator of GTP. *Proc. Natl. Acad. Sci. U. S. A.* **2002**, *99* (26), 16684–16688. https://doi.org/10.1073/pnas.262655299.

(166) El-Aziz, S. M. A.; Faraag, A. H. I.; Ibrahim, A. M.; Albrakati, A.; Bakkar, M. R. *Tyrosinase Enzyme Purification and Immobilization from Pseudomonas Sp. EG22 Using Cellulose Coated Magnetic Nanoparticles: Characterization of Bioactivity in Melanin Product*; preprint; In Review, 2023. https://doi.org/10.21203/rs.3.rs-3100351/v1.

(167) Khan, M. R. Immobilized Enzymes: A Comprehensive Review. *Bull. Natl. Res. Cent.* **2021**, *45* (1), 207. https://doi.org/10.1186/s42269-021-00649-0.

(168) Krishnaswamy, M.; Kenkare, U. W. The Effect of pH, Temperature, and Organic Solvents on the Kinetic Parameters of Escherichia Coli Alkaline Phosphatase. *J. Biol. Chem.* **1970**, *245* (15), 3956–3963. https://doi.org/10.1016/S0021-9258(18)62941-2.

(169) Hammer, S. C.; Knight, A. M.; Arnold, F. H. Design and Evolution of Enzymes for Non-Natural Chemistry. *Curr. Opin. Green Sustain. Chem.* **2017**, *7*, 23–30. https://doi.org/10.1016/j.cogsc.2017.06.002.

(170) Fogler, H. S. *Elements of Chemical Reaction Engineering*, 3rd ed., Eastern Economy

ed.; Prentice-Hall of India: New Delhi, 2006.
(171) Jensen, J. N. Approach to Steady State in Completely Mixed Flow Reactors. *J. Environ. Eng.* **2001**, *127* (1), 13–18. https://doi.org/10.1061/(ASCE)0733-9372(2001)127:1(13).
(172) Özdural, A. R.; Tanyolaç, D.; Boyacı, İ. H.; Mutlu, M.; Webb, C. Determination of Apparent Kinetic Parameters for Competitive Product Inhibition in Packed-Bed Immobilized Enzyme Reactors. *Biochem. Eng. J.* **2003**, *14* (1), 27–36. https://doi.org/10.1016/S1369-703X(02)00099-2.
(173) Weekman, V. W. Laboratory Reactors and Their Limitations. *AIChE J.* **1974**, *20* (5), 833–840. https://doi.org/10.1002/aic.690200502.
(174) Naramittanakul, A.; Buttranon, S.; Petchsuk, A.; Chaiyen, P.; Weeranoppanant, N. Development of a Continuous-Flow System with Immobilized Biocatalysts towards Sustainable Bioprocessing. *React. Chem. Eng.* **2021**, *6* (10), 1771–1790. https://doi.org/10.1039/d1re00189b.
(175) Adebar, N.; Nastke, A.; Löwe, J.; Gröger, H. Segmentierte Flow-Prozesse Zur Überwindung von Limitierungen Der Ganzzell-Biokatalyse in Gegenwart von Organischen Lösungsmitteln. *Angew. Chem.* **2021**, *133* (29), 15997–16004. https://doi.org/10.1002/ange.202015887.
(176) Wang, J.; Gu, S.-S.; Cui, H.-S.; Yang, L.-Q.; Wu, X.-Y. Rapid Synthesis of Propyl Caffeate in Ionic Liquid Using a Packed Bed Enzyme Microreactor under Continuous-Flow Conditions. *Bioresour. Technol.* **2013**, *149*, 367–374. https://doi.org/10.1016/j.biortech.2013.09.098.
(177) Trodler, P.; Pleiss, J. Modeling Structure and Flexibility of Candida Antarctica Lipase B in Organic Solvents. *BMC Struct. Biol.* **2008**, *8* (1), 9. https://doi.org/10.1186/1472-6807-8-9.
(178) Jaworek, M. W.; Gajardo-Parra, N. F.; Sadowski, G.; Winter, R.; Held, C. Boosting the Kinetic Efficiency of Formate Dehydrogenase by Combining the Effects of Temperature, High Pressure and Co-Solvent Mixtures. *Colloids Surf. B Biointerfaces* **2021**, *208*, 112127. https://doi.org/10.1016/j.colsurfb.2021.112127.
(179) Hassan, S. S.; Williams, G. A.; Jaiswal, A. K. Emerging Technologies for the Pretreatment of Lignocellulosic Biomass. *Bioresour. Technol.* **2018**, *262*, 310–318. https://doi.org/10.1016/j.biortech.2018.04.099.
(180) Follonier, S.; Panke, S.; Zinn, M. Pressure to Kill or Pressure to Boost: A Review on the Various Effects and Applications of Hydrostatic Pressure in Bacterial Biotechnology. *Appl. Microbiol. Biotechnol.* **2012**, *93* (5), 1805–1815. https://doi.org/10.1007/s00253-011-3854-6.
(181) Tufvesson, P.; Lima-Ramos, J.; Nordblad, M.; Woodley, J. M. Guidelines and Cost Analysis for Catalyst Production in Biocatalytic Processes. *Org. Process Res. Dev.* **2011**, *15* (1), 266–274. https://doi.org/10.1021/op1002165.

8. Appendix

This section provides additional and supplementary information.

8.1. Gas Chromatography

The GC chromatograms and the resulting calibration curves are given in Figure 44, Figure 45 and Figure 46.

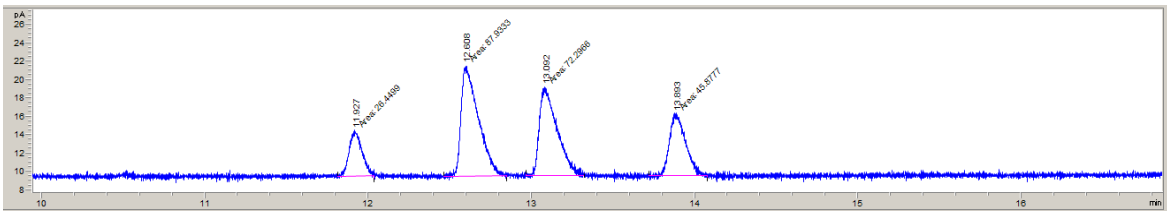

Figure 44: GC chromatograms of (*R*/*S*)-1-phenyl-2-propanol and (*R*/*S*)-1-phenyl-2-propanyl acetate

Typical resulting retention times are $t_{S\text{-PPA}} = 11.6$ min, $t_{S\text{-PP}} = 12.6$ min, $t_{R\text{-PP}} = 13.1$ min and $t_{R\text{-PPA}} = 13.7$ min.

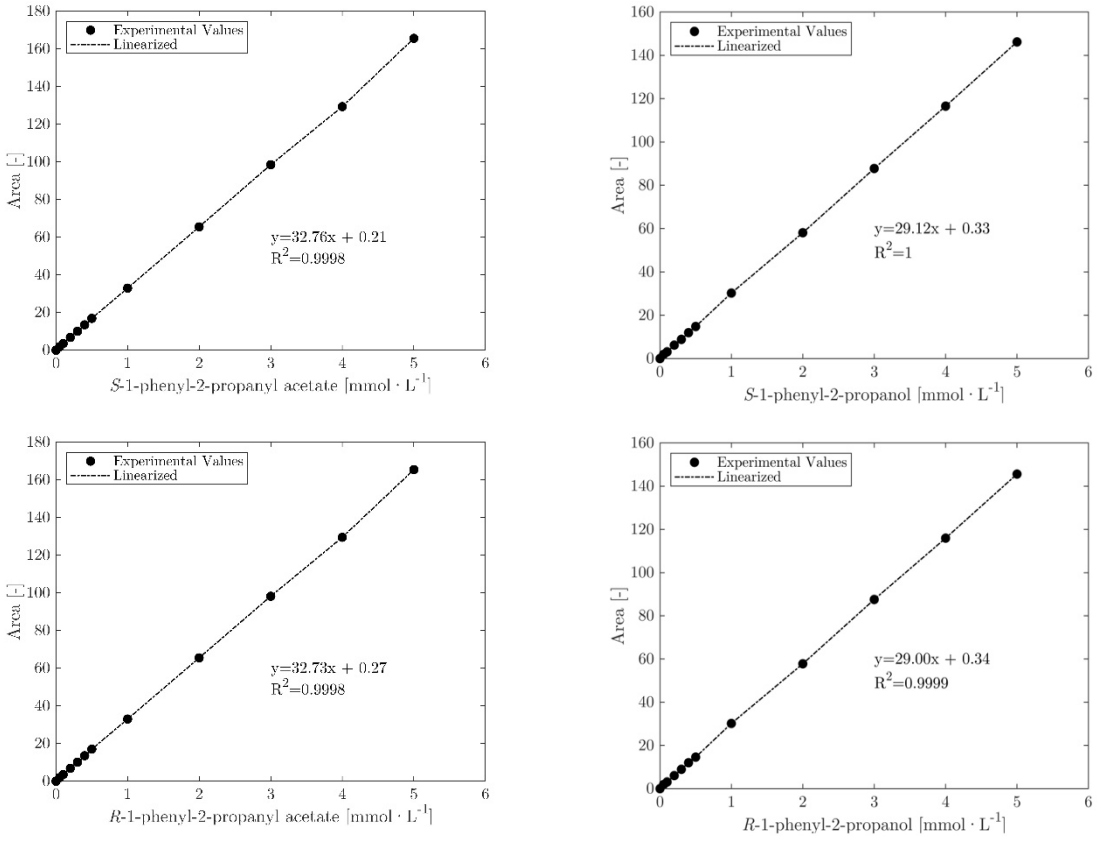

Figure 45: Calibration of (*R*/*S*)-1-phenyl-2-propanol and (*R*/*S*)-1-phenyl-2-propanyl acetate up to 5.0 mmol ·L^{-1}

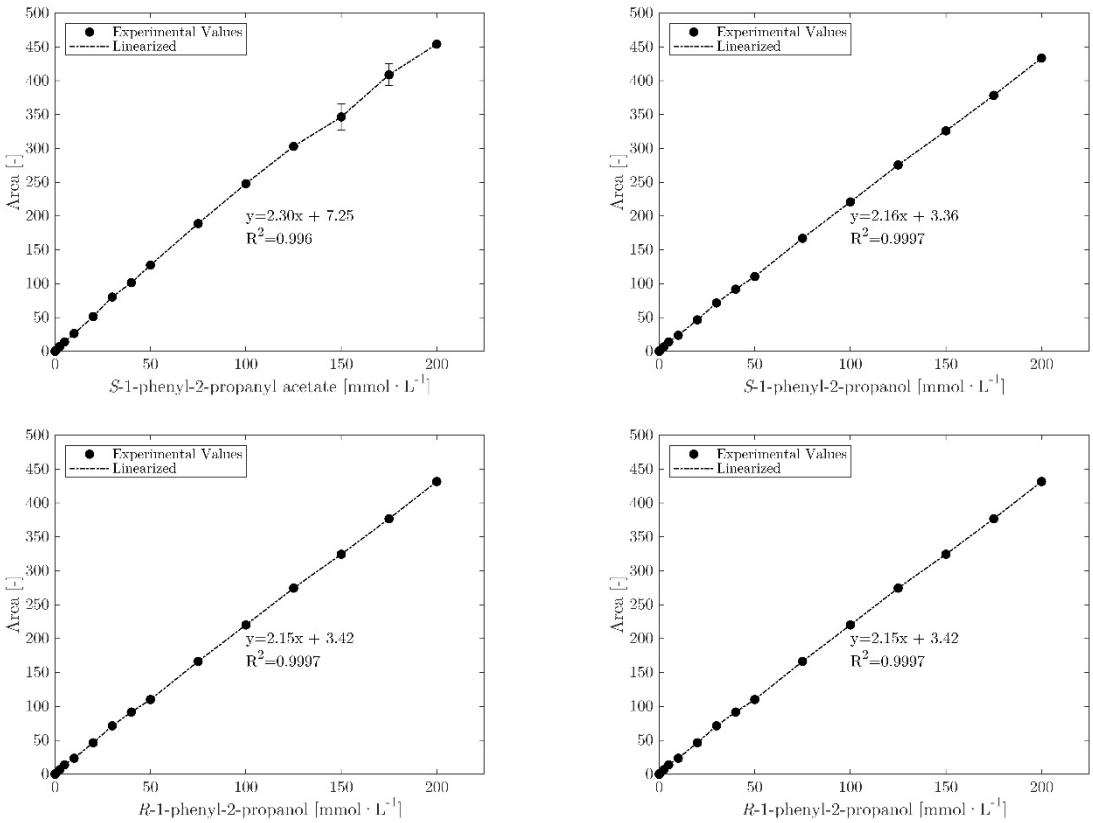

Figure 46: Calibration of (*R*/*S*)- 1-phenyl-2-propanol and (*R*/*S*)- 1-phenyl-2-propanyl acetate up to 200.0 mmol ·L^{-1}

8.2. High Pressure Liquid Chromatography

The HPLC chromatograms and the resulting calibration curves are given in Figure 47and Figure 48.

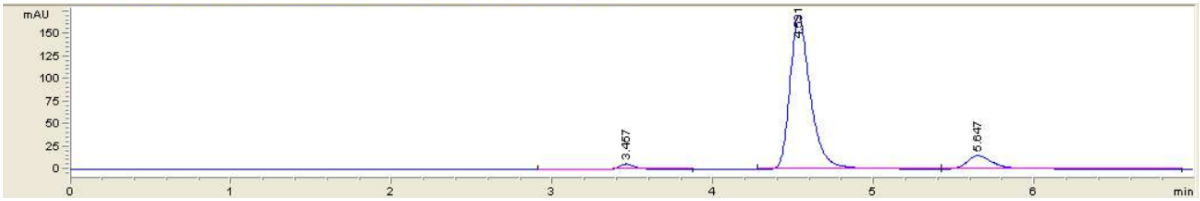

Figure 47: HPLC chromatograms of CMP, CDP and CTP

Typical resulting retention times are t_{CMP} = 3.4 min, t_{CDP} = 4.7 min and t_{CTP} = 5.6 min.

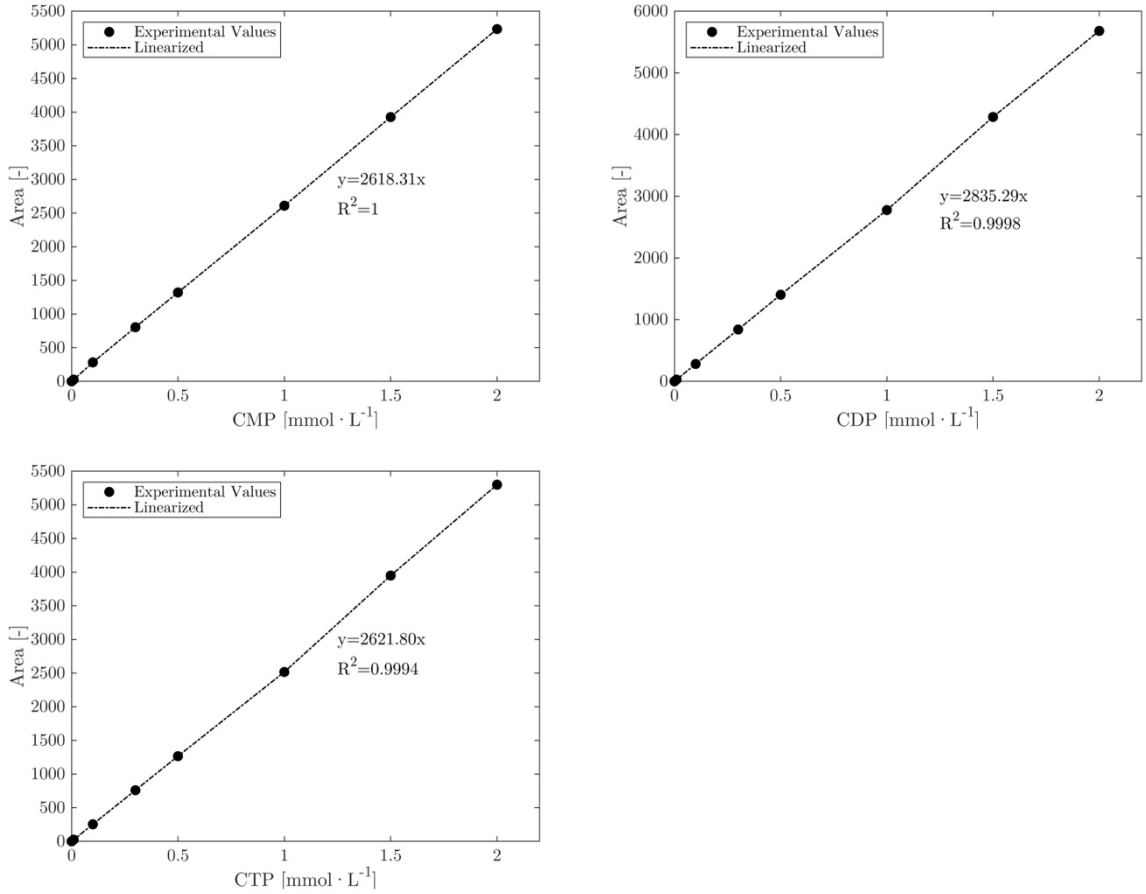

Figure 48: Calibration of CMP, CDP and CTP

8.3. Immobilization of *Candida rugosa* Lipase

Table 31 gives the number of the immobilization procedure with resulting enzyme loading and the immobilization yield.

Table 31: Immobilization experiment for CRL.

Immobilization Batch	Yield [%]	Enzyme Load [$\mu g_{enzyme} \cdot g_{carrier}^{-1}$]
TR 1	61.8	780.2
TR 2	14.3	240.5
TR 3	53.9	825.8
TR 4	77.4	568.8
TR 5	81.6	1261.2
TR 6	76.2	1955.4
TR 8	50.8	835.5
TR 9	77.1	3426.1
TR 10	70.6	1603.0
TR 11	47.0	979.9
TR 12	75.7	1144.7
TR 13	30.7	1200.5
TR 16	74.8	1141.7
TR 17	25.2	151.4
TR 20	74.6	5957.5
TR 21	75.4	8369.0

8.4. Immobilization of *Candida antarctica* Lipase B

Table 32 gives the number of the immobilization process with resulting enzyme loading and the immobilization yield.

Table 32: Immobilization experiment for CalB.

Immobilization Batch	Yield [%]	Enzyme Load [$\mu g_{enzyme} \cdot g_{carrier}^{-1}$]
TR 7	64.3	30171.5
TR 14	31.4	2642.1
TR 15	94.6	17366.9
TR 18	80.4	6035.0
TR 19	88.9	21152.7
TR 22	82.6	11057.8

8.5. Overview of *Candida antarctica* lipase B Experiments to Investigate the Dependency of the Specific Activity on Pressure and Temperature

The overview of *Candida antarctica* lipase B experiments to investigate the dependency of the specific activity on pressure and temperature is given in Table 33.

Table 33: Investigating of activity in dependency on pressure and temperature overview of used immobilization batches.

Experiment	Temperature [°C]	Pressure steps [bar]	Immobilization batch
HP_011	35	800, 1200	TR15
HP_012	35	800, 1200	TR15
HP_023	45	800, 1200	TR18
HP_024	45	800, 1200	TR18
HP_007	55	800, 1200	TR15
HP_008	55	800, 1200	TR15
HP_009	65	800, 1200	TR15
HP_010	65	800, 1200	TR15
HP_019	35	400, 600	TR15
HP_022	35	400, 600	TR18
HP_013	45	400, 600	TR15
HP_014	45	400, 600	TR15
HP_015	55	400, 600	TR15
HP_016	55	400, 600	TR15
HP_017	65	400, 600	TR15
HP_018	65	400, 600	TR15
HP_020	45	400, 600	TR17

8.6. Molecular Weight Analysis of Polyphosphate

Gel permeation chromatography (GPC) was used to determine the molecular weight distribution of the polyphosphate. A set-up consisting of a LC-20AT pump C (Shimadzu, Kyōto, Japan), a DEGASi conventional degasser (Biotech, Onsala, Sweden), a 3900 smart RI autosampler (Knauer, Berlin, Germany), a Viscotek 270 Dual refractive index detector (RID) (Malvern Panalytical, Malvern, UK), and an electronic range control (ERC) oven. For the separation, two PL-aquagel-OH mixed-H 8 µm, 300 × 7.5 mm columns (Agilent, Santa Clara, USA) were used in conjunction with an GPC/SEC guard column (Agilent, Santa Clara, USA), to prevent impurities from entering the analytical columns. The data analysis was performed using OmniSEC software (Malvern Panalytical, Malvern, UK). The mobile phase used was a 150.0 mmol $\cdot$ L^{-1} sodium chloride (NaCl) solution, stripped with helium gas for 20 min, to replace dissolved gasses, before being pumped through the system at a rate of 1.0 mL $\cdot$ min^{-1}. For the analysis, 125 mg of polyP MERCK EMPURA®; CAS-Number: 10361-03-2 (Merck KGaA, Darmstadt, Germany) was dissolved in 5 mL of water as the standard solution with a nominal concentration of 25 g $\cdot$ L^{-1}. The solution was filtered through a 0.2 µm pore size regenerated cellulose membrane syringe filter. A 1:10 dilution from the filtered standard solution was prepared at room temperature and vortexed thoroughly, before being analyzed.

The system was established using water in a stepwise increase starting at 0.3 $mL \cdot min^{-1}$, increasing to 0.6 $mL \cdot min^{-1}$, then 0.8 $mL \cdot min^{-1}$ and finally to 1.0 $mL \cdot min^{-1}$, holding the flow constant for 20 min between each step. Then the solvent was exchanged by lowering the flowrate to 0.8 $mL \cdot min^{-1}$, and starting the feed with the 150.0 $mmol \cdot L^{-1}$ NaCl Solution. The rate was held for 20 min before increasing to 1.0 $mL \cdot min^{-1}$ and maintained for 20 min allowing the system to equilibrate. After that point, samples were injected using the autosampler.

A 12-point calibration with narrow standards was performed, to estimate the molecular weight of polyP. Three polyethylene-oxide (PEO) / polyethylene-glycol (PEG) mixtures (Agilent, InfinityLab EasiVial PEG/PEO) each with four known standards were used to establish a wide-range calibration. The standards were obtained from Agilent (Agilent, Santa Clara, USA) with molecular weights between 106 to 1500000 $g \cdot mol^{-1}$. They were used to correlate the retention time with the molecular weight through the gel permeation chromatography set-up.

Determination of Polyphosphate Length

The size of commercially available polyP was measured using gel permeation chromatography (GPC). Commercially available sodium polyphosphate from MERCK EMPURA®; CAS-Number: 10361-03-2 (Merck KGaA, Darmstadt, Germany) was dissolved in water and passed through a separation column, to estimate the molecular size and distribution of polyP chains of different lengths. The correlation between the molecular weight and the retention time was done using three polyethylene-oxide (PEO) / polyethylene-glycol (PEG) mixtures of known molecular weight in a range from 106 to 1500000 $g \cdot mol^{-1}$. The result from the GPC is shown in Figure 49.

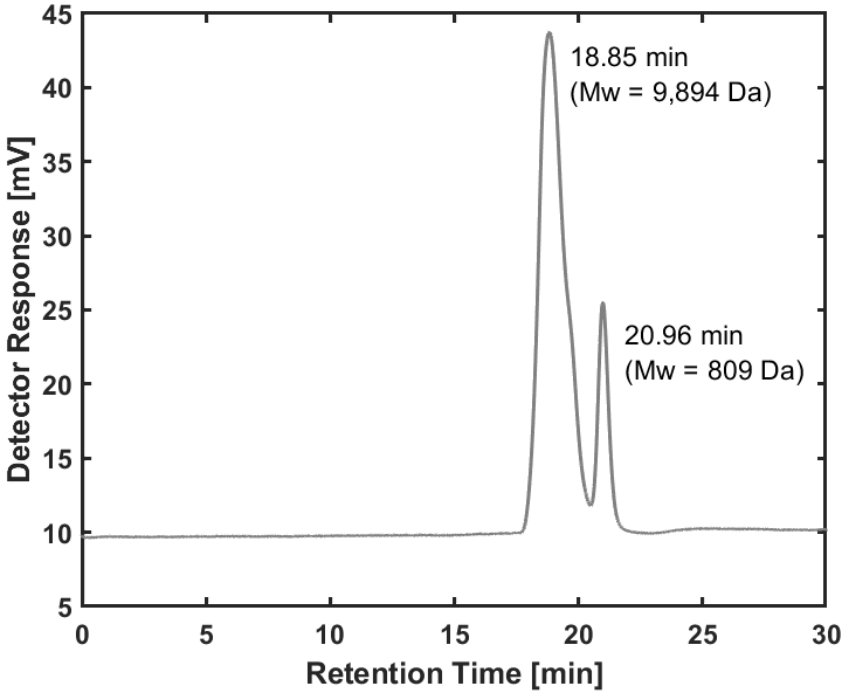

Figure 49: Separation of polyphosphate using gel permeation chromatography.

The sampled polyP shows a bimodal distribution with the majority (80.0-84.0 %) being long chains with an average molecular weight of over 9.9 kDa. The remaining fraction has an average molecular weight of 0.8 kDa. The overall molecular weight for polyP as a mixture of short and long chains is estimated to be 78 residues long (8.0 kDa).

8.7. Matlab Script for Kinetic Parameter Estimation

The following matlab script was used to determine the kinetic parameters of the PPK catalyzed cofactor regeneration along with the resulting confidence intervals. The same nonlinear regression method (nlinfit function, MATLAB 2019a) [76] was used to determine the kinetic parameters of CRL catalyzed transesterification.

```
clear all
close all
clc

%Kinetic of ppk-- Reading of the concentration and activity data from excel
DataGCreadCDP = readtable('Daten.xlsx','Sheet', 'CDP','Range','B1:B22');
ConcallCDP = table2array(DataGCreadCDP);

DataGCreadPP = readtable('Daten.xlsx','Sheet', 'PP','Range','B1:B22');
ConcallPP = table2array(DataGCreadPP);

DataGCreadv_m = readtable('Daten.xlsx','Sheet', 'Activity','Range','B1:B22');
v_m = table2array(DataGCreadv_m);

DataGCreadconmittel2 = readtable('Daten.xlsx','Sheet', 'conmittel2','Range','B1:B22');
conmittel2 = table2array(DataGCreadconmittel2);

DataGCreadactmittel2 = readtable('Daten.xlsx','Sheet', 'actmittel2','Range','B1:B22');
actmittel2 = table2array(DataGCreadactmittel2);

DataGCreadactstd2 = readtable('Daten.xlsx','Sheet', 'actstd2','Range','B1:B22');
actstd2 = table2array(DataGCreadactstd2);

DataGCreadconmittel2PP = readtable('Daten.xlsx','Sheet', 'conmittel2PP','Range','B1:B22');
conmittel2PP = table2array(DataGCreadconmittel2PP);

DataGCreadactmittel2PP = readtable('Daten.xlsx','Sheet', 'actmittel2PP','Range','B1:B22');
actmittel2PP = table2array(DataGCreadactmittel2PP);

DataGCreadactstd2PP = readtable('Daten.xlsx','Sheet', 'actstd2PP','Range','B1:B22');
actstd2PP = table2array(DataGCreadactstd2PP);

% Generation of Substrate Concentration Matrix
C = [ConcallCDP,ConcallPP]; %  concentration vector
CCDP = ConcallCDP; % CDP concentration vector
CPP = ConcallPP;  % PP concentration vector

% Starting parameters
```

```
vmax = 2; % U/mg
km_CDP = 12; % [mM]
km_PP = 50; % [mM]
ki_PP = 160; % [mM]
start_parameter = [vmax km_CDP km_PP ki_PP

%Non linear regression: for fitting of the kinetic parameter
disp('...Fitting of kinetic Parameter...')
parfit = zeros(4,3);
Res_all = zeros(21,3);
for plotten = 1:1:3
[parfit_pre, Res, Jac, Sigma] = nlinfit(C,v_m,@(parfit_pre,C)MMKinetik2(parfit_pre,C,plotten),start_parameter);
parfit(:,plotten) = parfit_pre;
Res_all(:,plotten) = Res;
CInt = nlparci(parfit(:,plotten), Res,'jacobian',Jac); % CInt is the matrix for the confidence interval in which the upper and lower limits are specified (in absolute values)
CInt = abs((CInt(:,1)-CInt(:,2))/2); % Calculates the average from the difference of the absolute values of CInt, so that they can be given as +- value

%Display of fitted kinetic parameter
fprintf('Parameters:\n\t\t Initial Calculated\t Confi.Int\t Unit\n')
formatSpec ='%s\t %2.1f \t %1.3f \t +- %1.3f \t %s \n';
kinpara={'vmax' 'kmCDP' 'kmPP' 'kiPP'};
paraunit={'U/mg' 'mM' 'mM' 'mM'};
for i=1:4
    fprintf(formatSpec, kinpara{i},start_parameter(i),parfit(i,plotten),CInt(i),paraunit{i})
end
end

% Data point generation to display the fitted parameters in a continuous MM-curve.
values_plot  = 150;
C_simCDP     = linspace(0,85,values_plot)'; % Vector with 150 simulated cCDP values from 0 to 85 with linear distances
C_simVinones = 44*ones(size(C_simCDP)); % Vector with same size as upper vector with cPP=44
C_sim1 = [C_simCDP,C_simVinones]; % Both vectors combined in a substrate conc. matrix
C_simPP      = linspace(0,850,values_plot)'; % Vector with 150 simulated cPP values from 0 to 850 with linear distances
C_simPPones = 70*ones(size(C_simPP)); % Vector with same size as upper vector with cCDP=70
C_sim2 = [C_simPPones,C_simPP]; % Both vectors combined in a substrate conc. matrix

v_sim1 = zeros(values_plot,3);
v_sim2 = zeros(values_plot,3);
```

```
for plotten = 1:1:3
v_sim1(:,plotten) = MMKinetik2(parfit(:,plotten),C_sim1,plotten); % Activity vector calculated via MMKinetics with simulated substrate conc.
v_sim2(:,plotten) = MMKinetik2(parfit(:,plotten),C_sim2,plotten); % Activity vector calculated via MMKinetics with simulated substrate conc.
end

%% Plotting

% RMSD CDP
RMSD_1 = sqrt(sum(Res_all(1:8,1).^2)); RSMD_1_str = num2str(round(RMSD_1,2));
RMSD_2 = sqrt(sum(Res_all(1:8,2).^2)); RSMD_2_str = num2str(round(RMSD_2,2));
RMSD_3 = sqrt(sum(Res_all(1:8,3).^2)); RSMD_3_str = num2str(round(RMSD_3,2));

% RMSD PP
RMSD_4 = sqrt(sum(Res_all(9:end,1).^2)); RSMD_4_str = num2str(round(RMSD_4,2));
RMSD_5 = sqrt(sum(Res_all(9:end,2).^2)); RSMD_5_str = num2str(round(RMSD_5,2));
RMSD_6 = sqrt(sum(Res_all(9:end,3).^2)); RSMD_6_str = num2str(round(RMSD_6,2));

%Experimental data (CDP) and fitted curve in Michelis-Menten plot:
figure('Name','Simulated Michaelis-Menten-Plot','NumberTitle','off')
plot(CCDP(1:9),v_m(1:9),'ok',C_simCDP,v_sim1(:,1),'-k',C_simCDP,v_sim1(:,2),'-
.k',C_simCDP,v_sim1(:,3),'--k','MarkerFaceColor','k','linewidth',1)
title('Michaelis-Menten-Plot')
hold on
errorbar(conmittel2, actmittel2,actstd2,'ok','markersize',4);
hold on
xlabel('Cytidine 5-diphosphate [mM]')
xlim([0 90])
ylabel('Specific Activity [U mg^-^1]')
ylim([0 1.4])
legend('experimental values','uncompetitive','competitive','non-competitive');
text(5,1.3,append('RMSD uncomp. = ',RSMD_1_str));
text(5,1.25,append('RMSD comp. = ',RSMD_2_str));
text(5,1.20,append('RMSD non-comp.= ',RSMD_3_str));

%Experimental data (PP) and fitted curve in Michelis-Menten plot:
figure('Name','Simulated Michaelis-Menten-Plot','NumberTitle','off')
plot(CPP(10:21),v_m(10:21),'ok',C_simPP,v_sim2(:,1),'-k',C_simPP,v_sim2(:,2),'-
.k',C_simPP,v_sim2(:,3),'--k','MarkerFaceColor','k','linewidth',1)
hold on
hold on
plot(CPP(10:21),v_m(10:21),'ok','MarkerFaceColor','k')
hold on
```

```
errorbar(conmittel2PP, actmittel2PP,actstd2PP,'ok','markersize',4);
title('Michaelis-Menten-Plot')
xlabel('Polyphosphate [mM]')
xlim([0 850])
ylabel('Specific Activity [U mg^-^1]')
ylim([0 1.2])
legend('experimental values','uncompetitive','competitive','non-competitive');
text(450,0.65,append('RMSD uncomp. = ',RSMD_4_str));
text(450,0.60,append('RMSD comp. = ',RSMD_5_str));
text(450,0.55,append('RMSD non-comp. = ',RSMD_6_str));

kin_legend = {'uncompetitive','competitive','non-competitive'};

function v=MMKinetik2(start_parameter,C,plotten) % Michaelis-Menten_Equation (One-Substrates)

%Start Concnetrations
cCDP = C(:,1);
cPP = C(:,2);

% Start Parameter
vmax = start_parameter(1); %U/mg
km_CDP = start_parameter(2); %[mM]
km_PP = start_parameter(3); %[mM]
ki_PP = start_parameter(4); %[mM]

if plotten == 1
    v = vmax.*(cCDP./(km_CDP+cCDP)).*(cPP./(km_PP+cPP.*(1+cPP./ki_PP))); % uncompetitive inhibition
elseif plotten == 2
    v = vmax.*(cCDP./(km_CDP+cCDP)).*(cPP./(cPP+km_PP.*(1+cPP./ki_PP))); % competitive inhibition
else
    v = vmax.*(cCDP./(km_CDP+cCDP)).*(cPP./((km_PP+cPP).*(1+cPP./ki_PP))); % noncompetitive inhibition
end
end
```

8.8. Experimental Data

This section provides experimental data that is not presented in the main part of this thesis.

8.8.1. Experimental Data: Investigation of Activity in Dependency on Pressure and Temperature

Table 34 gives the experimental data of the investigation of activity in dependency on pressure and temperature of CalB.

Table 34: Investigating of Activity in Dependency on Pressure and Temperature.
Reaction conditions: T = 35-65 °C; $\dot{V}$ = 0.5 ml ·min^{-1}; solvent: heptane; c_{PP} = 10.0 mmol ·L^{-1}; c_{vin} = 864.0 mmol ·L^{-1}; reactor dimensions: 50 x 3 mm; $m_{TR15/TR18}$ = 0.15 g; m_{CalB}(TR15) = 0.195 mg ; m_{CalB}(TR18) = 0.741 mg; p = 1 bar; n = 1-2.

Temperature [°C]	Pressure [bar]	Immobilizate Batch	Specific Activity [U ·mg^{-1}]	Note
35	1	TR15	0.5 ± 0.02	
35	400	TR15	0.5	n=1
35	600	TR15	0.6	n=1
35	800	TR15	0.6 ± 0.03	
35	1200	TR15	0.6 ± 0.03	
45	1	TR15	0.6	n=1
45	400	TR15	0.6	n=1
45	600	TR15	0.7	n=1
45	800	TR18	1.7 ± 0.00	not included
45	1200	TR18	1.9 ± 0.04	not included
55	1	TR15	0.7 ± 0.01	
55	400	TR15	0.8 ± 0.00	
55	600	TR15	0.8 ± 0.00	
55	800	TR15	0.8 ± 0.02	
55	1200	TR15	0.9 ± 0.02	
65	1	TR15	0.8 ± 0.00	
65	400	TR15	0.8 ± 0.01	
65	600	TR15	0.8 ± 0.00	
65	800	TR15	0.9 ± 0.02	
65	1200	TR15	1.0 ± 0.01	

8.8.2. Characterization of Immobilization Procedure of CalB

Table 35, Table 36 and Table 37 gives the experimental data of the investigation of the characterization of immobilization procedure of CalB according to the temperature and the used method.

Table 35: Immobilization of CalB with tube roller method.

	Temperature [°C]		
Time [h]	4	22	40
0	1 ± 0.15	1 ± 0.10	1+0.51
0.5	0.62 ± 0.21	0.20 ± 0.05	0.39 ± 0.21
1	0.34 ± 0.10	0.07 ± 0.02	0.12 ± 0.07
2	0.19 ± 0.06	0.03 ± 0.01	0.07 ± 0.04
4	0.09 ± 0.03	0.02 ± 0.01	0.07 ± 0.04
24	0.08 ± 0.02	0.02 ± 0.01	0.04 ± 0.03

Table 36: Immobilization of CalB with overhead shaker method.

	Temperature [°C]		
Time [h]	4	22	40
0	1 ± 0.13	1 ± 0.20	1 ± 0.52
0.5	0.60 ± 0.10	0.27 ± 0.12	0.21 ± 0.11
1	0.39 ± 0.09	0.10 ± 0.03	0.07 ± 0.04
2	0.23 ± 0.04	0.03 ± 0.01	0.03 ± 0.02
4	0.15 ± 0.03	0.03 ± 0.01	0.03 ± 0.02
6	0.11 ± 0.04	-	0.04 ± 0.02
24	-	0.06 ± 0.02	-

Table 37: Immobilization of CalB with shaking plate method.

	temperature [°C]		
time [h]	4	22	40
0	1 ± 0.17	1 ± 0.20	1 ± 0.15
0.5	0.37 ± 0.20	0.75 ± 0.23	0.37 ± 0.14
1	0.48 ± 0.14	0.22 ± 0.09	0.06 ± 0.04
2	0.37 ± 0.08	0.21 ± 0.06	0.06 ± 0.02
4	0.24 ± 0.05	0.17 ± 0.08	0.02 ± 0.01
6	0.21 ± 0.04	-	0.02 ± 0.01
24	-	0.02 ± 0.01	-